THE UNIVERSITY OF QUEENSLAND

AUSTRALIA

Characterisation of the Flaviviral Non-Structural Protein NS1'

Lucy Bernadette Young

Bachelor of Science – Honours Class 1

A thesis submitted for the degree of Doctor of Philosophy at
The University of Queensland in 2014

School of Chemistry and Molecular Biosciences

Abstract

Members of the genus Flavivirus (including Japanese Encephalitis virus and West Nile virus) are important disease causing agents that result in considerable morbidity and mortality worldwide. NS1' is a C-terminally extended form of the NS1 protein produced only by encephalitic flaviviruses from the Japanese Encephalitis virus serogroup. The function of this unique protein remains elusive, and a further understanding of its production and function during viral infection is necessary. This thesis aims to extend our knowledge of this protein by investigating potential functions and characteristics of NS1' (including localisation, dimer formation and secretion), as well as examining the effect of NS1' mutagenesis on viral infection.

As NS1' consists of the entire NS1 protein with a 52-amino acid C-terminal tail, it is possible that NS1' may behave similar to NS1 in infection. Here I show that WNV NS1' and NS1 localise to the same cellular compartments when expressed from plasmid DNAs and also co-localise to viral RNA replication sites in infected cells. Using complementation analysis with NS1-deleted WNV cDNA, I demonstrated that NS1' is able to substitute for the crucial function of NS1 in virus replication. Co-immunoprecipitation and mass spectrometry indicated that NS1' interacts with other non-structural proteins involved in the formation of the replication complex, further supporting a role for NS1' in viral replication.

The secretable heat-labile NS1 dimer has been extensively studied and is known to be important for viral infection. I show here that WNV NS1' is able to form a unique sub-population of heat and low pH stable dimers that are sensitive to reducing treatments. The stable nature of the NS1' dimers can be linked to amino acids 385-394, though not specifically to the single cysteine residue present within this region. NS1 and NS1' also form a heterodimer in both infected and co-transfected cells. Secretion of NS1' is lower than that of NS1, indicating that the frameshifted region of NS1' results in increased cellular retention of NS1' compared to NS1.

Current NS1'-lacking WNV_{KUN} mutants, such as A30A', abolish NS1' production through mutation of the ribosomal frameshift. This particular mutation results in decreased neurovirulence in weanling mice, however, this may be due to either the lack of NS1' or the frameshift itself. Separation of these potentially competing factors is necessary to fully understand the function of the NS1' protein. To do this, mutations were introduced to NS1' to create either a virus producing a C-terminally truncated version of NS1' (Stop Mutant) or a virus with mutated C-terminus of NS1' (SCMU). Analysis of these mutants showed that Stop Mutant was much like wild type WNV_{KUN}

with respect to protein production, localisation, growth kinetics, and mortality in weanling mice. This suggests that full length NS1' is not required for neurovirulence. SCMU on the other hand was surprisingly more pathogenic than WNV_{KUN} virus in weanling mice, though showed little difference to WNV_{KUN} with respect to growth kinetics (with the exception of C6/36 cells) and protein production in cells. Preliminary analysis indicates that the mutations introduced into both SCMU and Stop Mutant increase the frameshifting efficiency of the virus, suggesting that increased the ratio of structural to non-structural proteins induced by the frameshift is unlikely to affect viral pathogenicity. Both Stop Mutant and SCMU NS1' also showed an increase in NS1' secretion compared to wild type WNV_{KUN}, which indicates that the sequence of the last 20 amino acids of NS1' may be responsible for low level WNV_{KUN} NS1' secretion.

Throughout this project, I have shown that NS1' co-localises with NS1 and can substitute for NS1 in WNV replication; NS1' forms secretable heat-stable homodimers which are linked to amino acids 385-394; full length NS1' is not important for WNV_{KUN} like virulence; and that the frameshifting efficiency of the -1 PRF located in NS2A is unlikely to affect viral pathogenicity in a mouse model of infection.

Declaration by Author

This thesis is composed of my original work, and contains no material previously published or written by another person except where due reference has been made in the text. I have clearly stated the contribution by others to jointly-authored works that I have included in my thesis.

I have clearly stated the contribution of others to my thesis as a whole, including statistical assistance, survey design, data analysis, significant technical procedures, professional editorial advice, and any other original research work used or reported in my thesis. The content of my thesis is the result of work I have carried out since the commencement of my research higher degree candidature and does not include a substantial part of work that has been submitted to qualify for the award of any other degree or diploma in any university or other tertiary institution. I have clearly stated which parts of my thesis, if any, have been submitted to qualify for another award.

I acknowledge that an electronic copy of my thesis must be lodged with the University Library and, subject to the policy and procedures of The University of Queensland, the thesis be made available for research and study in accordance with the Copyright Act 1968 unless a period of embargo has been approved by the Dean of the Graduate School.

I acknowledge that copyright of all material contained in my thesis resides with the copyright holder(s) of that material. Where appropriate I have obtained copyright permission from the copyright holder to reproduce material in this thesis.

Publications during candidature

Young L, Melian E, Khromykh A. 2013. NS1′ colocalizes with NS1 and can substitute for NS1 in West Nile virus replication. J. Virol. **87**:9384–90.

Young L, Melian E, Setoh YX, Young P, Khromykh A. 2014. Last twenty amino acids of the West Nile Virus NS1' protein are responsible its retention in cells and formation of unique heat stable NS1' homodimers. Submitted to J. Virol.

Publications included in thesis

Young L, Melian E, Khromykh A. 2013. NS1′ colocalizes with NS1 and can substitute for NS1 in West Nile virus replication. J. Virol. **87**:9384–90. – Incorporated as Chapter 3.

Contributor	Statement of contribution
Lucy Young (Candidate)	Conducted experiments (100%) Designed experiments (50%) Wrote the paper (70%)
Ezequiel Balmori Melian	Designed experiments (25%) Wrote and edited paper (15%)
Alexander Khromykh	Designed experiments (25%) Wrote and edited paper (15%)

Young L, Melian E, Setoh YX, Young P, Khromykh A. 2014. Last twenty amino acids of the West Nile Virus NS1' protein are responsible its retention in cells and formation of unique heat stable NS1' homodimers. Submitted to J. Virol. – Incorporated as Chapter 5 and part of Chapter 6.

Contributor	Statement of contribution
Lucy Young (Candidate)	Conducted experiments (93%) Designed experiments (50%) Wrote the paper (70%)

Ezequiel Balmori Melian	Conducted experiments (2%) Designed experiments (20%) Wrote and edited paper (10%)
Yin Xiang Setoh	Conducted experiments (5%)
Paul Young	Designed experiments (10%) Wrote and edited paper (5%)
Alexander Khromykh	Designed experiments (20%) Wrote and edited paper (15%)

Contributions by others to the thesis

Prof. Alexander A. Khromykh: Was involved in experimental design, supervision, and interpretation of results. Assisted in editing this manuscript.

Dr Mario Lobigs: Was involved in experimental design and interpretation of results. Assisted in editing this manuscript.

Dr Ezequiel Balmori Melian: Was involved in experimental design and generated PC3 lysates (JEV and WNVNY99) used for experiment shown in Figure 5.2.

Professor Paul Young: Was involved in experimental design and interpretation of results.

Dr Yin Xiang Setoh: Conducted one animal experiment that was combined with my own results for Figure 6.8B.

Statement of parts of the thesis submitted to qualify for the award of another degree

None.

Acknowledgements

Firstly, this thesis would not have been possible without the support of my primary supervisor Alexander Khromykh. Thank you for taking me in for Honours in the first place and encouraging me to stay on for my PhD. Thank you for all the support you have given me, for pushing me to do better and to work harder; I would not be the scientist I am today without your guidance. Your knowledge and experience has made this project possible. Special thanks must also go to Mario Lobigs, who despite looming retirement was more than happy to step in as my secondary supervisor over this last year. Your brilliant advice and experience through my last mad rush of experiments and during the writing process has been invaluable. This thesis would not be what it is without the support you have given me.

Huge thanks must go to all the past and present post-docs and students from the Khromykh lab for their advice and friendship. To the post-docs, Judy, Penny, Eze, Brian, Andrea, Setoh, and Andrii, no matter how busy you were, you were always willing to give advice and help me out when I needed it. To everyone else in the lab who kept my sanity intact through the long (long) hours; Dan, Dougald, Erinke, Eelke, Quek, Nick, Victoria, Rory, Daniel, Giel, and particularly Shessy and Adriana. Your friendship and support has truly made this process not only bearable, but some of the best years of my life. I know that I have made life-long friends in this lab.

Thanks must go to Roy Hall for generously providing limitless amounts of antibodies and advice throughout the years. You have been a brilliant and supportive chair; who will always go above and beyond to help someone who needs it. To all the members of the Young and Hall labs for their friendship and advice throughout my degree; Cindy, Ash, Imogen, Jaelle, Lucas, Fi, Jody, Suz, Dan, Keith, Bree, Cait, and Nat; your friendship made these last few years such fun. In particular, to Dave, who keeps me honest, always has time for a chat over coffee (or at the pub), and who has taught me so much over the years.

To my friends and family, thank you for putting up with all my (numerous) work-related absences; it kept me going knowing you would still be there when I emerged from the other side. My dear sister Kate, whose wonderful encouragement and passion for life has been a constant inspiration. It means the world that you have always believed in me.

Thank you to my parents in particular, who have supported me unwaveringly throughout this long process; I am so lucky to have four amazing people looking out for me. To my step-dad

Geoff, whose constant enthusiasm and encouragement to “think like a virus” definitely made this thesis better; to my step-mother Cheryl, who has always been a source of inspiration and proof that one does not need to stay in academia to be successful and happy; to my incredible mum, words cannot describe how much I appreciate everything you have done for me - you will always be my role model; and, lastly, to my dad. While I know that there is no such thing as a “science gene”, I have no doubt that my love of science comes from you. Your passion and drive for this wonderful field of viruses is what drew me to it in the first place, and your constant teachings that no experiment, or month, or year will ever be bad enough to ruin the pure joy that comes from those amazing moments when something goes right is what keeps me here. It is truly wonderful to be able to share this with you, and I hope to one day be a fraction of the scientist you are.

Finally, to my amazing husband Justin. Your love and support throughout these last few years has made all this possible. Thank you for putting up with me, listening to me rant, cooking for me, and encouraging me no matter what. Quite simply, I could not have done this without you.

This thesis is for all of you. I hope I have done you proud.

Keywords

flavivirus, west nile, ns1, replication, dimer, secretion, ns1' mutant, pathogenesis

Australian and New Zealand Standard Research Classifications (ANZSRC)

ANZSRC code: 110804 Medical Virology, 100%

Fields of Research (FoR) Classification

FoR code: 1108, Medical Microbiology, 100%

Table of Contents

List of Figures

List of Tables

List of Abbreviations

3D	Three dimensional
ABTS	2,2'-azino-bis(3-ethylbenzothiazoline-6-sulphonic acid)
ACN	Acetonitrile
APS	Ammonium persulfate
BFA	Brefeldin A
BiP	Binding immunoglobulin protein
bp	Base-pairs
BHK	Baby hamster kidney
BSA	Bovine serum albumin
C	Capsid protein
°C	Degrees Celcius
cDNA	Complimentary deoxyribonucleic acid
CF	Culture fluid
CHO	Carbohydrate
cm	Centimeters
CM	Convoluted membrane
CMV	Cytomegalovirus
CNS	Central nervous system
CO_2	Carbon dioxide
CPE	Cytopathic effect
Da	Dalton
DAPI	4',6-diamidino-2-phenylindole
DC	Dendritic cell
DENV	Dengue virus
DEPC	Diethyl pyrocarbonate
dH_2O	Distilled water
DMEM	Dulbecco's modified Eagle's medium
DNA	Deoxyribonucleic acid
dsRNA	Double-stranded ribonucleic acid
DTT	Dithiothreitol
E	Envelope protein
ECL	Enhanced chemiluminescence
EDTA	Ethylenediaminetetraacetic acid

eEF-1α	Eukaryotic elongation factor 1α
ELISA	Enzyme-linked immunosorbent assay
ER	Endoplasmic reticulum
ESI	Electrospray ionisation
FCS	Foetal calf serum
fH	Factor H
FSSM	Frameshift silent motif
GAG	Glycosaminoglycans
GAPDH	Glyceraldehyde 3-phosphate dehydrogenase
GFP	Green fluorescent protein
GPI	Glycosyl-phosphatidylinositol-linked
h	Hours
HEK	Human embryonic kidney
HEPES	4-(2-hydroxyethyl)-1-piperazineethanesulfonic acid
HRP	Horse-radish peroxidase
hpi	Hours post infection
IFA	Immunofluorescence assay
IFN	Interferon
i.p.	Intraperitoneal
IPS	IFN-promoter stimulator
IRF	IFN regulatory factor
ISG	Interferon-stimulated gene
JEV	Japanese encephalitis virus
kb	Kilobase
kDa	Kilodaltons
KUN	Kunjin strain
kV	Kilovolts
LB	Luria Bertani
M	Molar
mAb	Monoclonal antibody
MALDI	Matrix-assisted laser desorption ionization
MAVS	Mitochondrial antiviral signalling
MDA5	Myeloma differentiation antigen 5
MEF	Mouse embryonic fibroblast
µF	Microfarad

µg	Microgram
mg	Milligram
min	Minutes
miRNA	Micro-ribonucleic acid
µl	Microlitre
ml	Millilitre
µM	Micromolar
mm	Millimeter
mM	Millimolar
MOI	Multiplicity of infection
MOPS	3-(N-morpholino)propanesulfonic acid
mRNA	Messenger ribonucleic acid
MS	Mass spectrometry
MVEV	Murray Valley encephalitis virus
NCR	Non-coding region
ng	Nanogram
NK	Natural killer cell
nLC	Nanoscale liquid chromatography
NLR	Nucleotide oligomerization domain (Nod)-like receptors
nm	Nanometer
NP-40	Nonidet P40
NS	Non-structural
NTP	Nucleoside triphosphate
NY	New York
OAS	Oligoadenylate synthase
PAMP	Pathogen-associated molecular pattern
PBS	Phosphate-buffered saline
PBST	Phosphate buffered saline Tween-20
PC	Paracrystalline array
PCR	Polymerase chain reaction
pfu	Plaque-forming unit
pH	Partial pressure of the hydronium ion
PKR	Protein kinase R
PMSF	Phenylmethylsulfonyl fluoride
ppm	Parts per million

PRF	Programmed ribosomal frameshift
prM	Pre-membrane protein
PRR	Pattern recognition receptor
RC	Replication complex
RdRp	RNA-dependent RNA polymerase
RER	Rough endoplasmic reticulum
RF	Replicative form
RIG-I	Retinoic-acid inducible gene-I
RLR	RIG-I-like receptor
RNA	Ribonucleic acid
RNAi	Ribonucleic acid interference pathway
RPMI	1640 Roswell Park Memorial Institute 1640 medium
RT	Room temperature
RT-PCR	Reverse transcriptase polymerase chain reaction
SCF	Soluble complement fixing antigen
SCMU	Scramble Mutant
SDS-PAGE	Sodium dodecyl sulphate polyacrylamide gel electrophoresis
sec	Seconds
SEM	Standard error of the mean
sfRNA	Subgenomic flavivirus ribonucleic acid
siRNA	Small interfering ribonucleic acid
SLEV	St Louis encephalitis virus
ssRNA	Single-stranded ribonucleic acid
TBEV	Tick-borne encephalitis virus
TEMED	Tetramethylethylenediamine
TFA	Trifluoroacetic acid
TLR	Toll-like receptor
TOF	Time-of-flight
U	Units
UPR	Unfolded protein response
UTR	Untranslated region
V	Volts
VP	Vesicle packets
WNF	West Nile fever
WNV	West Nile virus

WT	Wild-type
x *g*	Times gravity
YFV	Yellow fever virus

1 Literature Review

1.1 Flaviviruses

The family *Flaviviridae* consists of enveloped viruses with a positive-sense, single-stranded RNA genome encoding a single polyprotein. Within this family are four genera, *Hepacivirus*, *Pestivirus*, *Pegivirus*, and *Flavivirus* (6, 7). The genus *Flavivirus* can be further subdivided into 4 main groups: the mosquito-borne, tick-borne, no known vector and the insect-specific flavivirus groups (Figure 1.1) (8, 6, 9). This genus includes medically relevant pathogens, such as Dengue virus (DENV), Yellow Fever virus (YFV), Tick Borne encephalitis virus (TBEV) and the members of the Japanese encephalitis virus (JEV) serogroup. The clinical symptoms caused by the mosquito-borne viruses predominantly fall into two distinct categories; those that cause systemic disease, such as DENV and YFV, and those that cause encephalitic disease, grouped together in the JEV serogroup. Interestingly, these two distinct groups of viruses can be further distinguished by their predominant vector-host relationship. Encephalitic viruses are usually transmitted by *Culex* vectors and infect avian hosts, while systemic disease-causing viruses are typically transmitted by *Aedes* vectors and infect mammalian hosts (10). The JEV serogroup includes West Nile virus (WNV), JEV, Murray Valley encephalitis virus (MVEV) and St Louis encephalitis virus (SLEV).

1.2 West Nile Virus

1.2.1 Distribution

WNV is a mosquito-borne flavivirus within the JEV serogroup, and is currently the major cause of viral encephalitis in the United States. WNV is also the most widely distributed arbovirus, and has been endemic throughout Africa, the Middle East, Europe and parts of Asia since its first isolation in 1937 (11). It was introduced into the Americas in 1999 by a single point introduction in New York, now designated the WNV_{NY99} strain (12, 13). This was followed by a dramatic expansion across America, and resulted in WNV now being detected throughout Central and North America (14-17). WNV has been detected in at least 65 species of mosquito and 326 species of bird in North America alone, highlighting the ability of WNV to adapt to new host and vector species (15, 18). WNV can be divided into two main lineages (19, 20), though the possibility for eight distinct lineages has also been suggested (21-24, 450). Originally, to be classified as a WNV, lineages were defined as being less than 21% genetically divergent (25), however, the inclusion of the proposed lineages III to VII would result in more than 25% genetic divergence (21). The inclusion of these additional lineages is therefore still regarded as controversial.

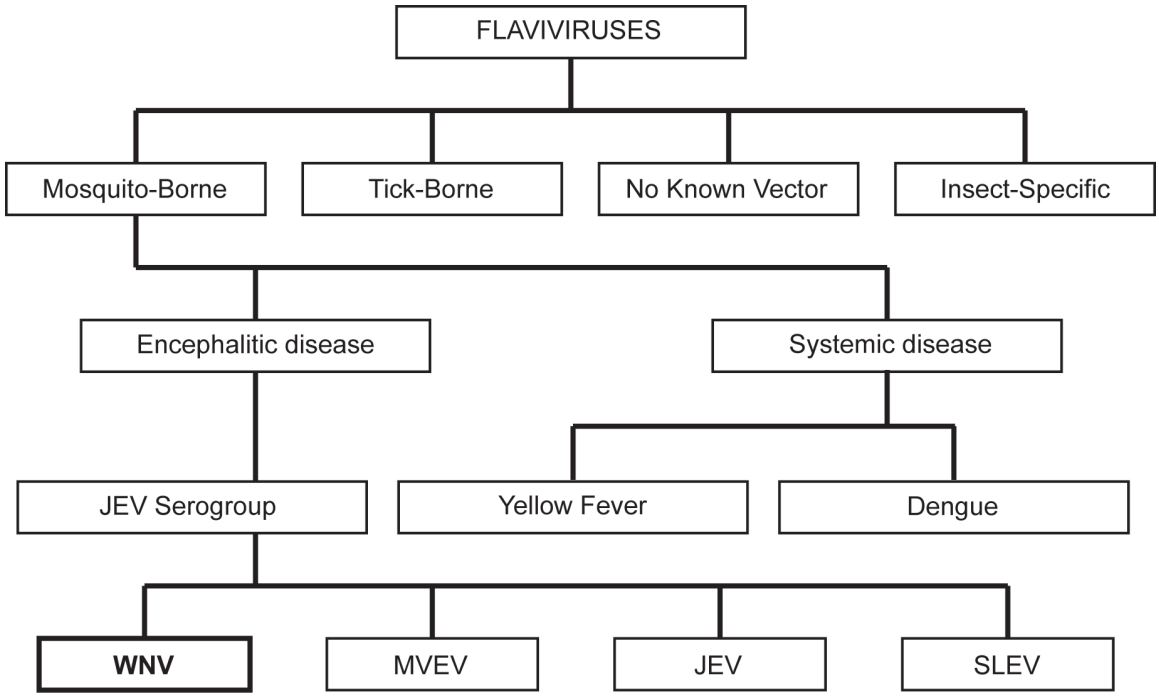

Figure 1.1 Genus *Flavivirus*. The genus *Flavivirus* is divided based into 4 distinct groups. The mosquito-borne flaviviruses are further divided based on clinical symptoms; either encephalitic or systemic. WNV is a mosquito-borne flavivirus within the JEV serogroup, and the focus of this thesis.

Lineage I is the most widely distributed of the lineages, causing disease prevalent in Africa, Asia, Europe, Australia, North America, and Central America (13). This lineage can be further divided into three sub-lineages: lineage Ia, which is well established in Africa, Europe and the Americas; lineage Ib, also known as Kunjin (WNV_{KUN}), and the only strain of WNV present in Australia; and lineage Ic, occurring throughout India (13). WNV lineage II is found primarily in Sub-Saharan Africa (26-28), with recent introductions detected in Europe and Russia (29-33).

1.2.2 Transmission

WNV transmission occurs predominantly between mosquitoes of the *Culex* genus and passeriform birds (Figure 1.2) (34, 35). The possibility of vertical transmission has also been shown, though it has only been observed at very low levels (36, 37). WNV does not usually cause widespread clinical disease in avian hosts, and the high mortality seen in birds during the WNV_{NY99} outbreaks is unique to Northern America (38). However, WNV can cause neurological symptoms in some avian species, with other species displaying variable levels of morbidity and mortality (39-41). Following ingestion of infected blood by mosquitoes, there are several barriers the virus must overcome to achieve transmission. First, the virus must successfully infect the midgut of the mosquito, and subsequently disseminate to the periphery. In order to then transmit the virus, high

levels of virus must be present within the salivary glands prior to transmission during the mosquito's next blood meal (42-45). The immune response of the mosquito is also involved in preventing successful virus infection. The primary innate immune response to viruses in mosquitoes is the RNA interference pathway (RNAi). The importance of this pathway has been shown through the use of small interfering RNAs (siRNAs) that mediate silencing through the RNAi pathway to provide immunity to WNV (46). However, classical innate immune pathways (such as Jak-STAT and Toll) are also involved in the mosquito innate immunity (47). WNV has the ability to infect humans and other mammals via the bite of an infected mosquito, though these are usually known as "dead-end" hosts as they are unable to generate a sufficiently high viraemia to transmit the virus further.

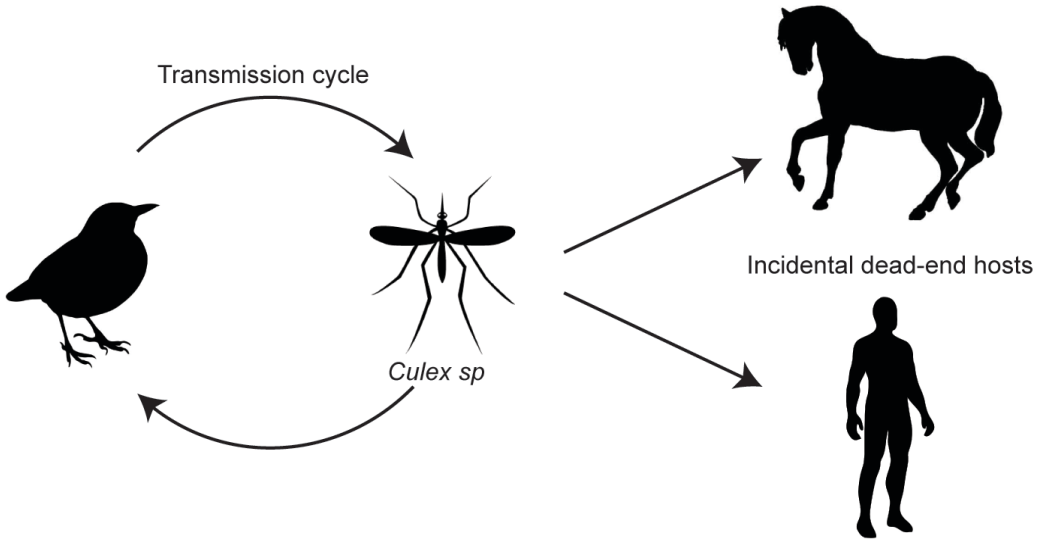

Figure 1.2 Transmission cycle of WNV. WNV is maintained through a transmission cycle between birds and *Culex* mosquitoes, while causing incidental infections in other mammals (particularly humans and horses).

1.2.3 Disease and pathogenesis

The incubation period of WNV in the mammalian host is usually between 2 and 14 days. Infections with WNV are predominantly asymptomatic, with 20-25% of infected individuals developing a mild West Nile fever (WNF) and 1 in 150–250 developing neurological complications (48-53). WNF is characterised by an abrupt onset of symptoms lasting 3-6 days, though they can last for weeks. These symptoms usually include headache, fever, malaise, and a morbilliform or maculopapular rash. In less than 1% of cases, a patient may develop West Nile neurological disease, which can last for weeks and up to several months, and may result in death. Again, an

abrupt onset of fever and headache is seen, with signs of involvement of the central nervous system (CNS), including meningitis, encephalitis and acute flaccid paralysis. This neurological disease can range from a fairly mild, self-limiting confusional state to severe encephalopathy, coma, and eventually death. The fatality rate of WNV infection is approximately 10% in those who develop neurological disease, and is notably higher in older patients (18). Lineage I of WNV is associated with both WNF and neurological disease, while lineage II causes predominantly WNF, with only a very rare occurrence of CNS complications (26, 13, 27, 28). However, even within lineage I different levels of pathogenesis are observed. WNV_{KUN}, the subtype within Australia, is a lineage I WNV and rarely associated with human disease (54, 55).

WNV initially replicates in keratinocytes, skin resident dendritic cells (DCs) and Langerhans DCs (56, 57). WNV infected DCs then migrate to draining lymph nodes from which viremia develops, leading to the spread of virus to peripheral organs, and potentially the CNS (58). It is still unclear precisely how WNV invades the CNS (59). It is thought that WNV infection may disrupt the blood brain barrier integrity by the induction of cytokines (81, 451-455); WNV may directly infect the vascular endothelium and transmigrate into the brain parenchyma (456); viral particles may enter the CNS via the trafficking of infected monocytes (457-459); or WNV may invade the CNS by retrograde axonal transport from infected peripheral nerves (460-462).

1.3 Immune response to WNV

1.3.1 Cell intrinsic innate immune response

The innate immune response is crucial for the control of WNV infection. It is predominantly the induction of interferon (IFN) triggered by the innate immune system (and its subsequent downstream effects) that is so essential. The cells of the innate immune system are the first point of encounter for WNV. Myeloid DCs, monocytes and macrophages are all key targets for virus infection, and are therefore crucial for antiviral immunity (60, 61). The host cell is able to sense infecting virus through the recognition of a pathogen-associated molecular pattern (PAMP) by a pattern recognition receptor (PRR). Plasmacytoid DCs, while resistant to direct infection, also contribute to the innate immune response via an interaction of the virus with PRRs present within endosomal compartments (61). Binding of PRRs to PAMPs results in a signalling cascade involving the activation of adaptor proteins, induction of transcription factors, and subsequent production of soluble mediators (such as proinflammatory cytokines and IFN). This leads to a potent antiviral response through the induction of antiviral effector genes, activation of innate immune cells, and humoral and cell-mediated immunity. Interferon and the PRRs (Toll-like receptors (TLRs), retinoic-

acid inducible gene-I (RIG-I)-like receptors [RLRs], and nucleotide oligomerisation domain (Nod)-like receptors [NLRs]) are all key players involved in the induction of the innate immune system (47, 62-64).

Pathogen Recognition Receptors (PRRs)

RLRs are a family of cytosolic RNA helicase proteins that detect the presence of foreign RNA (such as from an RNA virus) in the cytoplasm (65). Once activated, RLRs signal through IFN-promoter stimulator (IPS)-1 and mitochondrial antiviral signalling (MAVS) adaptor proteins to trigger the production of transcription factors IFN regulatory factor (IRF) 3 and IRF7. RNA from WNV has been shown to trigger RLR signalling through the receptors RIG-I and myeloma differentiation antigen 5 (MDA5), and the importance of this signalling cascade has been demonstrated at several stages (66-68). RIG-I and MDA5 knockout mice have increased mortality over wild-type when infected with WNV (67, 69). The absence of the adaptor protein MAVS correlates with a wider tissue tropism and CNS pathology, and an increase in viral load in both the periphery and CNS (70). Another RLR signalling factor (Caspase-12) has been shown to be essential for developing an anti-viral response against WNV (71). Both RIG-I and MDA5 are important for the immune response against WNV, with RIG-I appearing to function early in infection and MDA5 later in infection (72, 73).

The TLRs detect the presence of distinct forms of foreign RNA present in endosomes; TLR3 recognises dsRNA and TLR7/8 recognises ssRNA (74, 75). TLRs signal through various adaptor molecules to activate transcription factors (such as IRF3 and IRF7) controlling IFN and inflammatory cytokine production. There are many studies on the control of WNV by TLRs, and they appear to function in a cell specific manner (76-83). For example, TLR3 is important for controlling WNV infection in the CNS, functioning in neurons but not macrophages or DCs to promote IFN production (76). TLR7 on the other hand, can trigger IFN production in neurons, macrophages, and keratinocytes, but not DCs (79, 82).

NLR signalling occurs through the inflammasome (a signalling complex within the cytosol) and results in the production of cytokines. WNV has been shown to activate the NLRP3 inflammasome complex and induce production of IL-1β (84). The IL-1 receptor, NLRP3, apoptosis-associated speck-like protein containing a CARD (ASC) adaptor protein and caspase-1 (which are all components of inflammasome signalling) are all involved in mediating immunity

against WNV (85, 86, 84). In accordance with these findings, IL-1β signalling has also been implicated in the promotion of an anti-WNV response (87).

Interferon

Type-I IFNs are cytokines critical for the control of most viral infections. RLR and TLR signalling results in the upregulation of type-I IFNs (IFN-α and IFN-β). Type-I IFN has potent antiviral activity and is necessary for controlling viral replication and contributes to priming both B and T cell responses (88-90, 64, 91-93). One of the reasons IFN-α/β is particularly critical is that it is responsible for the downstream induction of many IFN stimulated genes (ISGs) that are also involved in inhibiting WNV infection. IFN-α/β secreted from cells binds to the IFN-α/β receptor (IFNAR) and signals through tyrosine kinase 2 (Tyk2) and Janus kinase 1 (Jak1) to activate signal transducer and activator of transcription (STAT) 1 and 2, leading to the induction of ISGs. Several ISG screens have been conducted, leading to the subsequent identification of a large number of genes that are upregulated during WNV infection (94-98). Many of these proteins have also been shown experimentally to have antiviral activity, for example, the IFIT family (99, 100, 98, 101); the IFITM family (102, 94, 98); RNase L and PKR (103-106); and viperin (94, 107). Type-II IFN, or IFN-γ, is also important for restricting WNV infection (108, 109), as is IFN-λ, a third type of interferon (110).

WNV interference with innate immune responses

Numerous studies have identified a wide range of mechanisms that WNV employs to evade the host innate immune response. WNV can evade detection by RLRs through an as of yet unknown mechanism (72). The envelope protein has been shown to inhibit a dsRNA-induced response (111). WNV NS1 appears to antagonise TLR3 signalling, though this result is somewhat controversial due to conflicting studies (112-114). WNV-produced sub-genomic flaviviral RNA (sfRNA) has been shown to inhibit IFN signalling (106). The viral non-structural proteins have been shown to inhibit STAT1 and STAT2 activation (115-119), activate the unfolded protein response (120, 121), and redistribute cellular cholesterol leading to downregulation of Jak-STAT signalling (122). WNV has also been implicated in the inhibition of Tyk2 phosphorylation (123) and degradation of IFNAR1 (124).

1.3.2 Cell-mediated innate immune response

Natural killer (NK) cells have been suggested to bridge the gap between the innate and the adaptive immune response (125). NK cells identify infected cells and induce cytokine production and mediate cell lysis. These cells have been shown to be involved in the antiviral response to WNV (126, 127). However, the precise involvement of NK cells in the induction of immunity to WNV is still unclear, as depletion of NK cells does not impact WNV infection (128, 129). In addition to NK cells, γδ T cells (a small subset of T cells with effector functions) are also important for protective immunity against WNV infection as an early source of IFN-γ. An absence of these cells was shown to be correlated with an enhanced susceptibility to WNV infection (130).

1.3.3 Complement-mediated innate immune response

The complement system is mediated by serum and surface proteins that are involved in recognition of PAMPs, altered self ligands, and immune complexes. This system consists of three pathways: the classical, lectin, and alternative pathways (131). Complement activation induces antiviral effector functions, including pathogen opsonisation and/or lysis, priming of B cells, and enhancement of T cell killing. Mice that are deficient in any one of numerous components of the complement pathway all show enhanced susceptibility to WNV infection, highlighting the importance of the complement system against WNV (132-135).

1.3.4 Adaptive immune response

The adaptive immune response is involved in promoting viral clearance, assists in the control of viral infection, and is crucial in preventing re-infection. Both the viral pathogens themselves and the innate immune responses they activate are involved in stimulating the adaptive immune response. This response can be broadly divided into antibody-mediated immunity and cell-mediated immunity. Antibody-mediated immunity, or humoral immunity, is controlled by B cells and is essential for the restriction of WNV infection. The production of antibodies specific to WNV antigens can result in neutralisation of viral particles and lysis of infected cells. A lack of B cells in WNV infected mice correlates with an enhanced mortality, highlighting their importance in controlling WNV infection (136, 137). The supply of WNV-specific antibodies prior to challenge with infectious virus can also protect against infection (138, 137, 139, 140).

Cell-mediated immunity is controlled by T cells, which can be sub-divided into different subsets of T cells with distinct roles. $CD8^+$ T cells and $CD4^+$ T cells are both critical for protection

against WNV (141-144). A lack of $CD8^+$ T cells leads to enhanced viral replication in the CNS (142). Interestingly, $CD8^+$ T cells also seem to have pathogenic role in WNV infection, with the presence of $CD8^+$ T cells contributing to an increase in mortality when a high viral dose is used (130). $CD4^+$ T cells play an essential role in priming B cell mediated antibody responses, mediating $CD8^+$ T cell responses, and secretion of anti-viral cytokines following WNV infection (145, 143). Regulatory T cells have also been implicated in modulating the immune response to WNV (146).

1.4 WNV genome

WNV is an enveloped virus with a virion structure of approximately 50nm diameter. A 30nm inner nucleocapsid is surrounded by a host-derived lipid membrane, in which the envelope and membrane proteins are inserted (147-150). The genome enclosed within the nucleocapsid is a single stranded positive sense RNA genome of approximately 11 000 nucleotides (151, 13, 152) and contains a type 1 cap (m^7GpppAmp) at the 5'-terminus but no 3' polyadenylate tail (20, 153, 154). The coding region of the WNV genome is flanked by 5' and 3' non-coding regions (NCR) that despite a lack of sequence conservation contain secondary structures that are highly conserved among flaviviruses (155-158). The 5'-NCR of WNV is approximately 100 nucleotides in length, and the 3'-NCR is between 600 and 700 nucleotides in length (159, 20). The WNV genome is translated as a single polyprotein that encodes 3 structural (capsid, membrane and envelope) and seven non-structural proteins (NS1, NS2A, NS2B, NS3, NS4A, NS4B and NS5) (Figure 1.3A).

1.5 Translation and processing

Following translation as a single open reading frame, the WNV polyprotein is cleaved both co- and post-translationally by host and viral proteases (20, 160-162). The presence of multiple transmembrane domains determines whether individual proteins will reside on the cytoplasmic or the luminal side of the ER membrane (Figure 1.4B). The prM, E and NS1 proteins are localised to the luminal side of the ER (20). Here, the host signal peptidase cleaves the polyprotein at the N-terminus of these proteins. For cleavage by the host signal peptidase to occur, a signal sequence is required. The prM, E, NS1 and NS4B proteins are all preceded a stretch of hydrophobic amino acids followed by Val-X-Ala (where X is His, Asn, or Ala), which is consistent with the -1, -3 rule for signalase cleavage (163-167). The capsid, NS3 and NS5 proteins are located on the cytoplasmic side of the membrane, while the NS2A, NS2B, NS4A and NS4B proteins span the ER membrane (20). The N-terminus of NS2B, NS3, NS4A and NS5 are all cleaved by the viral NS2B-NS3 protease (163, 168, 164-166). The enzyme involved in the cleavage of the NS1/NS2A junction is still unclear.

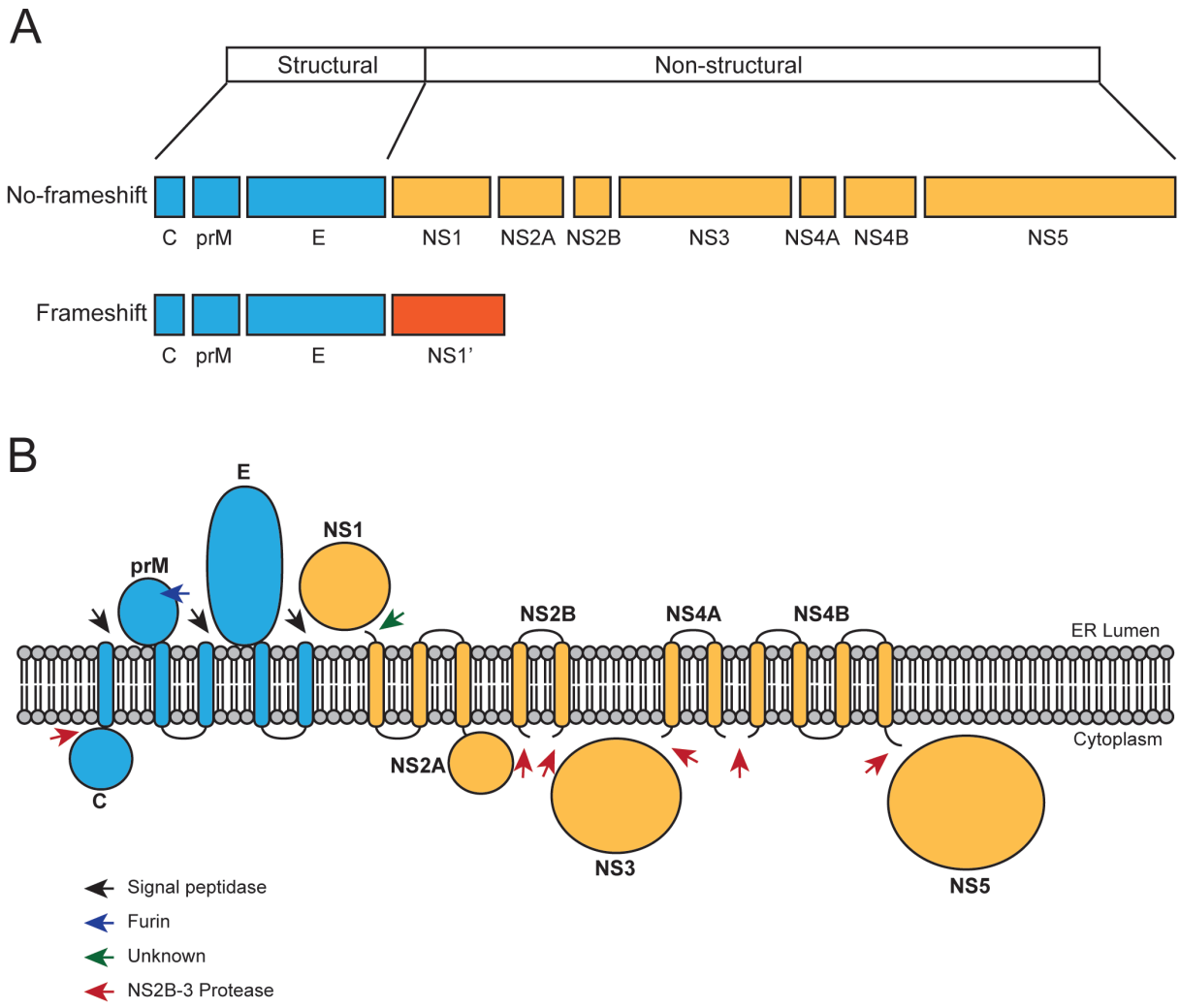

Figure 1.3 Organisation of the WNV genome and polyprotein. A. The polyprotein translated from the 11kB genome is processed into 3 structural (C, prM and E; blue) and 7 non-structural (NS; yellow) proteins. In 30-50% of translation events, a frameshift occurring within the NS2A coding region results in the production of a C-terminally extended form of NS1 (known as NS1'; orange) terminating in a stop codon. **B.** WNV polyprotein spans the ER membrane and is cleaved by host (signal peptidase, black arrow; furin, dark blue arrow; unknown, green arrow) and viral (NS2B-3; red arrow) proteases.

1.6 WNV proteins

1.6.1 Capsid

The flavivirus capsid (C) is the first gene encoded by the polyprotein, producing a 14kDa cytosolic protein. C is cleaved from prM by co-ordinated cleavage by both the ER resident host signalase (at the prM junction) and the viral NS2B-NS3 protease (on the cytosolic side of the ER membrane) (Figure 1.3B) (169-175). The primary function of the capsid protein is to form the nucleocapsid in association with the viral RNA genome. C has an affinity for both lipids and

nucleic acids (176, 177, 147, 178), and charged basic residues on both the N- and C-terminus interact with nucleic acids (179, 147). The exact structure of nucleocapsid is still unclear, though it is unlikely to fully enclose the viral RNA (180-182). In addition to forming the nucleocapsid, C is also involved in promoting viral replication and translation (183, 184).

1.6.2 Membrane

The flaviviral membrane (M) protein is a small, 8kDa protein that is cleaved from its precursor (prM; approximately 21kDa). During virion production, this precursor protein is anchored to the lipid membrane that encloses the viral nucleocapsid (185-187). Here it interacts with the viral envelope protein as a heterodimer and assembles on the membrane surface with two additional heterodimer complexes (188, 185). The key function of the prM protein is to stabilize the envelope protein during trafficking of the immature virion through the secretory pathway (189, 188, 190). In the trans-Golgi the prM precursor protein is cleaved by the host protease furin into mature M. However, the pr peptide appears to remain associated with the viral particle until it is released from the cell (191, 189, 188, 192-194). The prM protein is one of three viral glycoproteins (including the envelope and NS1 proteins), and the addition of glycans is important for particle production and pathogenesis (191, 195-197, 193). prM has also been suggested to assist in the folding of the envelope protein (198).

1.6.3 Envelope

The flaviviral envelope (E) protein is a 53kDa glycoprotein containing 6 disulfide bridges (199). This class II viral fusion protein resides in a dimeric form on the surface of viral particles and triggers fusion of the viral and host cell membranes. As E is the major protein on the surface of virions, it is also the primary target of neutralizing antibodies (148, 200). E consists of three distinct domains connected by flexible hinge regions; DI, DII, and DIII (201-205). Domain I is the central domain and functions as the hinge point for DII (465). DII mediates dimerisation of E, and includes a glycine rich tip that is important for membrane fusion (206, 189, 207). Through a number of studies, DIII has been suggested to contain binding sites for cellular proteins (208-210, 204). The glycosylation of the envelope protein is important for viral pathogenesis (195, 196, 211, 212), though the nature of glycosylation can be variable in different WNV strains (213-216, 205).

E is arranged in 90 homodimers on the surface of mature virions (201, 185). The low pH environment in the late endosomes following endocytosis of viral particles triggers a

conformational change in the E protein that leads to fusion between the viral and endosomal membranes. It has been suggested that the protonation of one or more His residues triggers this change (217-219). The conformational change results in the dissociation of dimeric E on the virion surface, and in the exposure of the fusion domain on the tip of DII. This domain subsequently interacts with the adjacent endosomal membrane, and monomeric E reassociates as a trimer (220). This triggers membrane fusion through a hemifusion intermediate, finally resulting in the formation of a fusion pore (219).

1.6.4 Non-structural membrane proteins

WNV expresses 4 small, multifunctional hydrophobic proteins with 2-3 membrane spanning regions. NS2A, NS2B, NS4A and NS4B are involved in a variety of roles throughout viral infection, from assembly, to viral RNA replication, to inhibition of the host immune system (221-224). In fact, all four hydrophobic proteins co-localise with dsRNA and other members of the replication complex (RC), and thus have been implicated in viral RNA replication (225, 221, 223, 226). In addition to this, NS2A, NS2B, NS4A and NS4B have been shown to be involved in the inhibition of the host immune system, specifically by blocking type 1 IFN signalling (227, 116-118, 228). Apart from a role in RNA replication and inhibition of IFN signalling, all four proteins have been shown to have additional and diverse functions throughout the virus life cycle.

NS2A is a 22kDa protein involved in virion assembly and IFN-independent apoptotic cell death (168, 229, 225, 230, 116, 221, 231, 232). The primary function of the small, 14kDa NS2B protein is a protease co-factor in combination with the C-terminal protease domain of NS3 (233, 164, 162, 234). The 16kDa NS4A protein has been implicated in reorganisation of host cell membranes, with expression of NS4A alone sufficient to induce membrane proliferation (235, 221, 222, 236, 237). In further support for this role of NS4A, structural predictions of the protein highlights the ability of NS4A to induce membrane curvature (238). NS4A forms oligomers that are important for viral infection, as mutations disrupting this result in a inhibition of viral replication (239). Protein binding studies carried out on NS4A show an association with the additional members of the replication complex, and thus supporting the theory of a role for NS4A in viral RNA replication (221). The 29kDa NS4B protein has also been implicated in membrane proliferation (223, 240). Recently, the presence of an alternative reading frame within NS4B was identified by bioinformatic analysis and determined to result in the production of a protein containing the N-terminus of NS4B with a unique C-terminus (241, 242). Both NS4A and NS4B

have been shown to activate the unfolded protein response, leading to an inhibition of antiviral signalling (121).

1.6.5 NS3

NS3 is a 70kDa protein consisting of two distinct functional domains, a serine protease and a helicase. NS3 is widely distributed throughout the cell, particularly in association with proliferating ER membranes. NS3 has been shown to co-localise with dsRNA and other non-structural proteins involved the formation of the replication complex, suggesting that this protein is also involved in RNA replication (226). The C-terminal domain of NS3 shows RNA-stimulated nucleoside triphosphatase (NTPase), ATPase/helicase and 5' triphosphatase (RTPase) activity (243-245). The RTPase activity is involved in dephosphorylation of the 5' end of RNA prior to the addition of a cap (246). The helicase domain is able to unwind RNA, driven by NTPase hydrolysis (247-250). This is the domain involved in viral RNA replication. An interaction between NS3 and NS5 has been shown, and NS5 appears to stimulate the NTPase/helicase activity (251-253). It has also been suggested that the helicase activity is enhanced by an association of NS3 with NS4B (254).

The N-terminal 175 residues of NS3 comprise a serine protease, which functions in association with NS2B (255, 243, 256). The NS3 sequence contains a conserved catalytic triad within the protease domain (His51, Asp75 and Ser135 for WNV) (255, 257, 243, 256). The structure of the NS2B-NS3 protease shows a predominantly closed confirmation, with NS2B wrapped around NS3 (258, 259). This protease activity results in cleavage after dibasic residues that are followed by a small side chain amino acid (257). This pattern occurs at multiple sites within the viral polyprotein, and the NS2B-NS3 protease mediated cleavage of the viral polyprotein (in addition to cleavage by host proteases) liberates the individual proteins (257, 260, 164, 261, 262).

The N-terminal protease and C-terminal NTPase/helicase appear to be segregated domains (263, 264). The two distinct functions of the NS3 protein are also likely to occur in separate regions of the cell, with the protease functioning in the induced convoluted membranes to cleave the viral polyprotein, and the helicase functioning at the site of RNA replication in vesicle packets. In addition to the helicase and protease activities, NS3 has also been implicated in virion assembly (5, 229, 261, 265, 266). In-frame deletions of the helicase domain result in an inability of virions to be assembled (5, 261).

1.6.6 NS5

NS5, the largest of the viral proteins, is a multifunctional 100kDa protein that is essential for viral replication (267, 268). It contains a characteristic RNA-dependent RNA polymerase (RdRp) in the C-terminal two thirds of the protein (269-273) and its role in viral RNA replication has been confirmed by numerous studies, including co-localisation of NS5 with both dsRNA and other non-structural proteins implicated in the formation of the flaviviral replication complex (274, 275, 252). This domain contains a conserved GDD active site at positions 665-667 in WNV, which is critical for the function of the polymerase (276, 267, 270, 277). The N-terminal region of NS5 contains an S-adenosyl methionine methyltransferase (MTase) with both N7 and 2'-O MTase activity. This domain can also function as a guanylyltransferase (278-281). Crystallisation of NS5 showed classic palm, thumb, and finger domains within the RdRp, in addition to highlighting an intra-molecular interaction between the MTase and RdRp domains (282, 272). NS5 also contains a nuclear localisation sequence; however this has little effect on virus replication (274, 283, 284).

1.7 Virus Replication Cycle

1.7.1 Attachment and entry

WNV can infect many different cell types in culture; however, in the course of an actual infection the tropism of WNV is more limited. WNV predominantly targets monocytes, macrophages, dendritic cells, endothelial cells and neurons (20, 285). The specific receptor on the cell surface that is used for initial viral binding is still unclear, and it appears that in fact, multiple receptors can bind to WNV. One example is a transmembrane cell receptor, $\alpha_V\beta_3$ integrin, which has been implicated in the binding and entry of both WNV and JEV. Knockdown of this particular receptor results in a decrease in the efficiency of WNV infection (286). In addition to this receptor, glycosaminoglycans have also been implicated in flaviviral receptor binding (218).

Following initial binding to the cell (Figure 1.4, step 1), viral particles enter the cell by receptor mediated endocytosis of clathrin coated pits and accumulate in early endosomes (287-293). Following endocytosis, viruses are trafficked to the late endosomes by microtubules (Figure 1.4, step 2) (288, 294, 295). Once in the late endosome, the environment becomes acidified, triggering a conformational change in the virion surface. The envelope protein, which forms the surface of the virion, is altered from a dimer form to a trimer form. This trimeric E protein mediates fusion of the viral and endosomal membranes, subsequently releasing the enclosed nucleocapsid (Figure 1.4, step

3) (296, 297). Once in the cytoplasm, the virus core uncoats, releasing the viral RNA (Figure 1.4, step 4) (289, 298).

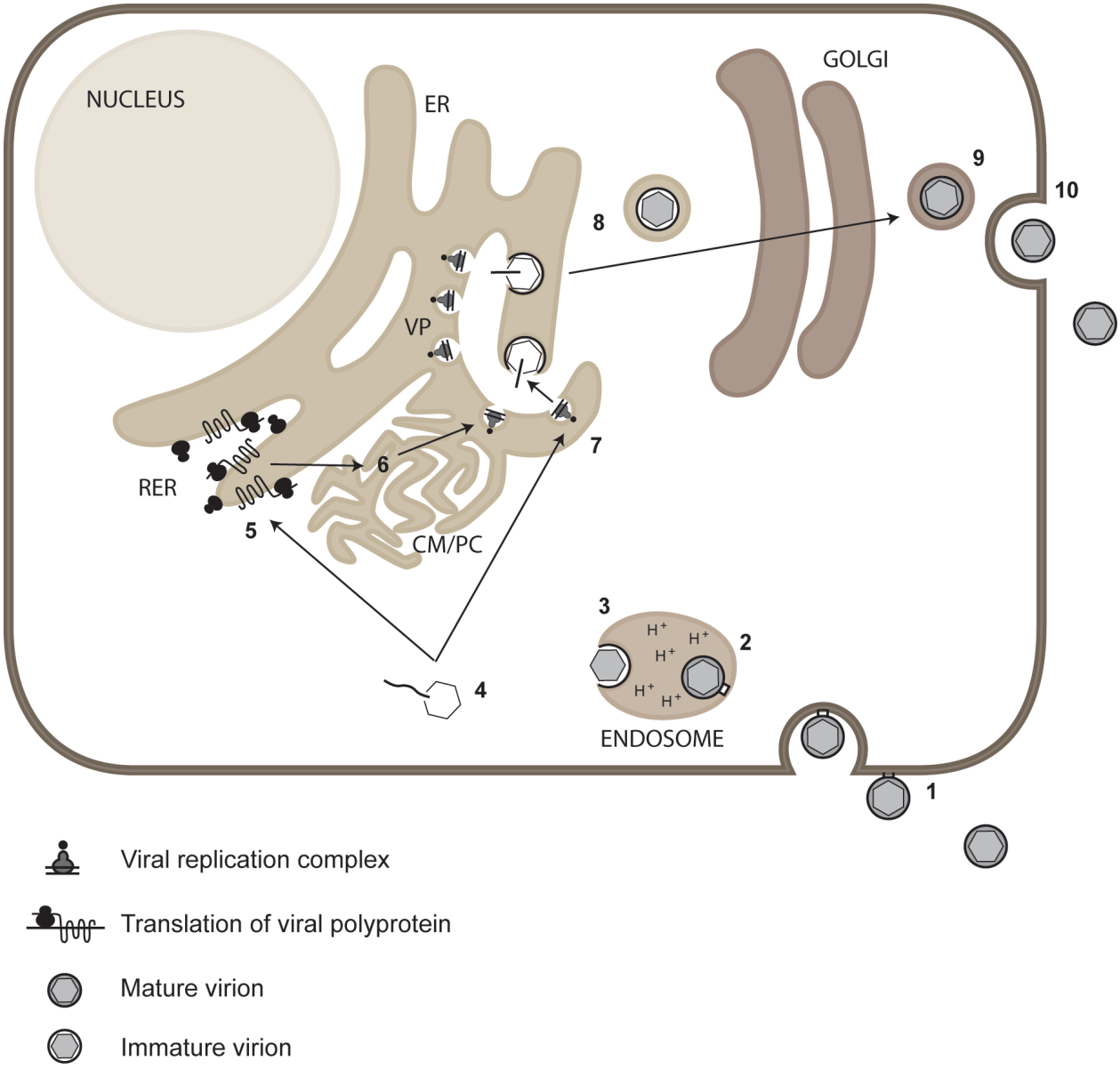

Figure 1.4 Flavivirus replication cycle. (1) Receptor attachment and endocytosis of clathrin-coated pits. **(2)** Trafficking to late endosome and subsequent acidification. **(3)** Fusion of virion and endosome membrane due to low-pH triggered conformational change in E. **(4)** Uncoating of viral RNA. **(5)** Translation of genome in rough endoplasmic reticulum (RER). **(6)** Non-structural proteins induce remodelling of cell membranes, including formation of vesicle packets (VP) and convoluted membranes/paracrystalline arrays (CM/PC). **(7)** Viral RNA replication occurs in VP. **(8)** Encapsidation of RNA and formation of immature virions. **(9)** Cleavage of pr from M and maturation of virion in trans-Golgi. **(10)** Release of mature progeny virus from cell.

1.7.2 Replication

All viral non-structural proteins have been identified in association with dsRNA and VPs by immunfluorescence and electron microscopy studies, and have thus been implicated in viral RNA replication. In addition to a role for the non-structural proteins in the RC, a number of host proteins also appear to be involved in flaviviral RNA replication (299, 300). One example is the eukaryotic elongation factor 1 alpha (eEF-1α), an abundant host protein involved in transporting tRNAs to translating ribosomes (301), which has been shown to interact with WNV RNA (302-304).

Initial translation of the incoming positive strand RNA viral genome provides the non-structural viral proteins required for RNA replication. The RC, comprised of both host and viral proteins, assembles on 3' end of the positive strand genomic RNA (305). Cyclization of the genome by 3'-5' long distance RNA-RNA interactions is required for minus strand RNA synthesis (306, 307, 2, 308). The low level of genomes available early in replication results in positive sense RNA molecules switching between a linear template for translation and a cyclic form for RNA synthesis. The RC transcribes minus strand RNA from the positive strand RNA, producing a double stranded RNA replicative form (RF). This initial replication can occur as early as 3 h post infection (309). Once negative sense RNA is generated, this RF acts as the template for the replication of positive sense RNA (310, 311). By 24 h, the exponential phase of genome synthesis begins (310), where multiple RNAs are simultaneously copied from a single minus strand template. As new positive strand RNA is being formed, it displaces the old strand. Throughout the virus life cycle, the level of minus strand RNA remains low in comparison to positive strand RNA, which functions as mRNA for translation and is also packaged to produce new viral particles.

1.7.3 Membrane reorganisation

WNV induces significant morphological changes in the host cell architecture. The initial production of non-structural proteins from incoming viral genomes is crucial for triggering the remodelling of the cellular architecture (312, 149). Viral non-structural proteins have been shown to induce proliferation of the ER membrane. This can be linked to an upregulation of cholesterol, that is redistributed to regions of the ER containing the replication complexes (122). This membrane proliferation produces two distinct structures (313-315, 226); vesicle packets (VP), which are produced early in infection (316, 221, 149), and convoluted membranes (CM), which are formed later (313, 149). Convoluted membranes may be randomly folded or arranged in highly ordered paracrystalline arrays (PC). VP represent the site of RNA replication, apart from very early in

infection (prior to membrane proliferation) (317, 318). The CM/PC on the other hand is formed as the site of polyprotein processing (313, 149).

1.7.4 Assembly and maturation

Once replicated, new positive strand genomes exit the VPs through a pore (318), after which they can be either replicated, translated, or assembled into virions. It is thought that the hydrophobic face of the capsid protein binds to the cytoplasmic side of the ER membrane, while the charged face binds to the RNA exiting a VP pore (147, 319). Both the envelope and membrane proteins also associate within the ER membrane. Assembly of virions then occurs when genomic RNA interacts with capsid in the same region where E and prM are associated. This leads to the budding of immature virions into the ER. These virions are subsequently transported through the secretory pathway, where glycans on prM and E are modified (320). The presence of the pr peptide in initial virion formation is required to protect the E protein from triggering membrane fusion within the low pH environment of the secretory pathway (188, 321, 190, 194). Within the trans-Golgi, prM is cleaved by furin to mature M. Prior to release from the cell, E is modified from the trimeric form to dimers, forming the mature viral particle (185, 190, 322-324). Subviral particles containing only the prM and E proteins, with no nucleocapsid, are also released during infection (321).

1.8 NS1 review

While the focus of this thesis is on the non-structural protein NS1', an understanding of the NS1 protein is crucial to further the studies on NS1'. NS1' is a C-terminally extended form of NS1, and so contains the entire NS1 sequence. It is possible that NS1' may therefore be able to function like NS1.

1.8.1 Introduction

NS1 was first identified in the brains of DENV infected mice in 1970, though was initially designated as a virion-derived soluble complement fixing (SCF) antigen (325). This SCF antigen was later identified as NS1, the first non-structural protein encoded in the flaviviral genome (162, 326). Flaviviral NS1 is fairly highly conserved, with a sequence consisting of 1056 nucleotides (327-329). NS1 is a 352 amino acid glycoprotein with a molecular weight of 46-55 kDa, depending on the glycosylation state (327, 326, 330). Initially produced in the ER, NS1 exists in several oligomeric forms as either cell associated or secreted protein (331-333). NS1 has been implicated in a wide range of functions during flaviviral infection, including performing a critical function in RNA replication, as well as both activation and inhibition of the host immune system (4).

1.8.2 Expression and processing

See Figure 1.5 for a depiction of NS1 processing and trafficking pathway.

During translation of the flaviviral polyprotein, NS1 is directed to the ER due to the presence of a signal sequence encoded by the last 24 amino acids of the preceding E protein (334). NS1 is cleaved from E at the N-terminus by the ER host signal peptidase (161) and at the C-terminus from NS2A by an unidentified host cell protease (335) (Figure 1.5, step 1). Monomeric NS1 contains 12 conserved cysteine residues that form 6 intramolecular disulfide bonds. The disulfide bond arrangement has been solved for MVEV, WNV and DENV (3, 336, 337), with the cysteine residues being linked as shown in Figure 1.6. The importance of these disulfide bonds has been determined previously, with mutagenesis studies indicating that at least the last 3 cysteine residues were critical for proper NS1 folding, and subsequently maturation, secretion, and oligomerisation (338).

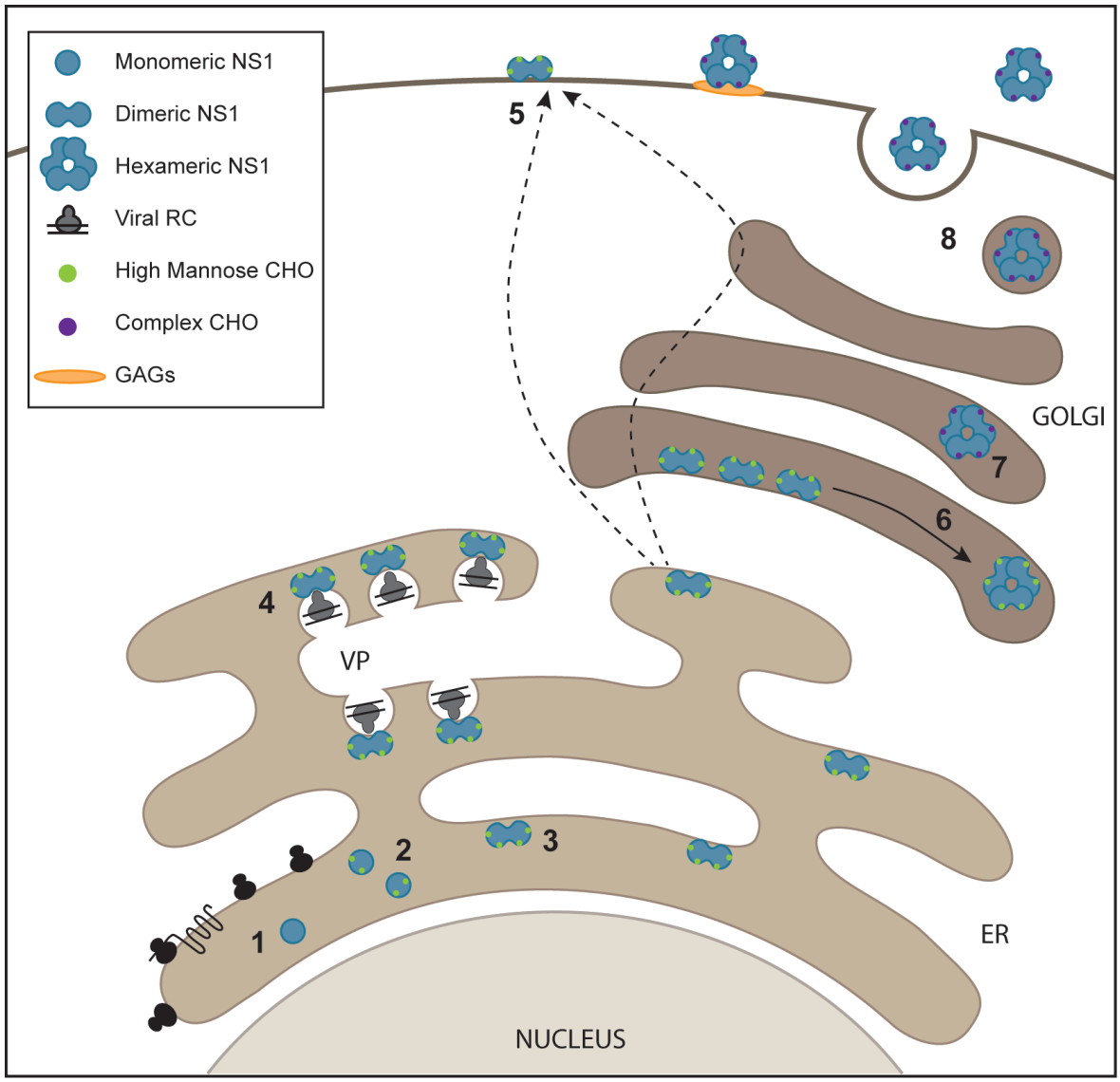

Figure 1.5 NS1 processing and trafficking in mammalian cells. During translation, NS1 is directed to the ER due to the presence of a signal sequence in the C-terminus of the preceding E protein. NS1 is cleaved from the adjacent E and NS2A genes forming a monomer (**step 1**) which is modified by the addition of high-mannose carbohydrates at 2 or 3 sites (depending on the flavivirus; **step 2**). Following glycosylation, NS1 rapidly dimerises and becomes membrane associated (**step 3**) due to an acquired hydrophobic nature. NS1 is then trafficked to 3 distinct locations in infected cells. NS1 is trafficked to the site of RNA replication in vesicle packets (VP), where it associates with other components of the viral replication complex (RC; **step 4**). Membrane associated NS1 is also trafficked to the cell surface by an as yet unidentified pathway (**step 5**). A subset of NS1 traffics through the Golgi, where the dimers associate to form a soluble hexamer (**step 6**). Here the high mannose carbohydrates are processed to more complex sugars (**step 7**), and the soluble hexamer is subsequently secreted to the extracellular fluid (**step 8**), where it can bind back to infected and uninfected cells via an association with glycosaminoglycans (GAGs). Figure modified from Muller and Young, 2013 (4).

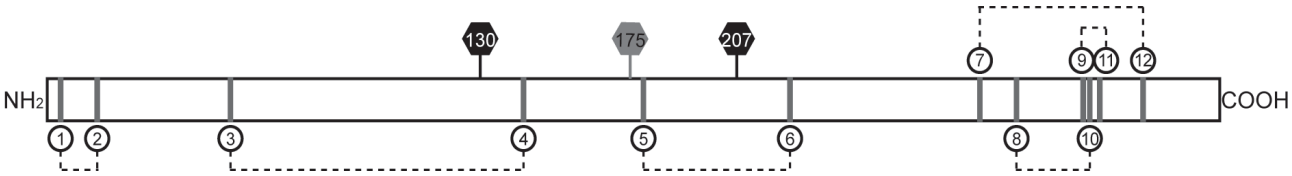

Figure 1.6 Schematic of NS1 protein. Disulfide linkages are shown between conserved cysteine residues (circles), and glycosylation sites are indicated by black (conserved Asn 130 and 207) and grey (additional glycosylation at Asn 175 for WNV, MVEV and SLEV) hexagons.

Following translation and cleavage, NS1 is glycosylated at multiple sites by the addition of high-mannose carbohydrates (Figure 1.5, step 2). The number of glycosylation sites varies depending on the flaviviral species. DENV, YFV and JEV contain 2 conserved sites (at Asn 130 and Asn 207) (339-341, 326, 342), while WNV, MVEV and SLEV each contain 3 sites (an additional site at Asn 175) (343, 336, 344, 345, 329, 346). Once glycosylated, NS1 forms a detergent resistant dimer that is sensitive to heat and low pH treatment (347, 348, 333). The formation of an NS1 dimer was first identified through SDS-PAGE analysis of infected mammalian or insect cell lysate and is a consistent feature of all flaviviruses (332, 333). The loss of NS1 dimers by a single amino acid substitution at residue 250 of WNV_{KUN} or MVEV NS1 resulted in attenuation of virus growth and a reduced virulence in mice. This work suggests that the NS1 dimer is important for viral pathogenesis (349, 350). However, as this mutation did not completely ablate virus replication, it is likely that dimeric NS1 is not critical for virus replication or that some dimerisation still occurred. NS1 dimers acquire a partially hydrophobic nature (348), which has been suggested to be the major factor in the subsequent association of NS1 with the ER membrane (4) (Figure 1.5, step 3).

NS1 is trafficked to three distinct locations in infected cells following dimerisation in the ER: the site of RNA replication; the cell surface (351, 348); and secreted to the extracellular fluid (331, 352). The majority of NS1 remains within the ER, where it is trafficked to the site of RNA replication in vesicle packets (Figure 1.5, step 4). Here, NS1 co-localises with dsRNA and other members of the replication complex (268, 353, 309, 316, 226). The critical role NS1 plays in viral RNA replication is outlined in section 1.8.3. In addition to remaining within the ER, membrane associated NS1 is also trafficked to the cell surface, by an as yet unknown pathway (Figure 1.5, step 5) (351, 348). Cross-linking of NS1 expressed on the surface of YFV infected cells indicates that cell surface NS1 is present in its dimeric form (351). For DENV NS1 only, a glycosyl-phosphatidylinositol (GPI)-linked form has been identified that is produced in the ER and subsequently trafficked to the cell surface (354-356). This GPI-anchored form is capable of signal

transduction; however, it only constitutes a small proportion of NS1 present on the cell surface (354).

Once dimerised, a subset of NS1 is trafficked to the Golgi, where three dimeric units associate to form a soluble hexamer (Figure 1.5, step 6). During passage through the Golgi, the high mannose carbohydrates are processed to more complex sugars (Figure 1.5, step 7). This hexamer is subsequently secreted from infected mammalian cells (Figure 1.5, step 8), though not from insect cells (357, 331, 352, 332). This further processing and glycosylation of NS1 has been shown to be important for not only NS1 secretion, but also viral replication and virulence (358, 359, 341, 360, 361). The absence of secretion from insect cells is likely to be due to insect cells lacking the machinery for proper processing of NS1 into a complex carbohydrate form (352, 332, 4). The formation of this hexameric NS1 form has thus far been confirmed to be produced from TBEV (357, 331), DENV (352), and WNV (362) infected cells. The NS1 hexamer is held together by weak hydrophobic interactions that are disrupted by detergent treatment (352). To detect this form, chemical cross-linking of extracellular fluid or SDS-PAGE with very low levels of SDS were performed. However, this was still only able to detect small amounts of the hexameric species, and neither technique showed complete retention of this native form (357, 331, 352).

Secreted DENV NS1 has been shown to bind to glycosaminoglycans (GAGs) on the surface of infected and uninfected cells (363). NS1 is also internalised from the surface of cells by endocytosis, where it accumulates in the late endosomes for up to 48 h (364). DENV and JEV NS1 have been shown to associate with lipid rafts in both infected and transfected cells (365, 355). Lipid rafts contain cholesterol, which has recently been implicated in flaviviral entry, RNA uncoating, and RNA replication (366, 365). A reciprocal relationship seems to exist between cell surface expression and NS1 secretion. The expression of NS1 on the surface of WNV infected cells has been shown to be greater than that of DENV NS1; however, the level of secreted NS1 is greater for DENV infected cells. This relationship was specifically linked to two N-terminal amino acids (10 and 11) that were different between WNV and DENV, and mutagenesis of these residues could confer the converse expression pattern (367).

Previous work using either cryoelectron microscopy or single particle analysis and 3D remodelling determined that NS1 forms a barrel-like structure comprising of three dimeric units (368, 369). Gutsche *et al* (368) also identified the presence of a central channel rich in lipids, consistent with the previous work showing an association of NS1 with lipid rafts (365, 355). Recently, the full crystal structure of WNV and DENV NS1 was solved (3). This work confirms the

barrel-like structure of the hexamer, with a hydrophobic interior consistent with the association with lipids. Briefly, the NS1 dimer was shown to consist of a central β-sheet "ladder" structure, containing 18 β-sheets (Figure 1.7). Each monomer was shown to have three distinct domains: a short β-roll dimerisation domain (amino acids 1-29; blue); a "wing" domain (amino acids 30-180; yellow and orange) that contained two glycosylation sites (for WNV NS1) and a mix of α-helices and β-sheets; and the third and most notable domain is a continuous β-sheet (amino acids 181-352; red), with each monomer contributing 9 strands to the central "ladder" structure. The β-roll and a connecter region within the "wing" domain form a distinctly hydrophobic surface (Figure 1.7C). In addition to the presence of amino acids involved in the interaction of NS1 with NS4B (370) within this region, this hydrophobicity suggested that this region is a likely candidate for an interaction with the ER membrane.

It is worth noting that while the characteristics described above and outlined in Figure 1.5 are generally accepted as being common to flaviviral NS1, some of the results have been obtained only for one (predominantly DENV) flaviviral species. Specifically, the identification of a GPI-anchored form of NS1, the ability of hexameric NS1 to bind back to cells via an interaction with GAGs, and the internalisation of cell surface NS1 by endocytosis have only been confirmed for DENV (364, 363, 354-356). Only YFV NS1 has been confirmed to be in a dimeric form on the surface of infected cells (351). It has also been shown that not all characteristics are the same between flaviviruses, for example, the correlation between surface expression and secretion seen for WNV and DENV NS1 (367). In addition to this, a clear variation in the glycosylation pattern of NS1 from different flaviviral species is evident (343, 336, 344, 345, 339, 329, 340, 341, 326, 346, 342). Inconsistencies in NS1 binding partners has also been identified, with a complement protein (factor H) interacting with WNV NS1, but not JEV NS1 (362, 371).

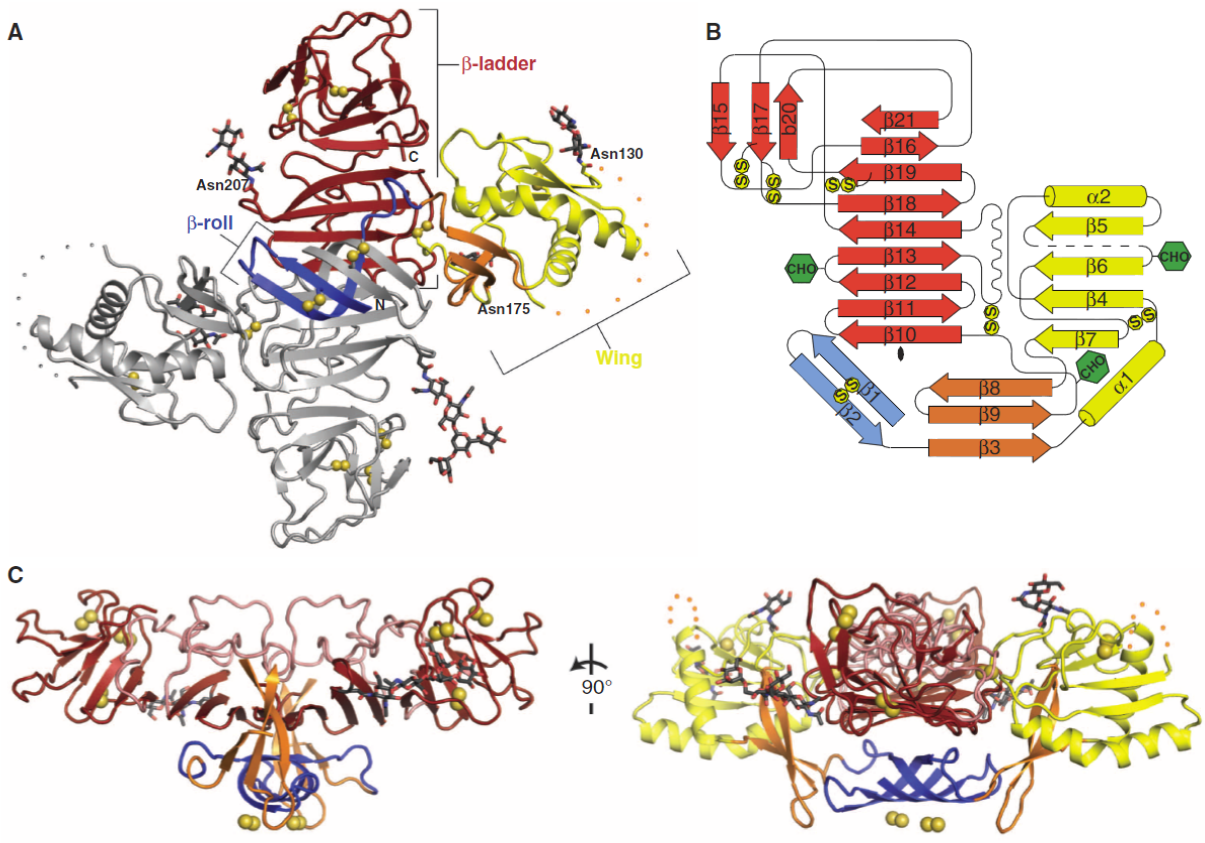

Figure 1.7 Crystal structure of NS1 dimer. Figure reproduced from Akey *et al*, 2014 (3). "(A) NS1 dimer with one subunit in gray and the other colored by domain (blue, b roll; yellow, wing with orange connector subdomain; red, central b ladder). Disulfides are shown as yellow spheres and N-linked glycosylation sites as black sticks. A 20-residue disordered region is indicated with dotted lines. C, C terminus; N, N terminus. **(B)** Topology diagram for NS1 monomer [colored in blue, yellow, orange, and red as in **(A)**]. Glycosylation sites are indicated with green hexagons and disulfides with yellow circles. **(C)** Perpendicular views of NS1 from the edge (left) and the end (right) of the b ladder. The b roll (blue) and b-connector subdomain (orange) of the wing form a protrusion on one face of the b ladder with the spaghetti loop (pink) and glycosylation sites on the other face. The wing domain is omitted from the left image for clarity."

1.8.3 Involvement of NS1 in Flaviviral replication

The first indication that NS1 is involved in viral RNA replication was the observation that DENV NS1 co-localised with dsRNA in vesicle packets with infected cells (316). This was further confirmed with WNV NS1, suggesting a role for NS1 in the RC (316, 226). Since then, mutagenesis studies (359, 372, 373) and *trans*-complementation experiments (268, 5, 309, 374, 375) have shown that NS1 performs a crucial function early in replication. As NS1 is physically separate from the remaining components of the RC, it has been suggested that it is likely to be involved in RNA replication by providing an anchor mechanism to hold the RC to the ER (4). This

is thought to happen through an interaction with one or several of the transmembrane proteins involved in the RC (Figure 1.8). An interaction of NS1 with both NS4A and NS4B has been shown by corresponding compensatory mutations (353, 370), while a physical interaction was shown only with NS4B (370).

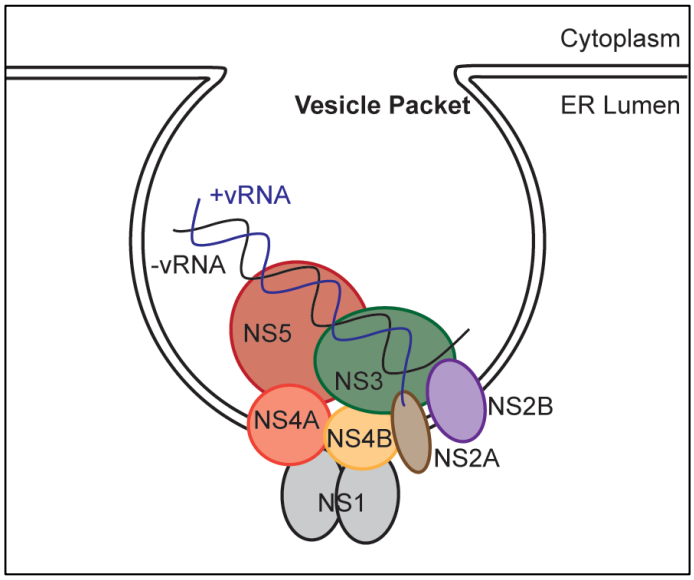

Figure 1.8 Schematic of the proposed replication complex. This schematic is based on the available information on the flaviviral replication complex (RC). The flaviviral RC resides within vesicle packets formed in the ER membrane. The majority of the components of the RC (including NS2A, NS2B, NS3, NS4A, NS4B and NS5) are present on the cytoplasmic face of the ER membrane, with NS1 present in the ER lumen. NS1 is hypothesised to form an anchor due to an interaction with NS4A, NS4B, or both. Positive sense viral RNA (vRNA) is transcribed from the negative sense vRNA by the polymerase domain of NS5. Figure modified from Muller and Young, 2013 (4).

The *trans*-complementation experiments indicated that NS1 can be supplied in *trans* to recover replication-deficient flavivirus RNA lacking functional NS1 (268, 5, 309, 374, 375). Further work on the recovery of a defective YFV genome showed that complementation was not successful with addition of DENV NS1, suggesting that *trans*-complementation is virus-specific (309). It was this work that identified the genetic link between NS4A and NS1, with a compensatory mutation in NS4A resulting in DENV NS1 being able to complement for the YFV NS1-deleted genome (353). Column bound NS4A was able to precipitate all members of the RC (including NS1), further supporting the theory that NS1 may interact with NS4A (221). The genetic interaction between NS1 and NS4B was suggested due to a compensatory mutation present in NS4B following passaging of a WNV NS1 containing two amino acids from DENV NS1.

Subsequently, co-immunoprecipitation and mass spectrometry identified a physical interaction between NS1 and NS4B (370).

Most recently, a group working with WNV_{NY99} confirmed the necessity of NS1 in the replication complex for this WNV strain (374). The authors showed that in the case of WNV_{NY99}, *trans*-complementation with NS1 from different flaviviral species was possible without the need for compensatory mutations, albeit to different degrees of success. JEV NS1 complemented to similar degree as WNV NS1, while DENV, YFV, and SLEV NS1 complemented less efficiently with complemented viruses showing reduced plaque size and lower titres (374).

1.8.4 Interaction of NS1 with the host immune response

An interaction between NS1 and the host immune system has been known since NS1 was first identified as a soluble complement fixing antigen (325). NS1 has the conflicting ability to both activate and inhibit the host immune system.

NS1 is potentially the major viral antigen responsible for the activation of the complement pathway (376, 377). Secreted NS1 is able to directly activate the complement pathway, resulting in an increase in the level of membrane attack complexes (376). In addition to this, the presence of NS1 on the surface of infected cells has also been shown to be involved in the activation of the complement response. Binding of NS1-specific antibodies to NS1 on the cell surface leads to the generation of C5b-9 membrane attack complexes. These in turn trigger cellular activation and production of inflammatory cytokines (376). NS1 binds directly to the complement inhibitory factor clusterin, which inhibits the formation of membrane attack complexes. NS1 binding therefore reduces the levels of clusterin, leading to an increase in C5b-9 formation (378).

In addition to being involved in the activation of the complement system, NS1 has also been implicated in the evasion of complement system, both the classical/lectin pathway and the alternative pathway. DENV secreted NS1 was identified through co-precipitation analysis to bind to the complement protein C4. This interaction was found to promote cleavage of C4 to C4a and C4b via the recruitment of the complement specific protease C1s. This mechanism limits the amount of C4 available and therefore can protect the virus from neutralisation (379). Secreted NS1 from DENV, WNV and YFV infected cells has been shown to interact with C4 binding protein (C4BP), which is also likely to increase the cleavage of C4, and therefore inhibit neutralisation. The presence of the C4BP-NS1 complex on the surface of infected cells may also prevent cells from

complement mediated lysis (380). WNV NS1 has also been observed to bind to factor H (fH), a regulator of the alternative complement pathway. This interaction leads to a reduction in the formation of membrane attack complexes on cells, and therefore protects infected cells from complement mediated cell lysis (362). However, this particular interaction is not conserved for all flaviviral NS1, as it has been reported that JEV NS1 is not able to bind fH (371).

In addition to a role in the complement pathway, NS1 has also been implicated in the inhibition of TLR3 signalling (113, 114). TLR3 signalling has been shown to protect against WNV infection (76, 78, 79, 81, 83), suggesting that an inhibition of TLR3 may contribute to WNV pathogenicity. The potential for an interaction between NS1 and TLR3 is still somewhat controversial, due to a similar study that failed to identify any inhibition of TLR3 signalling by DENV, YFV or WNV NS1 (112).

1.9 NS1' review

1.9.1 Introduction

NS1' is an additional non-structural protein that was first identified in JEV infected cells. Anti-NS1 antibodies reacted to two individual protein bands, the expected 42 kDa NS1 protein and an additional 58 kDa protein, which the authors designated NS1' (381). Since this first discovery, NS1' has been confirmed to be produced by members of the JEV serogroup, including JEV, MVEV, and WNV (both WNV_{KUN} and WNV_{NY99}) (382, 383). NS1' is absent from cells infected with viruses outside this serogroup, including DENV, YFV, and Kokobera (382, 330). This suggested that NS1' expression may be unique to the members of the JEV serogroup. NS1' was also shown to react with antibodies to the start of the NS2A coding region, suggesting that this additional non-structural protein was formed by an alternate cleavage site present within the NS2A gene (381).

1.9.2 Frameshifting and production

In 2009, computer modelling predicted the presence of an RNA pseudoknot at the beginning of the NS2A gene that was conserved between members of the JEV serogroup. Due to the presence of this pseudoknot, the authors hypothesised that the 5'-end of the NS2A RNA may contain a -1 programmed ribosomal frameshift (PRF) (384). A -1 frameshift at this site would produce a protein consistent with the observed molecular weight of NS1', containing the entire NS1 sequence plus 9 amino acids of NS2A prior to the frameshift and 43 residues after the frameshift, terminating in a stop codon (384). A -1 PRF requires two signals, a heptanucleotide “slippery” site and an RNA pesudoknot, separated by 6-8 bases (385). Both of these signals were present and conserved between the members of the JEV serogroup, further supporting this hypothesis (Figure 1.9) (384). Following this prediction, our laboratory experimentally demonstrated the requirement of both these signals for production of NS1' (1) Two different viral mutants were produced that affected either the slippery heptanucleotide (FSSM; frameshift silent motif) or the formation of the RNA pseudoknot (A30A'; silent alanine substitution at residue 30 of NS2A). Neither mutant virus expressed NS1', confirming that both the slippery heptanucleotide and RNA pseudoknot are required for NS1' production. This verified that NS1' is indeed the product of a ribosomal frameshift. The requirement for the pseudoknot has since been confirmed for JEV NS1' (386).

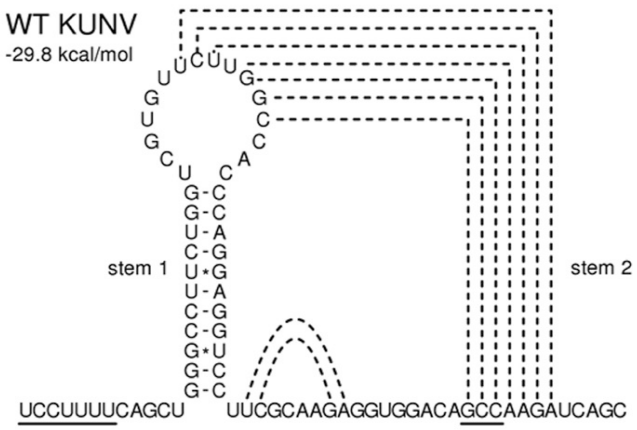

Figure 1.9 Predicted RNA pseudoknot structure in NS2A. Frameshift heptanucleotide (UCCUUUU) and codon 30 of NS2A (involved in A30A' mutation) are underlined and predicted RNA interactions contributing to formation of the pseudoknot are indicated by dashed lines. Figure reproduced from Melian *et al*, 2010 (1).

NS1' is produced in 30-50% of translation events, and is therefore present in infected cells at levels either slightly lower than or equal to the level of NS1 (332, 381, 1). NS1' has the same glycosylation pattern as NS1 (332), which is expected as NS1' contains the entire NS1 sequence and the frameshifted region contains no additional predicted glycosylation sites. Like NS1, JEV NS1' forms a heat-labile dimer in infected cells. However, NS1' does not appear to be secreted to the same degree as NS1, with only low levels of protein detected in the culture fluid of infected cells following pulse-chase (332). The presence of an NS1/NS1' heterodimer has also been suggested for both JEV and MVEV (382, 387, 388).

1.9.3 Role in neurovirulence

Although a specific function for NS1' in viral infection had not been identified, a role in viral neurovirulence has been suggested. Analysis of the NS1'-lacking mutants generated for examination of the -1 PRF (A30A' and FSSM) determined that while a lack of PRF/NS1' does not affect viral replication *in vitro*, it does correlate to attenuation in a mouse model. Weanling mice infected with wild-type WNV_{KUN} typically show an 80% mortality rate, while A30A' and FSSM showed only 30 and 40% mortality, respectively (1). Further work with the A30A' mutant determined that a lack of PRF/NS1' has no effect on RNA synthesis, cell-to-cell spread or virus-induced cytopathic effect (CPE) (389). It is as of yet unclear why the A30A' mutant is attenuated in mice.

In agreement with the work conducted in WNV_{KUN}, a study on the JEV vaccine strain (SA14-14-2) determined that a single point mutation abolished PRF and NS1' production. By introducing this single mutation into a JEV infectious clone, the authors determined that the lack of PRF and NS1' expression correlated with a reduction in neurovirulence (100% mortality of the parental strain *verses* 0% with the mutant), despite no effect on viral replication *in vitro* (390). This work, in combination with the work conducted in WNV_{KUN}, suggested a relationship between PRF/NS1' production and an enhanced virulence phenotype.

1.9.4 Additional predicted functions and characteristics of NS1'

NS1' has previously been implicated in the assembly of viral particles (391). During the development of RepliVAX D2 (a single-cycle chimeric DENV vaccine expressing DENV prM/E genes in a WNV backbone) mutations to enhance virion packaging were introduced through blind passaging of the vaccine in cell culture. One of these mutations, a single amino acid substitution in NS2A, eliminated the ribosomal frameshift, thereby abolishing NS1' production (392, 391). This mutation lead to an increase in viral packaging, though had no effect on genome replication, highlighting a possible link between NS1' and the structural proteins. This was not the case when this mutation was introduced to a non-chimeric WNV vaccine (RepliVAX WN (463, 464)), suggesting that production of NS1' inhibits assembly of virus particles only in association with DENV structural proteins. Therefore, it is unlikely that NS1' is involved in virion assembly during natural WNV infection, as the presence of NS1' has no effect on virion production or viral replication when expressed in association with WNV prM/E genes (1, 391).

Work carried out in a JEV expression system determined that NS1' is a substrate for caspase cleavage (386). In the process of generating expression plasmids for the examination of NS1' in isolation, the authors identified a small amount of truncated NS1'. This was further confirmed in JEV infected cells. Analysis of the C-terminal frameshifted region of JEV NS1' uncovered a potential caspase cleavage site (QEVDG), and the use of inhibitors confirmed that this truncated product was indeed due to caspase cleavage (386). The authors suggest that as caspases are activated to initiate apoptosis in flavivirus infected cells (393-395), NS1' may be able to modulate apoptosis (386). However, due to the low levels of cleaved NS1', it is unlikely to be involved in altering the apoptotic response.

Interestingly, several more recent studies have suggested that the importance of NS1' lies not within the mammalian system, but instead in mosquito and avian systems. Recently, work

carried out in our laboratory studied the effect of an NS1'-lacking WNV_{NY99} virus in wild-caught house sparrows. Titration of virus particles in serum from infected house sparrows showed attenuation of WNV_{NY99} A30A' compared to wild-type WNV_{NY99} at the peak time of viral replication (3.7 log_{10} pfu *verses* 4.4 log_{10} pfu, respectively). These results suggest that NS1' is important for virulence in birds (389).

A study using JEV infectious clones in avian cell culture and embryonated chicken eggs identified a role for NS1' in facilitating JEV infection in avian cells (396). NS1'-expressing viruses formed larger foci in chicken embryonic fibroblast (DF-1) cells and showed a log increase in virus production at both 48 and 72 hpi compared to viruses that lacked NS1'. The authors showed that this is likely due to enhanced viral RNA production, as the use of qRT-PCR determined that viruses expressing NS1' had significantly increased levels of RNA over those that lacked NS1'. This was not the case for infection of mammalian cells, as infection of BHK cells showed no difference in either viral titres or the level of viral RNA. A lack of NS1'-expression also correlated with a reduced mortality of embryonated chicken eggs. These results suggested that NS1' may be specifically functioning in an avian system (396). However, work conducted by our group in DF-1 cells failed to identify any differences in viral replication between NS1'-expressing and NS1'-lacking viruses (389). This suggests that the effect of NS1' on replication in these avian systems may be specific to JEV.

In addition to the work conducted in house sparrows, Melian *et al.* aimed to determine whether PRF/ NS1' was important for viral replication and transmission in mosquitoes (389). This worked examined the effect of mutations abolishing PRF and NS1' expression in the context of whole *Culex* mosquitoes, as opposed to previous work which has utilised insect cell culture (1). *Cx. annulirostris* mosquitoes were exposed to blood meal containing either wild-type WNV_{KUN} or A30A' (lacking PRF and NS1') virus. The level of virus present in both the body (a measure of the ability of the virus to initially infect) and legs (indicating the ability of the virus to disseminate) was lower for A30A' infected than wild-type infected mosquitoes. In addition to this, the amount of virus present in the saliva (indicative of the ability of the mosquito to transmit virus) was significantly lower in the absence of PRF and NS1'. This work suggested that PRF and/or NS1' are important for infection of and transmission by *Cx. annulirostris* mosquitoes (389).

1.10 Scope of thesis

The aim of this thesis is to further the understanding of the flaviviral NS1' protein. While NS1' was first identified more than 25 years ago, focused studies on this elusive protein have thus far been limited, resulting in very little being known about NS1'. While initially thought to be the product of an alternate cleavage occurring within the NS2A gene, a recent bioinformatic study (supported by subsequent experimental evidence) determined that NS1' is produced by a -1 PRF (384, 1, 386). This has allowed for the development of NS1'-only expressing plasmids for the examination of NS1' in isolation (375). By examining the NS1' protein in isolation from NS1, we hope to develop a better understanding of the characteristics of NS1'. The work conducted for this thesis asked two distinct questions; does NS1' share any similar functions and/or characteristics with NS1, and does NS1' possess any unique functions and/or characteristics that differ from NS1?

As NS1' consists of the entire NS1 protein, it is possible that NS1' may behave similar to NS1 in infection. Cellular localisation was examined to determine whether NS1' had similar distribution to NS1, and complementation analysis was used to establish whether NS1' can function in viral replication. The secretable heat-labile NS1 dimer has been extensively studied and is known to be important for viral infection. Therefore, the dimer formation and secretion of NS1' was examined. Co-immunoprecipitation and mass spectrometry was carried out to identify and compare protein-protein interactions of NS1 and NS1'.

PRF/NS1' has been implicated in viral pathogenesis in mice, though the precise mechanism of action is still unclear (1, 390). Indeed, the attenuation seen for PRF/NS1'-lacking mutants may be due to a loss of the NS1' protein itself, or a loss of the -1 PRF. This PRF has been implicated in controlling the ratio of structural to non-structural proteins (389), and may therefore have a role in pathogenesis separate to that of the NS1' protein. To fully understand the function of the NS1' protein, it is necessary to separate these factors. To do this, new viral mutants that affect only NS1' production and not the PRF were designed and characterised. These new mutants were used to study the effect of NS1' on viral pathogenesis.

In summary, the work conducted for this thesis had three main aims: 1) to identify similarities between the NS1' and NS1 proteins; 2) to investigate the formation of NS1' homodimers and NS1/NS1' heterodimers; and 3) to design and characterise viral mutants that affect NS1' production but not ribosomal frameshifting.

2 Materials and Methods

2.1 Cell Culture

Baby hamster kidney (BHK) and Vero76 (African green monkey) cells were maintained in Dulbecco's Modified Eagle Medium (DMEM; Gibco, USA) supplemented with 5% heat-inactivated Fetal Calf Serum (FCS; Moregate, Australia), 100 U/mL penicillin, 100 µg/mL streptomycin and 2 mM glutamax. Mouse embryonic fibroblasts (MEF) and human embryonic kidney (HEK) 293T cells were also grown in DMEM supplemented 10% FCS, 1 mM sodium pyruvate, and with glutamax, penicillin and streptomycin as above. *Aedes albopictus* cells (C6/36) were grown and maintained in Roswell Park Memorial Institute (RPMI) medium (Gibco, USA) containing 10% FCS, and glutamax, penicillin and streptomycin as above.

2.2 Virus Stocks

2.2.1 Electroporation

Full-length WNV_{KUN} infectious clone cDNA templates (FLSDX and mutants) were linearised with XhoI (New England BioLabs, MA, USA) as outlined below (section 2.3.3), and purified by phenol-chloroform extraction and ethanol precipitation. RNA was *in vitro* transcribed using 1 µg linearised DNA template, 40 U SP6 RNA polymerase (Roche, Switzerland), 10X SP6 transcription buffer (Roche, Switzerland), 1 mM rNTP/CAP mix (Promega, WI, USA), and 20 U RNasin (Promega, WI, USA) in a 20 µL reaction mixture at 37°C for 2 h. One U RQ1 DNase (Promega, WI, USA) was added and the reaction incubated at 37°C for a further 30 min to remove the template DNA. BHK cells were washed three times in ice-cold diethyl pyrocarbonate-phosphate buffered saline (DEPC-PBS) and suspended in DEPC-PBS to a final concentration of 5×10^6 cells/ml. Twenty µg of in vitro transcribed RNA was mixed with 2×10^6 cells in a 0.2 cm cuvette (Bio-Rad, CA, USA) and pulsed twice with a 10 sec interval by using a Bio-Rad Gene Pulser II (∞ Ω, 25 µF, 1.5 kV). Cells were incubated on ice for 5 min, resuspended in cell culture medium and seeded into culture flasks.

2.2.2 Production and titration of virus stocks

At 2 to 4 days post electroporation, P1 virus stocks were harvested and clarified by centrifugation at 1500 x g for 5 min at 4°C. To titrate P1 stocks, plaque assays were performed in six-well plates by infecting BHK cells for 2 h with virus stocks diluted from 10^{-2} to 10^{-7}. Infected

cells were overlaid with 2 mL of plaque assay medium (70% DMEM, 2.5% FCS, 13 mM sodium bicarbonate, 70 µg/mL streptomycin, 70 U/mL penicillin, 14 mM HEPES, 1.4 mM glutamax, and 0.35% low-melting-point agarose [Bio-Rad, CA, USA]) and incubated for 3 days at 37°C with 5% CO_2. Cells were fixed with 2 mL/well 4% formaldehyde in PBS and incubated for 1 h at room temperature. Contents of the well were discarded and cells stained with 0.2% crystal violet in 10% ethanol/90% PBS for 20 min. Stain was removed and plaques were counted to calculate plaque forming units per mL (pfu/mL).

Working virus stocks (P2) were generated by infection of BHK cells at low multiplicity of infection (MOI=0.1) with WNV_{KUN} or mutant viruses harvested from electroporated BHK cells (P1). Stocks were harvested at day 3 to 5 post infection and titrated as above.

WNV_{NY99} stock was provided by Judy Edmonds, and was generated by infection of Vero76 cells with virus harvested from BHK cells electroporated with RNA transcribed from infectious cDNA clone of NY99 4132 isolate as described previously (397). JEV FU strain, first isolated in 1995 (398), and MVEV 1-51, first isolated in 1951 (399), were kindly donated by Roy Hall.

2.2.3 Infection

Vero, BHK, WT MEF or C6/36 cells were seeded into 6-well plates and infected with WNV_{KUN} or mutant viruses at MOI 1 (unless otherwise stated) for 2 h. Cells were washed 3X and appropriate growth media was added. For growth kinetics, 100 µL per sample was harvested at the indicated times post infection, clarified by centrifugation and stored at -80°C. Virus titres were determined by plaque assay as described.

2.3 DNA Manipulations

2.3.1 Transformation

Chemical transformation. Plasmid DNA was combined with a 50 µL aliquot of chemically competent DH5α *E. coli* cells and incubated on ice for 30 min. The cells and DNA were subsequently heat-shocked for 45 sec at 42°C and immediately transferred to ice for a further 2 min. Pre-warmed Luria-Bertani (LB) broth (1% tryptone, 0.5% yeast extract, 1% NaCl) was added to the transformed cells which were allowed to recover at 37°C for 1 h. Transformed cells were spread on LB agar (LB broth with the addition of 1.5% agar) plates supplemented with ampicillin (100 µg/mL). Plates were incubated overnight at 37°C. Once bacterial colonies developed, individual

colonies were picked at random, added to 5 mL LB broth containing ampicillin (100 μL/mL) and grown overnight at 37°C in a shaker. Cultures to be grown for midiprepping were generated by adding 2 mL of the above culture to 100 mL LB broth containing ampicillin, and grown overnight in a shaker at 37°C.

Electrotransformation. For transformation into electrocompetent DH5α *E. coli*, 60 ng plasmid DNA was mixed with a 40 μL aliquot of competent cells. The bacteria and DNA were transferred to a 0.2 cm cuvette (Bio-Rad, CA, USA), pulsed once (200 Ω, 2.5 kV, 25μF) and transferred to ice. Electroporated cells were recovered in pre-warmed LB broth for 1 h at 37°C. Cells were subsequently spread onto LB agar/ampicillin plates and incubated overnight at 37°C. Once colonies developed, individual clones were picked and grown as described above.

2.3.2 Purification

Miniprep. Plasmid DNA was purified from 2 mL bacterial cultures using the Wizard Plus SV Plasmid Miniprep System (Promega, WI, USA) according to the manufacturer's instructions.

Midiprep. For purification of plasmids from larger bacterial cultures (~100 mL) NucleoBond® Xtra Midi kit (Macherey-Nagel, Germany) was used according to the manufacturer's instructions. For pcDNA-based plasmids, NucleoBond Finalizers were used according to the instructions. For purification of larger plasmids (FLSDX- and pKUN-based), isopropanol precipitation and ethanol washes were carried out without the use of the Finalizer. The concentration of plasmid DNA was determined using a NanoDrop ND-1000 Spectrophotometer (NanoDrop, DE, USA).

2.3.3 Enzyme digestion

All restriction enzymes were purchased from New England BioLabs (MA, USA). Digestion reactions were performed in 20-100 μL with 1 – 10 U enzyme, depending on the amount of DNA to be digested, with 10X reaction buffer and 10X bovine serum albumin (BSA) added as required. Reaction were incubated for a minimum of 2 h at 37°C, prior to DNA fragments being separated by gel electrophoresis as outlined below.

2.3.4 Gel Electrophoresis

For analysis of digested and undigested DNA, agarose gels were prepared by melting 1% agarose (Amresco, OH, USA) in 1X TAE buffer (40 mM Tris-acetate, 1 mM ethylenediaminetetraacetic acid [EDTA] pH 8.0), followed by the addition of 0.2 µg/mL ethidum bromide. Once gels were set, DNA samples were mixed with 6X loading dye (Fermentas, Lithuania) and loaded onto the gel. Electrophoresis was carried out in 1X TAE buffer at 100V for approximately 1 h to separate DNA fragments. DNA bands were visualised on a GelLogic 212 PRO UV/white light transilluminator (Carestream, NY, USA) and sizes were determined by comparison to the bands of a 1 kb DNA ladder (Fermentas, Lithuania).

2.3.5 DNA extraction from gels

The appropriate DNA fragment for purification was excised with a sterile scalpel, and DNA was purified from the gel fragment using the Wizard SV Gel and PCR Cleanup System (Promega, WI, USA) according to the manufacture's instructions.

2.3.6 Sequencing

Purified DNA samples (0.2 – 1 µg) for sequencing were prepared in 12 µL reactions with 0.85 µM sequencing primer and sterile water. Samples were submitted to the Australian Genome Research Facility (Brisbane, Australia) for analysis on an AB3730xl sequencer.

2.3.7 Polymerase Chain Reaction

For site-directed mutagenesis and cloning, high-fidelity PCR was carried out using Pfu DNA Polymerase (Promega, WI, USA). PCR was carried out in 50 µL reactions containing 20 ng template DNA, 10X Pfu DNA polymerase buffer (Promega, WI, USA), 1.25 µM each of forward and reverse primers, 1 µL of 10 mM dNTPs, 1 µL Pfu DNA polymerase and distilled water. A MyCycler Thermal Cycler (Bio-Rad, CA, USA) was used for reaction cycles, using the conditions outlined in Table 2.1 below.

Table 2.1 PCR cycle conditions

Cycle	Time	Temperature	Repeats
Initial denaturation	2 min	95°C	1X
Denaturation	30 sec	95°C	30X
Annealing	30 sec	45 - 60°C	
Elongation	2 min per kb	72°C	
Final elongation	20 min	72°C	1X
Hold	∞	15°C	

2.3.8 Ligations

Ligation reactions were carried out in a total volume of 15 µL, which included 100 ng vector DNA, 3-5X molar more insert DNA, 1.5 µL 10X ligation buffer and 0.5 µL T4 DNA ligase (New England BioLabs, MA, USA). Controls with no insert DNA (vector only), no vector DNA (insert only) and no T4 DNA ligase were included. Ligation reactions were incubated overnight at 16°C prior to transformation into competent cells as outlined above (section 2.3.1).

2.3.9 Transfections

293T cells were seeded at 80-90% confluency in antibiotic-free medium 24 h prior to experiments. Transfections were carried out using Lipofectamine® 2000 (Invitrogen, OR, USA), according to the manufacturer's instructions. A ratio of 0.8 µg DNA to 2 µL reagent for a 24-well plate was used as standard, and scaled appropriately for well size.

2.4 Protein Analysis

2.4.1 Cell lysis

RIPA buffer. Transfected or infected cells were lysed at the indicated time post transfection or infection with 200 µL RIPA buffer per well of a 12-well plate (50mM Tris HCl pH 7.5, 150mM NaCl, 0.5% sodium deoxycholate, 1% Nonidet P40 [NP40], 0.1% sodium dodecyl sulfate [SDS], complete protease inhibitor cocktail [Roche, Switzerland]), scraped into suspension and incubated on ice for 30 min. Membranous material was removed by centrifugation at 14,000 x g for 10 min at 4°C and cell lysate was subsequently stored at -80°C.

Co-IP buffer. Cells for co-immunoprecipitation and mass spectrometry analysis were washed 2X in PBS, lysed for 30 min on ice with Co-IP lysis buffer (50mM Tris HCl pH 7.5, 250mM NaCl, 5mM EDTA, 0.02% sodium azide, 1% NP40, 1 mM sodium orthovanadate, complete protease inhibitor cocktail, 1 mM phenylmethanesulfonylfluoride [PMSF]) and clarified by centrifugation as above.

2.4.2 SDS-PAGE

Sodium dodecyl sulfate polyacrylamide gel electrophoresis (SDS-PAGE) was carried out using either a Mini-PROTEAN® Tetra Handcast system (Bio-Rad, CA, USA) or Bolt® Mini-Gel system (Novex, USA). Using the Mini-PROTEAN® system, SDS-PAGE gels were prepared with a 10% resolving (2.5 mL Milli-Q H_2O, 1.25 mL 40% Bis-Acrylamide [Bio-Rad, CA, USA], 1.25 mL 1.5 M Tris-HCl [pH 8.8], 50 µL 10% SDS, 25 µL 10% ammonium persulfate [APS] and 25 µL tetramethylethylenediamine [TEMED; Bio-Rad, CA, USA]) and 4% stacking gel (2.5 mL Milli-Q H_2O, 1.25 mL 40% Bis-Acrylamide, 1.25 mL 1.5 M Tris-HCl [pH8.8], 50 µL 10% SDS, 25 µL 10% APS and 25 µL TEMED). Bolt® 4-12% Bis-Tris Plus Gel (Novex, USA) were used with the Bolt® Mini-gel system.

To carry out SDS-PAGE, cell lysate was added to 4X NuPAGE® SDS-PAGE loading buffer (Novex, USA) and samples were heated (70°C for 10 min) or left untreated as indicated. For protein samples that were to be reduced, lysate was incubated with 5% β-mercaptoethanol prior to heat treatment. Protein samples were loaded into the wells of an SDS-PAGE gel and electrophoresed for 1 to 2 h (as required for separation) at 130 V (Mini-PROTEAN® system) or 200 V (Bolt® system) in Tris-Glycine running buffer.

2.4.3 Western Blot transfer

Following SDS-PAGE, samples were transferred from the gel to a nitrocellulose membrane (Hybond-ECL; GE Healthcare Limited, Buckinghamshire, UK) using the Mini Trans-Blot System (Bio-Rad, CA, USA). The transfer cassette was assembled (fibre pad, 3 pieces of Whatman filter paper, gel, membrane, 3 pieces of filter paper and a second fibre pad) and submerged in cold transfer buffer (25 µM Tris base, 200 µM glycine, 0.1% SDS and 20% methanol) in the gel tank. Protein transfer was carried out at 100 V for 1.5 h. Membranes were removed from the transfer apparatus and washed in 1X PBS Tween-20 (PBST).

2.4.4 Immunoblotting

Membranes to be immunoblotted were blocked with 2.5% non-fat milk (Bio-Rad, CA, USA) in PBS overnight at 4°C. The blocking solution was removed by 3 x 5 min washes with PBST prior to incubation with the primary antibody at an appropriate dilution in 2.5% non-fat milk for 1 h at room temperature. Primary antibody was removed by 3 x 10 min washes in PBST and the membrane incubated with the secondary antibody at an appropriate dilution (1:1000 for AlexaFluor680-conjugated secondary antibodies [Molecular Probes, USA] and 1:5000 for horseradish peroxidase [HRP]-conjugated secondary antibodies [Cell Signalling Technology, MA, USA]) in PBST for 1 h at room temperature protected from light (depending on secondary antibody). The secondary antibody was removed by 3 x 10 min washes in PBST. If AlexaFluor680-conjugated secondary antibodies were used, signal from membranes was detected using an Odyssey machine. For membranes probed with HRP-conjugated secondary antibodies, signal was developed using Pierce ECL Plus Western Blotting Substrate (Thermo Scientific, IL, USA) according to the manufacture's instructions. Membranes were exposed to X-ray film in an X-ray cassette at -80°C and developed.

2.4.5 Co-immunoprecipitation

Immunoprecipitation was carried out with 25 to 50 µL Dynabeads® Protein G (Life Technologies, USA) per sample according to the manufacture's instructions. Briefly, beads were incubated with the described amount of antibody diluted in 200 µL PBST per sample for 30 min then washed to remove unbound antibody. The Dynabead®/antibody complex was incubated for 1 h at room temperature with the appropriate cell lysate. Subsequent washes were carried out with PBS and proteins were eluted in 30 µL of elution buffer (20 µL 50 mM glycine [pH2.8] plus 10 µL NuPAGE SDS sample buffer unless otherwise stated).

2.4.6 Mass spectrometry processing

Eluted protein samples for mass spectrometry (MS) analysis were reduced (5 mM DTT for 30 min at 56°C) and alkylated (25 mM iodoacetamide for 30 min at room temperature) prior to in solution digestion with 2-4 ng/µL trypsin overnight at 37°C. Resulting peptide mixtures were concentrated and purified using solid-phase extraction (C18 ZipTip; ZipTip® Pipette Tips, Millipore, Germany) after washes with 5% acetonitrile (ACN)/ 0.1% trifluoroacetic acid (TFA) and elution in 10 µL 80% ACN/ 0.1% TFA. Samples were diluted in 90 µL water prior to analysis.

Samples were separated using reversed-phase chromatography on a Shimadzu Prominence nanoLC system. Using a flow rate of 30 µL/min, samples were first desalted on an Agilent C18 trap (0.3 x 5 mm, 5 µm) for 3 min, followed by separation on a Vydac Everest C18 (300 A, 5 µm, 150 mm x 150 µm) column at a flow rate of 1 µL/min. A gradient of 10-60% buffer B in buffer A over 30 min where buffer A = 1 % ACN / 0.1% FA and buffer B = 80% ACN / 0.1% FA was used to separate peptides. Eluted peptides were directly analysed on a TripleTof 5600 instrument (ABSciex) using a Nanospray III interface. Gas and voltage settings were adjusted as required. MS TOF scan across m/z 350-1600 was performed for 0.5 sec followed by information dependent acquisition for 20 peptides across m/z 40-1600 (0.05 sec per spectra) using high sensitivity mode. A collision energy spread (CE = 40 +/-15 V) was used for fragmentation.

Data was converted to mascot generic format (mgf) and searched in MASCOT accessed via the Australian Proteome Computational Facility. Database was set to 'SwissProt', searching all species, using 'tryspin' as enzyme with up to 2 mis-cleavages, and carbamidomethyl of cysteine (fixed) and oxidation of methionine (variable) modifications were included. Mass tolerances of 50 ppm (MS) and 0.1 Da (MS/MS) were used.

2.4.7 Immunofluorescence

Transfection or infection of cells seeded in a 24-well plate on coverslips was carried out as described above (section 2.3.9 and 2.2.3, respectively). At the stated time point, cells were washed in PBS and fixed with either 300 µL 4% paraformaldehyde in PBS containing 0.1% Triton X-100 for 20 min, or 80% acetone in PBS for 5 min. Acetone fixation was used in combination with the anti-NS1' polyclonal antibody, due to fixation specificity of this antibody. After fixation, cells were washed 3 times with PBS and blocked in 1% BSA in PBS. Coverslips were incubated cell side down on 50 µL spots of primary antibody at an appropriate dilution in a solution of 1% BSA in PBS for 1 h at room temperature. Coverslips were washed 5 times with PBS, incubated cell side down on 50 µL spots of secondary antibody at an appropriate dilution in 1% BSA in PBS and incubated for 1 hour at room temperature. Cells were washed with PBS and incubated with a 1:5000 dilution of DAPI in PBS for 10 min, to counterstain the cell nuclei. DAPI was removed and coverslips washed a further 5 times with PBS. Cells on coverslips were mounted onto glass slides with Mowiol® 4-88 Mounting Media (Polysciences, Inc) and images captured using ZEISS LSM 510 META Laser Scanning Confocal Microscope at 200X magnification, unless otherwise stated.

2.4.8 Antibodies

Primary antibodies used throughout this thesis are listed below in Table 2.2, and secondary antibodies are listed in Table 2.3.

Table 2.2 Primary antibodies used throughout thesis.

Name	Specificity	Dilution (WB)	Dilution (IFA)
4G4	NS1 and NS1'	1:1000	1:200
Biotinylated 4G4	NS1 and NS1'	NA	1:10000
FS-ab	NS1'	1:500	1:80
3.67G	E	NA	1:50
Anti-NS3	NS3	NA	1:200
Anti-Myc	Myc tag	NA	1:200
Anti-Calnexin	ER marker	NA	1:200
Anti-GM130	Golgi marker	NA	1:200
Anti-EEA-1	Early endosomes marker	NA	1:400
Anti-dsRNA	dsRNA	NA	1:10000

Table 2.3 Secondary antibodies used throughout thesis.

Name	Supplier	Dilution (WB)	Dilution (IFA)
Anti-mouse HRP	Cell Signalling Technology	1:5000	NA
Anti-rabbit HRP	Cell Signalling Technology	1:5000	NA
AlexaFluor680 goat anti-mouse	Molecular Probes	1:1000	NA
AlexaFluor680 goat anti-rabbit	Molecular Probes	1:1000	NA
AlexaFluor488 goat anti-mouse	Molecular Probes	NA	1:1000
AlexaFluor488 goat anti-rabbit	Molecular Probes	NA	1:1000
AlexaFluor594 goat anti-mouse	Molecular Probes	NA	1:1000
AlexaFluor555 goat anti-rabbit	Molecular Probes	NA	1:1000

2.4.9 Metabolic labelling of proteins

Pulse-chase analysis was carried out in 6-well plates of infected Vero cells (infected at an appropriate MOI with KUN or mutant KUN viruses) or transfected 293T cells (transfected with pcDNA-NS1, pcDNA-NS1' or both plasmids) at 24, 48 or 72 h. At the indicated time post infection or transfection, cells were starved for 30 min in methionine- and cysteine-free DMEM (Gibco, USA), followed by labelling for 1 to 2 h (as indicated) with 100 μCi ^{35}S-methionine (TRAN^{35}S-LABEL; MP Biomedicals, USA). After labelling, cells were washed once in PBS and twice in DMEM, and chased for the indicated amount of time in normal medium. For the radioactive secretion experiments, cell monolayers were placed on ice and the culture fluids were removed, clarified by centrifugation at 1500 g for 5 min, and mixed with an equal volume of 2X lysis buffer (20 mM Tris-HCI [pH 7.5], 150 mM NaCI, 10 mM EDTA, 2% sodium deoxycholate, 2% Triton X-l00, 0.2% SDS containing a 2X concentration of complete protease inhibitor cocktail [Roche, Switzerland]). The cell monolayer was rinsed with ice-cold PBS (pH 7.4), scraped from the plate in 1X lysis buffer (10 mM Tris-HCI [pH 7.5], 150 mM NaCI, 5 mM EDTA, 1% sodium deoxycholate, 1% Triton X-l00, 0.1% SDS) containing protease inhibitors, incubated for 30 min on ice, and clarified by centrifugation for 10 min at 14,000 g. For experiments examining the structural to non-structural protein ratio, cell monolayers were lysed in RIPA buffer as outlined in section 2.4.1. Resulting protein preparations were immunoprecipitated with NS1-reactive mAb 4G4 using 25 μL Dynabeads® Protein G per sample as described above (section 2.4.5). Eluted proteins were loaded onto SDS-PAGE gels, electrophoresed and labelled proteins were transferred to nitrocellulose membranes as per sections 2.4.2 and 2.4.3. Membranes were exposed to a phosphor screen and scanned on a Typhoon scanner (GE Healthcare Limited, Buckinghamshire, UK) or exposed to X-ray film in an X-ray cassette at -80°C and developed. To quantify labelled proteins, individual band intensities were determined by Image J software.

2.4.10 pH treatment of lysate

Nine microliters of harvested lysate was incubated with 3 μL 1 M glycine at the indicated pH for 1 h at room temperature. Samples were combined with 4X NuPAGE® SDS-PAGE loading buffer and subjected to SDS-PAGE and Western blotting as described above.

2.5 RNA manipulations

2.5.1 RNA isolation and Northern blotting

Total RNA was harvested from transfected cells at the indicated time point using TriReagent (Sigma-Aldrich, St Louis, USA) according to the manufacturer's instructions. Cells were lysed in 1 mL TriReagent and all other reagent amounts were altered accordingly. Samples were resuspended in 20 µL RNAse-free H_2O and concentrations determined by Nanodrop. Isolated RNA (5 µg for each sample) was prepared with northern blot loading buffer (0.72 mL formamide, 0.16 mL 10X MOPS, 0.26 mL 37% formaldehyde, 0.18 mL DEPC- H_2O, 0.1mL 80% glycerol, 0.08 mL bromophenol blue) and samples were denatured at 65°C for 10 min. Samples were loaded onto a denaturing 1.5% agarose gel (1.5 g agarose, 5 mL 20X MOPS, 90 mL DEPC-H_2O, 5.4 mL 37% formaldehyde and 2 µL ethidium bromide) and run at 75 V for 2 h using 1X MOPS as running buffer. Gel was equilibrated in 10X SSC for 45 min and RNA was transferred overnight to Hybond-N membranes (GE Healthcare Limited, Buckinghamshire, UK) by upward capillary transfer. RNA was crosslinked to the membrane by UV-irradiation (using UV Stratalinker® 1800 [Stratagene]) and Northern hybridization with a [^{32}P]-labeled (Perkin Elmer, Waltham, USA) WNV_{KUN} specific 3'-UTR probe was carried out to detect accumulation of viral RNA. Briefly, the membrane was pre-hybridized with warmed ExpressHyb hybridization solution (Clontech, CA, USA) for 1.5 h at 68°C before addition of 3'-UTR radioactive probe for 2 h to detect genomic RNA. The membrane was subsequently washed to remove unbound radioactivity, exposed to a phosphor screen overnight and scanned on a Typhoon scanner.

2.5.2 miRNA isolation

For miRNA isolation, cells were seeded in 10 cm culture dishes at an appropriate density and infected at MOI=1 with the indicated viruses. Small RNAs, including miRNAs, were harvested from infected cells at the indicated time point using the *mir*Vana™ miRNA Isolation Kit (Ambion, TX, USA), as per the manufacture's instructions. Cells were lysed using 600 µL Lysis/Binding solution per plate and all other reagent volumes were altered accordingly.

2.5.3 Small RNA Northern Blot

A total of 5 µg of RNA was suspended in 40 µL with RNA Loading Buffer II (Ambion, TX, USA) and denatured by heating at 85°C for 5 min. The samples were loaded onto a pre-run 15% polyacrylamide Tris-borate-EDTA (TBE)-Urea gel (Invitrogen, OR, USA), and electrophoresed at

180 V for 65 min in 1X TBE. RNA was stained with ethidium bromide for visualisation and subsequently transferred to Amersham Hybond-N^+ membranes (GE Healthcare Limited, Buckinghamshire, UK) at 35 V for 90 min in 0.5X TBE. Transferred RNA was cross-linked to the membrane by UV cross-linking. Prehybridization was carried out at 37°C in ExpressHyb hybridization solution (Clontech, CA, USA) for 90 min. Probes to detect the predicted miRNA were prepared by labelling of a DNA oligonucleotide complementary to the stem-loop structure with [γ-^{32}P] dATP (Perkin-Elmer, MA, USA) using T4 polynucleotide kinase (Roche, Switzerland). Gel filtration using Illustra MicroSpin G-25 columns (GE Healthcare Limited, Buckinghamshire, UK) was carried out to remove unincorporated nucleotides. Purified probes were hybridized to membranes overnight at 37°C in ExpressHyb hybridization solution. Following hybridization, the membranes were washed 4X for 15 min with Northern wash buffer (1% SDS, 1X SSC [0.15 M NaCl, 0.015 M sodium citrate]) at 37°C, and exposed overnight to a phosphor screen (GE Healthcare Limited, Buckinghamshire, UK). Exposed screens were scanned on a Typhoon scanner.

2.6 Animal experimentation

2.6.1 Mouse strain

Swiss outbred CD1 weanling mice (18-19 days old) were used for all experimentations. Animal experiments were covered under the University of Queensland Animal Ethics (SCMB/405/11/NHMRC "The role of small, flaviviral RNA as well as non-structural protein 2 in West Nile virus pathogenicity") in accordance with the Australian code of practice for the care and use of animals for scientific purposes (NHMRC, Australia).

2.6.2 Infection and observation of mortality

Groups of 10-20 mice were infected intraperitoneally with 100 or 1000 pfu of either WNV_{KUN} or mutant viruses in 100 µL additive-free DMEM. Mice were monitored daily for signs of illness and euthanized when signs of encephalitis (severally hunched posture, partial or full paralysis) were evident. At the conclusion of the experiment, surviving animals were anaesthetized by i.p. injection of ketamine/xylazol/PBS (1:1:8) mixture, blood was collected via cardiac puncture, and mice were euthanized by cervical dislocation. Blood was collected in serum separator tubes, and serum subsequently separated from cellular content via centrifugation at 4,800 x g for 5 min at RT.

2.6.3 ELISA

C6/36 cells were seeded in sterile, flat-bottomed tissue culture grade 96-well plates (1X confluent T-175 flask {approximately 1 x 10^8 cells} resuspended in 17.3 ml of 2% FCS RPMI medium seeds 12 plates). On the following day, cells were infected at MOI ~ 0.1 with WNV_{KUN} and incubated for 7 days at 28°C. Plates were fixed for 2 h at 4°C with fixative buffer (20% acetone, 0.2% BSA in PBS). Fixative was discarded, plates dried overnight at room temperature and stored at -20°C. Negative control plates were prepared in the same way, with no WNV_{KUN} infection.

To check surviving mice for seroconversion, a fixed plate ELISA was carried out using infected and uninfected C6/36 cells. Plates were blocked in 2.5% skim milk powder in PBST for 1 h at 37°C. Following blocking, duplicate 5-fold dilutions (starting at 1:50) of mouse serum in blocking buffer was carried out down 4 wells of infected fixed plates. The same dilutions were carried out on uninfected plates, though not in duplicate. Serum was incubated on fixed cells for 1 h at 37°C, followed by 3X washes with PBST. Secondary antibody (1:20000 goat anti-mouse HRP-conjugated antibody) diluted in PBST was added and incubated for 1 h at 37°C, followed by washing as before. Plates were developed with ABTS substrate buffer (25 mM citric acid, 25 mM trisodium citrate, 5 mg/mL ABTS, 0.012% H_2O_2) until sufficient colour developed, and absorbance at 405 nm was read using a Multiskan EX plate reader. An infected well reading double the corresponding result on the uninfected plate was recorded as positive. Serum samples that were recorded as negative indicated that the mouse did not seroconvert and was therefore excluded from survival analysis.

3 NS1' cellular localisation and role in replication

3.1 Introduction

NS1' is produced by a -1 PRF occurring at the beginning of the adjacent NS2A gene that adds an additional 52 amino acids to the NS1 protein: 9 amino acids of NS2A followed by 43 amino acids of frameshifted sequence (384, 1, 386). Produced in 30 – 50% of translation events, it is present in cells at levels similar to NS1 (1). This protein has been shown to be stably produced in cells and have a similar glycosylation state to NS1 (387, 332), suggesting that NS1' is a functional protein rather than a rapidly degraded by-product. As NS1' contains the entire NS1 coding sequence, with only a 52 amino acid extension, it was hypothesised that NS1' may be able to perform similar functions to NS1 during infection.

NS1 is known to localise to the ER (317, 316, 4, 226) due to the presence of a signal sequence encoded by the last 24 amino acids of the preceding E protein (334). NS1 is cleaved at the N-terminus by the ER-resident host signal peptidase (161) and at the C-terminus from NS2A by an unidentified host cell protease (335). NS1 is glycosylated at multiple sites (depending on the flavivirus) (341, 333) and rapidly dimerizes (348, 333). This dimer acquires a partially hydrophobic nature (348), which has been suggested to be the major factor in the subsequent association of NS1 with the ER membrane (4). Once dimerised, NS1 is trafficked to three distinct locations in infected cells: the site of RNA replication; the cell surface (351, 348); and secreted through the Golgi to the extracellular fluid (331, 352). The majority of NS1 remains associated with the ER, where it co-localises with dsRNA and other members of the replication complex (316, 226). See Figure 1.6 for a depiction of the processing and trafficking of NS1 outlined above.

NS1 performs a crucial function in replication, given that mutations or deletions in the NS1 gene result in a lack of detectable RNA replication. *Trans*-complementation of replication-deficient flavivirus RNA lacking functional NS1 has been shown by several groups. It was first shown using Sindbis virus replicons for stable expression of YFV NS1 in cell culture: while an internal deletion of 260 codons from NS1 in the YFV 17D cDNA clone completely ablated virus replication in vector-only expressing cells, successful RNA replication was recovered in cells expressing NS1 in trans (309). Similarly, a lethal mutation of WNV_{KUN} NS1 which resulted in a complete lack of RNA replication could be complemented *in trans* by expression of wild-type WNV_{KUN} NS1 (268). This *trans*-complementation of replication was also seen for NS1-deleted viral RNA by NS1 expressed from WNV_{KUN} replicon RNA (5). It is this large (~80%), in-frame deletion of NS1 that was used

for the design of the CMV-promoter driven WNV_{KUN} genomic cDNA (pKUNdNS1) used in the *trans*-complementation experiments shown in this chapter.

To enable studies on the NS1' and NS1 proteins, CMV promoter-based plasmids expressing NS1' or NS1 (pcDNA-NS1' and pcDNA-NS1, respectively) were designed previously as shown in Figure 3.1A (published in (375)). Both constructs contained the WNV_{KUN} envelope protein (E) signal sequence at the N terminus followed by cDNA for the protein of interest and C-terminal Myc and Flag tags to assist in protein detection. pcDNA-NS1' was generated by inserting an additional nucleotide (Figure 3.1B, boxed nucleotide) at the frameshift site to induce the change in reading frame that leads to NS1' synthesis. To prevent further frameshifting, two single-nucleotide mutations were also introduced into the slippery heptanucleotide of the frameshift motif, as published previously (1) (Figure 3.1B, circled nucleotides). Protein production from the designed plasmids was confirmed by SDS-PAGE and Western blotting with 4G4, a monoclonal antibody that recognizes both NS1 and NS1' proteins (400). NS1 (monomer) was detected in lysates from pcDNA-NS1-transfected cells and NS1' proteins (both monomer and dimers) were detected in lysates from pcDNA-NS1'-transfected cells (Figure 3.1C). These plasmids were utilized for both localisation and complementation analyses.

The goal of this study was to determine whether the C-terminal 52 amino acid extension of NS1' interferes with the function of NS1 part of NS1' in viral RNA replication as well as to determine whether NS1' can substitute for NS1 in RNA replication. As NS1 localise predominantly to the ER and the sites of RNA replication, co-staining with antibodies against an ER marker (calnexin) and antibodies against dsRNA was carried out to determine cellular localisation of NS1'. Complementation analysis of NS1-deleted viral RNA with either pcDNA-NS1 or pcDNA-NS1' was performed to determine whether NS1' is able to substitute NS1 in viral RNA replication.

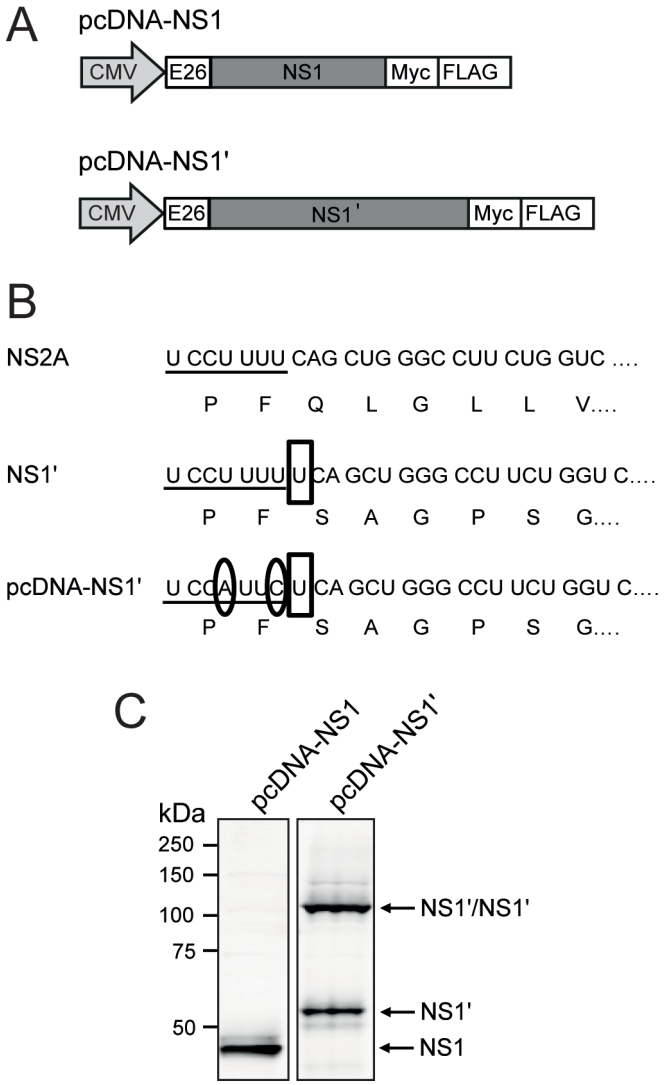

Figure 3.1 Design and characterization of plasmid DNAs expressing NS1 and NS1' genes. A. Plasmid constructs pcDNA-NS1 and pcDNA-NS1', for expression of NS1 and NS1', respectively, contain an N-terminal signal sequence consisting of the last 26 codons of the preceding WNV E protein and Myc and Flag tags at the C terminus for easy detection. **B.** Alignment of the nucleic and amino acid sequences of NS2A, NS1' and pcDNA-NS1' showing the -1 frameshift occurring at the beginning of the NS2A gene that leads to the generation of NS1'. Underlining shows the slippery heptanucleotide of the frameshift motif, open boxes show inserted nucleotides, and circles show mutated bases. **C.** Western blot showing expression of NS1 and NS1' from pcDNA-NS1 and pcDNA-NS1', respectively. Lysates were heat denatured and analyzed by Western blotting with anti-NS1 MAb (4G4).

3.2 Results

3.2.1 Cellular localisation of NS1' is similar to that of NS1 in plasmid DNA-transfected and virus-infected cells.

To examine whether NS1' co-localises to the ER with NS1, immunofluorescence assays were carried out on cells expressing NS1' or NS1 proteins. HEK293T cells transfected with pcDNA-NS1 or pcDNA-NS1' plasmids were fixed at 48 h post transfection and stained with 4G4, to detect both NS1 and NS1', and with NS1'-specific (FS-ab) antibodies (1). As expected, FS-ab stained only pcDNA-NS1' transfected cells, while 4G4 stained both pcDNA-NS1 and pcDNA-NS1' transfected cells (Figure 3.2A). As 4G4 is able to detect both NS1 and NS1', it is not possible to distinguish NS1 and NS1' localisation in cells infected with WNV_{KUN}, given that both proteins are produced. FS-ab on the other hand only recognizes NS1' protein. As the mutant virus A30A' does not produce NS1' protein (1), comparative co-staining with 4G4 and FS-ab of cells infected with wild type or A30A' mutant WNV_{KUN} viruses was carried out to assess whether NS1 and NS1' proteins localise to the same or different cellular compartments. Vero76 cells infected with either WNV_{KUN} or A30A' mutant virus and fixed at 24 hpi were co-stained with 4G4 and FS-ab. In WNV_{KUN} infected cells, 4G4-labeled proteins co-localise with FS-ab-labeled proteins, indicating that NS1 and NS1' are found in the same cellular compartments (Figure 3.2B). No FS-ab-specific staining was seen in A30A' infected cells and staining with the NS1-specific (4G4) mAb was similar to that seen in WNV_{KUN} infected cells stained with 4G4 or FS-ab.

Using 4G4 in addition to antibodies recognizing markers for various cellular compartments, the localisation of NS1' and NS1 in transfected cells was further examined. HEK293T cells transfected with pcDNA-NS1 or pcDNA-NS1' plasmids were fixed and permeablised at 48 h post transfection, and stained with biotinylated 4G4 and antibodies recognizing markers of the ER (rabbit polyclonal antibody against calnexin [Sigma Aldrich]), Golgi apparatus (mouse monoclonal antibody against GM130 [Becton Dickinson]) or endosomes (mouse monoclonal antibody against EEA-1 [BD Transduction Laboratories]). Both NS1 and NS1' localised predominantly to the ER (Figure 3.3A), with a small degree of localisation in the Golgi (Figure 3.3B), and no distinct localisation to the endosomes (Figure 3.3C). To detect cell surface NS1 and NS1', fixed and non-permeablised cells were stained with 4G4, washed extensively and subsequently permeablised to counter stain with anti-calnexin; confirming that 4G4 staining observed was indeed on the cell surface (Figure 3.3D). Moreover, there did not appear to be any differences in the cellular distribution of plasmid- expressed NS1' compared to NS1, leading to the conclusion that NS1' resides in the same cellular compartments as NS1.

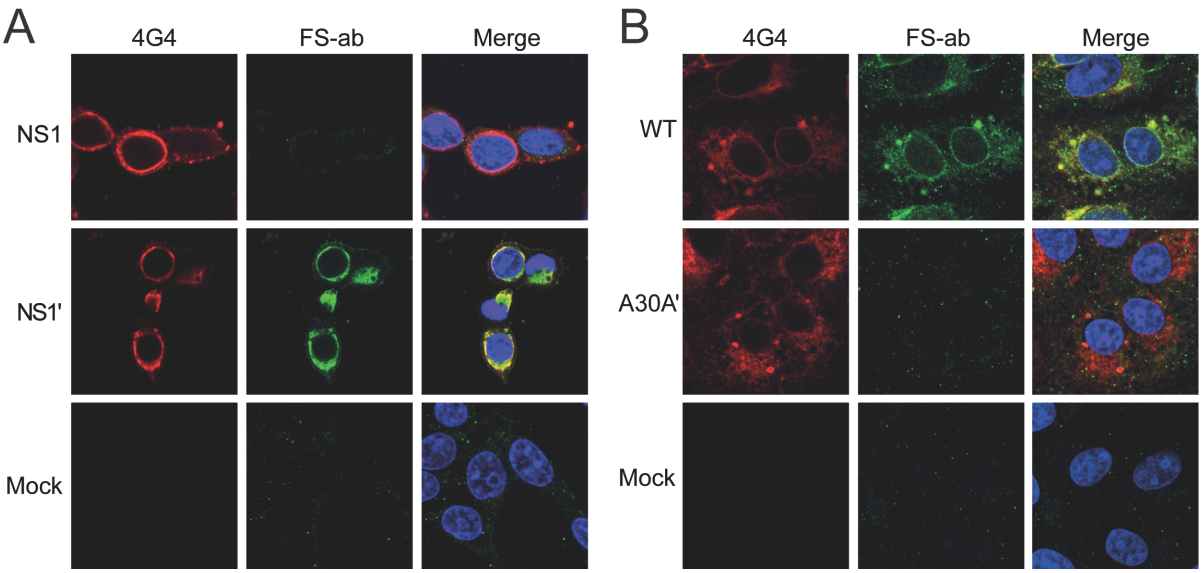

Figure 3.2 Cellular localisation of NS1' and NS1. A. Immunofluorescence analysis showing production of NS1 and NS1' using 4G4 (staining both NS1 and NS1') and FS-ab (NS1'-specific antibody) in transfected HEK293T cells. **B.** Immunofluorescence analysis showing co-localisation of NS1 and NS1' in infected Vero76 cells using 4G4 and FS-ab.

To confirm that the cellular distribution of NS1 and NS1' detected in transfected cells is the same as in infected cells, immunofluorescence analysis was again carried out with antibodies detecting marker proteins for ER, Golgi apparatus and endosomes. Vero76 cells infected with WNV_{KUN} or A30A' viruses were fixed at 24 h pi and stained with biotinylated 4G4 and either anti-calnexin, anti-GM130 or anti-EEA-1 antibodies. As in transfected cells, NS1 and NS1' localised predominantly to the ER (Figure 3.4A), with a small degree of co-localisation with the Golgi (Figure 3.4B) and no localisation to the endosomes (Figure 3.4C). Again, 4G4 staining of non-permeablised cells was carried out to detect NS1 and NS1' cell surface expression. Subsequent permeablisation of stained cells and counterstaining with anti-calnexin confirmed that NS1 specific cell surface staining was seen (Figure 3.4D) A comparison between WNV_{KUN} and A30A' infected cells might show unique NS1'-specific staining, since A30A' does not produce NS1'. However, no differences in anti-NS1 staining between WNV_{KUN} and A30A' infected cells indicate that NS1' and NS1 localise to the same cellular compartments. These results, in combination with the results from plasmid-transfected cells, indicate that NS1' protein has similar cellular distribution to NS1 during viral infection or when expressed as individual proteins.

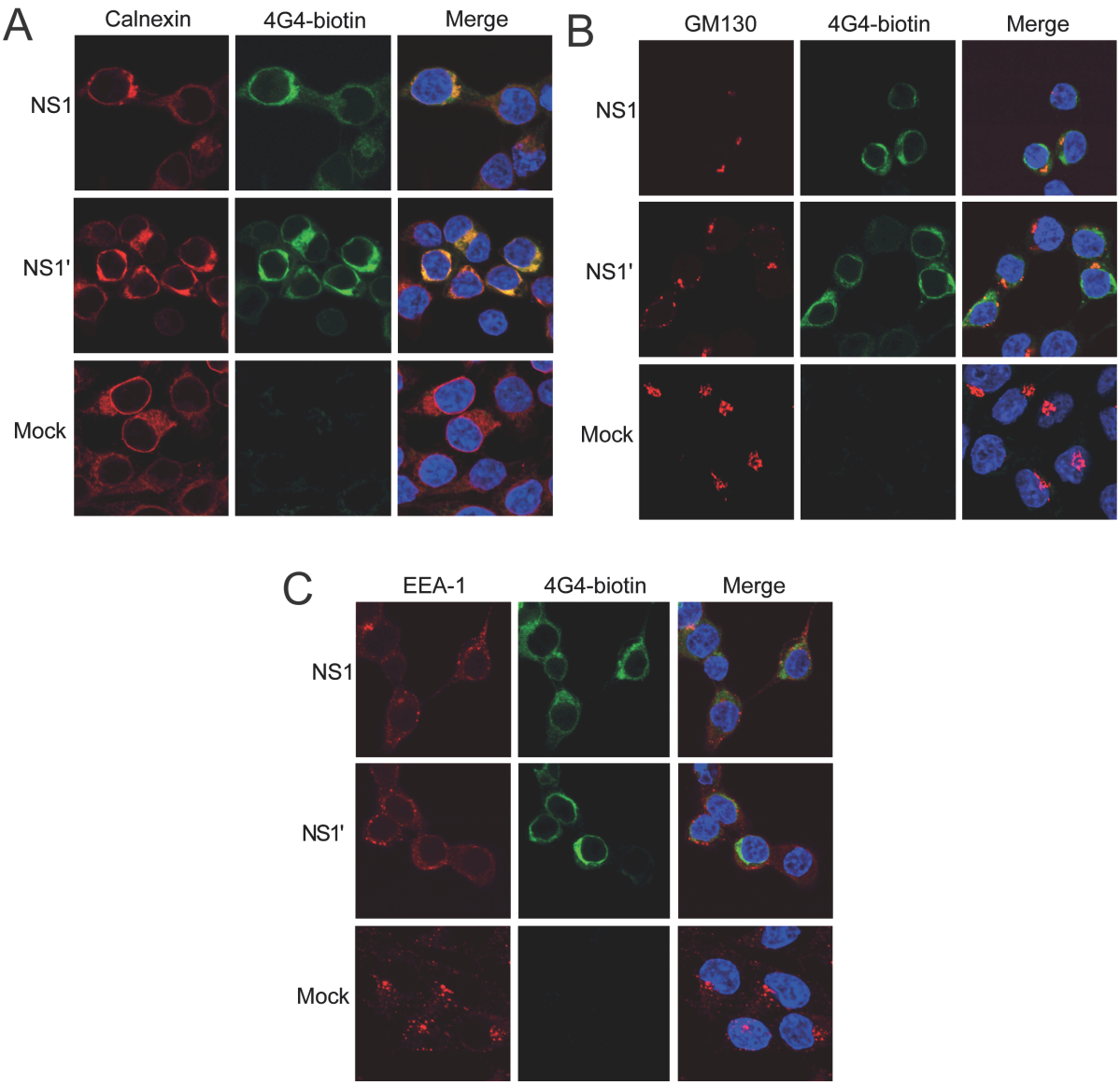

Figure 3.3 Cellular localisation of plasmid-expressed NS1' and NS1. Immunofluorescence analysis to investigate co-localisation of plasmid-expressed NS1 and NS1' with (**A**) the ER, (**B**) the Golgi, and (**C**) endosomes. Transfected HEK293T cells were stained with antibodies to organelle-specific markers (calnexin, GM130 or EEA-1 respectively; red) and biotinylated anti-NS1 (4G4; green). **D.** Transfected HEK293T cells were stained with 4G4 (red) prior to permeablisation and counterstaining with anti-calnexin (green) to visualize surface expression.

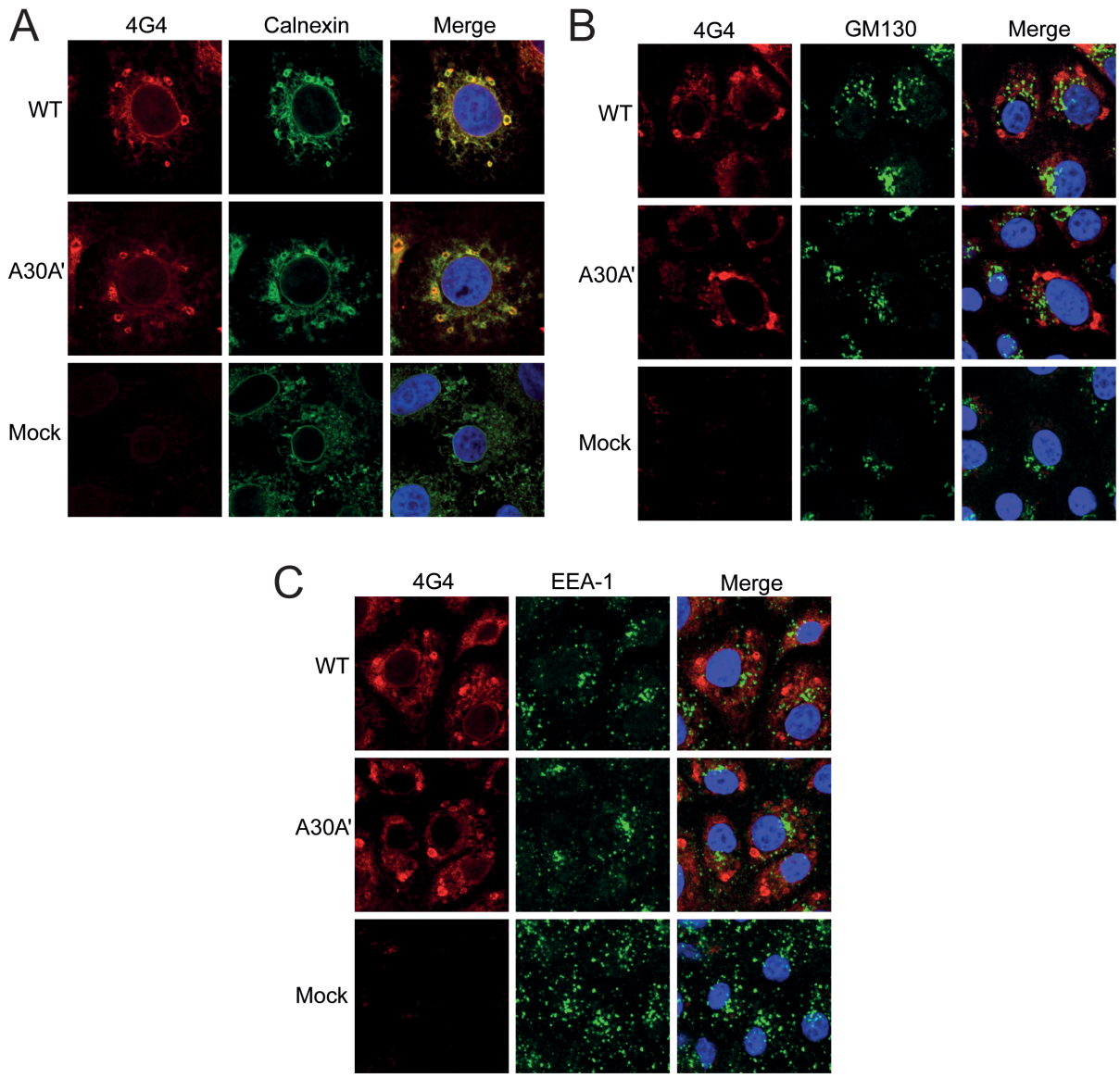

Figure 3.4 Localisation of NS1' and NS1 in WNV_{KUN}-infected cells. Immunofluorescence analysis to investigate co-localisation of virally expressed NS1 and NS1' with (**A**) the ER, (**B**) the Golgi, and (**C**) endosomes. Infected cells were stained with antibodies to organelle-specific markers (calnexin, GM130 or EEA-1 respectively) and biotinylated anti-NS1 (4G4). **D.** Infected Vero76 cells were stained with 4G4 (green) prior to permeablisation and counterstaining with anti-calnexin (red) to visualize surface expression.

NS1 co-localises with dsRNA at the sites of flavivirus RNA replication in WNV_{KUN} infected cells (226). To determine whether NS1' also co-localises with dsRNA, Vero76 cells infected with WNV_{KUN} or A30A' were fixed at 24 hpi and co-stained with an anti-dsRNA antibody and either biotinylated 4G4 or FS-ab. Proteins stained with both 4G4 and FS-ab co-localised with dsRNA (Figure 3.5A and B respectively), demonstrating that NS1' is also associated with dsRNA, and therefore with the sites of viral RNA replication.

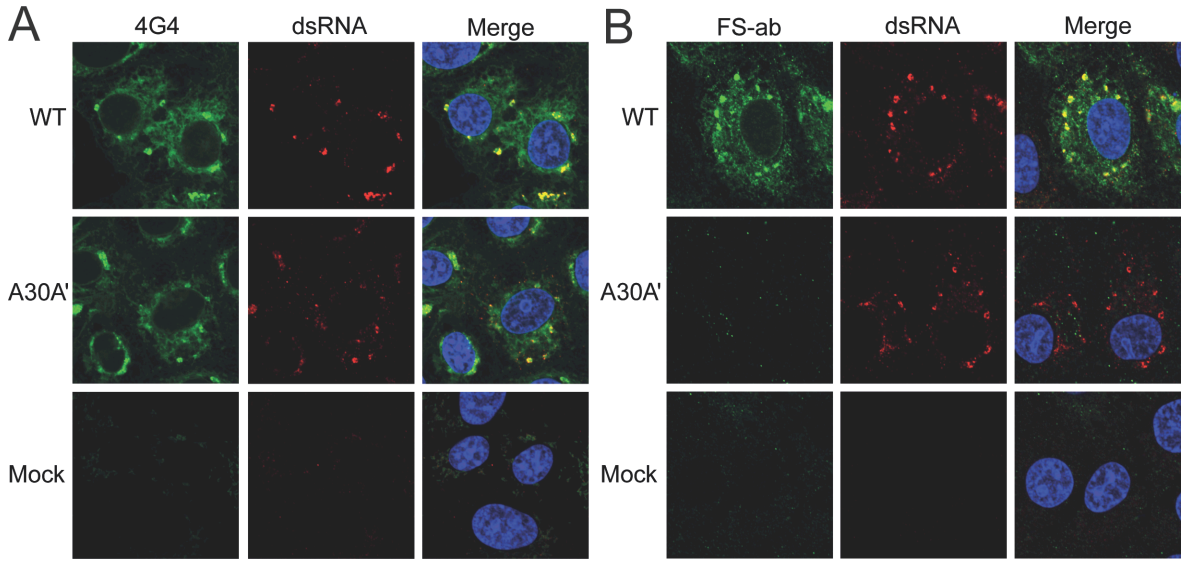

Figure 3.5 Co-localisation of NS1' and NS1 with dsRNA in WNV_{KUN}-infected cells. Immunofluorescence analysis to investigate co-localisation of NS1 and NS1' with dsRNA in infected cells stained with an anti-dsRNA Ab and either biotinylated 4G4 (**A**) or FS-ab (**B**).

3.2.2 NS1' complements replication of NS1-deleted viral RNA.

Due to the co-localization of NS1' with NS1 in the ER and with dsRNA, it was hypothesised that NS1', in addition to NS1, could also play a role in viral RNA replication. To test whether NS1' can substitute for the function of NS1 in viral replication, a CMV-promoter driven WNV_{KUN} genomic cDNA with a large (~80%) internal deletion of the NS1 gene was constructed (pKUNdNS1, Figure 3.6A; see Appendix 9.2 for cloning strategy). This deletion (dNS1.1) has been used previously in an RNA based system to demonstrate *trans*-complementation of replication of NS1-deleted viral RNA by the NS1 expressed from WNV_{KUN} replicon RNA (5). HEK293T cells were co-transfected with pKUNdNS1 and either pcDNA-NS1 or pcDNA-NS1' plasmids to determine whether expression *in trans* of NS1 or NS1' could rescue replication of replication-deficient pKUNdNS1 (see Figure 3.6B for experimental design). Transfection of repBHK cells expressing all of the WNV_{KUN} non-structural proteins, including NS1 and NS1', with pKUNdNS1 was also performed as a positive control (5), and co-transfection of pKUNdNS1 with a green fluorescent protein (GFP) expressing plasmid was included as a negative control.

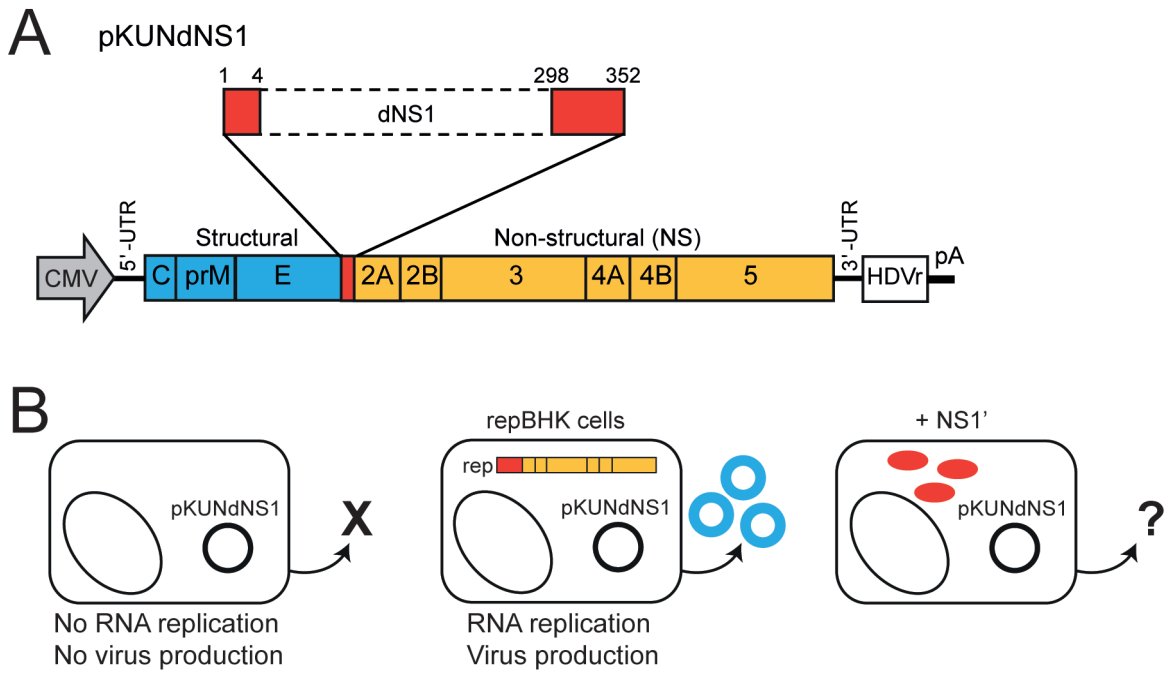

Figure 3.6 Experimental design to test complementation of NS1-deleted viral RNA. A. Schematic diagram of pKUNdNS1 plasmid DNA containing a large deletion in the NS1 gene (amino acid 4 to amino acid 298) of WNV_{KUN} genomic cDNA. CMV – Cytomegalovirus promoter, HDVr – Hepatitis delta virus ribozyme, pA – polyA signal, UTR – untranslated region. **B.** Experimental design. pKUNdNS1 alone does not replicate or produce virus particles. Transfection into cells stably expressing the non-structural proteins (repBHK cells) recovers replication and virus particle production. Experiment assessed whether expression of NS1' alone can *trans*-complement for the absence of NS1.

To examine rescue of RNA replication, total RNA was harvested from co-transfected cells at 2 or 4 days post transfection. Isolated RNA (5μg) was subjected to denaturing 1.5% agarose gel electrophoresis followed by transfer to Hybond-N membranes (GE Healthcare Limited, Buckinghamshire, UK). RNA was crosslinked to the membrane by UV-irradiation, and Northern hybridization with a [^{32}P]-labeled (Perkin Elmer, Waltham, USA) WNV_{KUN} specific 3'-UTR probe was carried out to detect accumulation of viral RNA. No viral RNA was detected in mock-transfected cells (Figure 3.7A, lanes 9 and 10), and transfection of repBHK cells with pKUNdNS1 resulted in increasing accumulation of viral genomic RNA (Figure 3.7A, lanes 11 and 12). A small level of RNA accumulation in the pKUNdNS1 only transfected cells was detected as expected (Figure 3.7A, lanes 1 and 2), due to the transcription of NS1-deficient RNA driven by CMV promoter. However, the levels of accumulated RNA were notably higher in cells co-transfected with either pcDNA-NS1 (5.5-fold increase at day 2 and 10-fold increase at day 4) (Figure 3.7A, lanes 3 and 4) or pcDNA-NS1' plasmids (3-fold increase at day 2 and a 5-fold increase at day 4) (Figure 3.7A, lanes 5 and 6) compared to those in pKUNdNS1 only transfected cells. Notably, some variations in the Northern blot detection of complemented genomic RNA between three different complementation experiments (not shown) were observed, producing a range of fold increases for pcDNA-NS1 complementation between 1.5 and 14 fold, and for pcDNA-NS1'-complementation between 1 and 5 fold. No distinct band for genomic RNA was detected in cells co-transfected with GFP-expressing plasmid (Figure 3.7A, lanes 7 and 8), possibly due to either inhibitory effect of GFP expression on transcription of pKUNdNS1 RNA or enhanced degradation of pKUNdNS1 RNA in the presence of GFP expression. Notably, the accumulation of viral RNA in NS1 and NS1' complementation experiments decreased from day 2 to day 4 after transfections, while transfection of pKUNdNS1 into repBHK cells led to an increase in RNA level (Figure 3.7A). This is likely due to the ability of complemented virus to spread in repBHK cells, where 100% of cells express complementing NS1 and NS1' proteins, while the spread of complemented virus is not possible in co-transfection experiments, as untransfected cells do not support replication and thus spread of complemented virus.

Trans-complementation of viral RNA replication by NS1' was further supported by immunofluorescence analysis of co-transfected HEK293T cells using staining with a mouse monoclonal anti-cmyc antibody (9E10 hybridoma, ATCC) (recognises myc-tagged NS1 or NS1' proteins) and rabbit polyclonal anti-NS3 antiserum (226) (recognising pKUNdNS1-expressed NS3 protein). Increased production of NS3 protein in pcDNA-NS1 and pcDNA-NS1' co-transfected cells, compared to pKUNdNS1 only transfected cells (Figure 3.7B), further demonstrated that

trans-complementation of replication of the NS1-deleted viral RNA was successful. Therefore, it was concluded that NS1' protein can rescue the replication deficiency of NS1-deleted viral RNA.

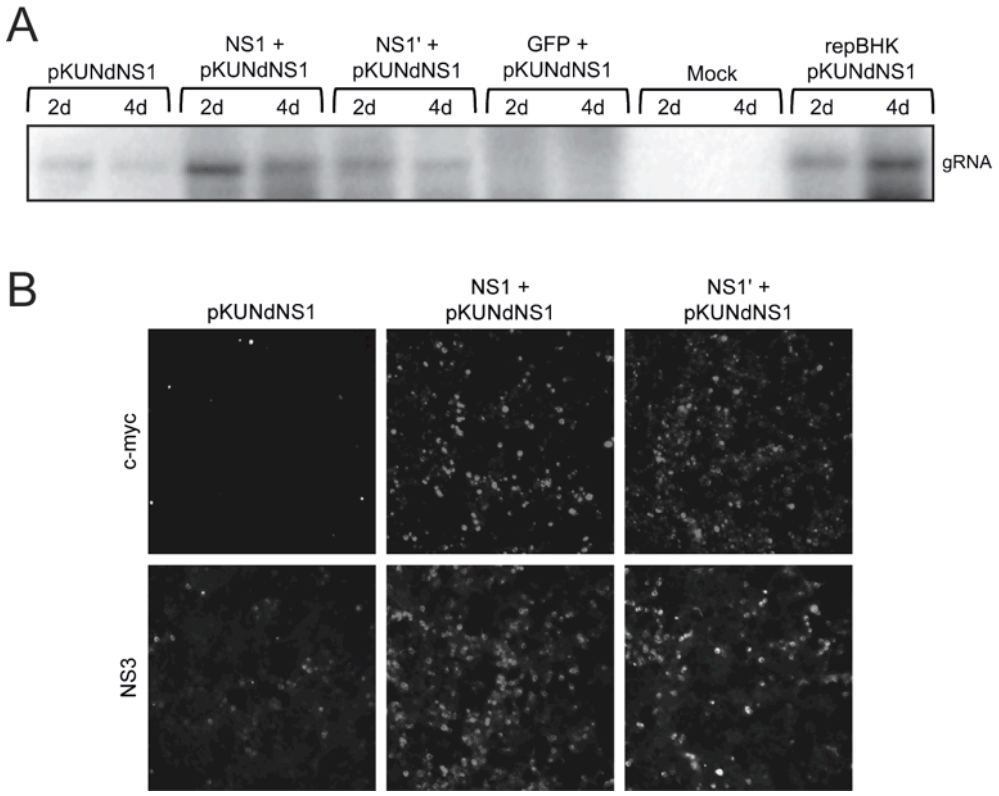

Figure 3.7 NS1' complements replication of NS1-deleted viral RNA. A. Northern blot with a radiolabelled 3'-UTR probe showing replicating genomic RNA. RNA was harvested from co-transfected cells at 2 or 4 d post transfection. **B.** Immunofluorescence of HEK293T cells co-transfected with pKUNdNS1 and either NS1 or NS1' at 2 days post transfection. Co-transfected cells were stained for cmyc and NS3. Transfected cells were imaged at 20X magnification.

To detect infectious virus production from co-transfected cells, and therefore further confirm successful complementation, culture fluid from transfected HEK293T cells was harvested at 2 and 4 days post transfection and used to infect repBHK cells. If complementation was successful, viral particles containing the NS1-deleted RNA would be able to infect the repBHK cells, replicate, and form viral particles due to the continuing expression of NS1 and NS1' in the repBHK cells. Prior to infection the culture fluid was treated with 10 units RQ1 DNase (Promega, Madison, USA) and 10 µg RNase A for 2 hours at room temperature to digest any remaining plasmid DNA or uncoated RNA. Two days after infection, cells were fixed and stained with an anti-E antibody to detect infected cells. Immunofluorescence images of repBHK cells infected with undiluted culture fluids and stained with 3.67G, a monoclonal anti-E antibody (213), showed that

only cells that were co-transfected with either pcDNA-NS1 or pcDNA-NS1' plasmids produced infectious viral particles (Figure 3.8A). No infectious virus was produced in pKUNdNS1 only transfected cells and in cells co-transfected with pKUNdNS1 and GFP-expressing plasmid (Figure 3.8A). The lack of E-positive repBHK cells infected with DNase- and RNase-treated undiluted culture fluids from pKUNdNS1 only transfected and pKUNdNS1 plus GFP-expressing plasmid co-transfected cells also demonstrates that no transfected DNA or uncoated viral RNA was carried over into the infection experiment.

To determine the titres of secreted viral particles, repBHK cells infected with serial 10-fold dilutions of collected culture fluids were stained with anti-E antibodies and foci of E-positive cells were counted. Titration of viral particles was carried out for two independent complementation experiments and the average viral titres were determined. The viral titres were similar from NS1 and NS1' complemented cells and both were similar to the viral titres obtained in repBHK cells at 2 days after transfection (Figure 3.8B). Notably, the accumulation of viral RNA and viral titres in NS1 and NS1' complementation experiments decreased from day 2 to day 4 after transfections, while transfection of pKUNdNS1 into repBHK cells led to a corresponding increase in RNA level and no decrease in viral titres (Figure 3.7A and 3.8B). This is likely due to the ability of complemented virus to spread in repBHK cells where 100% of cells are expressing complementing NS1 and NS1' proteins, while the spread of complemented virus is not possible in co-transfection experiments as un-transfected cells will not support replication and spread of complemented virus. From these results, it was concluded that NS1' could successfully complement for deleted NS1 in virus replication and that there was no significant difference in the efficiency of complementation between NS1 and NS1'.

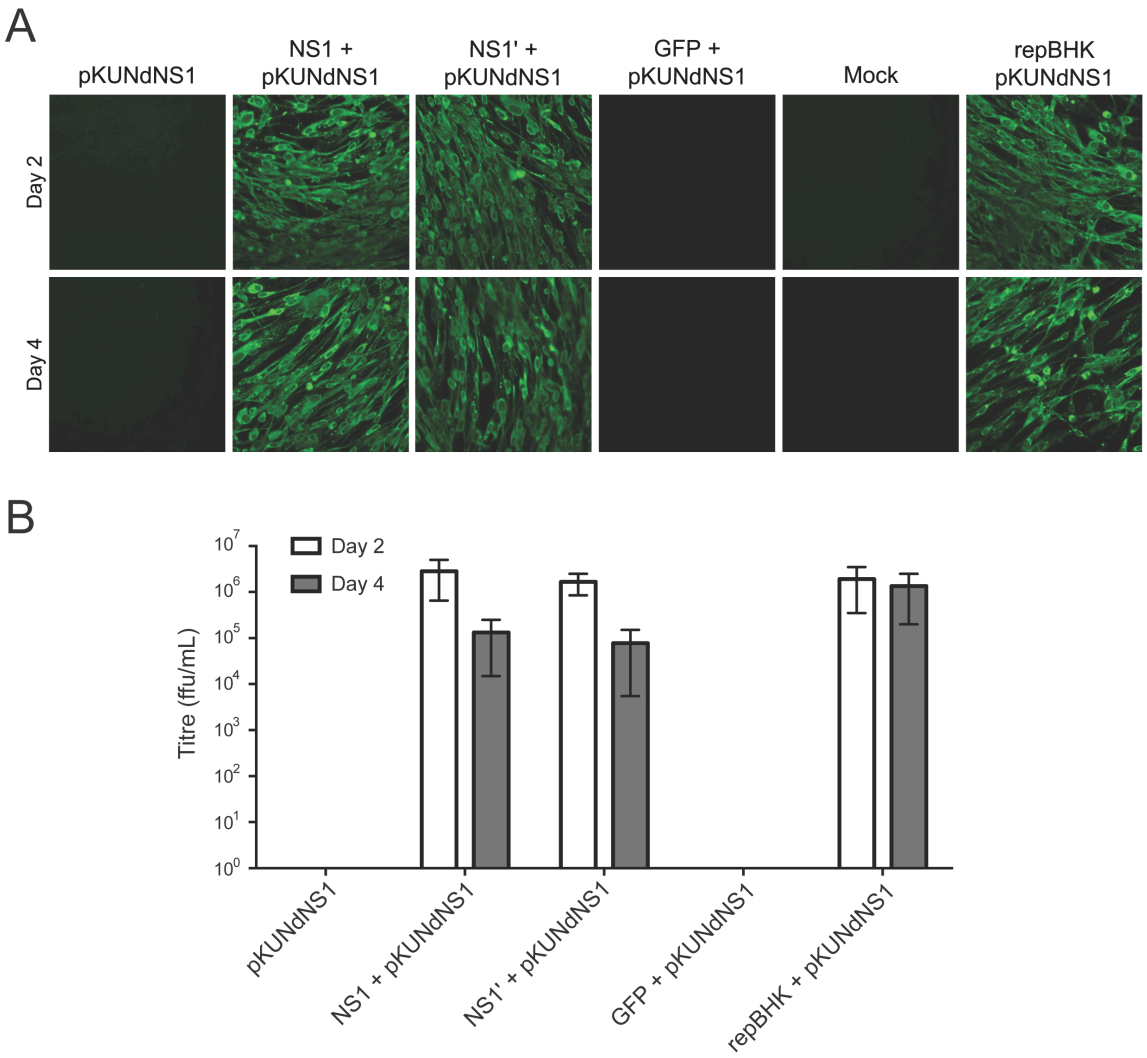

Figure 3.8 NS1' complements replication of NS1-deleted viral RNA. A. Immunofluorescence analysis showing production of infectious particles from cells co-transfected with pKUNdNS1 and either NS1 or NS1'. Culture fluid (CF) was harvested from co-transfected cells and used to infect repBHK cells. Infected repBHK cells were stained for E and imaged at 20X magnification. **B.** Titres were determined by infection of repBHK cells with serial dilutions of CF from co-transfected cells collected at day 2 (white bars) or 4 (grey bars) post transfection and counting E-positive foci at day 2 post infection. The graph is representative of two independent experiments, with error bars showing SEM. Difference in titres of complemented viruses between NS1 and NS1' was not significant ($P > 0.05$) as determined by a standard one-way ANOVA test.

3.3 Discussion

The experiments in this chapter were designed to analyse whether the C-terminal extension of the NS1' protein prevents NS1' from functioning as NS1 during RNA replication. Prior to any functional analysis, it was necessary to determine the cellular localisation of NS1' in relation to NS1. It would only be reasonable to examine whether NS1' can function similar to NS1 if it is localised to the same cellular compartments where NS1 functions.

Using immunofluorescence analysis of transfected cells (pcDNA-NS1 or pcDNA-NS1') and infected cells, it was concluded that the cellular localisation of NS1' is similar to that of NS1. Both proteins localised predominantly to the ER, with only a small degree of co-localisation with the Golgi (Figure 3.3 and 3.4). This localisation is consistent with what was expected, with the majority of NS1 and NS1' being localised to the ER, where it is initially produced, glycosylated and assembled into dimers. Moreover, given that both NS1 and NS1' are secreted proteins, it was also expected to find NS1/NS1'-specific staining in the Golgi compartment, which is part of the secretory pathway of the cell. After dimerization, a large portion of NS1 is trafficked to ER-derived membranes that constitute the site of RNA replication. Distinct co-localisation of NS1 with dsRNA is consistent with what has been seen previously (226). Interestingly, NS1' was also seen to co-localise with dsRNA in infected cells (Figure 3.5), suggesting a possible role for NS1' in RNA replication.

In relation to virally infected cells, it was not possible to determine unique NS1' localisation. From the nature of the antibodies used, it would have been possible to see unique NS1 staining (although there was none) as there would be no co-staining of NS1 antibodies (4G4) with NS1'-specific antibodies (FS-ab). However, it is not possible to detect unique NS1' staining, as both 4G4 and FS-ab detect NS1'. Co-staining with 4G4 and FS-ab may therefore either represent NS1' alone or co-localisation of NS1 and NS1'. Experiments therefore relied on the comparison of NS1'-expressing and NS1'-lacking virus infected cells to identify unique NS1' localisation. Comparison of WNV_{KUN} (NS1'-expressing) and A30A' (NS1'-lacking) infected cells showed no distinct regions of staining unique to WNV_{KUN}, confirming that NS1' has a similar cellular localisation to NS1.

In addition to being localised to the ER, NS1 is expressed on the cell surface of infected cells (351, 348). Moreover, NS1' glycan modifications (a mixture of high mannose and complex carbohydrates) are also consistent with transport of this protein to the plasma membrane (387, 332). The data shown in Figure 3.3D confirmed cell surface staining for NS1' expressed from pcDNA-

NS1'. While it was possible to detect cell surface expression of NS1' on transfected cells, specific detection of NS1' on the surface of infected cells was not possible with the available antibodies. Nevertheless, it would be reasonable to assume that if NS1' expressed from transfected cells is trafficked to the cell surface, a similar scenario would occur for virally encoded NS1'. However, this could not be confirmed, as FS-ab staining was only successful in cells fixed in acetone, which permeabilises the plasma membrane. The surface staining shown in this chapter was carried out by fixation of infected or transfected cells in PFA and staining with anti-NS1 (4G4) prior to cell permeablisation (Figure 3.3D and 3.4D). FS-ab did not work efficiently in PFA fixed cells, suggesting that the protein cross-linking caused by PFA affects the FS-ab binding epitope.

Once it was confirmed that NS1' has similar cellular localisation as NS1, experiments to examine whether NS1' can substitute for the function of NS1 in replication were carried out. This was also supported by the fact that co-localisation of NS1' with dsRNA was observed, already suggesting a role for NS1' in viral replication. Initial plans for trans-complementation experiments were similar to those that have been conducted previously: with the use of NS1-deleted viral RNA and NS1 or NS1' expressing stable cell lines (268, 5, 309). Unfortunately, the development of the stable cell lines was not successful. While transient expression of NS1' was evident in transfected cells, and DNA from the appropriate plasmids was detected in the stable cell lines, there was no expression of NS1' from the stable cell lines following antibiotic selection (data not shown). Although the optimal system was not successfully developed, co-transfection of a plasmid cDNA (pKUNdNS1) with either NS1 or NS1' from transient plasmids showed the ability of NS1 and NS1' to complement for the replication-deficient cDNA. There was also no significant difference in the efficiency of complementation between NS1 and NS1', supporting the hypothesis that the C-terminal tail does not interfere with the ability of NS1' to function in RNA replication.

The *trans*-complementation results in this chapter showing recovery of a replication-deficient NS1-deleted WNV_{KUN} RNA with NS1' have since been confirmed by another group working with WNV_{NY99} (374). Using NS1' produced from VEEV replicon expressing BHK cells, the authors showed successful recovery of a replication-deficient WNV_{NY99} infectious clone that contained a similar internal deletion of the NS1 gene used in the experiments shown here. These results, in combination with those shown in this thesis chapter, provide strong evidence for a role for NS1' in RNA replication during flaviviral infection.

While the data shown here do not rule out the possibility that NS1' may have a unique function in virus infection that is different from NS1, they do show that NS1' can substitute for NS1

protein in RNA replication. Given that NS1' does contain the entire NS1 coding region, it was not entirely unexpected that NS1' has a similar localization and can perform the same function(s) as NS1 in the virus life cycle. Although only the function of NS1' in viral RNA replication was examined in this thesis, NS1' may also be involved in other reported functions of NS1, such as interactions with the complement system (379, 376, 362, 378, 401) and inhibition of TLR3 signaling (114). This was outside the scope of this thesis; however, future studies on this would provide further insight into the ability of NS1' to function as NS1. Moreover, the question of why some flaviviruses generate significant amounts of NS1' still remains to be answered.

4 Attempt to identify unique NS1' interacting proteins

4.1 Introduction

To identify proteins interacting with NS1 and NS1', a technique known as nanoscale liquid chromatography mass spectrometry (nLC-MS) was used (402, 403). Briefly, a mixture of proteins is enzymatically digested (in this case, using trypsin digestion) and the resulting peptide fragments are separated by nanoscale reverse phase liquid chromatography (nLC). This separation technique uses a hydrophobic solid phase that results in peptides being separated by hydrophobicity (404). Once separated, the eluted peptides are ionised by electrospray ionisation (ESI) and analysed by MS. In this case, tandem mass spectrometry (MS/MS) was used, involving both a quadrupole (QUAD) analyser and time of flight (TOF) analyser. QUAD analysers use radio frequency and direct current voltage to determine the mass to charge ratio of ions. TOF on the other hand, uses a voltage gradient to accelerate the ions, and measures the flight time of the ions; which is proportional to the square root of the mass to charge ratio (405). Peptide sequences are then identified based on the mass to charge ratio of the ionised samples. Databases (for example, MASCOT) are then utilised to match the identified peptides to known genomic sequences to identify the protein.

One approach to examine potential functions of a protein is to use immunoprecipitation and MS to identify protein-protein interactions. The identification of a specific protein interacting with NS1' may reveal a previously unknown function. This is a widely utilised technique that has been used previously to successfully identify a number of protein-protein interactions for flaviviruses (362, 184, 406-408, 370). For example, an interaction between the JEV NS5 protein and heat shock protein 70 (Hsp70), Ras related nuclear protein (Ran) and eukaryotic translation elongation factor 1 alpha (eEF-1α) was identified using affinity purification and MS (408). The interaction of WNV NS1 with factor H and subsequent confirmation that NS1 is involved in evasion of the host complement system was also identified by co-purification and MS (362).

Co-immunoprecipitation, and also MS, has been utilised previously to examine the role of NS1 in the replication complex. The exact function of NS1 in replication is still unknown, as NS1 is located on the lumenal side of the ER and physically separated from the remaining components of the replication complex. It has been suggested that it may provide structural support to the replication complex by anchoring it to the ER membrane (4). Previous *trans*-complementation work showed that complementation of NS1 is species-specific, as DENV NS1 could not complement for

a YFV NS1-deleted genome. This specificity was overcome by a compensatory mutation in NS4A, suggesting an interaction between the two proteins. In addition to this, column bound NS4A was shown to interact with all components of the replication complex, including NS1 (309). Recently, an interaction between NS1 and NS4B has been shown by immunoprecipitation and a combination of western blotting and MS analysis. The authors suggested that in fact it is this interaction of NS1 with NS4B that provides an anchor for the replication complex to the ER membrane. In addition to co-immunoprecipitation with NS4B, the authors showed that NS1 can also pull down NS3 (370). Whether this shows a direct interaction or an indirect link through other interacting proteins is still unclear.

Our group has previously utilised MS to experimentally confirm that a predicted ribosomal frameshift is responsible for NS1' production (384, 1). Matrix-assisted laser desorption ionization–time of flight (MALDI-TOF) MS identified several peptide fragments consistent with the predicted frameshift sequence present in the excised and digested NS1' protein band following anti-NS1 immunoprecipitation of WNV_{KUN} infected cell lysate (1). This work was crucial to the experimental confirmation that NS1' is indeed produced by a -1 PRF.

To identify proteins interacting with NS1 and NS1', two approaches were designed. The first (immunoprecipitation with anti-NS1 antibody [4G4]) aimed to identify unique NS1' interactions by comparison of wild-type WNV_{KUN} (expressing both NS1 and NS1') and A30A' (expressing only NS1) infected cells. In addition, comparison of proteins immunoprecipitated with NS1 or NS1' from pcDNA-NS1 and pcDNA-NS1' transfected cells, respectively, was carried out. This approach will ideally highlight protein interactions that are unique to WNV_{KUN} infected (or pcDNA-NS1' transfected) samples, indicating that they are NS1'-specific interactions. The second approach was to perform NS1'-specific immunoaffinity purification from WNV_{KUN} infected cells using FS-ab. This would identify any proteins specifically interacting with NS1', and confirm whether proteins immunoprecipitated from WNV_{KUN} infected cells using 4G4 were interacting with NS1, NS1', or both. Both approaches are required, as comparison of NS1' (FS-ab bound) and NS1/NS1' (4G4 mAb bound) associated proteins is necessary to identify which interactions are unique to NS1'.

4.2 Results

To identify proteins uniquely interacting with NS1' (but not NS1), immunoaffinity purification and nLC-MS were carried out as outlined in Figure 4.1. Following infection with either WNV_{KUN} or A30A', cells were lysed in NP-40 lysis buffer and resulting cell lysate was incubated with either anti-NS1 mAb (4G4) or anti-NS1' antiserum (FS-ab) bound Protein G Dynabeads®. Bound proteins were eluted in non-denaturing buffer, reduced and alkylated prior to overnight in-solution trypsin digestion. Peptide fragments were subsequently subjected to MS analysis (see Figure 4.1 for experimental design). In addition to infected cell lysates, pcDNA-NS1 and pcDNA-NS1' transfected cell lysates were also subjected to immunoaffinity purification and MS analysis.

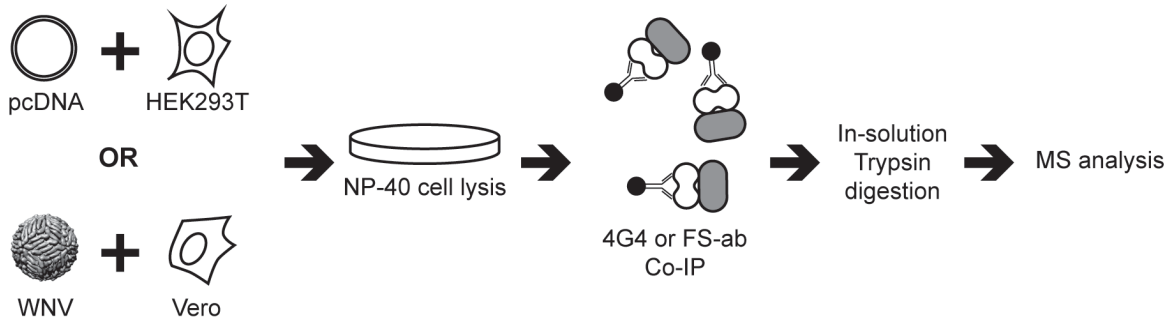

Figure 4.1 Experimental design for identifying interacting proteins by MS analysis. pcDNA-NS1, pcDNA-NS1' or mock transfected 293T cells, or WNV_{KUN}, A30A' or mock infected Vero76 cells, were lysed in NP-40 lysis buffer and immunoprecipitated with 4G4 or FS-ab coupled with Protein G Dynabeads®. Eluted proteins were reduced, alkylated and digested with trypsin prior to MS analysis.

4.2.1 Anti-NS1 immunoprecipitation

To confirm that anti-NS1 and NS1' immunoprecipitations with 4G4 mAb were successful, SDS-PAGE analysis of the original infected cell lysate, unbound proteins following Dynabead® immunoprecipitation, and eluted proteins (prior to reducing) was carried out. NS1 and NS1' were both detected in all WNV_{KUN} samples, while only NS1 was detected in A30A' samples (Figure 4.2). While not all NS1 and NS1' had been immunoprecipitated (as evident by the presence of NS1 and NS1' in the unbound fraction), detectable levels of both NS1 and NS1' were seen in the precipitated and eluted fraction.

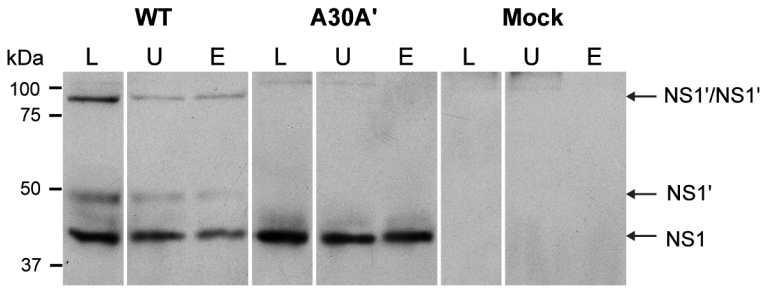

Figure 4.2 Western blot confirming that NS1 immunoaffinity purification was successful. Western blot with anti-NS1 (4G4) mAb of 4G4 immunoprecipitates showing presence of NS1 and NS1' in wild-type (WT) WNV_{KUN} lysate (L), unbound (U) and eluted (E) fractions, and NS1 only in A30A' samples.

Once it was confirmed that NS1 immunoaffinity purification was successful, protein samples from both infected and transfected cells were digested with trypsin and analysed by MS. Following MS analysis of infected samples, peptide hits corresponding to several viral proteins (E, NS3 and NS4B) were detected in both wild-type WNV_{KUN} and A30A' infected cell lysate in multiple independent experiments (Table 4.1). In addition to this, binding immunoglobulin protein (BiP; an ER resident molecular chaperone protein) was detected in WNV_{KUN} samples from all 7 experiments, and in A30A' samples from 3 experiments. Peptide hits that were present in less than two repeat independent experiments were not included in the summary of protein matches, neither were any peptides also identified in mock samples. BiP was also detected in pcDNA-NS1' transfected samples (Table 4.2), as was alpha-1-antiproteinase (a serum trypsin inhibitor). eEF-1α and glyceraldehyde 3-phosphate dehydrogenase (GAPDH) were detected in both pcDNA-NS1 and -NS1' transfected samples, suggesting a possible interaction with both NS1 and NS1'.

Table 4.1 Proteins co-isolated with NS1/NS1' in wild-type (WT) WNV_{KUN} and NS1 in A30A' infected cells. Results shown are from 7 independent experiments.

Protein	**# Experiments detected**	
	WT	**A30A'**
E	6	5
NS3	4	4
NS4B	5	5
BiP	7	3

Table 4.2 Proteins co-isolated with NS1 or NS1' in pcDNA-NS1 or pcDNA-NS1' transfected cells, respectively. Results shown are from 6 independent experiments.

Protein	# Experiments detected	
	pcDNA-NS1	pcDNA-NS1'
eEF-1α	2	5
GAPDH	4	1
BiP	-	2
Alpha-1-antiproteinase	-	2

4.2.2 Anti-NS1' immunoprecipitation

To determine whether the protein interactions seen for 4G4 immunoprecipitation in infected cells was a result of NS1 or NS1' protein binding, immunoprecipitation with anti-NS1' antiserum (FS-ab) was carried out for both infected and transfected cells. This would also confirm the NS1'-interacting proteins observed in transfected cells. Again, to confirm successful immunoprecipitation, SDS-PAGE analysis of the cell lysate, unbound fraction and eluted protein was carried out. While not all the NS1' protein was immunoprecipitated (similar to the results seen for 4G4 pull downs) the anti-NS1' immunoaffinity purification was successful, with eluted protein only being detected for wild-type WNV_{KUN} samples (Figure 4.3).

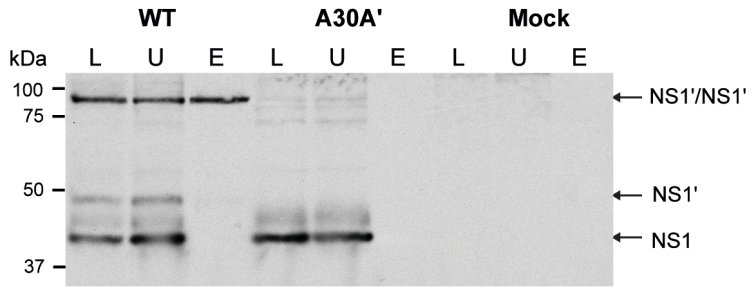

Figure 4.3 Western blot confirming that NS1' immunoaffinity purification was successful. Western blot with anti-NS1 (4G4) mAb of FS-ab immunoprecipitates showing presence of NS1' in wild-type (WT) WNV_{KUN} lysate (L), unbound (U) and eluted (E) fractions, and NS1 only in wild-type WNV_{KUN} and A30A' lysate and unbound samples.

Following MS analysis of infected cells, several peptide hits unique to wild-type WNV_{KUN} samples were detected in multiple independent experiments (Table 4.3). The same viral proteins detected following NS1 immunoaffinity purification of infected lysates (E, NS3 and NS4B) were again detected following immunoprecipitation with anti-NS1' serum. BiP was detected in wild-type WNV_{KUN} infected samples for two independent experiments. Immunoprecipitation of transfected cell lysate with anti-NS1' resulted in the detection of several different peptide matches, including eEF-1α, GAPDH and BiP (Table 4.4), which was consistent with the results from anti-NS1 immunoprecipitation in transfected cells. In addition to these hits, several new peptide matches were seen in multiple repeat experiments of transfected cell lysate immunoaffinity purification (see Table 4.4 for full list).

Table 4.3 Proteins co-isolated with NS1' in wild-type (WT) WNV_{KUN} or A30A' infected cells. Results shown are from 4 independent experiments.

Protein	**# Experiments detected**	
	WT	**A30A'**
E	4	-
NS3	3	-
NS4B	3	-
BiP	2	-

Table 4.4 Proteins co-isolated with NS1' in pcDNA-NS1 or pcDNA-NS1' transfected cells. Results shown are from 4 independent experiments.

Protein	**# Experiments detected**	
	pcDNA-NS1	**pcDNA-NS1'**
eEF-1α	-	3
GAPDH	-	2
BiP	-	2
ADP-ATP translocase 2	-	4
ATP synthase subunit α	-	4
ATP synthase subunit β	-	2
Prohibitin 1	-	3
Prohibitin 2	-	2
Prosaposin	-	2
T-complex protein 1 subunit β	-	2
T-complex protein 1 subunit ζ	-	2
Voltage dependent anion selective channel protein 1	-	2
Voltage dependent anion selective channel protein 2	-	2
L-lactate dehydrogenase A chain	-	2

4.3 Discussion

Mass spectrometry has previously been used successfully to identify flavivirus-host protein interactions, as well as interactions between the different flaviviral proteins (184, 406-408). Specifically for NS1, co-immunoprecipitation identified a role for NS1 in inhibition of the host complement pathway, and an interaction with NS4B that has provided insight into how NS1 may function in replication (362, 370).

The data presented in this chapter has identified both host and viral proteins interacting with NS1 and NS1'. Work conducted in MVEV infected cells identified the presence of both an E-NS1 and an E-NS1' complex (382). The E protein has also previously been immunoprecipitated with either NS1 or NS1' from WNV_{KUN} infected cells (370). The work shown in this chapter confirms this association (Table 4.1 and 4.3), and through the use of A30A' (lacking NS1') and an NS1'-specific antibody, verifies that E is in fact interacting with both NS1 and NS1'. This E-NS1 product has been suggested previously to be a non-functional aggregate, as NS1 and E did not dissociate at any time during infection. However, the nature of these heterodimers has not been further examined. It is possible that this interaction is due to an involvement of NS1 in the folding of E, thereby promoting virion production. It is as of yet unconfirmed whether E proteins interacting with NS1 can dissociate and subsequently be involved in the virion envelope.

Immunoprecipitation of WNV_{KUN} infected cell lysate with an anti-NS1 mAb has been previously shown to pull down components of the flaviviral replication complex (NS3 and NS4B) (370). While the authors claimed this to indicate a physical interaction between NS1 and NS4B, no distinction between NS1 and NS1' was made in this pull-down, suggesting that this result could indicate an interaction of NS4B with either NS1 or NS1'. The work shown in this chapter is the first confirmation that both NS1 and NS1' interact with these viral proteins. NS3 and NS4B were detected in both wild-type WNV_{KUN} (expressing NS1 and NS1') and A30A' (expressing only NS1) infected cell lysate immunoprecipitated with an anti-NS1 mAb, verifying that NS1 is interacting with these viral proteins (Table 4.1). In addition, NS3 and NS4B were also detected in immunoprecipitates from WNV_{KUN} infected cell lysate when NS1'-specific ab was used (Table 4.3), confirming that NS1' also interacts with these proteins. The detection of this interaction between NS1' and members of the flaviviral replication complex supports the finding that NS1' is functioning in the WNV replication complex during viral infection, as outlined in chapter 3 of this thesis.

In contrast to what has been previously seen, no co-precipitation of NS5 with NS1 or NS1' was observed. Work conducted previously in JEV infected mammalian (BHK) and avian (DF-1) cells indicated that NS1 co-precipitates with NS5 (396). In the work carried out for this chapter, NS5 did not co-precipitate with either NS1 or NS1'. Takamatsu *et al* (396) did show an increased interaction between JEV NS1' and NS5 in avian cells, and a repeat of the work shown in this chapter in avian cells may indicate whether this species specific enhancement of the interaction may also hold true for NS1' of WNV_{KUN}.

The work shown in this chapter identified several host cell proteins co-precipitating with NS1 and/or NS1', with the most consistent peptide hits being against BiP, eEF-1α and GAPDH. BiP (also known as the 78 kDa glucose-regulated protein, or GRP78) is a well characterised ER-resident molecular chaperone protein involved in the unfolded protein response (UPR) and in directing protein folding and assembly, among other functions (409, 410). BiP has been shown previously to be involved in folding and oligomerisation of several viral proteins, particularly secreted or cell surface expressed glycoproteins (411-418). One example is the interaction between BiP and the influenza virus hemagglutinin protein, where BiP has been suggested to shield cysteine residues during folding and prevent the formation of intermediate disulfide bonds (418). The role of BiP in the unfolded protein response is via an interaction with all three key proteins that control the UPR (protein kinase R (PKR)-like ER kinase [PERK], activating transcription factor 6 [ATF6], and inositol-requiring enzyme 1 [IRE1]), which prevents their activation. Following disassociation from these proteins and activation of the UPR, an increased production of chaperone proteins (including BiP itself) occurs. BiP has previously been implicated in several flaviviral protein interactions, and likely impacts on virus production. This chaperone protein has been shown to be secreted during JEV infection and impact on the infectivity or release of the virus. The authors did not observe any impact on viral replication, and suggested that BiP may be involved in the maturation of virus particles (419). In addition to a role in JEV infection, BiP has also been implicated in DENV infection. Previous studies have determined that BiP interacts with the DENV E protein and can increase production of infectious virions (415). BiP has also been suggested as a possible receptor for DENV in HepG2 cells (a human liver cell line) (420). The upregulation of BiP by activation of the UPR has been shown during WNV infection (121, 421, 422). Moreover, another group has shown by IFA that BiP co-localises with NS1 in WNV infected cells (120). This upregulation of BiP expression may have lead to the observed interaction of BiP with NS1 and NS1' (Table 4.1 – 4.4). It is likely that BiP is functioning to assist in viral protein folding as both virally-expressed and plasmid-expressed NS1 and NS1' could bind to BiP. This in turn may result in the effect on virus infection seen previously (415, 419).

Both eEF-1α and GAPDH were detected in plasmid transfected samples (Table 4.2 and 4.4). While this may be an artefact of overexpression of NS1 and NS1', both eEF-1α and GAPDH have previously been shown to interact with flaviviral proteins. eEF-1α is a well conserved ubiquitous protein that is involved in protein synthesis. This protein interacts with the WNV genomic RNA, co-localises with the WNV replication complex (as shown by co-staining with both dsRNA and NS5/NS3), and has been shown to co-precipitate with JEV NS5 (302, 304, 408). These results suggest that eEF-1α is likely to be involved in the flaviviral replication complex. However, the work shown in this chapter only detected an interaction of NS1 and NS1' with eEF-1α in plasmid transfected cells (Table 4.2 and 4.4), and not in infected cells. As eEF-1α is widely involved in protein translation, it is possible that the interaction between NS1 and eEF-1α is due to co-precipitation with ribosomes during the high level of protein synthesis occurring in plasmid transfected cells. However, the recognition site of the anti-NS1' antibody that was used is towards the C-terminus of the protein, and therefore unlikely to bind to proteins that are still undergoing translation. Therefore, this result is more likely indicative of a protein-protein interaction occurring post-translation.

GAPDH has previously been shown to co-localise with JEV NS5 in infected cells. Though no direct binding between NS5 and GAPDH was observed, the authors determined that GAPDH was able to associate with NS5 via an interaction with viral RNA (423). However, as NS1 and NS1' co-precipitated with GAPDH in transfected cells only, it is unlikely that this interaction is related to the possible role GAPDH has in flaviviral replication. In addition to being localised predominantly to the nucleus and cytosol (424), GAPDH has also been identified on the cell surface. A previous study on surface expressed GAPDH identified a possible role in endocytosis, as a mutation in GAPDH affected the endocytic pathway (specifically the interaction of late endosomes with mirotubules) (425, 426). Interestingly, NS1 has also been shown to accumulate in late endosomes following internalisation of surface bound NS1 by endocytosis (364). Immunofluorescence staining of pcDNA-NS1 and pcDNA-NS1' transfected cells confirmed the presence of NS1 and NS1' on the cell surface (Figure 3.3D). It is possible that the overexpression in transfected cells may have led to an interaction of NS1 and NS1' with GAPDH on the cell surface or in the late endosomes.

The NS1' immunoaffinity purification of transfected cells identified a number of potential NS1'-specific interactions. While these proteins initially seemed to be interacting with NS1', several are unlikely to represent true interactions, based solely on their cellular localisation. For example, ADP-ATP translocase 2, which was detected in all 4 independent experiments, is a transporter

protein localised to the mitochondria (427-429). ATP synthase, various subunits of which were identified in all 4 experiments, is an enzyme also localised to the mitochondria that is involved in ATP synthesis (430). T-complex protein 1, detected in two independent experiments, is a molecular chaperone protein, though it is usually present in the cytosol (431), and therefore unlikely to interact with NS1' in cells. L-lactate dehydrogenase is also located in the cytosol of cells and involved in lactate metabolism (432). While the voltage dependent anion selective channel protein 1 has more recently been identified on the plasma membrane of cells, it is better characterised as a mitochondrial protein (433, 434). The proteins outlined here have a distinct cellular localisation that indicates that the co-precipitation with NS1' seen is more likely due to an artificial interaction during or after cell lysis preparation.

However, not all of the proteins identified in NS1' affinity purification of transfected cells have such a clear cellular localisation that suggests an artificial interaction. Prohibitin is predominantly localised to the mitochondria, but both prohibitin 1 and 2 have been identified to have varying cellular localisation (435). Interestingly, prohibitin has been suggested to have some activity as a viral receptor protein, having been identified as a receptor for Chikungunya virus (CHIKV) in microglial cells (436) and DENV (but specifically not JEV) in insect cells (437). Prosaposin is a precursor protein that is processed into four individual glycoportiens known as saposins A-D. While it is predominantly localised to lysosomal compartments where processing to individual saposins occurs, prosaposin also exists as a membrane-bound and secretory protein (438). It is unclear why these particular proteins were detected in anti-NS1' and not anti-NS1 immunoprecipitation, however, this suggests that they are unlikely to be true interactions. These interactions may be observed due to some unforeseen effect of the immunoaffinity purification that only occurred in transfected cells combined with the anti-NS1' antibody.

In this chapter, we were unable to successfully identify unique proteins interacting with NS1'. However, the results shown here have confirmed that NS1' interacts with members of the replication complex during infection, and is therefore likely to be functioning in viral replication. The interaction of NS1 and NS1' with the molecular chaperone protein BiP is likely indicative of the stressed state of the infected or transfected cells, resulting in an upregulation of chaperone proteins to assist in protein folding. It is unclear from the results shown in this chapter whether this interaction between NS1/NS1' and BiP is important for viral replication. The observed interactions of NS1 and NS1' with eEF-1α and GAPDH are more likely due to the overexpression of NS1 and NS1', and may not represent true protein-protein interactions that would occur during viral infection. Several of the potential NS1'-specific interactions observed in NS1' immunoaffinity

purification of transfected cells were likely due to an artificial interactions occurring during or after lysing cells, as the known cellular localisation of these protein suggests that they would not come in contact with NS1'. In addition to this, the failure to confirm these potential protein interactions in any of the other three conditions used reinforces the hypothesis that these interactions represent an artefact of the procedure.

The lack of detection of unique NS1'-interacting proteins and confirmation of NS1' functioning in viral replication further supports the hypothesis that NS1' may not have a unique function in viral infection. The production of NS1' may simply be a consequence of regulation of viral gene expression by the -1 PRF. Further work examining the protein-protein interactions identified here is necessary to confirm NS1' functioning as NS1.

5 NS1' secretion and stable dimerisation

5.1 Introduction

Following NS1 cleavage from the flaviviral polyprotein (335, 161), it is glycosylated at either 2 or 3 sites (341, 333) and rapidly dimerises (348, 333). The formation of an NS1 dimer is a consistent feature of all flaviviruses. This detergent resistant, heat-sensitive dimer (347, 333) was first identified through SDS-PAGE analysis of infected mammalian or insect cell lysate (332, 333). Formation of NS1 dimers relies on 12 cysteine residues in NS1 that form 6 intramolecular disulfide bonds. The importance of these disulfide bonds has been shown previously, with mutagenesis studies indicating that at least the C-terminal 3 cysteine residues were critical for proper folding of NS1, and subsequently maturation, secretion and oligomerisation (338). The NS1 dimer has been shown to be important for viral pathogenesis, with a single amino acid substitution at residue 250 of WNV_{KUN} and MVEV NS1 resulting in a lack of detectable NS1 dimers that correlated with reduced neuroinvassiveness in mice (349, 350). However, this mutation did not completely ablate virus replication, suggesting that dimeric NS1, while important for pathogenesis, is not essential for virus replication.

Once dimerised, a proportion of NS1 is trafficked through the Golgi, where the high mannose carbohydrates are processed to more complex sugars. Here NS1 forms a soluble hexamer, which is subsequently secreted from infected mammalian cells, though not from insect cells (439, 440, 357, 331, 352, 400, 332). This is likely to be due to insect cells lacking the machinery for proper processing of NS1 glycans into complex carbohydrate forms (4). The hexameric form of NS1 is held together by weak hydrophobic interactions which are disrupted by detergent treatment (352). Observation of the hexamer without prior cross-linking is therefore difficult, as detergents that disrupt the hexameric form to dimers are present in lysis buffers and during SDS-PAGE analysis. Chemical cross-linking of extracellular fluid, or SDS-PAGE carried out with very low levels of SDS are required to detect even small amounts of the hexameric species, though neither technique shows complete retention of this native form (357, 331, 352).

To examine the NS1' protein in isolation, an NS1'-expressing plasmid (pcDNA-NS1') was developed as outlined in chapter 3 of this thesis (Section 3.1). During the initial characterisation of the pcDNA-NS1' plasmid, the presence of a sub-population of heat-stable NS1' dimers was discovered (Figure 5.1A). These heat-stable dimers had not been identified previously. Work conducted in JEV infected cells noted only the presence of heat-labile NS1' dimers in addition to

the well-characterised heat-labile dimers formed by NS1 (387). The presence of heat-stable NS1' dimers was also detected in WNV_{KUN} infected cells (Figure 5.1B), confirming that this property was not an artefact of plasmid expression. The heat-stable dimers were sensitive to treatment with reducing agents (results obtained during my honours project), suggesting that the heat-stability may be due to the presence of an intermolecular disulfide bond. In addition to the formation of NS1 and NS1' homodimers, the presence of a NS1/NS1' heterodimer has previously been suggested for both JEV and MVEV (382, 387, 388). Initial work in infected cells conducted during my honours project has indicated that this heterodimer may be formed during WNV_{KUN} infection as well (Figure 5.1B).

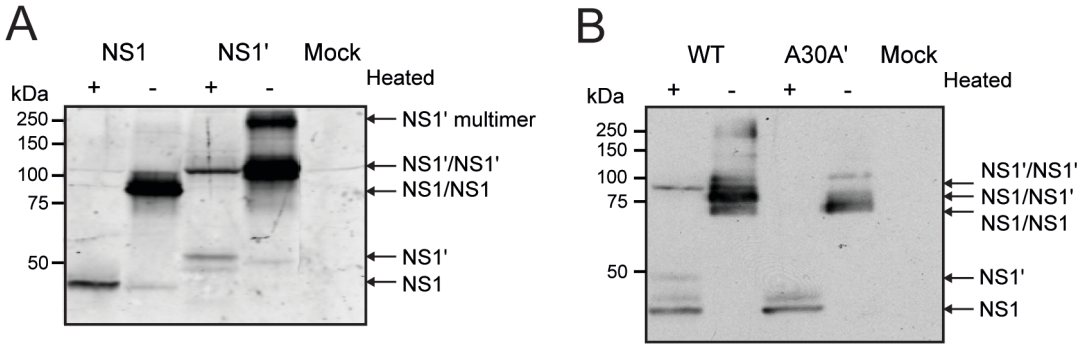

Figure 5.1 Identification of heat-stable NS1' dimers in transfected and infected cells. A. Western blot showing expression of NS1 and NS1' from pcDNA-NS1 and pcDNA-NS1' transfected 293T cells, respectively. Lysates were heat denatured or left untreated and analyzed by Western blotting with anti-NS1 (4G4). **B.** Western blot showing expression of NS1 and NS1' from WNV_{KUN} and NS1 only from A30A' mutant infected Vero76 cells. Lysates were heat denatured or left untreated and analyzed as above.

The work presented in this chapter aims to further characterize the heat-stable nature of the NS1' dimer and determine the region of the frameshifted sequence that contributes to heat stability. In addition, secretion of WNV_{KUN} NS1' was examined, as previous work conducted in JEV infected cells suggested that there is only low level secretion of NS1' during JEV infection (387, 332). Dimerisation and secretion of NS1 are important for flaviviral pathogenesis, and a clearer understanding of these properties of the NS1' protein may lead to the identification of a unique role for NS1' in viral infection.

5.2 Results

5.2.1 Heat-stable NS1' dimers are unique to WNV.

Previous studies on JEV NS1' have shown only the presence of heat-labile NS1' dimers (387), which is contrary to our findings for WNV_{KUN} NS1'. To examine this further, lysates from JEV, MVEV, WNV_{NY99} and WNV_{KUN} infected Vero76 cells were subjected to SDS-PAGE and Western blotting with anti-NS1 antibodies to determine the presence or absence of heat-stable NS1' dimers. Heat-stable NS1' dimers were only detected in heated WNV (NY99 and KUN) samples (Figure 5.2, lanes 5 and 7), but not JEV or MVEV samples, showing that these dimers are unique to WNV.

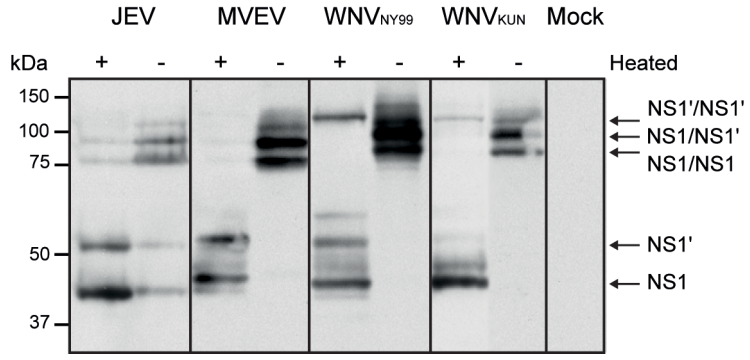

Figure 5.2 Heat-stable NS1' dimers are unique to WNV infected cells. Lysates harvested from JEV, MVEV, WNV_{NY99} and WNV_{KUN} infected Vero cells were heated (70°C for 10 min) or left untreated and proteins were separated by SDS-PAGE. Proteins were transferred to nitrocellulose membranes and NS1 and NS1' were detected with an anti-NS1 mAb (4G4).

5.2.2 WNV NS1' dimers are heat and low pH resistant.

Previous work by Falconar and Young (347) has shown that NS1 dimers are stable at low pH (pH 3.5). To assess the pH stability of NS1' dimers, pcDNA-NS1 or -NS1' transfected cell lysates (Figure 5.3A) and WNV_{KUN} or A30A' infected cell lysates (Figure 5.3B) were incubated for 1 h with 1M glycine buffered to the indicated pH prior to separation by electrophoresis. NS1 dimers were indeed stable until the pH was lowered to 3.5, while a sub-population of NS1' dimers were still stable at the lowest pH tested, pH 2.2. A range of temperature treatments was also tested on the same lysates to further examine the heat-stability (Figure 5.4). While NS1 dimers were stable at room temperature, heating to 60°C for 30 min was enough to begin to disrupt the dimeric interaction. NS1' on the other hand, forms a sub-population of dimers that were still stable at the

highest temperature tested. The sub-population of NS1' that does not have this heat-stable nature has a similar stability to NS1 dimers, with respect to both temperature and pH treatment.

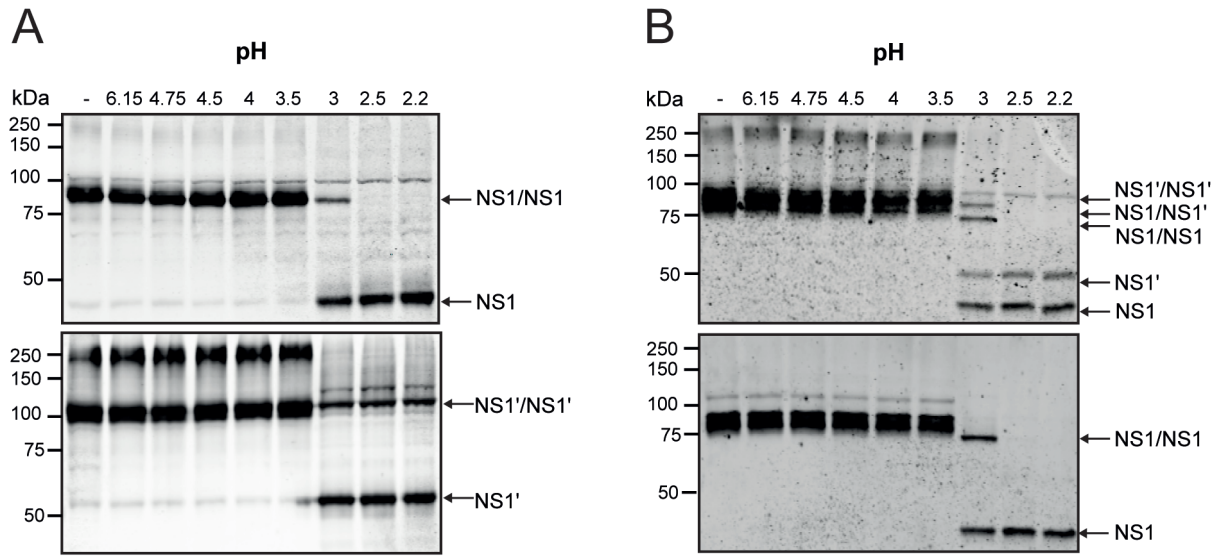

Figure 5.3 pH-stability of NS1 and NS1' dimers. Lysate from **A**) transfected or **B**) infected cells was incubated with 1M glycine at the indicated pH prior to separation by electrophoresis and western blotting with anti-NS1 (4G4). Top panel is either pcDNA-NS1 transfected (A) or WNV_{KUN} infected (B) and bottom panel is either pcDNA-NS1' transfected (A) or A30A' infected (B).

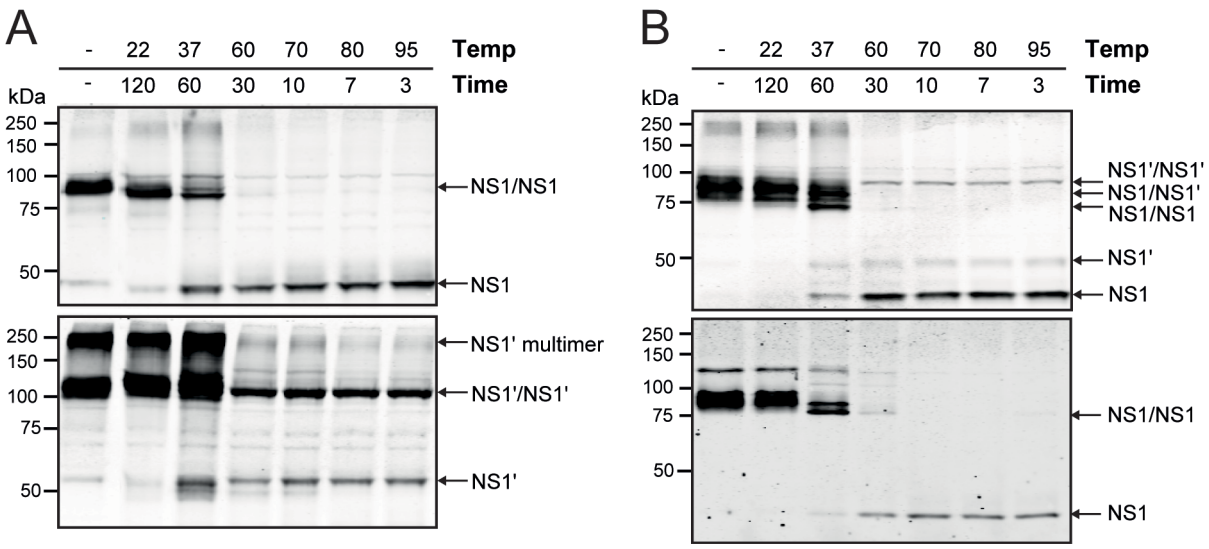

Figure 5.4 Heat-stability of NS1 and NS1' dimers. Lysate from **A**) transfected or **B**) infected cells was incubated at the indicated temperature for the time shown prior to separation by electrophoresis and western blotting anti-NS1 (4G4). Top panel is either pcDNA-NS1 transfected (A) or WNV_{KUN} infected (B) and bottom panel is either pcDNA-NS1' transfected (A) or A30A' infected (B).

5.2.3 NS1' dimer stability resides within penultimate 10 amino acids.

As the NS1' heat-stable dimers are distinct from the heat-labile dimers formed by NS1, the stability must be linked to the presence of the frameshifted region of NS1'. To determine the region contributing to this stability, C-terminal 10- and 20-amino acid truncations of NS1' were generated by PCR mutagenesis of pcDNA-NS1' (Figure 5.5A). The presence of heat-stable dimers was determined by SDS-PAGE and Western blot analysis of heated or unheated lysates generated from HEK293T cells transfected with pcDNA-NS1, -NS1', -NS1'del10 or -NS1'del20. NS1' and NS1'del10 both formed a sub-population of heat-stable dimers (Figure 5.5B, lanes 3-4 and 5-6 respectively), while NS1'del20 formed only heat-labile dimers (lanes 7-8), similar to those produced by NS1 (lanes 1-2). Interestingly, NS1'del20 also eliminated NS1' multimer that can be observed in both NS1' and NS1'del10 unheated samples (Figure 5.5 lanes 4 and 6 respectively). This indicates that the stable nature of the NS1' dimers can be linked to the penultimate 10 amino acids.

To determine whether the loss of heat-stable dimers in pcDNA-NS1'del20 transfected cells was due to the specific amino acid sequence, or to a minimum length requirement of the frameshifted region, amino acids 385 to 393 were mutated to alanine (Figure 5.5A). SDS-PAGE and Western blot analysis of lysate from pcDNA-NS1'Ala transfected cells showed that NS1'Ala is similar to NS1'del20, as it does not form heat-stable dimers (Figure 5.5B, lanes 9 and 10). This confirms that the heat-stable dimerisation is linked to the specific sequence of amino acids 385-394, rather than to the length of NS1'.

Due to the presence of a cysteine (Cys) residue within the mutated 10 aa region of NS1', we hypothesized that a disulfide bond may be forming between monomeric units, creating the heat-stability seen. This was also supported by the fact that the dimers are sensitive to treatment with reducing agents. However, mutagenesis of this Cys residue to Ser (Figure 5.5A) failed to prevent the formation of the heat-stable NS1' dimers (Figure 5.5B, lanes 11 and 12) showing that this Cys is not involved in formation of heat-stable NS1' dimers.

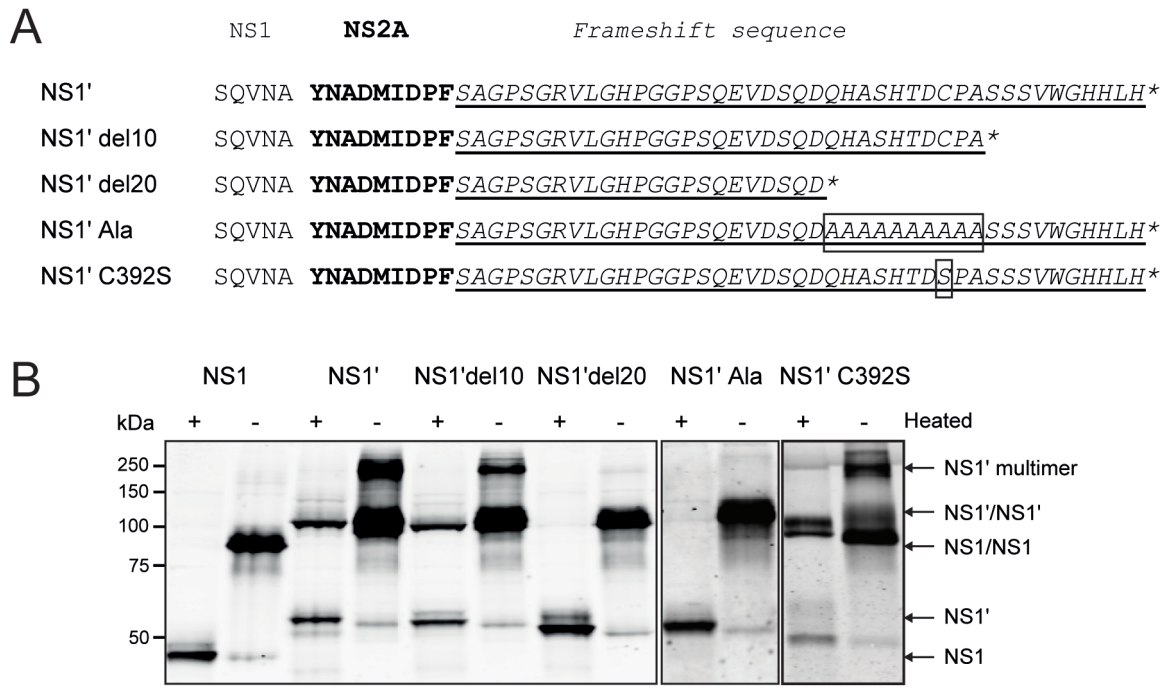

Figure 5.5 Region at the C-terminus of NS1' contributing to formation of heat-stable dimers. A. Design of C-terminally truncated (NS1'del10 and NS1'del20) or mutated (NS1'Ala and NS1' C392S) pcDNA-NS1' constructs to assess the region of NS1' contributing to heat-stable dimers. Underlining shows the frameshifted region of NS1', boxed residues show amino acid substitutions and asterisk (*) shows stop codons. **B.** Lysates harvested from HEK293T cells transfected with pcDNA-NS1, -NS1', -NS1'del10, -NS1'del20, -NS1'Ala or -NS1' C392S were heated (70°C for 10 min) or left untreated and proteins were separated by SDS-PAGE. Proteins were transferred to nitrocellulose membranes and detected with anti-NS1 mAb (4G4).

5.2.4 NS1 and NS1' form heterodimers in infected and co-transfected cells.

The presence of NS1/NS1' heterodimers has been suggested previously for JEV and MVEV (382, 387, 388). From the work shown in this chapter in infected cells, it was apparent that this heterodimer is also produced in WNV_{KUN} and WNV_{NY99} infected cells, as three distinct dimeric bands were identified in unheated cell lysate (Figure 5.2, lanes 8 and 6 respectively). To confirm that this is indeed an NS1/NS1' heterodimer, 293T cells were singularly-transfected or co-transfected with pcDNA-NS1 and pcDNA-NS1'. Cell lysates were either heated or left untreated prior to separation by SDS-PAGE. Proteins were transferred to nitrocellulose membrane and analysed by Western blotting with anti-NS1 mAb (4G4), to detect both NS1 and NS1'. As expected, single dimeric bands corresponding to the NS1 and NS1' homodimer were detected in unheated pcDNA-NS1 and pcDNA-NS1' singularly-transfected samples, respectively (Figure 5.6, lanes 2 and 4). However, in the unheated co-transfected sample, three distinct dimeric bands were observed

(Figure 5.6, lane 6). The heterodimer was dissociated by heat-treatment, suggesting that unlike the NS1' homodimer, the NS1/NS1' heterodimer is heat-labile. This indicates that also in the absence of a viral infection, NS1 and NS1' are able to form heat-labile heterodimers.

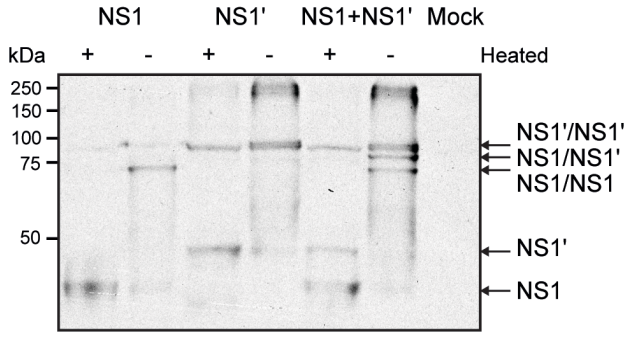

Figure 5.6 Formation of NS1/NS1' heterodimers in transfected cells. Lysate from 293T cells transfected with pcDNA-NS1, pcDNA-NS1' or co-transfected with both pcDNA-NS1 and pcDNA-NS1' was heated (70°C for 10 min) or left untreated and proteins were separated by polyacrylamide gel electrophoresis. Proteins were transferred to nitrocellulose membranes and detected with anti-NS1 (4G4) antibodies.

5.2.5 WNV NS1' is secreted less efficiently than NS1.

It has been shown previously that JEV NS1', unlike NS1, is not secreted efficiently from infected cells (387, 332). To determine whether this is also the case for WNV_{KUN} NS1', pulse-chase experiments were carried out. Radiolabelled NS1 and NS1' were detected in both the cell monolayer and culture fluid of WNV_{KUN} infected Vero76 cells at 24 or 72 h pi (Figure 5.7A and B, respectively). Quantification of individual protein bands and determination of the extracellular/intracellular ratio (E/I) showed that NS1' is consistently secreted to a lower degree compared to NS1 (Figure 5.7). To confirm the low level secretion of NS1' seen in infected cells is not due to the presence of other viral proteins, the secretion of NS1 and NS1' was examined in the context of plasmid transfected cells. A similar secretion pattern could be seen for NS1 and NS1' expressed from pcDNA-NS1 and pcDNA-NS1' transfected 293T cells (both co- and individually-transfected) at 24 and 48 h post transfection (Figure 5.8A and B, respectively). Again, the E/I ratio showed that NS1' (whether individually- or co-transfected) was secreted to a significantly lower degree than NS1 (Figure 5.8C). These results indicate that the frameshifted region of NS1' results in increased cellular retention of NS1' compared to NS1.

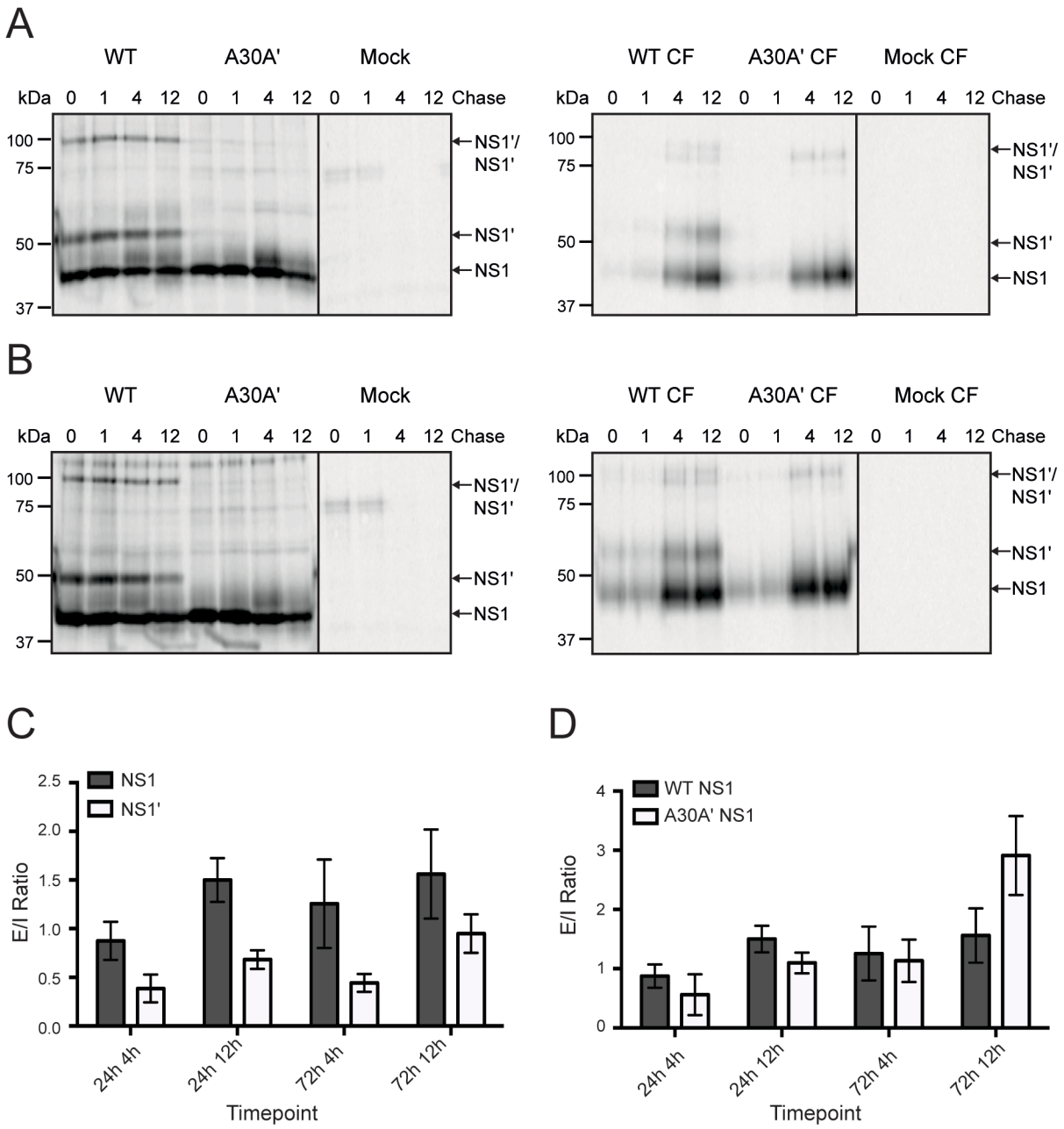

Figure 5.7 NS1 and NS1' production and secretion from infected cells. A-B. Production and secretion of NS1 and NS1' from Vero cells infected with WNV_{KUN} or A30A'. Pulse-chase was performed at **A**. 24 or **B**. 72hpi, culture fluids (CF) were clarified by centrifugation and cell monolayers were lysed as described. Protein preparations were immunoprecipitated with anti-NS1 (4G4) using Dynabeads® Protein G. Antibody-bound proteins were eluted and samples subjected to electrophoresis. Labeled proteins were transferred to nitrocellulose membranes and exposed to phosphor screen for 1 day. Left-hand panels show immunoprecipitated cell monolayer lysate and right-hand panel shows CF. **C**. Extracellular/intracellular ratio for NS1 and NS1' produced by infected cells confirms that NS1' is secreted to a lower degree compared to NS1. **D.** E/I ratio for WT NS1 and A30A' NS1 indicates that the presence of NS1' does not affect the secretion of NS1. Results are expressed as the mean ± SEM of two independent experiments.

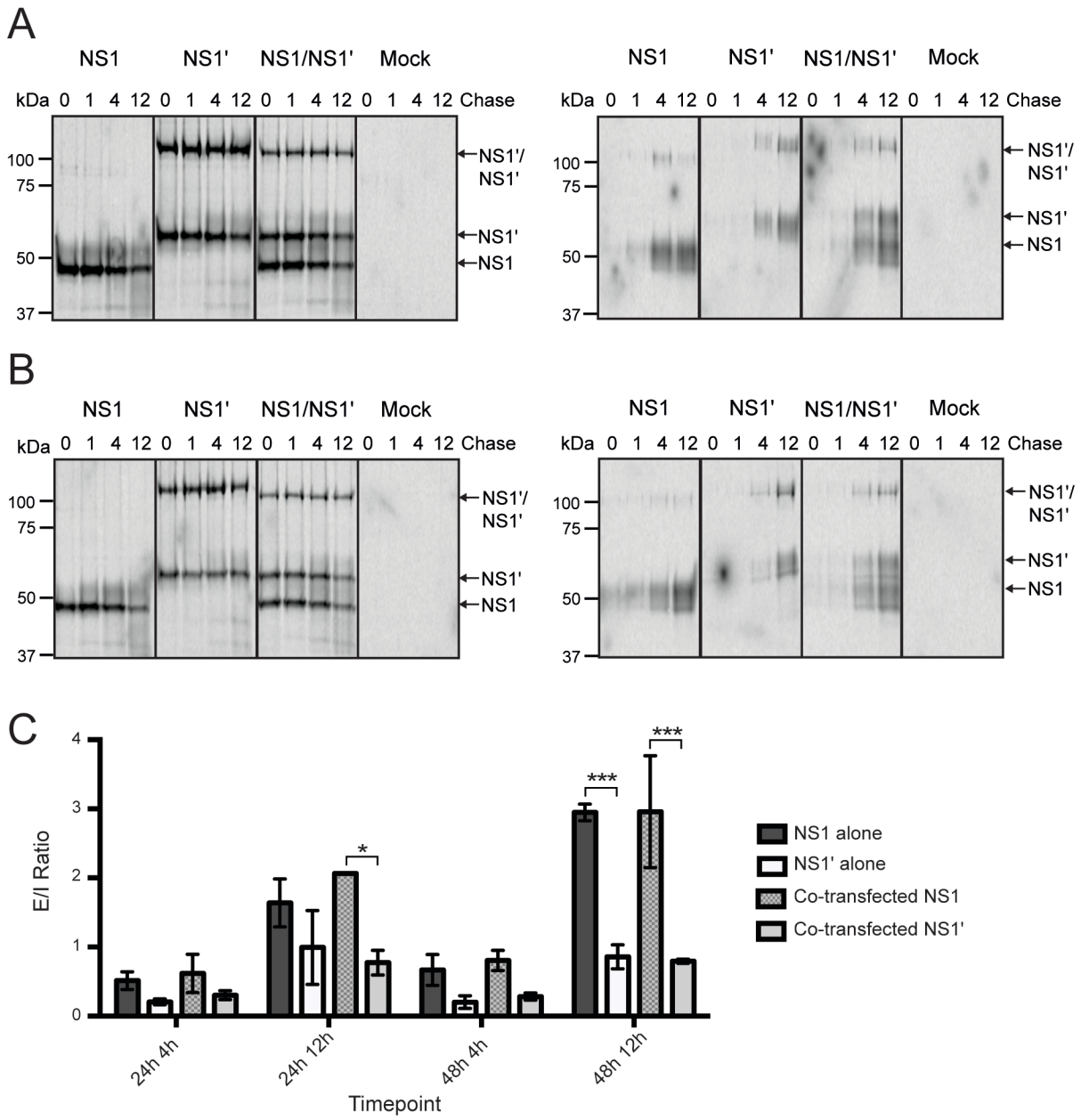

Figure 5.8 NS1 and NS1' production and secretion from transfected cells. A-B. Production and secretion of NS1 and NS1' from transfected or co-transfected 293T cells. Pulse-chase was performed at **A**. 24 or **B**. 48 hours post transfection and samples processed as outlined in Figure 5.8. Left-hand panels show immunoprecipitated cell monolayer lysate and right-hand panel shows CF. **C**. Extracellular/intracellular ratio for NS1 and NS1' produced by transfected cells confirms that NS1' is secreted to a lower degree compared to NS1. Results are expressed as the mean ± SEM of two independent experiments and significance (*** [$P < 0.001$] or * [$P < 0.01$]) determined by 2-way ANOVA.

As NS1 and NS1' form a heterodimer in both infected and co-transfected cells, it is possible that this interaction may affect NS1 secretion. In spite of this interaction, comparison of the E/I ratio for either co- or singularly-transfected NS1 or NS1' indicates that the presence of NS1' does not affect the secretion of NS1, and vice versa (Figure 5.8C). This can also be seen in the comparison between NS1 expressed from WNV_{KUN} infected cells and A30A' infected cells (Figure 5.7D), where the presence of NS1' (in WNV_{KUN} infected cells) does not affect the efficiency of NS1 secretion.

5.3 Discussion

The work shown in this chapter was carried out to further investigate a sub-population of heat-stable NS1' dimers that are produced in infected and plasmid transfected cells. This is the first identification of heat-stable NS1' dimers and results shown here indicate that this heat-stability is so far unique to WNV (Figure 5.2). This is consistent with previous studies carried out with JEV or MVEV that have identified only the presence of heat-labile NS1' dimers (382, 387, 383, 332, 381). The heat-stable dimerisation could be linked to the specific sequence between amino acids 385-394 (Figure 5.5). This does not mean that the sequence contributing to heat-stable dimerisation must be entirely contained within this region, but it is likely to at least span these amino acids. Interestingly, although there is ~46% conservation between the examined flaviviruses, there is no conservation at all for amino acids 385-394 between WNV NS1' (both WNV_{KUN} and WNV_{NY99}) and the other encephalitic flavivirus NS1' (Figure 5.9). WNV_{KUN} and WNV_{NY99} have 8 conserved residues between amino acids 385-394, suggesting that the two non-conserved residues are not involved in the formation of heat-stable dimers. Future work to further narrow down the region resulting in heat-stable dimerisation would be particularly interesting to determine whether the potential dimerisation motif present is conserved through additional WNV lineages.

	NS2A	*Frameshift sequence*
		385 394
WNV_{KUN}	**YNADMIDPF**	*SAGPSGRVLGHPGGPSQEVDSQDQHASHTDCPASSSVWGHHLH**
WNV_{NY99}	**YNADMIDPF**	*SVGPSGRVLGHPGGPSQEVDSQDQHASYTDCSASPGVWGHYLH**
JEV	**FNGEMVDPF**	*SAGPSGDVSGHPGGPSQEVDGQIDHSCGFGGPTCADAWGHHLH**
MVEV	**FNGDMIDPF**	*SVRPSGDVSGHPGGLEEEVDGQTYSASSGWGSASPPPWGHYLH**
WNV conserved	YNADMIDPFS	GPSGRVLGHPGGPSQEVDSQDQHAS TDC AS VWGH LH*
JEV serogroup conserved	N M DPFS	PSG V GHPGG EVD Q WGH LH*

Figure 5.9 NS1' frameshift sequence conservation. Underlining shows the frameshifted region contributing to heat-stable dimer formation and asterisk (*) shows stop codons. Amino acids conserved for WNV species only or conserved between all examined members of JEV serogroup (WNV, JEV and MVEV) are indicated. Virus sequences used: WNV_{KUN} – GenBank:AY274504; WNV_{NY99} – GenBank:NC_009942; JEV – GenBank:NC_001437; MVEV – GenBank:NC_000943.

The increased stability observed here for NS1' has provided insight into the cell associated form of NS1', and potentially NS1. Due to the increase in dimer stability, it is possible to observe higher order oligomeric forms in unheated SDS-PAGE analysis of WNV_{KUN} NS1'. Indeed, when

this dimer stability was abolished by truncation or mutation, not only were the heat-stable dimers affected, but also the detergent-stable oligomers. Based on the observed size on SDS-PAGE gels, these are likely to be hexamers; however, further confirmation would be required. These higher order oligomers are still observed in SDS-PAGE analysis when cell lysates were treated with iodoacetamide (to prevent disulfide exchange post-lysis), suggesting that the potential hexamer seen is a natural state, not a product of lysis (data not shown). This data may also shed light on the cell associated form of NS1, which is still unknown (4). The NS1 hexamer is held together by only weak hydrophobic interactions that are disrupted to dimers by detergent treatment (352), such as those required for cell lysis. The observation of higher order oligomers formed by NS1' may indicate that the subtle increase in stability seen for WNV_{KUN} NS1' is enough to allow us to observe the natural state of intra-cellular NS1' without the need for cross-linking.

One key characteristic examined in this chapter was the inefficient secretion of NS1', despite no distinct hydrophobic region present in the frameshifted sequence. The results shown here indicate that NS1' is secreted from infected and transfected cells, although less efficiently than NS1 (Figure 5.7 and 5.8). In contrast to what has been shown in this chapter, and what has been seen in infected cells (Fig. 5.7 and 5.8, and (332)), previous work with plasmid expression of JEV NS1 and NS1' has suggested that NS1' is not secreted at all from transfected cells (388). However, this work was conducted prior to the confirmation that NS1' is produced by a ribosomal frameshift (384, 1, 390), when it was assumed to be an alternate cleavage product. The plasmid design for NS1' (NS1 with an additional 60 amino acids of NS2A; (388)) was likely to have been producing a fusion of NS1-NS2A, possibly without effectively frameshifting to produce NS1' itself. As the authors suggested, the hydrophobic nature of the N-terminal NS2A amino acids may have been resulting in the inhibition of protein secretion seen. However, we have shown here that when properly produced, NS1' is secreted from plasmid transfected cells.

NS1 is trafficked to several different locations during viral infection, including the cell surface and secreted to the extracellular fluid. Secretion of NS1 to the extracellular fluid occurs through the Golgi pathway, and while a small amount of secreted NS1 has been shown to bind back to cells via an interaction with glycosaminoglycans (363), the majority of NS1 present on the surface of infected cells is due to an as yet unclear trafficking pathway, that is likely distinct from Golgi trafficking (4). Lin *et al* has previously suggested that the presence of NS1' affects the normal trafficking of NS1 (388). The authors determined that co-expression of JEV NS1 with authentic NS1' (through the use of a full-length NS1-NS2A plasmid system) reduced the cell surface expression of NS1 (388). The work conducted in this chapter suggests that the presence of WNV

NS1' does not impact on secretion of NS1 from cells, highlighting potential differences between NS1 trafficking to the cell surface and NS1 secretion. This work examined the presence of NS1 and NS1' in the extracellular fluid, and determined that the presence of NS1' (through co-transfection of pcDNA-NS1 and pcDNA-NS1' and through comparison of NS1'-expressing and NS1'-lacking viruses) does not affect NS1 secretion. The observation that NS1' may affect NS1 surface expression (388) but not secretion (work shown in this chapter) could be explained in several ways. First, it is possible that JEV and WNV NS1 and NS1' behave differently. There have been several previous studies highlighting differences between flaviviral NS1 species (371, 367), with one recent paper identifying just two N-terminal amino acid differences between WNV and DENV NS1 (RQ10NK) directly impacting on secretion vs. cell surface localisation (367). The same analysis has not yet been conducted for JEV, which contains arginine at position 10 (same as WNV) and lysine at position 11 (same as DENV). Secondly, it is possible that differences in glycosylation states affect secretion vs. cell surface expression. JEV and WNV NS1 have a different glycosylation pattern (344, 339), and it has been shown previously that glycosylation affects secretion to the extracellular fluid but not trafficking to the cell surface (367). Finally, it is possible that the presence of NS1' may affect trafficking to the cell surface, but not to the extracellular fluid. The specific pathway NS1 takes to the cell surface remains unclear, and it is possible that the presence of NS1' may impact this pathway alone. Previous work suggests that cell surface NS1 exists as a dimer (351), while it is secreted as a hexamer (352). It has been suggested that dimer trafficking to the cell surface occurs earlier in infection, and that increased concentrations of NS1 later in infection increases the chance of dimers forming hexamers (332, 4). It is therefore possible that heterodimerisation with NS1' may affect early NS1 trafficking to the cell surface, but not secretion to the extracellular fluid once NS1 concentrations have increased.

The presence of heat-stable NS1' dimers that are sensitive to reducing agents suggested the presence of a disulfide bond; however, mutagenesis of the Cys residue within the frameshifted region indicates that it is not due to a simple interaction between the C-terminal Cys residues of two monomers. It has previously been suggested (M. Lobigs, personal communication) that NS1 may itself catalyse disulfide bond exchange. Viral proteins have been identified previously to contain the disulfide isomerisation motif, CXXC. One example is the Human T-cell leukemia virus 1 envelope protein, which contains a CXXC motif that controls intersubunit disulfide isomerisation, mediating the viral fusion reaction (441). NS1 contains a CXXC motif that is conserved for DENV, YFV and the JEV serogroup. These Cys residues (C10 and C11) have been shown previously to be important for dimer formation and NS1 secretion (338). It has been hypothesised that NS1 may be involved in its own folding, as well as that of other flaviviral proteins, such as E. This may explain the

interaction between NS1 and E seen during viral infection (382). It is possible that the presence of the frameshifted region in NS1' may in fact impede folding of this C-terminally extended NS1 protein. The heat-stable dimers observed may therefore represent folding intermediates involving intermolecular disulfide bonds between covalently linked NS1' monomers. On the other hand, as these heat-stable dimers appear to be secreted to some degree (Figure 5.7 and 5.8), they are unlikely to represent misfolded protein, as this would be retained in the cell. However, only a small amount of NS1' is secreted from the cell, and it is therefore difficult to conclusively determine the dimer stability. Further work analysing the nature of these heat-stable NS1' dimers and the possibility of the involvement of NS1 in disulfide bond exchange is necessary.

The research carried out for this chapter has identified a sub-population of heat-stable NS1' dimers unique to WNV that is produced and secreted in infected and plasmid transfected cells. The stability of these dimers is dependent on amino acids 385-394; though not specifically to the cysteine reside at position 392. This heat-stable nature is distinct from the heat-labile dimers formed by NS1, and in combination with the inefficient secretion compared to NS1, suggests that the NS1' protein may not solely behave like NS1.

6 NS1' Mutagenesis

6.1 Introduction

While initially thought to be the product of an alternate cleavage site present in NS2A (381), it has since been determined that NS1' is produced by a -1 programmed ribosomal frameshift (PRF) occurring at the beginning of the adjacent NS2A gene (384). This ribosomal frameshift consists of two conserved motifs, a heptanucleotide "slippery" site followed by an RNA pseudoknot. The requirement of both these signals for the production of the WNV_{KUN} NS1' protein was previously confirmed experimentally by our group. This was done through the use of two mutant viruses: A30A', which mutates two nucleotides involved in the formation of the pseudoknot (NS2A nucleotides C90U and G93A), and FSSM (or frameshift silent motif), which introduced two mutations into the slippery heptanucleotide (NS2A nucleotides U24A and U27C). Neither of these mutant viruses produce NS1', and both showed reduced virulence in a mouse model without notably affecting viral replication in BHK or C6/26 cells (1). The requirement for the pseudoknot in the formation of JEV NS1' has also been shown experimentally, with mutations disrupting the pseudoknot abolishing NS1' production (386). In agreement with the work carried out in WNV_{KUN}, JEV mutant viruses lacking the PRF and NS1' showed attenuation of virulence in a mouse model (390).

As the flaviviral genome is translated as a single polyprotein, the presence of the PRF (and subsequent stop codon producing NS1') was hypothesized to alter the ratio of proteins upstream of the frameshift site *vs* those downstream from equimolar to a greater amount of those upstream. Therefore, frameshifting could be measured as a ratio of structural proteins (such as E) to non-structural proteins (such as NS5). Abolishing the PRF in the mutant viruses (such as A30A') would result in a decrease in the ratio of structural to non-structural proteins relative to the wild-type virus. Experimental work conducted in our laboratory confirmed this hypothesis by measuring the structural to non-structural protein ratio for wild-type WNV_{KUN} and A30A', showing that the ratio is indeed reduced for the PRF-lacking virus (389). The authors also showed that a lack of PRF/NS1' results in a reduced virulence in house sparrows, and affected viral replication, spread and transmission in *Culex* mosquitoes. However, while this study clearly showed an effect of the PRF on the ratio of structural to non-structural proteins, this cannot be conclusively linked to the attenuation seen in sparrows and mosquitoes, as the virus used (A30A') lacks both the PRF and NS1'.

Recent work carried out with JEV has suggested a possible role for NS1' in assisting virus production in avian cells by increasing viral RNA levels (396). The authors also showed that NS1' was in fact expressed more efficiently in avian cells than mammalian cells (chicken embryonic fibroblasts, DF-1, *vs* baby hamster kidney, BHK, cells). Finally, it was shown that infection with NS1'-exressing viruses resulted in a higher mortality rate in embryonated chicken eggs (ECEs). These data suggested that NS1' facilitates JEV viral infection in an avian system (396). However, as with the work carried out with WNV_{KUN} NS1'-lacking viral mutants, the observed effect could be either due to the function of NS1', the presence of the PRF itself, or a combination of both factors.

NS1'-lacking WNV_{KUN} mutants that are currently utilized, such as A30A', abolish NS1' production through mutation eliminating the ribosomal frameshift. Any subsequent effect observed may be due to either the lack of NS1' or the frameshift itself. Separation of these competing factors is necessary to fully understand the function of the NS1' protein. This chapter aims to characterise new viral mutants designed specifically to affect wild-type NS1' production and not the ribosomal frameshift.

6.2 Results

6.2.1 Design of Stop Mutant and SCMU

Two mutant WNV_{KUN} viruses, Stop Mutant and Scrambled Mutant (SCMU), were designed to affect wild-type NS1' production without affecting the predicted frameshift (Figure 6.1). Stop mutant introduces a premature stop codon 20 amino acids from the end of NS1', resulting in a truncated version of the protein. Due to the nature of the ribosomal frameshift, and NS1' being encoded in the -1 open reading frame of NS2A, it was not possible to create an alanine mutant in the viral context without affecting the coding sequence of NS2A. Instead, SCMU was created, which altered 19 of the last 20 amino acids based on what nucleotide changes could be made without affecting NS2A (Figure 6.1). The purpose of these mutants was to separate the effect of the frameshift (which should still be intact) from that of the NS1' protein per se on virus growth and virulence properties.

Figure 6.1 Design of mutant viruses with altered NS1' production. A. Nucleotide sequence of the frameshifted region of wild-type (WT), Stop Mutant and SCMU NS1'. Single nucleotide mutations were introduced to the WT NS1' sequence to introduce a stop codon (green) or to alter the amino acid sequence in NS1' (yellow). **B.** Amino acid sequence of WT, Stop Mutant and SCMU NS1'. Underlining shows the frameshifted region of NS1', boxed nucleotides show mutated amino acids and asterisks (*) shows stop codons.

Prior to cloning these mutations into the full-length infectious clone, the mutations were introduced into a cassette containing the C-terminal 26 amino acids of E through to the end of NS2A (pcDNA-E-NS2A). This was carried out to ensure that the designed mutations, which did not directly mutate the nucleotides involved in pseudoknot formation, did not have an unforeseen effect on the ribosomal frameshift. Using site directed PCR mutagenesis, a single point mutation was introduced into pcDNA-E-NS2A to generate pcDNA-E-NS2A-StopMutant. Similarly, 19 nucleotide changes were introduced into the NS2A gene to generate pcDNA-E-NS2A-SCMU. The presence of NS1 and NS1' was determined by SDS-PAGE and Western blot analysis of heated or unheated lysates generated from HEK293T cells transfected with pcDNA-E-NS2A-StopMutant or pcDNA-E-NS2A-SCMU. Both 4G4 (anti-NS1 monoclonal antibody) and NS1'-specific antibodies (FS-ab) detected a protein band corresponding to the predicted size of the truncated NS1' in pcDNA-E-NS2A-StopMutant transfected lysate (Figure 6.2). While a clear protein band at the expected size of NS1' was detected by 4G4 in SCMU samples, there was poor detection of this same band by NS1'-specific antibodies. This suggests that the nature of the mutations in SCMU may have affected the recognition site of the NS1'-specific antibody, not by direct mutation of the site, but possibly by affecting protein folding.

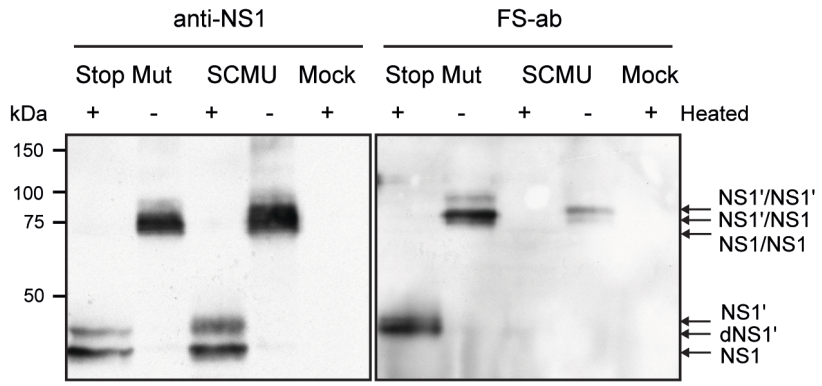

Figure 6.2 Production of NS1 and NS1' from mutated pcDNA-E-NS2A cassettes. Western blot showing expression of NS1 and NS1' from pcDNA-E-NS2A-Stop Mutant and -SCMU transfected 293T cells. Lysates were heat denatured or left untreated and analysed by Western blotting with anti-NS1 (4G4) or NS1'-specific antibodies (FS-ab).

6.2.2 Characterisation of WNV_{KUN} viruses with Stop and SCMU mutations.

Following confirmation that the two mutations did not abolish ribosomal frameshifting, and that versions of NS1' (either truncated or mutated) were produced from the expression cassettes, the mutations were next cloned into the WNV_{KUN} infectious clone, FLSDX. Once these mutations were introduced into FLSDX, it was necessary to verify that the ribosomal frameshift was still functional during translation of the full-length RNA. The presence of NS1' was determined by SDS-PAGE and Western blot analysis of lysate from infected Vero76, BHK, C6/36 or MEF cells. Similar to the results seen subgenomic expression in cells transfected with plasmid DNAs expressing mutant cassettes, both 4G4 and FS-ab detected a protein band corresponding to the predicted size of the truncated NS1' in Stop Mutant infected lysate for the different cells examined. Again, a protein band likely to correspond to NS1' was detected by 4G4 in SCMU samples, although there was poor detection by NS1'-specific antibodies. Interestingly, detection of Stop Mutant and SCMU NS1' by western blotting with anti-NS1 (4G4) antibody suggested that NS1' production was increased in the mutant viruses relative to wild-type virus. However, detection of wild-type NS1' with NS1'-specific antibodies was greater than detection with 4G4, suggesting that this may be an issue of antibody detection.

To further characterise Stop Mutant and SCMU NS1', immunofluorescence analysis of WNV_{KUN}, A30A', Stop Mutant or SCMU infected cells was carried out to assess NS1 and NS1' cellular localization. Infected Vero76 cells stained with anti-NS1 (4G4) and counter-stained with anti-calnexin (ER marker) antibodies showed that the truncation or mutation of NS1' did not alter cellular localisation compared to NS1' encoded by the wild-type WNV_{KUN} (Figure 6.4), which was shown in chapter 3 of this thesis to be predominantly ER localised (Figure 3.3 and 3.4).

To analyze the effect of truncation or mutation of NS1' on virus replication in cell culture, BHK, Vero76, C6/36 and MEFs were infected with the wild-type WNV_{KUN}, A30A', Stop mutant and SCMU viruses at MOI=1 (and MOI=0.1 for C6/36 cells), and virus titres in the culture fluid determined every 12h (24h for C6/36) for up to 120 hpi. The results showed that truncation of NS1' (Stop Mutant) did not affect virus replication in any of the cell lines (Figure 6.5) suggesting that full-length NS1' is not required for efficient virus growth. Mutation of NS1' in SCMU had no effect on virus growth in BHK, Vero76 or MEF cells, however, resulted in a slight increase in virus growth in C6/36 cells at later time points post infection (Figure 6.5). This increase in replication was seen for C6/36 cells infected at both MOI=1 and 0.1. In addition, a slight attenuation of A30A' viral growth was observed in C6/36 cells infected at MOI=0.1 at later time points.

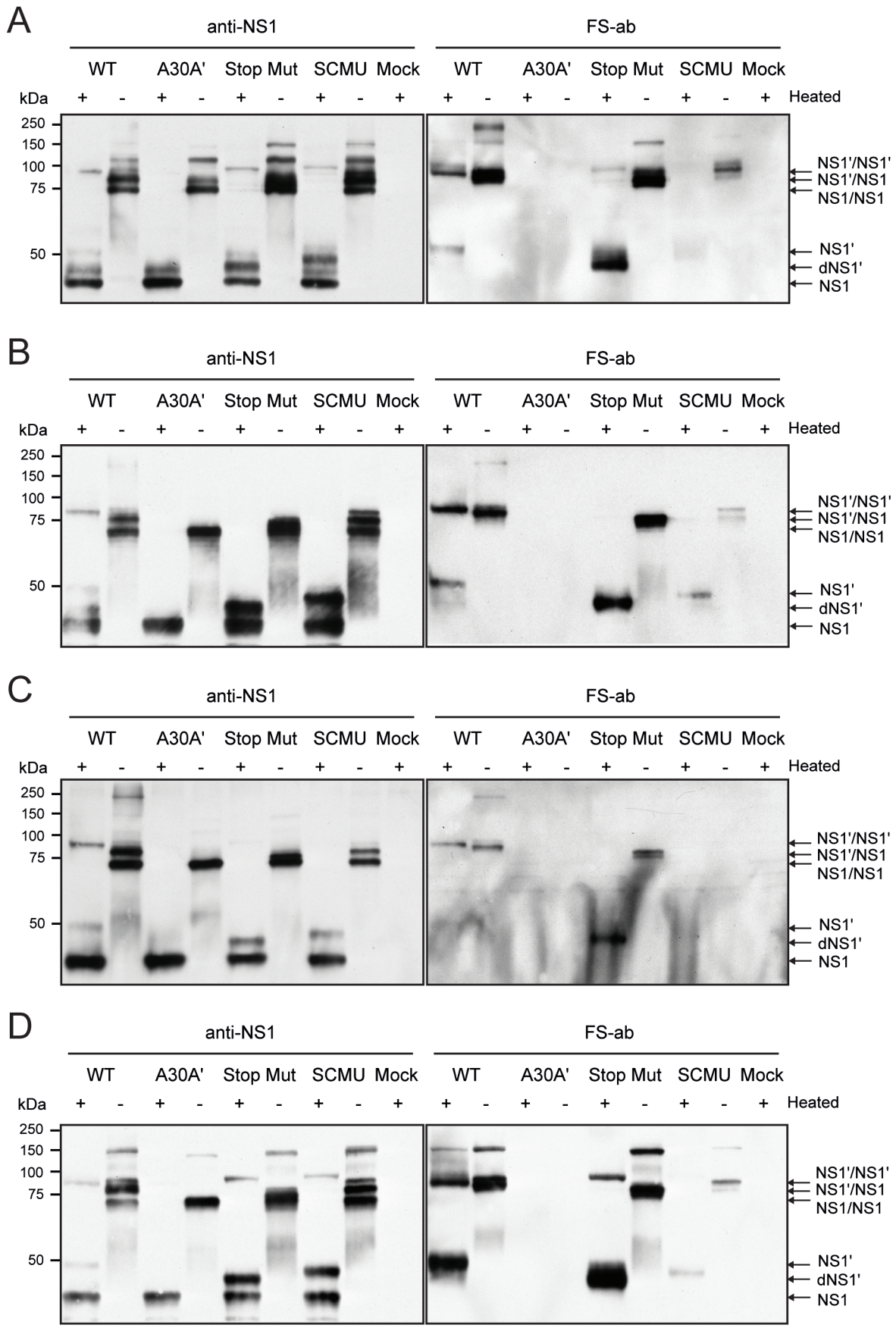

Figure 6.3 Production of NS1 and NS1' in infected cells. Western blots showing expression of NS1 and NS1' in wild-type (WT), A30A', Stop Mutant or SCMU FLSDX infected **A.** Vero76, **B.** BHK, **C.** Mouse

embryonic fibroblast (MEFs), or **D.** C6/36 cells. Lysates were heat denatured or left untreated, and analysed by Western blotting with anti-NS1 (4G4) or NS1'-specific antibodies (FS-ab).

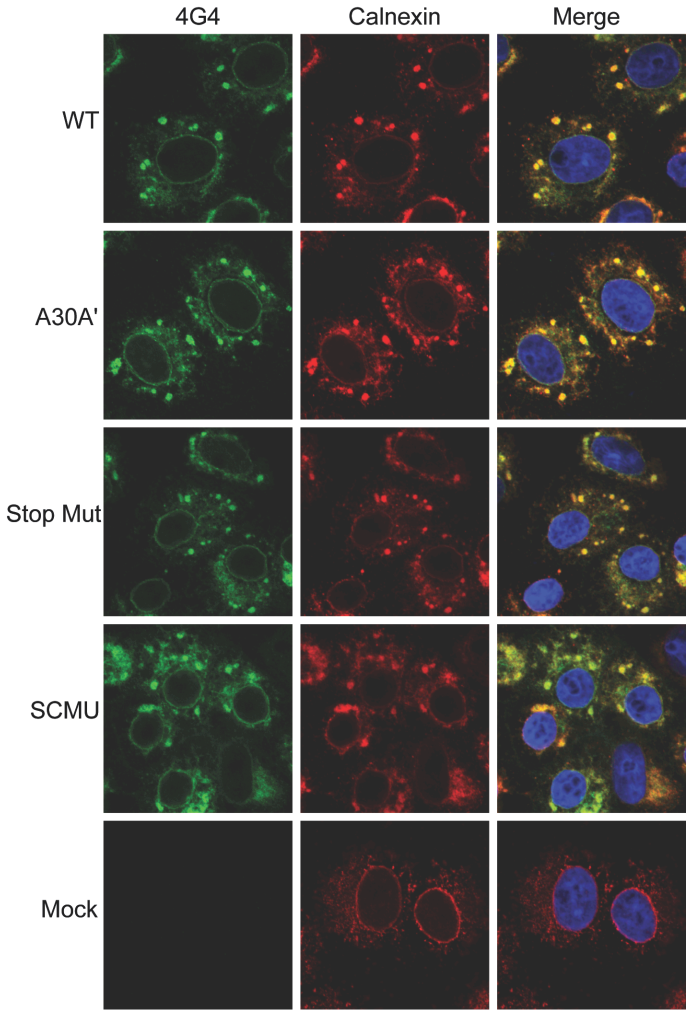

Figure 6.4 Localization of NS1' and NS1 in WNV_{KUN}, A30A', Stop Mutant or SCMU infected cells. Immunofluorescence analysis showing co-localization of virally expressed NS1 and NS1' with the ER. Infected cells were stained with anti-calnexin and anti-NS1 (4G4).

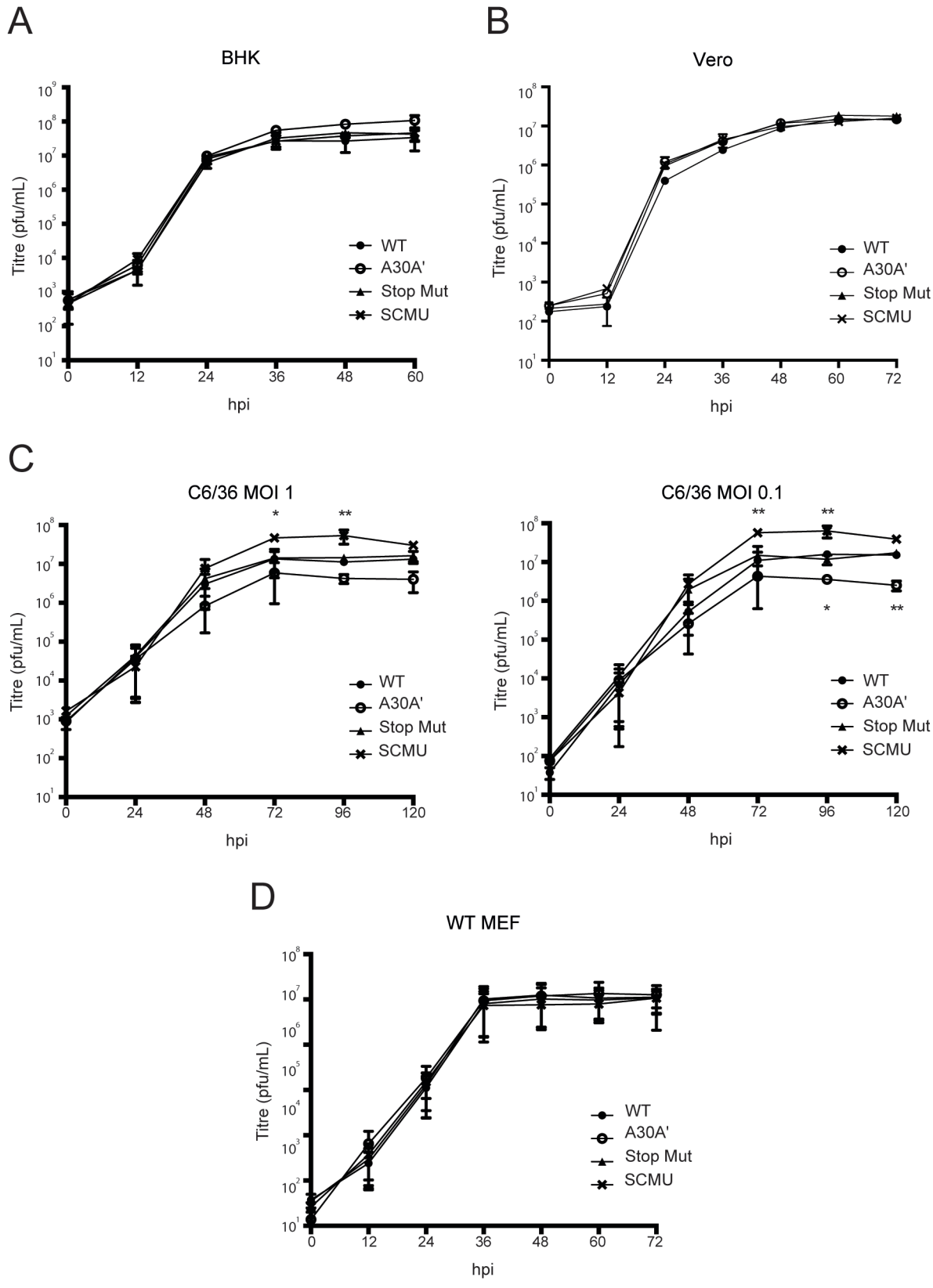

Figure 6.5 Growth kinetics of WNV_{KUN}, A30A', Stop Mutant and SCMU in **A.** BHK, **B.** Vero76, **C.** C6/36 or **D.** MEF cells. Cells were infected at MOI=1 (or 0.1 for C6/36 cells) and viral titers were determined up to 120 hpi by plaque assay. Results are expressed as the mean ± SEM of two independent experiments and significance (* [$P < 0.01$] or ** [$P < 0.005$]) determined by 2-way ANOVA.

Previous work carried out by our group indicated that abolishing the PRF affects the ratio of structural to non-structural proteins (389). Using the same experimental design, the structural to non-structural protein ratio of Stop Mutant and SCMU was examined. Vero76 cells were infected with WNV_{KUN} or mutant viruses and at 24 and 48hpi, pulse-chase ^{35}S-labelling was carried out in the presence of brefeldin A (BFA). BFA (at 5 mg/mL) was added to the cells during the 2 hours of labelling and 4 h chase to inhibit secretion of structural proteins, which could bias the ratio of structural to non-structural proteins. SDS-PAGE of culture fluid harvested from BFA treated or non-treated infected cells during pulse-chase analysis confirmed that the BFA treatment inhibited protein secretion (Appendix 9.2). Radiolabelled cell lysates were immunoprecipitated with anti-NS5 or anti-E antibodies and eluted proteins visualised by exposure to X-ray film following separation on SDS-PAGE gels (Figure 6.6A). The majority of E and NS5 produced by infected cells was immunoprecipitated, as shown by detection of only low levels of protein following a repeat pull-down on the unbound fraction (Appendix 9.3). Quantitation of individual protein bands was carried out and the structural to non-structural protein ratio determined for each virus (Figure 6.6B). At 24hpi there was no difference in the structural to non-structural protein ratio seen between wild-type and mutant viruses. However, by 48hpi, both Stop Mutant and SCMU showed a significant increase in the ratio of structural to non-structural proteins over wild-type WNV_{KUN}. These results suggest that the mutations introduced into SCMU and Stop Mutant increase frameshifting efficiency of the viruses. Interestingly, no significant difference between the ratio of structural to non-structural proteins of WNV_{KUN} and A30A' was seen.

Due to the increased hydrophobicity of the SCMU NS1' relative to wild-type NS1', the secretion pattern of NS1' was tested for both mutant viruses. Results shown in chapter 5 (Figure 5.7 and 5.8) confirmed that WNV_{KUN} NS1', like JEV NS1' (387), has an increased cellular retention compared to NS1. As the mutations introduced into SCMU increased the hydrophobicity of NS1', it was hypothesized that SCMU NS1' may have an increased cellular retention over that of wild-type WNV_{KUN} NS1'. Pulse-chase analysis of infected cells showed that NS1 and NS1' were both secreted from Stop Mutant and SCMU infected cells (Figure 6.7A). Quantification of individual protein bands showed while the level of intracellular NS1' was similar for all viruses (with the exception of A30A', which does not produce NS1'), the secretion of both Stop Mutant and SCMU NS1' was increased compared to WNV_{KUN}.

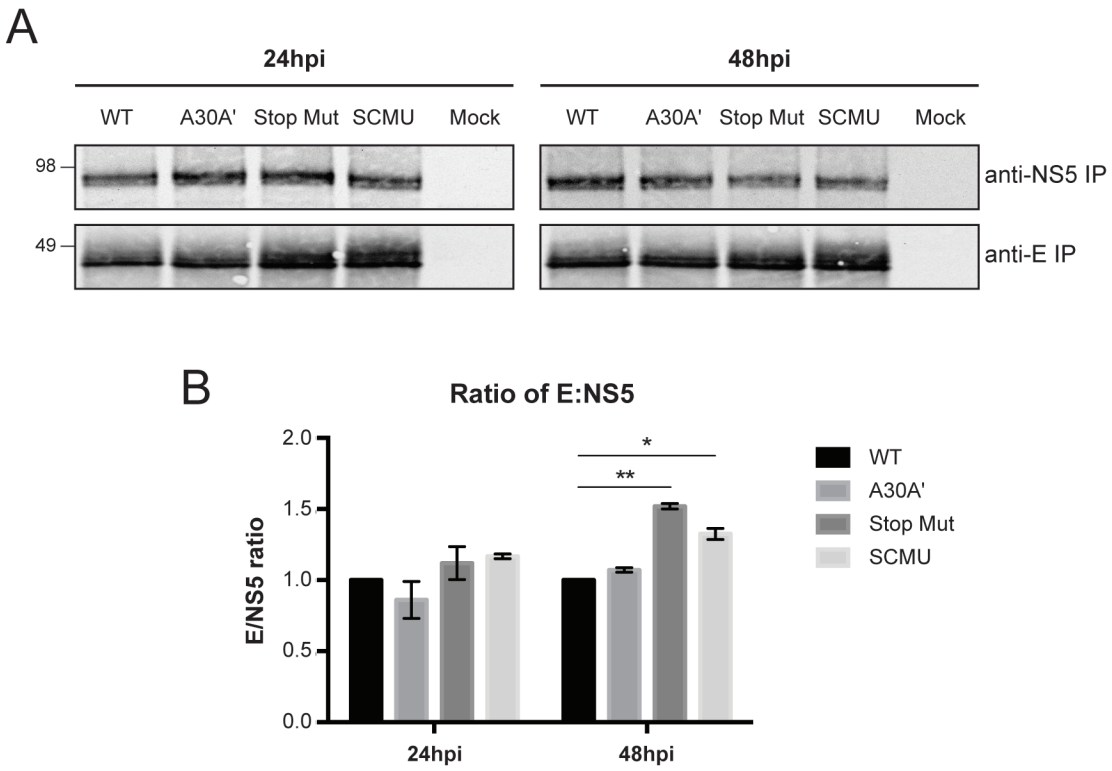

Figure 6.6 Infection with Stop Mutant and SCMU result in increased ribosomal frameshifting efficiency at 48hpi. A. Pulse-chase was performed at 24 and 48hpi and cell monolayers were lysed with RIPA buffer as described in chapter 2 of this thesis. Protein preparations were immunoprecipitated with anti-NS5 (5H1) or anti-E (3.91D) using Dynabeads® Protein G. Antibody-bound proteins were eluted and samples subjected to electrophoresis. Labelled proteins were transferred to nitrocellulose membranes and exposed to X-ray film. **B.** NS5 and E protein band intensities were determined and ratio of E/NS5 was calculated for wild-type (WT; black bar), A30A' (medium grey bar), Stop Mutant (dark grey bar) and SCMU (light grey bar) WNV_{KUN} at 24 or 48 hpi. Ratios were normalised to WT WNV_{KUN}. Results are expressed as the mean ± SEM of two independent experiments and significance (* [$P < 0.01$] or ** [$P < 0.005$]) determined by 2-way ANOVA.

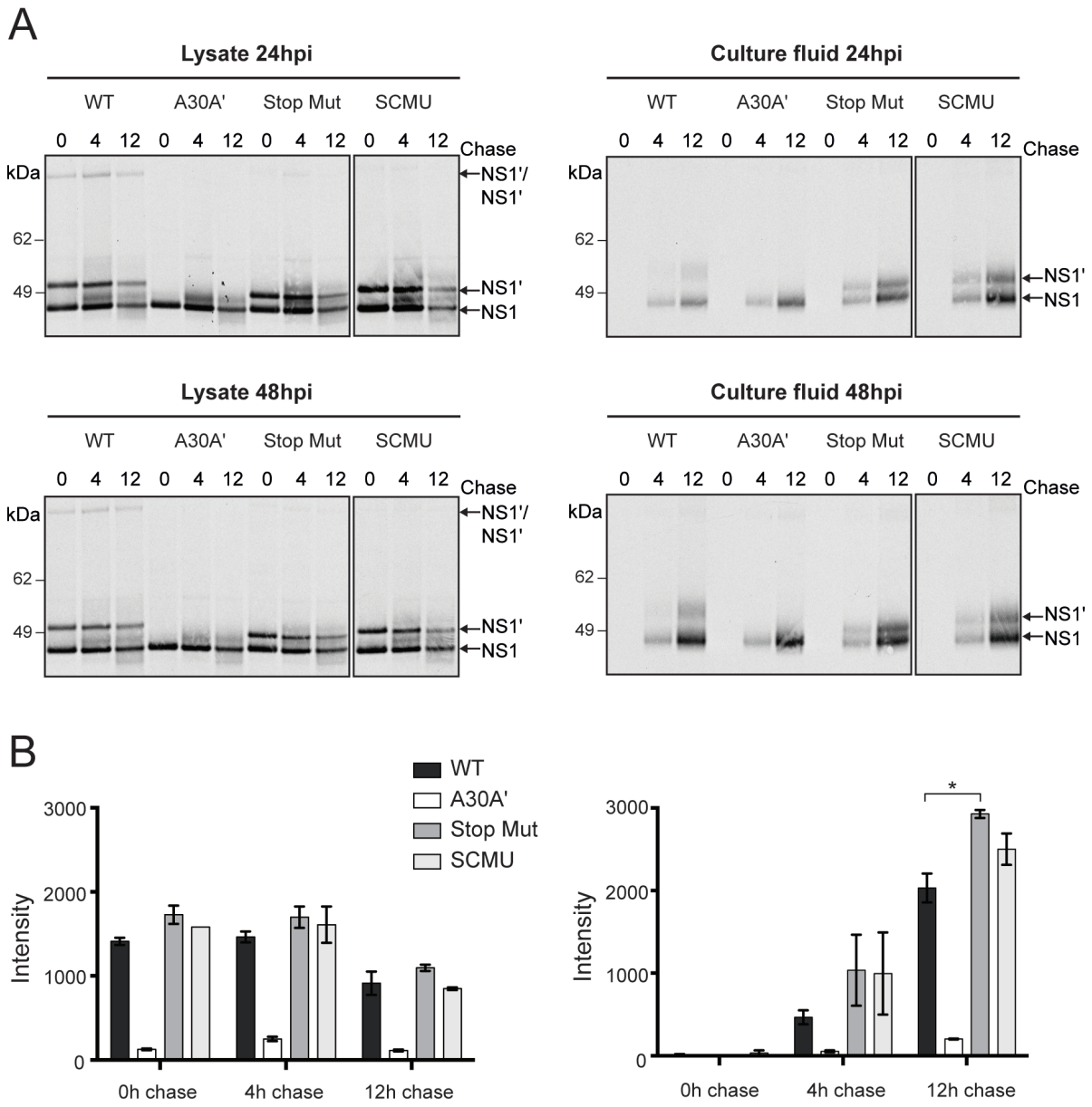

Figure 6.7 NS1' protein secretion by Stop Mutant and SCMU is increased compared to that of the WT WNV_{KUN} NS1'. A. Pulse (90 min)-chase (0, 4 or 12 h as indicated) was performed at 24 and 48hpi, culture fluids were clarified by centrifugation and cell monolayers were lysed as described in chapter 2 of this thesis. Protein preparations were immunoprecipitated with anti-NS1 (4G4) using Dynabeads® Protein G. Antibody-bound proteins were eluted and samples subjected to electrophoresis. Labelled proteins were transferred to nitrocellulose membranes and exposed to X-ray film. B**.** Quantification of intracellular (left-hand graph) or secreted (right-hand graph) NS1' band intensity from WNV_{KUN} (dark grey bar), A30A' (white bar), Stop Mutant (medium grey bar) or SCMU (light grey bar) infected cells at 48 hpi. Results are expressed as the mean ± SEM of two independent experiments and significance ($P < 0.01$) determined by 2-way ANOVA.

6.2.3 Virulence of Stop Mutant and SCMU in mice

It was shown previously that A30A' virus, lacking both the PRF and NS1', is attenuated in weanling mice compared to WNV_{KUN} (1). The attenuation of A30A' may be due to the absence of NS1' itself, the elimination of the ribosomal frameshift, or a combination of both. In contrast to A30A', the Stop and SCMU mutations prevent production of wild-type NS1', without affecting the ribosomal frameshift. To determine whether lack of wild-type NS1' production alone affects virus neuroinvasiveness, groups of ten 18 day-old mice were infected intraperitoneally with 100 or 1000 pfu of either WNV_{KUN}, A30A', Stop Mutant or SCMU and monitored daily for signs of encephalitis. These results showed that the virulence of Stop Mutant was not significantly different to that of wild-type WNV_{KUN} in mice infected with either 100 or 1000 pfu (~30% and ~40% survival for Stop Mutant compared to ~50% and ~20% survival for the wild type WNV_{KUN}, respectively) (Figure 6.8). Interestingly, A30A' in this particular experiment showed a slightly increased virulence at 1000 pfu to what has been seen previously (only 45% survival for A30A' compared to 60% survival seen previously) (1). As there was no significant difference between Stop Mutant and wild-type WNV_{KUN}, this suggests that a lack of full length NS1' does not affect neurovirulence. Although SCMU showed a similar mortality to WNV_{KUN} at 100 pfu (Figure 6.8A), it was surprisingly more pathogenic at 1000 pfu, showing 100% mortality as early as 8 days post infection (Figure 6.8B; WNV_{KUN} *verses* SCMU $P = 0.001$ as determined by Logrank test).

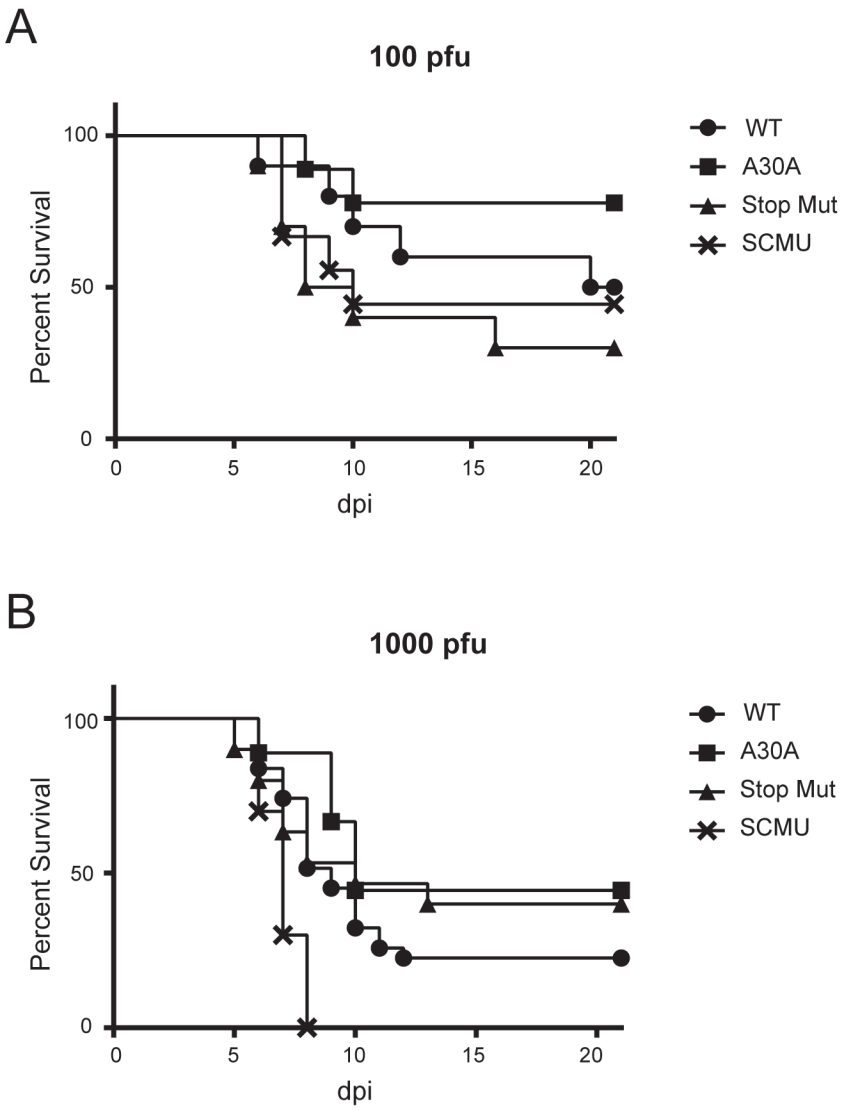

Figure 6.8 Virulence of WNV_{KUN}, A30A', Stop Mutant and SCMU in weanling mice. Groups of ten to twenty 18-day old weanling Swiss-outbred CD1 mice were infected intraperitoneally with **A.** 100 pfu (10 mice per group) or **B.** 1000 pfu (wild-type (WT) WNV_{KUN} and Stop Mutant, 30 mice per group total; A30A' and SCMU, 10 mice per group) and monitored daily for signs of encephalitis. WT WNV_{KUN} *vs* SCMU at 1000 pfu statistically significant (P = 0.001) as determined by Logrank test.

6.2.4 SCMU Predicted miRNA

Although subtle differences between SCMU and wild-type WNV_{KUN} (other than virulence phenotypes) have been identified, such as an increase in NS1' protein secretion and an increase in the ratio of structural to non-structural proteins, these are unlikely to be involved in the increase in virulence seen. Similar increases in frameshift efficiency and NS1' secretion was also seen for Stop Mutant, which shows no difference in pathogenicity compared to wild type WNV_{KUN}. This suggested that another factor may be involved in increased SCMU virulence. Analysis of the mutated region of RNA identified a potential hairpin structure present in SCMU but not wild-type WNV_{KUN} or Stop Mutant, suggesting the possibility of an introduced pre-micro-RNA that can be processed into micro RNA (miRNA; Figure 6.9A). A WNV_{KUN} encoded miRNA, KUN-miR-1, has been shown previously to impact on virus replication in insect cells (442). Interestingly, the role of KUN-miR-1 was shown to impact viral RNA replication specifically in insect cells, which would correlate with the increase in replication of SCMU in C6/36 cells (Figure 6.5) if SCMU has indeed produceda novel miRNA. To determine whether SCMU produces a novel miRNA, Vero76, C6/36 or MEF cells were infected with wild-type WNV_{KUN} or SCMU and enriched small RNAs were subjected to northern blotting with probes designed against the 5' or 3' stem of the predicted hairpin (probe 1 and 2 respectively; Figure 6.9A). Unfortunately, there was no RNA band coinciding with the expected size of a miRNA (20-25 nucleotides) seen for any of the cell types analyzed while larger bands that are likely to be RNA degradation products were detected (Figure 6.9B). These results show that while the pre-miRNA-like stem-loop structure encoded as the result of introduced mutations in SCMU was predicted, it does not result in production of a small RNA of the size expected for miRNA.

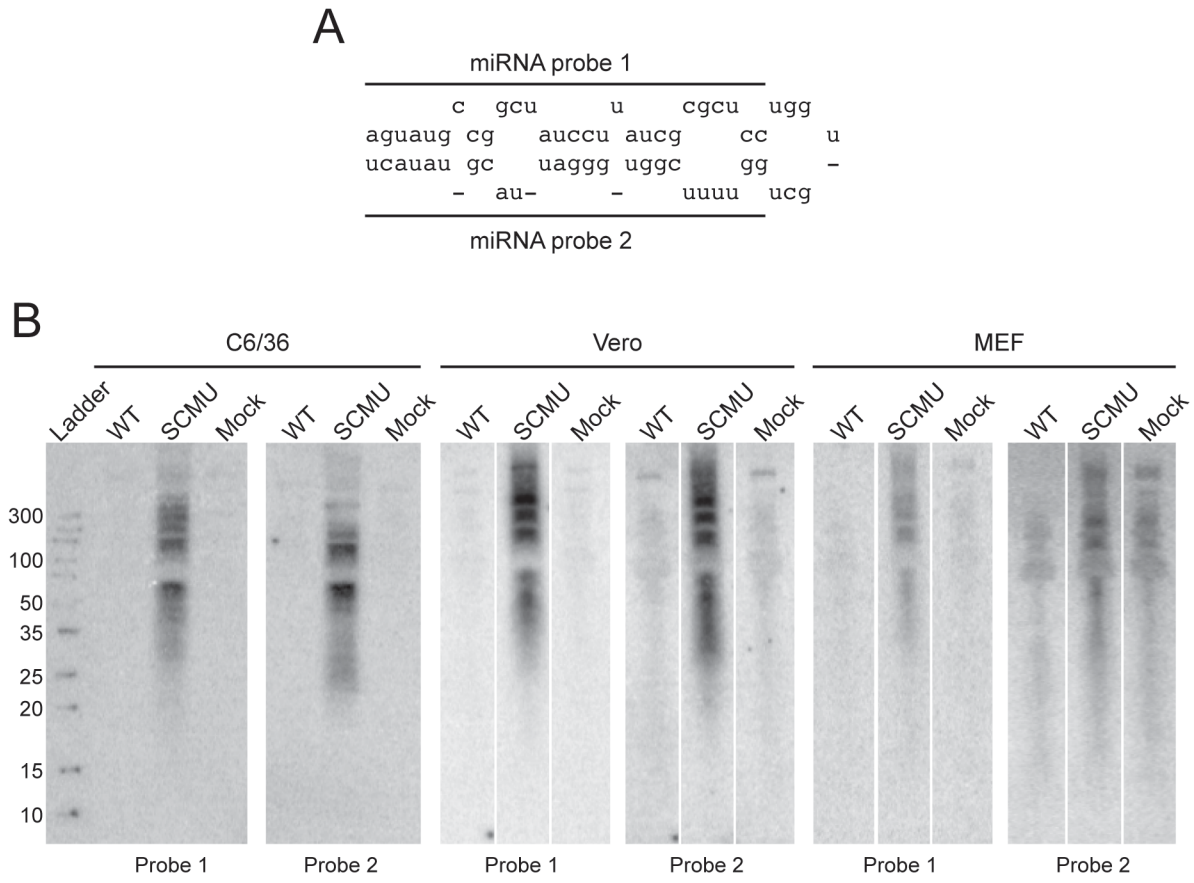

Figure 6.9 Predication and experimental analysis of potential miRNA encoded by SCMU. A. Nucleotide sequence and secondary structure of the predicted SCMU hairpin. Locations of probes used for analysis of miRNA production are shown. **B.** Northern blot of small RNAs harvested from wild-type (WT) WNV_{KUN}, SCMU or mock infected C6/36, Vero76 or MEF cells using miRNA probe 1 and 2, as shown in part A.

6.3 Discussion

The Stop Mutant and SCMU were designed specifically to separate the function of wild-type NS1' from that of the ribosomal frameshift itself. Stop Mutant contains a single nucleotide substitution that introduces a premature stop codon in NS1', which generates a 20 amino acid C-terminally truncated version of NS1'. SCMU on the other hand, introduces 19 point mutations that affect the sequence of 19 from the last 20 amino acids of NS1', but does not change NS2A amino acid sequence.

Due to the intricate relationship between the ribosomal frameshift and the production of NS1', it is difficult to determine whether attenuation of NS1'-lacking viruses is a result of the loss of the NS1' protein, or the frameshift itself (1, 390). It is possible that the frameshift evolved to control the ratio of structural to non-structural proteins (389), and that NS1' is merely its byproduct. However, it is unlikely to be a non-functioning byproduct, as NS1' has been shown to be functional in RNA replication (chapter 3, Figure 3.7 and 3.8; (375)). Another hypothesis is that NS1' may behave in infection as additional NS1. The frameshift event is hypothesized to have evolved for the control of structural to non-structural protein ratio (389), with NS1' being produced mainly to increase the relative level of functioning NS1.

The key finding from the work presented throughout this chapter is that truncation of NS1' did not detrimentally affect virus growth in mammalian and insect cell culture (Figure 6.5), or affect WNV_{KUN} pathogenicity in mice (Figure 6.8). These results strongly support the theory that full-length NS1' may not have a biological function that contributes to viral pathogenesis in a mammalian system. Furthermore, the finding that mutation of NS1' (in SCMU) actually resulted in a significant improvement in virus growth in mosquito cells and increased virulence in mice, strengthens the conclusion that wild-type NS1' does not perform a critical function in viral infection.

One key characteristic identified here is that the decreased secretion of NS1' compared to that of NS1 identified in chapter 5 (Figure 5.7 and 5.8) of this thesis can be linked to the last 20 amino acids of NS1' as shown by the secretion of the truncated Stop Mutant NS1' and mutated SCMU NS1' (Figure 6.7). This data suggests that the increase in secretion of NS1' in cells infected with Stop Mutant or SCMU is likely due to the loss of a potential cell retention signal in the final 20 amino acids of NS1'. Interestingly, the sequence of the frameshifted region is not well conserved between flaviviruses, with only five amino acids in the last 20 conserved between WNV_{KUN},

WNV_{NY99}, JEV and MVEV (Figure 5.9); however JEV has been shown previously to also have poor NS1' secretion (387). As an increase in NS1' secretion is a feature of both Stop Mutant and SCMU, which either truncate or mutate NS1', respectively (Figure 6.7), it is unlikely that this characteristic is dependent solely on the length of the C-terminal extension, supporting the hypothesis of a loss of a cell retention signal. However, although the increase in secretion seen for SCMU was noticeable, it was not significant (determined by 2-way ANOVA), and further repeats of this experiment will confirm whether the mutations introduced to NS1' cause a significant increase in protein secretion. In addition, while Stop Mutant increases NS1' secretion, the pathogenesis in mice is similar to that of wild-type WNV_{KUN}. This suggests that the inefficient secretion identified in chapter 5 of this thesis, while an intriguing characteristic of NS1' that is distinct from NS1, is unlikely to contribute to virulence in the mammalian system.

As Stop Mutant and SCMU were originally designed to affect wild-type WNV_{KUN} NS1' production but not the ribosomal frameshift, the frameshifting efficiency of the viruses was investigated. This was done by examining the ratio of structural to non-structural proteins, as has recently been published for the wild-type WNV_{KUN} and A30A' mutant. This recent publication showed that a lack of the ribosomal frameshift (in A30A') results in a decreased ratio of structural to non-structural proteins (389). As the mutations introduced into Stop Mutant and SCMU should not affect the formation of the frameshift itself, it was expected that neither mutations would have an impact on the structural to non-structural protein ratio. The data presented here indicates that both Stop Mutant and SCMU actually resulted in an increased ratio at 48 hpi (Figure 6.6). Due to the introduction of a novel stem-loop structure into the SCMU virion RNA (Figure 6.9A), it is tempting to speculate that the increased base pairing at the frameshift site further increases the frameshifting frequency. However, Stop Mutant also results in an increase in frameshifting frequency, and does not have this additional stem-loop structure. Given that Stop Mutant does not affect virulence and SCMU has an increased virulence in mice, this result is in clear contrast to the recent results with A30A' mutant, which suggested that a decrease in this ratio may be linked to attenuation (389).These results suggest that the ratio of structural to non-structural proteins is unlikely to impact pathogenicity.

Interestingly, the work carried out for this chapter is not consistent with the recent results showing reduction in the structural to non-structural protein ratio for A30A' compared to that of wild-type WNV_{KUN} (389). The results shown here indicate that in fact, the mutation of the pseudoknot and elimination of the frameshift in A30A' does not appear to impact on the ratio of structural to non-structural proteins, as there was no difference seen between wild-type WNV_{KUN}

and A30A' (Figure 6.6). The inconsistency seen here may be due to subtle differences between the experiments. Previous experiments utilized BHK cells, whereas the experiments conducted in this chapter used Vero76 cells to maintain consistency with additional characterization experiments. In addition, the previous work was carried out by immunoprecipitating lysate using a cocktail of anti-E and anti-NS5 antibodies. In the design of experiments for this thesis, it was thought that carrying out separate pull downs would be preferable, as this would ensure maximum protein binding. This was shown to be true through the repeat immunoprecipitation on the unbound fraction during the Dynabeads® pull down (Appendix 9.3). This confirmed that the SDS-PAGE gels run for quantification (Figure 6.6) were an accurate representation of the majority of E and NS5 protein present in the samples. No such control was included in previous experiments, and therefore the decrease in protein ratio seen for A30A' may have simply been an incomplete detection of all of the E and NS5 produced.

Western blotting with anti-NS1 antibodies (4G4) of lysates from cells infected with WNV_{KUN} or mutant viruses suggested that the production of NS1' is lower for wild-type WNV_{KUN} than for Stop Mutant and SCMU (Figure 6.3). However, detection with NS1'-specific antibodies (FS-ab) did not show such a significant decrease in protein expression between the wild-type and mutant viruses. It is possible that the reduction in 4G4 signal seen for wild-type WNV_{KUN} is solely due to an issue with antibody binding that was not apparent with FS-ab. Based on the data showing an increase in frameshifting efficiency for Stop Mutant and SCMU (Figure 6.6), it is also possible that there is indeed an increase in the production of NS1', however, the pulse-chase data showing the level of protein in viral lysates (Figure 6.7) does not support this.

The reason for the increased virulence of the SCMU mutant over that of wild-type WNV_{KUN} has yet to be uncovered. It is unlikely to be due to the increase in NS1' secretion, or the increase in the ratio of structural to non-structural proteins identified, as Stop Mutant also displayed these characteristics and has a no effect on virulence in mice. While further work to investigate the nature of the increased virulence of SCMU is appealing, it must be kept in mind that the mutations introduced into the virus were not specifically selected for pathogenesis, as there were limited possibilities for these mutations without affecting the sequence of NS2A. These arbitrary mutations may therefore have had an unforeseen effect that may have little to do with the properties and functions of NS1' itself. Instead, they may have simply resulted in a misfolded protein that triggered an unexpected response *in vivo*, leading to increased pathogenicity. Future work may introduce one or more mutations from SCMU at a time, in an effort to isolate the sequence contributing to pathogenesis, though this is unlikely to further the understanding of the NS1' protein. On the other

hand, it should be noted that gain-of-virulence phenotypes of viruses generated by targeted mutagenesis (without the use of known virulence determinants) are rare. Further work on the SCMU virus may therefore assist in determining the influence of natural selection on the mutability of this region.

The goal of the experiments outlined in this chapter were to design and characterize new mutant viruses to separate the function of wild-type NS1' from that of the PRF. SCMU, which introduces 19 amino acid changes into the C-terminal 20 amino acids of NS1' is not an ideal candidate, as this virus displayed characteristics unlikely to be due to the function of the NS1' protein. In spite of the slight difference in frameshifting efficiency seen between WNV_{KUN} and Stop Mutant, this mutant virus (which introduced a premature stop codon into NS1') is a promising candidate to further examine the function of full-length NS1' in viral replication.

7 Conclusions and Future directions

This thesis has identified new characteristics of the WNV NS1' protein, determined NS1 and NS1' binding partners, uncovered a role for NS1' in flaviviral replication, and has developed new resources for future studies on NS1'.

7.1 NS1' synthesis and trafficking

In combination with previously published studies, the work conducted for this thesis has determined that NS1' functions like NS1, with some differences in dimerisation and secretion. NS1', like NS1, predominantly resides within the lumen of the ER (Figure 3.3 and 3.4). Following initial translation, NS1' is glycosylated at the same number of sites as NS1 (as determined for JEV NS1') (387, 332). Similar to NS1, NS1' forms a dimer, though WNV NS1' has been shown in this thesis to form a heat-stable dimer distinct from the NS1 heat-labile dimer (chapter 5). Following dimerisation, NS1' is trafficked to the same locations in the cell as NS1: the site of RNA replication, the cell surface, and the extracellular fluid. NS1' was shown to co-localise with dsRNA in infected cells and function in RNA replication (chapter 3). NS1' was detected on the cell surface following plasmid transfection of 293T cells (Figure 3.3D), and is likely to also be expressed on the surface of WNV infected cells, though further confirmation of this is necessary. NS1' was determined to be secreted from both infected and plasmid-transfected cells, albeit to a lower degree than NS1 (Figure 5.7 and 5.8). This is in agreement with previous work examining the secretion of NS1' from JEV infected cells (332). Whether this extracellular form of NS1' is hexameric (like NS1) is yet to be determined.

Results shown in chapter 4 indicates that both NS1 and NS1' interact with the molecular chaperone protein BiP, likely within the lumen of the ER. BiP has been implicated previously in the folding of viral proteins, particularly viral glycoproteins (411-418). In plasmid transfected cells, BiP was only co-purified with NS1' and not NS1 (Table 4.2), suggesting that the interaction of BiP with NS1' is either stronger or more frequent than the interaction between BiP and NS1. This could indicate that NS1' is seen as misfolded or requires more assistance with folding than NS1. BiP was also immunoprecipitated more frequently from wild-type WNV_{KUN} infected lysate than A30A' infected lysate (7/7 *vs* 3/7 times, respectively; Table 4.1), supporting the theory that BiP has an increased interaction with NS1' over NS1. It is also possible that the unfolded protein response (UPR) is upregulated in wild-type WNV_{KUN} infected cells compared to A30A' infected cells, leading to increased expression of BiP during WNV_{KUN} infection. This could lead to the increased

interaction with NS1/NS1' that was observed. However, confirmation of this theory would require an analysis of the UPR in wild-type WNV_{KUN} and A30A' infected cells.

The suggestion that NS1' may have an increased interaction with BiP due to difficulties in protein folding supports the hypothesis that the sub-population of heat-stable dimers is due to misfolded intermediates with alternate disulfide bonds. It is also consistent with the reduction in NS1' secretion compared to NS1, suggesting that NS1' may be retained within the ER where it interacts with BiP. The C-terminal frameshifted region of NS1' would be located at the ends of the β-ladder of the NS1 dimer (see Figure 1.7 for NS1 crystal structure), and in close proximity to three disulfide bonds. While the crystal structure of NS1' has not been solved, it would be intriguing to determine whether it is consistent with the structure of NS1, or whether the C-terminal extension disrupts folding of the remainder of the protein. It would be particularly interesting to determine whether NS1' has a consistent structure, or whether the structure is in fact variable. This would shed light on whether the heat-stable dimers are formed due to misfolded intermediates that disrupts the disulfide bonds within NS1.

The pulse-chase experiments examining NS1' protein secretion indicates that the small amount of NS1' that is secreted has the same secretion kinetics as NS1 (Figure 5.7 and 5.8). This suggests that at least a proportion of the NS1' protein is folded, dimerised and trafficked through the secretory pathway at the same rate as NS1. In addition, NS1' is secreted when transfected on its own (Figure 5.8), and is therefore unlikely to only be secreted due to heterodimer formation with NS1. A proportion of this secreted NS1' is also present in its heat-stable dimer form, indicating that this form is unlikely to be a folding intermediate as misfolded protein would most likely be retained in the cell. However, only a small amount of NS1' is secreted from the cell, and it is therefore difficult to conclusively determine the dimer stability.

Previous work by other groups has suggested the possibility for unique functions for NS1'. JEV NS1' has been identified as a substrate for caspase cleavage, with the hypothesized cleavage site being highly conserved between NS1' from different flaviviral species (386). However, in spite of this conservation, the cleaved NS1' product was not observed by SDS-PAGE analysis of WNV_{KUN} infected or pcDNA-NS1' plasmid transfected cell lysates in our experiments. While this was not confirmed by an extensive analysis, it does suggests that caspase cleavage may be unique to JEV NS1'.

NS1' and/or the ribosomal frameshift has previously been implicated in assembly of viral particles (391). During the development of a chimeric DENV vaccine expressing DENV prM/E genes in a WNV backbone, a mutation that eliminated the ribosomal frameshift (thereby abolishing NS1' production) was determined to enhance virion packaging (392, 391). However, this mutation had no effect on genome replication, highlighting a possible link between NS1' and the structural proteins. This was not the case when this mutation was introduced to a non-chimeric WNV vaccine, suggesting that production of NS1' and/or the ribosomal frameshift somehow inhibits assembly of virus particles only in association with DENV structural proteins. Both NS1 and NS1' have been suggested to form a complex with E (382), and it is possible that an interaction of NS1' with DENV E, given that DENV does not naturally produce NS1', negatively impacts formation of the envelope. However, it is unlikely that NS1' assists in virion assembly during natural WNV infection, as the presence of NS1' has no effect on virion production or viral replication when expressed in association with WNV prM/E genes (1, 391). It is also possible that since the acquired mutation affects the formation of the frameshift, it may affect the ratio of structural to non-structural proteins. Abolishing the frameshift may therefore increase the relative expression of another non-structural protein that may be involved in enhancing assembly, rather than NS1' inhibiting assembly.

7.2 Function of NS1' in RNA replication

One of the key findings from the work presented in this thesis is the identification of a role of NS1' in flaviviral replication. Our *trans*-complementation studies determined that NS1' can substitute for NS1 in viral replication, and shows no difference in the efficiency of complementation compared to NS1 (Figure 3.7 and 3.8). This work alone suggests only that the C-terminal tail of NS1' does not interfere with NS1' functioning in replication in the absence of NS1. A role for NS1' in natural viral replication was supported by immunofluorescence data showing co-localisation of NS1' with dsRNA in infected cells (Figure 3.5), suggesting that NS1' was present at the site of viral RNA replication during WNV_{KUN} infection. This was further confirmed by the results showing a direct interaction of NS1' with components of the viral replication complex (specifically NS4B and NS3; Table 4.3). Taken together, the data presented throughout this thesis suggests that NS1' is indeed functioning in viral replication during WNV_{KUN} infection.

This function is not critical for viral replication, as a lack of NS1' has been shown previously (and been confirmed here; Figure 6.5) to not affect viral growth in several different cell types (1). It is more likely that NS1' simply functions in replication as additional NS1. When NS1' is not expressed (such as in the A30A' mutant), the level of NS1 produced is sufficient to maintain

viral replication. This data also has implications for the folding of NS1', as it suggests that the C-terminal tail is unlikely to significantly impact on the folding of the NS1 portion of the protein.

7.3 NS1' and PRF

Ribosomal frameshifting is a strategy used by RNA viruses to minimise the size of their genome (443, 444). This mechanism has been identified in several medically relevant viruses, such as HIV-1 and SARS-CoV (445, 446). A -1 PRF has also been identified to occur in alphaviruses, such as Sindbis virus and Chikungunya virus. Similar to the initial identification of the pseudoknot in the JEV serogroup, the presence of a predicted -1 PRF was identified to occur in the 6K structural protein in alphaviruses (447). This frameshift was predicted to produce an extension of the 6K protein, resulting in an 8 kDa protein termed TransFrame (TF). TF was identified in both Sindbis and Chikungunya virus infected cells, and further analysis determined that a lack of this frameshifted protein correlated with reduced pathogenicity and a reduction in virion particle release (448).

Unlike the alphavirus TF protein, the data shown throughout this thesis supports the theory that NS1' does not have a unique function in viral infection in a mammalian system. The actual frameshifted region of the NS1' protein is poorly conserved between different species (~40% conservation between WNV, JEV and MVEV NS1'), however, the stop codon (and therefore protein length) is very well conserved. This suggests that the NS1' protein is only produced as a byproduct of the ribosomal frameshift, and the conserved length of the protein ensured that NS1' could function as NS1. However, even viruses lacking both the PRF and NS1' have only a subtle effect on pathogenesis in the mammalian system, while perhaps having more profound effect in mosquitoes and birds (389). It is highly unlikely that such a conserved mechanism as -1 PRF producing a stable protein has evolved in a distinct group of viruses without a significant impact on viral growth/transmission properties in at least one of the vector or host systems. As these viruses predominantly cycle through the *Culex* mosquito and avian system, it is more likely that this is where the PRF and NS1' initially evolved, and therefore where it is likely to have a significant impact on pathogenesis.

7.4 Future directions for NS1'

As NS1' is produced as the result of PRF only by members of the JEV serogroup (encephalitic flaviviruses), it leads to the question whether this novel protein may have an effect on

the neurovirulence of the virus. Mosquito-borne flaviviruses causing systemic disease, and therefore outside of the JEV serogroup, do not express NS1'. The initial work conducted in our laboratory and others, identified a difference in neurovirulence in mice between PRF/NS1'-producing and PRF/NS1'-lacking viruses (1, 390), supporting this hypothesis. Work conducted for this thesis determined that full-length NS1' was not required for neurovirulence in mice. This suggests that it may be the PRF itself rather than its by-product NS1' that is important for neurovirulence in mammalian hosts. Further work in characterising the role of the PRF in WNV pathogenesis in the mammalian system is required.

The JEV serogroup is also distinguished by its vector/host relationship. Viruses within the JEV serogroup are predominantly transmitted by *Culex* mosquitoes and infect avian hosts, while mosquito-borne flaviviruses outside of this serogroup are transmitted by *Aedes* mosquitoes and infect mammalian hosts. Rather than a link between NS1' and the development on encephalitic disease, there may instead be a link between the *Culex*/avian relationship. Recent work conducted in the mosquito and avian systems supports this theory, with a difference in pathogenicity in house sparrows and transmission in *Culex* mosquitoes observed between viruses encoding PRF and expressing NS1' and those lacking PRF/NS1' (389).

In addition, work conducted in chicken embryonic fibroblasts (DF-1 cells) and embryonated chicken eggs identified a role for JEV PRF/NS1' in facilitating virus production in avian cells by increasing viral RNA levels (396). This is in contrast to previous work which has shown that viral growth in mammalian is not different between viruses lacking PRF/NS1' and those encoding PRF and expressing NS1' (1, 390). This suggests that PRF/NS1' may behave in a species-specific manner to assist in viral replication. Work in our laboratory conducted in DF-1 cells with WNV_{KUN} failed to identify any differences between PRF/ NS1'-producing and PRF/NS1'-lacking viruses, suggesting that the effect of PRF/NS1' on replication may be specific to JEV (389). Further studies comparing replication of NS1'-truncated Stop Mutant generated in this thesis and previously generated PRF/NS1'-lacking WNV viruses (such as A30A') in avian cell culture will establish whether the function of NS1' in viral replication in avian cells is conserved between NS1' from different flaviviral species and whether NS1' role in replication is dependent on full-length NS1' protein.

In addition to already conducted analysis in DF-1 cells performed at 37 degrees (389), examining the effect of the absence or truncation of NS1' in avian cells incubated at a higher temperature may shed light on the importance of the heat-stable NS1' dimers. The average body temperature of avian species is closer to 40°C, and can increase to 44°C at times of high activity

(449). While this seems only a subtle difference in temperature compared to the 37°C predominantly used for cull culture, some disruption in dimer stability is already observed at 37°C (Figure 5.4). Prolonged exposure to slightly higher body temperatures may therefore result in improved potential function of the more stable NS1' dimer.

As a role was identified for NS1' in functioning as additional NS1 protein in viral RNA replication, it would be intriguing to determine whether NS1' is also involved in other NS1 functions. One key function of NS1 is in the inhibition of the complement system (379, 380, 362, 371). However, this function is carried out predominantly by secreted NS1, and due to low levels of NS1' secreted from infected cell, it is unlikely that NS1' is also involved in complement inhibition. Similarly, while a role for secreted NS1 in TLR3 signaling inhibition has been identified (113, 114), low level NS1' secretion suggests that NS1' is not likely to be involved in TLR3 inhibition either.

The work conducted for this thesis has expanded the knowledge of the WNV NS1' protein, identifying and confirming its function as additional NS1 protein in viral RNA replication. As NS1' is inefficiently secreted compared to NS1, its primary function as additional NS1 is likely to reside intracellularly where viral RNA replication occurs. It is also likely that NS1' is simply a non-functional by-product of the -1 PRF, and that the frameshift itself rather than NS1' is important for viral infection. The work shown here examining the truncated NS1' produced by the Stop Mutant virus supports this hypothesis (chapter 6), as truncation of NS1' did not have a significant impact on WNV_{KUN} virulence in mammalian hosts (mice). Future work on examining the requirement of NS1' for viral replication in the mosquito and avian hosts will identify whether NS1' protein has a function in this vector-host system.

8 References

1. **Melian EB, Hinzman E, Nagasaki T, Firth AE, Wills NM, Nouwens AS, Blitvich BJ, Leung J, Funk A, Atkins JF, Hall R, Khromykh AA.** 2010. NS1' of Flaviviruses in the Japanese Encephalitis Virus Serogroup Is a Product of Ribosomal Frameshifting and Plays a Role in Viral Neuroinvasiveness. Journal of Virology **84:**1641 - 1647.

2. **Khromykh AA, Varnavski AN, Sedlak PL, Westaway EG.** 2001. Coupling between replication and packaging of flavivirus RNA: evidence derived from the use of DNA-based full-length cDNA clones of Kunjin virus. Journal of Virology **75:**4633-4640.

3. **Akey DL, Brown WC, Dutta S, Konwerski J, Jose J, Jurkiw TJ, DelProposto J, Ogata CM, Skiniotis G, Kuhn RJ, Smith JL.** 2014. Flavivirus NS1 structures reveal surfaces for associations with membranes and the immune system. Science **343:**881-885.

4. **Muller DA, Young PR.** 2013. The flavivirus NS1 protein: molecular and structural biology, immunology, role in pathogenesis and application as a diagnostic biomarker. Antiviral Res **98:**192-208.

5. **Khromykh AA, Sedlak PL, Westaway EG.** 2000. cis- and trans-acting elements in flavivirus RNA replication. Journal of Virology **74:**3253-3263.

6. **Cook S, Moureau G, Kitchen A, Gould EA, de Lamballerie X, Holmes EC, Harbach RE.** 2012. Molecular evolution of the insect-specific flaviviruses. Journal of General Virology **93:**223-234.

7. **Heinz FX, Purcell MS, Gould EA, Howard CR, Houghton M, Moormann RJM, Rice CM, Thiel HJ.** 2000. Family Flaviviridae, p. 860-878. *In* Regenmortel CF, Bishop DHL, Carstens EB, Estes MK (ed.), Virus Taxonomy. Academic Press, San Diego, CA, USA.

8. **Cook S, Holmes EC.** 2006. A multigene analysis of the phylogenetic relationships among the flaviviruses (Family: Flaviviridae) and the evolution of vector transmission. Arch Virol **151:**309-325.

9. **Kuno G, Chang GJ, Tsuchiya KR, Karabatsos N, Cropp CB.** 1998. Phylogeny of the genus Flavivirus. J Virol **72:**73-83.

10. **Gaunt MW, Sall AA, de Lamballerie X, Falconar AK, Dzhivanian TI, Gould EA.** 2001. Phylogenetic relationships of flaviviruses correlate with their epidemiology, disease association and biogeography. J Gen Virol **82:**1867-1876.

11. **Smithburn KC, Hughes TP, Burke AW, Paul. JH.** 1940. A neurotropic virus isolated from the blood of a native of Uganda. Amer Jour Trop Med **20:**471-492.

12. **Ebel GD, Dupuis AP, 2nd, Ngo K, Nicholas D, Kauffman E, Jones SA, Young D, Maffei J, Shi PY, Bernard K, Kramer LD.** 2001. Partial genetic characterization of West Nile virus strains, New York State, 2000. Emerg Infect Dis **7:**650-653.

13. **Lanciotti RS, Roehrig JT, Deubel V, Smith J, Parker M, Steele K, Crise B, Volpe KE, Crabtree MB, Scherret JH, Hall RA, MacKenzie JS, Cropp CB, Panigrahy B, Ostlund E, Schmitt B, Malkinson M, Banet C, Weissman J, Komar N, Savage HM, Stone W, McNamara T, Gubler DJ.** 1999. Origin of the West Nile virus responsible for an outbreak of encephalitis in the northeastern United States. Science **286:**2333-2337.

14. **Bosch I, Herrera F, Navarro JC, Lentino M, Dupuis A, Maffei J, Jones M, Fernandez E, Perez N, Perez-Eman J, Guimaraes AE, Barrera R, Valero N, Ruiz J, Velasquez G, Martinez J, Comach G, Komar N, Spielman A, Kramer L.** 2007. West Nile virus, Venezuela. Emerg Infect Dis **13:**651-653.

15. **Hayes EB, Komar N, Nasci RS, Montgomery SP, O'Leary DR, Campbell GL.** 2005. Epidemiology and transmission dynamics of West Nile virus disease. Emerg Infect Dis **11:**1167-1173.

16. **Komar N, Clark GG.** 2006. West Nile virus activity in Latin America and the Caribbean. Rev Panam Salud Publica **19:**112-117.

17. **Morales MA, Barrandeguy M, Fabbri C, Garcia JB, Vissani A, Trono K, Gutierrez G, Pigretti S, Menchaca H, Garrido N, Taylor N, Fernandez F, Levis S, Enria D.** 2006. West Nile virus isolation from equines in Argentina, 2006. Emerg Infect Dis **12:**1559-1561.

18. **Petersen LR, Brault AC, Nasci RS.** 2013. West Nile virus: review of the literature. JAMA **310:**308-315.

19. **Berthet FX, Zeller HG, Drouet MT, Rauzier J, Digoutte JP, Deubel V.** 1997. Extensive nucleotide changes and deletions within the envelope glycoprotein gene of Euro-African West Nile viruses. J Gen Virol **78 (Pt 9):**2293-2297.

20. **Brinton MA.** 2014. Replication cycle and molecular biology of the West Nile virus. Viruses **6:**13-53.

21. **Bondre VP, Jadi RS, Mishra AC, Yergolkar PN, Arankalle VA.** 2007. West Nile virus isolates from India: evidence for a distinct genetic lineage. J Gen Virol **88:**875-884.

22. **Prilipov AG, Kinney RM, Samokhvalov EI, Savage HM, Al'khovskii SV, Tsuchiya KR, Gromashevskii VL, Sadykova GK, Shatalov AG, Vyshemirskii OI, Usachev EV, Mokhonov VV, Voronina AG, Butenko AM, Larichev VF, Zhukov AN, Kovtunov AI, Gubler DJ, L'Vov D K.** 2002. [Analysis of new variants of West Nile fever virus]. Vopr Virusol **47:**36-41.

23. **Scherret JH, Poidinger M, Mackenzie JS, Broom AK, Deubel V, Lipkin WI, Briese T, Gould EA, Hall RA.** 2001. The relationships between West Nile and Kunjin viruses. Emerg Infect Dis **7:**697-705.

24. **Vazquez A, Sanchez-Seco MP, Ruiz S, Molero F, Hernandez L, Moreno J, Magallanes A, Tejedor CG, Tenorio A.** 2010. Putative new lineage of west nile virus, Spain. Emerg Infect Dis **16:**549-552.

25. **Charrel RN, Brault AC, Gallian P, Lemasson JJ, Murgue B, Murri S, Pastorino B, Zeller H, de Chesse R, de Micco P, de Lamballerie X.** 2003. Evolutionary relationship

between Old World West Nile virus strains. Evidence for viral gene flow between Africa, the Middle East, and Europe. Virology **315:**381-388.

26. **Ciccozzi M, Peletto S, Cella E, Giovanetti M, Lai A, Gabanelli E, Acutis PL, Modesto P, Rezza G, Platonov AE, Lo Presti A, Zehender G.** 2013. Epidemiological history and phylogeography of West Nile virus lineage 2. Infect Genet Evol **17:**46-50.

27. **May FJ, Davis CT, Tesh RB, Barrett AD.** 2010. Phylogeography of West Nile virus: from the cradle of evolution in Africa to Eurasia, Australia, and the Americas. J Virol **85:**2964-2974.

28. **Papa A, Bakonyi T, Xanthopoulou K, Vazquez A, Tenorio A, Nowotny N.** 2011. Genetic characterization of West Nile virus lineage 2, Greece, 2010. Emerg Infect Dis **17:**920-922.

29. **Bagnarelli P, Marinelli K, Trotta D, Monachetti A, Tavio M, Del Gobbo R, Capobianchi M, Menzo S, Nicoletti L, Magurano F, Varaldo P.** 2011. Human case of autochthonous West Nile virus lineage 2 infection in Italy, September 2011. Euro Surveill **16**.

30. **Bakonyi T, Ivanics E, Erdelyi K, Ursu K, Ferenczi E, Weissenbock H, Nowotny N.** 2006. Lineage 1 and 2 strains of encephalitic West Nile virus, central Europe. Emerg Infect Dis **12:**618-623.

31. **McMullen AR, Albayrak H, May FJ, Davis CT, Beasley DW, Barrett AD.** 2012. Molecular evolution of lineage 2 West Nile virus. J Gen Virol **94:**318-325.

32. **Papa A, Xanthopoulou K, Gewehr S, Mourelatos S.** 2011. Detection of West Nile virus lineage 2 in mosquitoes during a human outbreak in Greece. Clin Microbiol Infect **17:**1176-1180.

33. **Valiakos G, Touloudi A, Iacovakis C, Athanasiou L, Birtsas P, Spyrou V, Billinis C.** 2011. Molecular detection and phylogenetic analysis of West Nile virus lineage 2 in sedentary wild birds (Eurasian magpie), Greece, 2010. Euro Surveill **16**.

34. **Brault AC.** 2009. Changing patterns of West Nile virus transmission: altered vector competence and host susceptibility. Vet Res **40:**43.

35. **Ciota AT, Kramer LD.** 2013. Vector-virus interactions and transmission dynamics of West Nile virus. Viruses **5:**3021-3047.

36. **Dohm DJ, Sardelis MR, Turell MJ.** 2002. Experimental vertical transmission of West Nile virus by Culex pipiens (Diptera: Culicidae). J Med Entomol **39:**640-644.

37. **Nelms BM, Fechter-Leggett E, Carroll BD, Macedo P, Kluh S, Reisen WK.** 2013. Experimental and natural vertical transmission of West Nile virus by California Culex (Diptera: Culicidae) mosquitoes. J Med Entomol **50:**371-378.

38. **Kramer LD, Bernard KA.** 2001. West Nile virus in the western hemisphere. Curr Opin Infect Dis **14:**519-525.

39. **Dusek RJ, McLean RG, Kramer LD, Ubico SR, Dupuis AP, 2nd, Ebel GD, Guptill SC.** 2009. Prevalence of West Nile virus in migratory birds during spring and fall migration. Am J Trop Med Hyg **81:**1151-1158.

40. **Komar N, Langevin S, Hinten S, Nemeth N, Edwards E, Hettler D, Davis B, Bowen R, Bunning M.** 2003. Experimental infection of North American birds with the New York 1999 strain of West Nile virus. Emerg Infect Dis **9:**311-322.

41. **McLean RG, Ubico SR, Docherty DE, Hansen WR, Sileo L, McNamara TS.** 2001. West Nile virus transmission and ecology in birds. Ann N Y Acad Sci **951:**54-57.

42. **Chamberlain RW, Sudia WD.** 1961. Mechanism of transmission of viruses by mosquitoes. Annu Rev Entomol **6:**371-390.

43. **Grimstad PR, Paulson SL, Craig GB, Jr.** 1985. Vector competence of Aedes hendersoni (Diptera: Culicidae) for La Crosse virus and evidence of a salivary-gland escape barrier. J Med Entomol **22:**447-453.

44. **Hardy JL, Houk EJ, Kramer LD, Reeves WC.** 1983. Intrinsic factors affecting vector competence of mosquitoes for arboviruses. Annu Rev Entomol **28:**229-262.

45. **Kramer LD, Hardy JL, Presser SB, Houk EJ.** 1981. Dissemination barriers for western equine encephalomyelitis virus in Culex tarsalis infected after ingestion of low viral doses. Am J Trop Med Hyg **30:**190-197.

46. **Chotkowski HL, Ciota AT, Jia Y, Puig-Basagoiti F, Kramer LD, Shi PY, Glaser RL.** 2008. West Nile virus infection of Drosophila melanogaster induces a protective RNAi response. Virology **377:**197-206.

47. **Arjona A, Wang P, Montgomery RR, Fikrig E.** 2011. Innate immune control of West Nile virus infection. Cell Microbiol **13:**1648-1658.

48. **Donadieu E, Bahuon C, Lowenski S, Zientara S, Coulpier M, Lecollinet S.** 2013. Differential virulence and pathogenesis of West Nile viruses. Viruses **5:**2856-2880.

49. **Gyure KA.** 2009. West Nile virus infections. J Neuropathol Exp Neurol **68:**1053-1060.

50. **Hayes EB, Gubler DJ.** 2006. West Nile virus: epidemiology and clinical features of an emerging epidemic in the United States. Annu Rev Med **57:**181-194.

51. **Mostashari F, Bunning ML, Kitsutani PT, Singer DA, Nash D, Cooper MJ, Katz N, Liljebjelke KA, Biggerstaff BJ, Fine AD, Layton MC, Mullin SM, Johnson AJ, Martin DA, Hayes EB, Campbell GL.** 2001. Epidemic West Nile encephalitis, New York, 1999: results of a household-based seroepidemiological survey. Lancet **358:**261-264.

52. **Petersen LR, Carson PJ, Biggerstaff BJ, Custer B, Borchardt SM, Busch MP.** 2012. Estimated cumulative incidence of West Nile virus infection in US adults, 1999-2010. Epidemiol Infect **141:**591-595.

53. **Zou S, Foster GA, Dodd RY, Petersen LR, Stramer SL.** 2010. West Nile fever characteristics among viremic persons identified through blood donor screening. J Infect Dis **202:**1354-1361.

54. **Hall RA, Broom AK, Smith DW, Mackenzie JS.** 2002. The ecology and epidemiology of Kunjin virus. Current Topics in Microbiology and Immunology **267:**253-269.

55. **Hall RA, Scherret JH, Mackenzie JS.** 2001. Kunjin virus: an Australian variant of West Nile? Annals of the New York Academy of Sciences **951:**153-160.

56. **Lim PY, Behr MJ, Chadwick CM, Shi PY, Bernard KA.** 2011. Keratinocytes are cell targets of West Nile virus in vivo. J Virol **85:**5197-5201.

57. **Schneider BS, Higgs S.** 2008. The enhancement of arbovirus transmission and disease by mosquito saliva is associated with modulation of the host immune response. Trans R Soc Trop Med Hyg **102:**400-408.

58. **Johnston LJ, Halliday GM, King NJ.** 2000. Langerhans cells migrate to local lymph nodes following cutaneous infection with an arbovirus. J Invest Dermatol **114:**560-568.

59. **Cho H, Diamond MS.** 2012. Immune responses to West Nile virus infection in the central nervous system. Viruses **4:**3812-3830.

60. **Rios M, Zhang MJ, Grinev A, Srinivasan K, Daniel S, Wood O, Hewlett IK, Dayton AI.** 2006. Monocytes-macrophages are a potential target in human infection with West Nile virus through blood transfusion. Transfusion **46:**659-667.

61. **Silva MC, Guerrero-Plata A, Gilfoy FD, Garofalo RP, Mason PW.** 2007. Differential activation of human monocyte-derived and plasmacytoid dendritic cells by West Nile virus generated in different host cells. J Virol **81:**13640-13648.

62. **Diamond MS, Gale M, Jr.** 2012. Cell-intrinsic innate immune control of West Nile virus infection. Trends Immunol **33:**522-530.

63. **Quicke KM, Suthar MS.** 2013. The innate immune playbook for restricting West Nile virus infection. Viruses **5:**2643-2658.

64. **Rossini G, Landini MP, Gelsomino F, Sambri V, Varani S.** 2013. Innate host responses to West Nile virus: Implications for central nervous system immunopathology. World J Virol **2:**49-56.

65. **Kato H, Takeuchi O, Sato S, Yoneyama M, Yamamoto M, Matsui K, Uematsu S, Jung A, Kawai T, Ishii KJ, Yamaguchi O, Otsu K, Tsujimura T, Koh CS, Reis e Sousa C, Matsuura Y, Fujita T, Akira S.** 2006. Differential roles of MDA5 and RIG-I helicases in the recognition of RNA viruses. Nature **441:**101-105.

66. **Chang TH, Liao CL, Lin YL.** 2006. Flavivirus induces interferon-beta gene expression through a pathway involving RIG-I-dependent IRF-3 and PI3K-dependent NF-kappaB activation. Microbes Infect **8:**157-171.

67. **Errett JS, Suthar MS, McMillan A, Diamond MS, Gale M, Jr.** 2013. The essential, nonredundant roles of RIG-I and MDA5 in detecting and controlling West Nile virus infection. J Virol **87:**11416-11425.

68. **Shipley JG, Vandergaast R, Deng L, Mariuzza RA, Fredericksen BL.** 2012. Identification of multiple RIG-I-specific pathogen associated molecular patterns within the West Nile virus genome and antigenome. Virology **432:**232-238.

69. **Lazear HM, Pinto AK, Ramos HJ, Vick SC, Shrestha B, Suthar MS, Gale M, Jr., Diamond MS.** 2013. Pattern recognition receptor MDA5 modulates CD8+ T cell-dependent clearance of West Nile virus from the central nervous system. J Virol **87:**11401-11415.

70. **Suthar MS, Ma DY, Thomas S, Lund JM, Zhang N, Daffis S, Rudensky AY, Bevan MJ, Clark EA, Kaja MK, Diamond MS, Gale M, Jr.** 2010. IPS-1 is essential for the control of West Nile virus infection and immunity. PLoS Pathog **6:**e1000757.

71. **Wang P, Arjona A, Zhang Y, Sultana H, Dai J, Yang L, LeBlanc PM, Doiron K, Saleh M, Fikrig E.** 2010. Caspase-12 controls West Nile virus infection via the viral RNA receptor RIG-I. Nature Immunology **11:**912-919.

72. **Fredericksen BL, Gale M, Jr.** 2006. West Nile virus evades activation of interferon regulatory factor 3 through RIG-I-dependent and -independent pathways without antagonizing host defense signaling. J Virol **80:**2913-2923.

73. **Fredericksen BL, Keller BC, Fornek J, Katze MG, Gale M, Jr.** 2008. Establishment and maintenance of the innate antiviral response to West Nile Virus involves both RIG-I and MDA5 signaling through IPS-1. J Virol **82:**609-616.

74. **Alexopoulou L, Holt AC, Medzhitov R, Flavell RA.** 2001. Recognition of double-stranded RNA and activation of NF-kappaB by Toll-like receptor 3. Nature **413:**732-738.

75. **Heil F, Hemmi H, Hochrein H, Ampenberger F, Kirschning C, Akira S, Lipford G, Wagner H, Bauer S.** 2004. Species-specific recognition of single-stranded RNA via toll-like receptor 7 and 8. Science **303:**1526-1529.

76. **Daffis S, Samuel MA, Suthar MS, Gale M, Jr., Diamond MS.** 2008. Toll-like receptor 3 has a protective role against West Nile virus infection. Journal of Virology **82:**10349-10358.

77. **Kong KF, Delroux K, Wang X, Qian F, Arjona A, Malawista SE, Fikrig E, Montgomery RR.** 2008. Dysregulation of TLR3 impairs the innate immune response to West Nile virus in the elderly. J Virol **82:**7613-7623.

78. **Sabouri AH, Marcondes MC, Flynn C, Berger M, Xiao N, Fox HS, Sarvetnick NE.** 2014. TLR signaling controls lethal encephalitis in WNV-infected brain. Brain Res **1574:**84-95.

79. **Szretter KJ, Daffis S, Patel J, Suthar MS, Klein RS, Gale M, Jr., Diamond MS.** 2010. The innate immune adaptor molecule MyD88 restricts West Nile virus replication and spread in neurons of the central nervous system. J Virol **84:**12125-12138.

80. **Town T, Bai F, Wang T, Kaplan AT, Qian F, Montgomery RR, Anderson JF, Flavell RA, Fikrig E.** 2009. Toll-like receptor 7 mitigates lethal West Nile encephalitis via interleukin 23-dependent immune cell infiltration and homing. Immunity **30:**242-253.

81. **Wang T, Town T, Alexopoulou L, Anderson JF, Fikrig E, Flavell RA.** 2004. Toll-like receptor 3 mediates West Nile virus entry into the brain causing lethal encephalitis. Nat Med **10:**1366-1373.

82. **Welte T, Reagan K, Fang H, Machain-Williams C, Zheng X, Mendell N, Chang GJ, Wu P, Blair CD, Wang T.** 2009. Toll-like receptor 7-induced immune response to cutaneous West Nile virus infection. J Gen Virol **90:**2660-2668.

83. **Xia J, Winkelmann ER, Gorder SR, Mason PW, Milligan GN.** 2013. TLR3- and MyD88-dependent signaling differentially influences the development of West Nile virus-specific B cell responses in mice following immunization with RepliVAX WN, a single-cycle flavivirus vaccine candidate. J Virol **87:**12090-12101.

84. **Ramos HJ, Lanteri MC, Blahnik G, Negash A, Suthar MS, Brassil MM, Sodhi K, Treuting PM, Busch MP, Norris PJ, Gale M, Jr.** 2012. IL-1beta signaling promotes CNS-intrinsic immune control of West Nile virus infection. PLoS Pathog **8:**e1003039.

85. **Durrant DM, Robinette ML, Klein RS.** 2013. IL-1R1 is required for dendritic cell-mediated T cell reactivation within the CNS during West Nile virus encephalitis. J Exp Med **210:**503-516.

86. **Kumar M, Roe K, Orillo B, Muruve DA, Nerurkar VR, Gale M, Jr., Verma S.** 2013. Inflammasome adaptor protein Apoptosis-associated speck-like protein containing CARD (ASC) is critical for the immune response and survival in west Nile virus encephalitis. J Virol **87:**3655-3667.

87. **Byrne SN, Halliday GM, Johnston LJ, King NJ.** 2001. Interleukin-1beta but not tumor necrosis factor is involved in West Nile virus-induced Langerhans cell migration from the skin in C57BL/6 mice. J Invest Dermatol **117:**702-709.

88. **Lazear HM, Pinto AK, Vogt MR, Gale M, Jr., Diamond MS.** 2011. Beta interferon controls West Nile virus infection and pathogenesis in mice. J Virol **85:**7186-7194.

89. **Pinto AK, Daffis S, Brien JD, Gainey MD, Yokoyama WM, Sheehan KC, Murphy KM, Schreiber RD, Diamond MS.** 2011. A temporal role of type I interferon signaling in CD8+ T cell maturation during acute West Nile virus infection. PLoS Pathog **7:**e1002407.

90. **Purtha WE, Chachu KA, Virgin HWt, Diamond MS.** 2008. Early B-cell activation after West Nile virus infection requires alpha/beta interferon but not antigen receptor signaling. J Virol **82:**10964-10974.

91. **Samuel MA, Diamond MS.** 2005. Alpha/beta interferon protects against lethal West Nile virus infection by restricting cellular tropism and enhancing neuronal survival. J Virol **79:**13350-13361.

92. **Seo YJ, Hahm B.** 2010. Type I interferon modulates the battle of host immune system against viruses. Adv Appl Microbiol **73:**83-101.

93. **Suthar MS, Brassil MM, Blahnik G, McMillan A, Ramos HJ, Proll SC, Belisle SE, Katze MG, Gale M, Jr.** 2013. A systems biology approach reveals that tissue tropism to West Nile virus is regulated by antiviral genes and innate immune cellular processes. PLoS Pathog **9:**e1003168.

94. **Jiang D, Weidner JM, Qing M, Pan XB, Guo H, Xu C, Zhang X, Birk A, Chang J, Shi PY, Block TM, Guo JT.** 2010. Identification of five interferon-induced cellular proteins that inhibit west nile virus and dengue virus infections. J Virol **84:**8332-8341.

95. **Krishnan MN, Ng A, Sukumaran B, Gilfoy FD, Uchil PD, Sultana H, Brass AL, Adametz R, Tsui M, Qian F, Montgomery RR, Lev S, Mason PW, Koski RA, Elledge SJ, Xavier RJ, Agaisse H, Fikrig E.** 2008. RNA interference screen for human genes associated with West Nile virus infection. Nature **455:**242-245.

96. **Li J, Ding SC, Cho H, Chung BC, Gale M, Jr., Chanda SK, Diamond MS.** 2013. A short hairpin RNA screen of interferon-stimulated genes identifies a novel negative regulator of the cellular antiviral response. MBio **4:**e00385-00313.

97. **Qian F, Chung L, Zheng W, Bruno V, Alexander RP, Wang Z, Wang X, Kurscheid S, Zhao H, Fikrig E, Gerstein M, Snyder M, Montgomery RR.** 2013. Identification of genes critical for resistance to infection by West Nile virus using RNA-Seq analysis. Viruses **5:**1664-1681.

98. **Schoggins JW, Wilson SJ, Panis M, Murphy MY, Jones CT, Bieniasz P, Rice CM.** 2011. A diverse range of gene products are effectors of the type I interferon antiviral response. Nature **472:**481-485.

99. **Daffis S, Szretter KJ, Schriewer J, Li J, Youn S, Errett J, Lin TY, Schneller S, Zust R, Dong H, Thiel V, Sen GC, Fensterl V, Klimstra WB, Pierson TC, Buller RM, Gale M, Jr., Shi PY, Diamond MS.** 2010. 2'-O methylation of the viral mRNA cap evades host restriction by IFIT family members. Nature **468:**452-456.

100. **Perwitasari O, Cho H, Diamond MS, Gale M, Jr.** 2011. Inhibitor of kappaB kinase epsilon (IKK(epsilon)), STAT1, and IFIT2 proteins define novel innate immune effector pathway against West Nile virus infection. J Biol Chem **286:**44412-44423.

101. **Szretter KJ, Daniels BP, Cho H, Gainey MD, Yokoyama WM, Gale M, Jr., Virgin HW, Klein RS, Sen GC, Diamond MS.** 2012. 2'-O methylation of the viral mRNA cap by West Nile virus evades ifit1-dependent and -independent mechanisms of host restriction in vivo. PLoS Pathog **8:**e1002698.

102. **Brass AL, Huang IC, Benita Y, John SP, Krishnan MN, Feeley EM, Ryan BJ, Weyer JL, van der Weyden L, Fikrig E, Adams DJ, Xavier RJ, Farzan M, Elledge SJ.** 2009. The IFITM proteins mediate cellular resistance to influenza A H1N1 virus, West Nile virus, and dengue virus. Cell **139:**1243-1254.

103. **Gilfoy FD, Mason PW.** 2007. West Nile virus-induced interferon production is mediated by the double-stranded RNA-dependent protein kinase PKR. J Virol **81:**11148-11158.

104. **Samuel MA, Whitby K, Keller BC, Marri A, Barchet W, Williams BR, Silverman RH, Gale M, Jr., Diamond MS.** 2006. PKR and RNase L contribute to protection against lethal

West Nile Virus infection by controlling early viral spread in the periphery and replication in neurons. J Virol **80:**7009-7019.

105. **Scherbik SV, Paranjape JM, Stockman BM, Silverman RH, Brinton MA.** 2006. RNase L plays a role in the antiviral response to West Nile virus. J Virol **80:**2987-2999.

106. **Schuessler A, Funk A, Lazear HM, Cooper DA, Torres S, Daffis S, Jha BK, Kumagai Y, Takeuchi O, Hertzog P, Silverman R, Akira S, Barton DJ, Diamond MS, Khromykh AA.** 2012. West Nile virus noncoding subgenomic RNA contributes to viral evasion of the type I interferon-mediated antiviral response. J Virol **86:**5708-5718.

107. **Szretter KJ, Brien JD, Thackray LB, Virgin HW, Cresswell P, Diamond MS.** 2011. The interferon-inducible gene viperin restricts West Nile virus pathogenesis. J Virol **85:**11557-11566.

108. **Getts DR, Matsumoto I, Muller M, Getts MT, Radford J, Shrestha B, Campbell IL, King NJ.** 2007. Role of IFN-gamma in an experimental murine model of West Nile virus-induced seizures. J Neurochem **103:**1019-1030.

109. **Shrestha B, Wang T, Samuel MA, Whitby K, Craft J, Fikrig E, Diamond MS.** 2006. Gamma interferon plays a crucial early antiviral role in protection against West Nile virus infection. J Virol **80:**5338-5348.

110. **Ma D, Jiang D, Qing M, Weidner JM, Qu X, Guo H, Chang J, Gu B, Shi PY, Block TM, Guo JT.** 2009. Antiviral effect of interferon lambda against West Nile virus. Antiviral Res **83:**53-60.

111. **Arjona A, Ledizet M, Anthony K, Bonafe N, Modis Y, Town T, Fikrig E.** 2007. West Nile virus envelope protein inhibits dsRNA-induced innate immune responses. J Immunol **179:**8403-8409.

112. **Baronti C, Sire J, de Lamballerie X, Querat G.** 2010. Nonstructural NS1 proteins of several mosquito-borne Flavivirus do not inhibit TLR3 signaling. Virology **404:**319-330.

113. **Crook KR, Miller-Kittrell M, Morrison CR, Scholle F.** 2014. Modulation of innate immune signaling by the secreted form of the West Nile virus NS1 glycoprotein. Virology **458-459:**172-182.

114. **Wilson JR, Sessions PFd, Leon MA, Scholle F.** 2008. West Nile Virus Nonstructural Protein 1 Inhibits TLR3 Signal Transduction. Journal of Virology **82:**8262 - 8271.

115. **Laurent-Rolle M, Boer EF, Lubick KJ, Wolfinbarger JB, Carmody AB, Rockx B, Liu W, Ashour J, Shupert WL, Holbrook MR, Barrett AD, Mason PW, Bloom ME, Garcia-Sastre A, Khromykh AA, Best SM.** 2010. The NS5 protein of the virulent West Nile virus NY99 strain is a potent antagonist of type I interferon-mediated JAK-STAT signaling. J Virol **84:**3503-3515.

116. **Liu WJ, Chen HB, Wang XJ, Huang H, Khromykh AA.** 2004. Analysis of adaptive mutations in Kunjin virus replicon RNA reveals a novel role for the flavivirus nonstructural protein NS2A in inhibition of beta interferon promoter-driven transcription. Journal of Virology **78:**12225-12235.

117. **Liu WJ, Wang XJ, Clark DC, Lobigs M, Hall RA, Khromykh AA.** 2006. A single amino acid substitution in the West Nile virus nonstructural protein NS2A disables its ability to inhibit alpha/beta interferon induction and attenuates virus virulence in mice. J Virol **80:**2396-2404.

118. **Liu WJ, Wang XJ, Mokhonov VV, Shi PY, Randall R, Khromykh AA.** 2005. Inhibition of interferon signaling by the New York 99 strain and Kunjin subtype of West Nile virus involves blockage of STAT1 and STAT2 activation by nonstructural proteins. Journal of Virology **79:**1934-1942.

119. **Suthar MS, Brassil MM, Blahnik G, Gale M, Jr.** 2012. Infectious clones of novel lineage 1 and lineage 2 West Nile virus strains WNV-TX02 and WNV-Madagascar. J Virol **86:**7704-7709.

120. **Ambrose RL, Mackenzie JM.** 2013. ATF6 signaling is required for efficient West Nile virus replication by promoting cell survival and inhibition of innate immune responses. J Virol **87:**2206-2214.

121. **Ambrose RL, Mackenzie JM.** 2011. West Nile virus differentially modulates the unfolded protein response to facilitate replication and immune evasion. J Virol **85:**2723-2732.

122. **Mackenzie JM, Khromykh AA, Parton RG.** 2007. Cholesterol manipulation by West Nile virus perturbs the cellular immune response. Cell Host Microbe **2:**229-239.

123. **Keller BC, Fredericksen BL, Samuel MA, Mock RE, Mason PW, Diamond MS, Gale M, Jr.** 2006. Resistance to alpha/beta interferon is a determinant of West Nile virus replication fitness and virulence. J Virol **80:**9424-9434.

124. **Evans JD, Crown RA, Sohn JA, Seeger C.** 2011. West Nile virus infection induces depletion of IFNAR1 protein levels. Viral Immunol **24:**253-263.

125. **Vivier E, Raulet DH, Moretta A, Caligiuri MA, Zitvogel L, Lanier LL, Yokoyama WM, Ugolini S.** 2011. Innate or adaptive immunity? The example of natural killer cells. Science **331:**44-49.

126. **Hershkovitz O, Rosental B, Rosenberg LA, Navarro-Sanchez ME, Jivov S, Zilka A, Gershoni-Yahalom O, Brient-Litzler E, Bedouelle H, Ho JW, Campbell KS, Rager-Zisman B, Despres P, Porgador A.** 2009. NKp44 receptor mediates interaction of the envelope glycoproteins from the West Nile and dengue viruses with NK cells. J Immunol **183:**2610-2621.

127. **Zhang M, Daniel S, Huang Y, Chancey C, Huang Q, Lei YF, Grinev A, Mostowski H, Rios M, Dayton A.** 2010. Anti-West Nile virus activity of in vitro expanded human primary natural killer cells. BMC Immunol **11:**3.

128. **Larena M, Regner M, Lobigs M.** 2013. Cytolytic effector pathways and IFN-gamma help protect against Japanese encephalitis. Eur J Immunol **43:**1789-1798.

129. **Vogt MR, Dowd KA, Engle M, Tesh RB, Johnson S, Pierson TC, Diamond MS.** 2011. Poorly neutralizing cross-reactive antibodies against the fusion loop of West Nile virus envelope protein protect in vivo via Fcgamma receptor and complement-dependent effector mechanisms. J Virol **85:**11567-11580.

130. **Wang T, Scully E, Yin Z, Kim JH, Wang S, Yan J, Mamula M, Anderson JF, Craft J, Fikrig E.** 2003. IFN-gamma-producing gamma delta T cells help control murine West Nile virus infection. J Immunol **171:**2524-2531.

131. **Stoermer KA, Morrison TE.** 2011. Complement and viral pathogenesis. Virology **411:**362-373.

132. **Fuchs A, Pinto AK, Schwaeble WJ, Diamond MS.** 2011. The lectin pathway of complement activation contributes to protection from West Nile virus infection. Virology **412:**101-109.

133. **Mehlhop E, Diamond MS.** 2006. Protective immune responses against West Nile virus are primed by distinct complement activation pathways. J Exp Med **203:**1371-1381.

134. **Mehlhop E, Fuchs A, Engle M, Diamond MS.** 2009. Complement modulates pathogenesis and antibody-dependent neutralization of West Nile virus infection through a C5-independent mechanism. Virology **393:**11-15.

135. **Mehlhop E, Whitby K, Oliphant T, Marri A, Engle M, Diamond MS.** 2005. Complement activation is required for induction of a protective antibody response against West Nile virus infection. J Virol **79:**7466-7477.

136. **Chambers TJ, Droll DA, Walton AH, Schwartz J, Wold WS, Nickells J.** 2008. West Nile 25A virus infection of B-cell-deficient ((micro)MT) mice: characterization of neuroinvasiveness and pseudoreversion of the viral envelope protein. J Gen Virol **89:**627-635.

137. **Diamond MS, Shrestha B, Marri A, Mahan D, Engle M.** 2003. B cells and antibody play critical roles in the immediate defense of disseminated infection by West Nile encephalitis virus. J Virol **77:**2578-2586.

138. **Ben-Nathan D, Lustig S, Tam G, Robinzon S, Segal S, Rager-Zisman B.** 2003. Prophylactic and therapeutic efficacy of human intravenous immunoglobulin in treating West Nile virus infection in mice. J Infect Dis **188:**5-12.

139. **Engle MJ, Diamond MS.** 2003. Antibody prophylaxis and therapy against West Nile virus infection in wild-type and immunodeficient mice. J Virol **77:**12941-12949.

140. **Oliphant T, Engle M, Nybakken GE, Doane C, Johnson S, Huang L, Gorlatov S, Mehlhop E, Marri A, Chung KM, Ebel GD, Kramer LD, Fremont DH, Diamond MS.** 2005. Development of a humanized monoclonal antibody with therapeutic potential against West Nile virus. Nat Med **11:**522-530.

141. **Netland J, Bevan MJ.** 2013. CD8 and CD4 T cells in west nile virus immunity and pathogenesis. Viruses **5:**2573-2584.

142. **Shrestha B, Diamond MS.** 2004. Role of CD8+ T cells in control of West Nile virus infection. J Virol **78:**8312-8321.

143. **Sitati EM, Diamond MS.** 2006. CD4+ T-cell responses are required for clearance of West Nile virus from the central nervous system. J Virol **80:**12060-12069.

144. **Suthar MS, Diamond MS, Gale M, Jr.** 2013. West Nile virus infection and immunity. Nat Rev Microbiol **11:**115-128.

145. **Brien JD, Uhrlaub JL, Nikolich-Zugich J.** 2008. West Nile virus-specific CD4 T cells exhibit direct antiviral cytokine secretion and cytotoxicity and are sufficient for antiviral protection. J Immunol **181:**8568-8575.

146. **Lanteri MC, O'Brien KM, Purtha WE, Cameron MJ, Lund JM, Owen RE, Heitman JW, Custer B, Hirschkorn DF, Tobler LH, Kiely N, Prince HE, Ndhlovu LC, Nixon**

DF, Kamel HT, Kelvin DJ, Busch MP, Rudensky AY, Diamond MS, Norris PJ. 2009. Tregs control the development of symptomatic West Nile virus infection in humans and mice. J Clin Invest **119:**3266-3277.

147. **Khromykh AA, Westaway EG.** 1996. RNA binding properties of core protein of the flavivirus Kunjin. Arch Virol **141:**685-699.

148. **Kitano T, Suzuki K, Yamaguchi T.** 1974. Morphological, chemical, and biological characterization of Japanese encephalitis virus virion and its hemagglutinin. J Virol **14:**631-639.

149. **Murphy FA, Harrison AK, Gary GW, Jr., Whitfield SG, Forrester FT.** 1968. St. Louis encephalitis virus infection in mice. Electron microscopic studies of central nervous system. Lab Invest **19:**652-662.

150. **Nishimura C, Nomura M, Kitaoka M.** 1968. Comparative studies on the structure and properties of two selected strains of Japanese encephalitis virus. Jpn J Med Sci Biol **21:**1-10.

151. **Boulton RW, Westaway EG.** 1977. Togavirus RNA: reversible effect of urea on genomes and absence of subgenomic viral RNA in Kunjin virus-infected cells. Arch Virol **55:**201-208.

152. **Stollar V, Schlesinger RW, Stevens TM.** 1967. Studies on the nature of dengue viruses. III. RNA synthesis in cells infected with type 2 dengue virus. Virology **33:**650-658.

153. **Cleaves GR, Dubin DT.** 1979. Methylation status of intracellular dengue type 2 40 S RNA. Virology **96:**159-165.

154. **Wengler G, Gross HJ.** 1978. Studies on virus-specific nucleic acids synthesized in vertebrate and mosquito cells infected with flaviviruses. Virology **89:**423-437.

155. **Brinton MA, Dispoto JH.** 1988. Sequence and secondary structure analysis of the 5'-terminal region of flavivirus genome RNA. Virology **162:**290-299.

156. **Brinton MA, Fernandez AV, Dispoto JH.** 1986. The 3'-nucleotides of flavivirus genomic RNA form a conserved secondary structure. Virology **153:**113-121.

157. **Cahour A, Pletnev A, Vazielle-Falcoz M, Rosen L, Lai CJ.** 1995. Growth-restricted dengue virus mutants containing deletions in the 5' noncoding region of the RNA genome. Virology **207:**68-76.

158. **Rauscher S, Flamm C, Mandl CW, Heinz FX, Stadler PF.** 1997. Secondary structure of the 3'-noncoding region of flavivirus genomes: comparative analysis of base pairing probabilities. RNA **3:**779-791.

159. **Beasley DW, Li L, Suderman MT, Barrett AD.** 2001. West Nile virus strains differ in mouse neurovirulence and binding to mouse or human brain membrane receptor preparations. Ann N Y Acad Sci **951:**332-335.

160. **Lindenbach BD, Rice CM.** 2003. Molecular biology of flaviviruses. Advances in Virus Research **59:**23-61.

161. **Nowak T, Farber PM, Wengler G.** 1989. Analyses of the terminal sequences of West Nile virus structural proteins and of the in vitro translation of these proteins allow the proposal of a complete scheme of the proteolytic cleavages involved in their synthesis. Virology **169:**365-376.

162. **Rice CM, Lenches EM, Eddy SR, Shin SJ, Sheets RL, Strauss JH.** 1985. Nucleotide sequence of yellow fever virus: implications for flavivirus gene expression and evolution. Science **229:**726-733.

163. **Cahour A, Falgout B, Lai CJ.** 1992. Cleavage of the dengue virus polyprotein at the NS3/NS4A and NS4B/NS5 junctions is mediated by viral protease NS2B-NS3, whereas NS4A/NS4B may be processed by a cellular protease. J Virol **66:**1535-1542.

164. **Falgout B, Pethel M, Zhang YM, Lai CJ.** 1991. Both nonstructural proteins NS2B and NS3 are required for the proteolytic processing of dengue virus nonstructural proteins. J Virol **65:**2467-2475.

165. **Speight G, Coia G, Parker MD, Westaway EG.** 1988. Gene mapping and positive identification of the non-structural proteins NS2A, NS2B, NS3, NS4B and NS5 of the flavivirus Kunjin and their cleavage sites. Journal of General Virology **69 (Pt 1):**23-34.

166. **Speight G, Westaway EG.** 1989. Carboxy-terminal analysis of nine proteins specified by the flavivirus Kunjin: evidence that only the intracellular core protein is truncated. J Gen Virol **70 (Pt 8):**2209-2214.

167. **von Heijne G.** 1983. Patterns of amino acids near signal-sequence cleavage sites. Eur J Biochem **133:**17-21.

168. **Chambers TJ, McCourt DW, Rice CM.** 1989. Yellow fever virus proteins NS2A, NS2B, and NS4B: identification and partial N-terminal amino acid sequence analysis. Virology **169:**100-109.

169. **Amberg SM, Rice CM.** 1999. Mutagenesis of the NS2B-NS3-mediated cleavage site in the flavivirus capsid protein demonstrates a requirement for coordinated processing. J Virol **73:**8083-8094.

170. **Lobigs M.** 1993. Flavivirus premembrane protein cleavage and spike heterodimer secretion require the function of the viral proteinase NS3. Proc Natl Acad Sci U S A **90:**6218-6222.

171. **Lobigs M, Lee E.** 2004. Inefficient signalase cleavage promotes efficient nucleocapsid incorporation into budding flavivirus membranes. J Virol **78:**178-186.

172. **Lobigs M, Lee E, Ng ML, Pavy M, Lobigs P.** 2010. A flavivirus signal peptide balances the catalytic activity of two proteases and thereby facilitates virus morphogenesis. Virology **401:**80-89.

173. **Schrauf S, Schlick P, Skern T, Mandl CW.** 2008. Functional analysis of potential carboxy-terminal cleavage sites of tick-borne encephalitis virus capsid protein. J Virol **82:**2218-2229.

174. **Stocks CE, Lobigs M.** 1998. Signal peptidase cleavage at the flavivirus C-prM junction: dependence on the viral NS2B-3 protease for efficient processing requires determinants in C, the signal peptide, and prM. J Virol **72:**2141-2149.

175. **Yamshchikov VF, Compans RW.** 1994. Processing of the intracellular form of the west Nile virus capsid protein by the viral NS2B-NS3 protease: an in vitro study. J Virol **68:**5765-5771.

176. **Ivanyi-Nagy R, Lavergne JP, Gabus C, Ficheux D, Darlix JL.** 2008. RNA chaperoning and intrinsic disorder in the core proteins of Flaviviridae. Nucleic Acids Res **36:**712-725.

177. **Jones CT, Ma L, Burgner JW, Groesch TD, Post CB, Kuhn RJ.** 2003. Flavivirus capsid is a dimeric alpha-helical protein. J Virol **77:**7143-7149.

178. **Markoff L, Falgout B, Chang A.** 1997. A conserved internal hydrophobic domain mediates the stable membrane integration of the dengue virus capsid protein. Virology **233:**105-117.

179. **Khromykh AA, Varnavski AN, Westaway EG.** 1998. Encapsidation of the flavivirus kunjin replicon RNA by using a complementation system providing Kunjin virus structural proteins in trans. J Virol **72:**5967-5977.

180. **Kiermayr S, Kofler RM, Mandl CW, Messner P, Heinz FX.** 2004. Isolation of capsid protein dimers from the tick-borne encephalitis flavivirus and in vitro assembly of capsid-like particles. J Virol **78:**8078-8084.

181. **Lopez C, Gil L, Lazo L, Menendez I, Marcos E, Sanchez J, Valdes I, Falcon V, de la Rosa MC, Marquez G, Guillen G, Hermida L.** 2009. In vitro assembly of nucleocapsid-like particles from purified recombinant capsid protein of dengue-2 virus. Arch Virol **154:**695-698.

182. **Zhang Y, Kostyuchenko VA, Rossmann MG.** 2007. Structural analysis of viral nucleocapsids by subtraction of partial projections. J Struct Biol **157:**356-364.

183. **Bhuvanakantham R, Ng ML.** 2013. West Nile virus and dengue virus capsid protein negates the antiviral activity of human Sec3 protein through the proteasome pathway. Cell Microbiol **15:**1688-1706.

184. **Katoh H, Mori Y, Kambara H, Abe T, Fukuhara T, Morita E, Moriishi K, Kamitani W, Matsuura Y.** 2011. Heterogeneous nuclear ribonucleoprotein A2 participates in the replication of Japanese encephalitis virus through an interaction with viral proteins and RNA. J Virol **85:**10976-10988.

185. **Kuhn RJ, Zhang W, Rossmann MG, Pletnev SV, Corver J, Lenches E, Jones CT, Mukhopadhyay S, Chipman PR, Strauss EG, Baker TS, Strauss JH.** 2002. Structure of dengue virus: implications for flavivirus organization, maturation, and fusion. Cell **108:**717-725.

186. **Zhang W, Chipman PR, Corver J, Johnson PR, Zhang Y, Mukhopadhyay S, Baker TS, Strauss JH, Rossmann MG, Kuhn RJ.** 2003. Visualization of membrane protein domains by cryo-electron microscopy of dengue virus. Nat Struct Biol **10:**907-912.

187. **Zhang Y, Corver J, Chipman PR, Zhang W, Pletnev SV, Sedlak D, Baker TS, Strauss JH, Kuhn RJ, Rossmann MG.** 2003. Structures of immature flavivirus particles. EMBO J **22:**2604-2613.

188. **Heinz FX, Stiasny K, Puschner-Auer G, Holzmann H, Allison SL, Mandl CW, Kunz C.** 1994. Structural changes and functional control of the tick-borne encephalitis virus glycoprotein E by the heterodimeric association with protein prM. Virology **198:**109-117.

189. **Guirakhoo F, Bolin RA, Roehrig JT.** 1992. The Murray Valley encephalitis virus prM protein confers acid resistance to virus particles and alters the expression of epitopes within the R2 domain of E glycoprotein. Virology **191:**921-931.

190. **Mackenzie JM, Westaway EG.** 2001. Assembly and maturation of the flavivirus Kunjin virus appear to occur in the rough endoplasmic reticulum and along the secretory pathway, respectively. J Virol **75:**10787-10799.

191. **Castle E, Nowak T, Leidner U, Wengler G.** 1985. Sequence analysis of the viral core protein and the membrane-associated proteins V1 and NV2 of the flavivirus West Nile virus and of the genome sequence for these proteins. Virology **145:**227-236.

192. **Junjhon J, Lausumpao M, Supasa S, Noisakran S, Songjaeng A, Saraithong P, Chaichoun K, Utaipat U, Keelapang P, Kanjanahaluethai A, Puttikhunt C, Kasinrerk W, Malasit P, Sittisombut N.** 2008. Differential modulation of prM cleavage, extracellular particle distribution, and virus infectivity by conserved residues at nonfurin consensus positions of the dengue virus pr-M junction. J Virol **82:**10776-10791.

193. **Li L, Lok SM, Yu IM, Zhang Y, Kuhn RJ, Chen J, Rossmann MG.** 2008. The flavivirus precursor membrane-envelope protein complex: structure and maturation. Science **319:**1830-1834.

194. **Yu IM, Holdaway HA, Chipman PR, Kuhn RJ, Rossmann MG, Chen J.** 2009. Association of the pr peptides with dengue virus at acidic pH blocks membrane fusion. J Virol **83:**12101-12107.

195. **Goto A, Yoshii K, Obara M, Ueki T, Mizutani T, Kariwa H, Takashima I.** 2005. Role of the N-linked glycans of the prM and E envelope proteins in tick-borne encephalitis virus particle secretion. Vaccine **23:**3043-3052.

196. **Hanna SL, Pierson TC, Sanchez MD, Ahmed AA, Murtadha MM, Doms RW.** 2005. N-linked glycosylation of west nile virus envelope proteins influences particle assembly and infectivity. J Virol **79:**13262-13274.

197. **Kim JM, Yun SI, Song BH, Hahn YS, Lee CH, Oh HW, Lee YM.** 2008. A single N-linked glycosylation site in the Japanese encephalitis virus prM protein is critical for cell type-specific prM protein biogenesis, virus particle release, and pathogenicity in mice. J Virol **82:**7846-7862.

198. **Lorenz IC, Allison SL, Heinz FX, Helenius A.** 2002. Folding and dimerization of tick-borne encephalitis virus envelope proteins prM and E in the endoplasmic reticulum. J Virol **76:**5480-5491.

199. **Roehrig JT, Hunt AR, Johnson AJ, Hawkes RA.** 1989. Synthetic peptides derived from the deduced amino acid sequence of the E-glycoprotein of Murray Valley encephalitis virus elicit antiviral antibody. Virology **171:**49-60.

200. **Pierson TC, Diamond MS.** 2008. Molecular mechanisms of antibody-mediated neutralisation of flavivirus infection. Expert Rev Mol Med **10:**e12.

201. **Heinz FX, Mandl CW, Holzmann H, Kunz C, Harris BA, Rey F, Harrison SC.** 1991. The flavivirus envelope protein E: isolation of a soluble form from tick-borne encephalitis virus and its crystallization. J Virol **65:**5579-5583.

202. **Kanai R, Kar K, Anthony K, Gould LH, Ledizet M, Fikrig E, Marasco WA, Koski RA, Modis Y.** 2006. Crystal structure of west nile virus envelope glycoprotein reveals viral surface epitopes. J Virol **80:**11000-11008.

203. **Nybakken GE, Nelson CA, Chen BR, Diamond MS, Fremont DH.** 2006. Crystal structure of the West Nile virus envelope glycoprotein. J Virol **80:**11467-11474.

204. **Rey FA, Heinz FX, Mandl C, Kunz C, Harrison SC.** 1995. The envelope glycoprotein from tick-borne encephalitis virus at 2 A resolution. Nature **375:**291-298.

205. **Wengler G, Castle E, Leidner U, Nowak T.** 1985. Sequence analysis of the membrane protein V3 of the flavivirus West Nile virus and of its gene. Virology **147:**264-274.

206. **Bressanelli S, Stiasny K, Allison SL, Stura EA, Duquerroy S, Lescar J, Heinz FX, Rey FA.** 2004. Structure of a flavivirus envelope glycoprotein in its low-pH-induced membrane fusion conformation. EMBO J **23:**728-738.

207. **Modis Y, Ogata S, Clements D, Harrison SC.** 2004. Structure of the dengue virus envelope protein after membrane fusion. Nature **427:**313-319.

208. **Bhardwaj S, Holbrook M, Shope RE, Barrett AD, Watowich SJ.** 2001. Biophysical characterization and vector-specific antagonist activity of domain III of the tick-borne flavivirus envelope protein. J Virol **75:**4002-4007.

209. **Chu JJ, Rajamanonmani R, Li J, Bhuvanakantham R, Lescar J, Ng ML.** 2005. Inhibition of West Nile virus entry by using a recombinant domain III from the envelope glycoprotein. J Gen Virol **86:**405-412.

210. **Lee E, Lobigs M.** 2000. Substitutions at the putative receptor-binding site of an encephalitic flavivirus alter virulence and host cell tropism and reveal a role for glycosaminoglycans in entry. J Virol **74:**8867-8875.

211. **Lee E, Leang SK, Davidson A, Lobigs M.** 2010. Both E protein glycans adversely affect dengue virus infectivity but are beneficial for virion release. J Virol **84:**5171-5180.

212. **Mondotte JA, Lozach PY, Amara A, Gamarnik AV.** 2007. Essential role of dengue virus envelope protein N glycosylation at asparagine-67 during viral propagation. J Virol **81:**7136-7148.

213. **Adams SC, Broom AK, Sammels LM, Hartnett AC, Howard MJ, Coelen RJ, Mackenzie JS, Hall RA.** 1995. Glycosylation and antigenic variation among Kunjin virus isolates. Virology **206:**49-56.

214. **Beasley DW, Whiteman MC, Zhang S, Huang CY, Schneider BS, Smith DR, Gromowski GD, Higgs S, Kinney RM, Barrett AD.** 2005. Envelope protein glycosylation status influences mouse neuroinvasion phenotype of genetic lineage 1 West Nile virus strains. J Virol **79:**8339-8347.

215. **Botha EM, Markotter W, Wolfaardt M, Paweska JT, Swanepoel R, Palacios G, Nel LH, Venter M.** 2008. Genetic determinants of virulence in pathogenic lineage 2 West Nile virus strains. Emerg Infect Dis **14:**222-230.

216. **Shirato K, Miyoshi H, Goto A, Ako Y, Ueki T, Kariwa H, Takashima I.** 2004. Viral envelope protein glycosylation is a molecular determinant of the neuroinvasiveness of the New York strain of West Nile virus. J Gen Virol **85:**3637-3645.

217. **Harrison SC.** 2008. The pH sensor for flavivirus membrane fusion. J Cell Biol **183:**177-179.

218. **Mukhopadhyay S, Kuhn RJ, Rossmann MG.** 2005. A structural perspective of the flavivirus life cycle. Nat Rev Microbiol **3:**13-22.

219. **Stiasny K, Fritz R, Pangerl K, Heinz FX.** 2009. Molecular mechanisms of flavivirus membrane fusion. Amino Acids **41:**1159-1163.

220. **Liao M, Sanchez-San Martin C, Zheng A, Kielian M.** 2010. In vitro reconstitution reveals key intermediate states of trimer formation by the dengue virus membrane fusion protein. J Virol **84:**5730-5740.

221. **Mackenzie JM, Khromykh AA, Jones MK, Westaway EG.** 1998. Subcellular localization and some biochemical properties of the flavivirus Kunjin nonstructural proteins NS2A and NS4A. Virology **245:**203-215.

222. **Miller S, Kastner S, Krijnse-Locker J, Buhler S, Bartenschlager R.** 2007. The non-structural protein 4A of dengue virus is an integral membrane protein inducing membrane alterations in a 2K-regulated manner. J Biol Chem **282:**8873-8882.

223. **Miller S, Sparacio S, Bartenschlager R.** 2006. Subcellular localization and membrane topology of the Dengue virus type 2 Non-structural protein 4B. J Biol Chem **281:**8854-8863.

224. **Westaway EG, Mackenzie JM, Khromykh AA.** 2002. Replication and gene function in Kunjin virus. Current Topics in Microbiology and Immunology **267:**323-351.

225. **Leung JY, Pijlman GP, Kondratieva N, Hyde J, Mackenzie JM, Khromykh AA.** 2008. Role of Nonstructural Protein NS2A in Flavivirus Assembly. Journal of Virology **82:**4731 – 4741.

226. **Westaway EG, Mackenzie JM, Kenney MT, Jones MK, Khromykh AA.** 1997. Ultrastructure of Kunjin virus-infected cells: colocalization of NS1 and NS3 with double-stranded RNA, and of NS2B with NS3, in virus-induced membrane structures. Journal of Virology **71:**6650-6661.

227. **Evans JD, Seeger C.** 2007. Differential effects of mutations in NS4B on West Nile virus replication and inhibition of interferon signaling. Journal of Virology **81:**11809-11816.

228. **Munoz-Jordan JL, Laurent-Rolle M, Ashour J, Martinez-Sobrido L, Ashok M, Lipkin WI, Garcia-Sastre A.** 2005. Inhibition of alpha/beta interferon signaling by the NS4B protein of flaviviruses. Journal of Virology **79:**8004-8013.

229. **Kummerer BM, Rice CM.** 2002. Mutations in the yellow fever virus nonstructural protein NS2A selectively block production of infectious particles. J Virol **76:**4773-4784.

230. **Liu WJ, Chen HB, Khromykh AA.** 2003. Molecular and functional analyses of Kunjin virus infectious cDNA clones demonstrate the essential roles for NS2A in virus assembly and for a nonconservative residue in NS3 in RNA replication. J Virol **77:**7804-7813.

231. **Melian EB, Edmonds JH, Nagasaki TK, Hinzman E, Floden N, Khromykh AA.** 2013. West Nile virus NS2A protein facilitates virus-induced apoptosis independently of interferon response. J Gen Virol **94:**308-313.

232. **Nestorowicz A, Chambers TJ, Rice CM.** 1994. Mutagenesis of the yellow fever virus NS2A/2B cleavage site: effects on proteolytic processing, viral replication, and evidence for alternative processing of the NS2A protein. Virology **199:**114-123.

233. **Erbel P, Schiering N, D'Arcy A, Renatus M, Kroemer M, Lim SP, Yin Z, Keller TH, Vasudevan SG, Hommel U.** 2006. Structural basis for the activation of flaviviral NS3 proteases from dengue and West Nile virus. Nat Struct Mol Biol **13:**372-373.

234. **Wengler G, Nowak T, Castle E.** 1990. Description of a procedure which allows isolation of viral nonstructural proteins from BHK vertebrate cells infected with the West Nile flavivirus in a state which allows their direct chemical characterization. Virology **177:**795-801.

235. **Lin C, Amberg SM, Chambers TJ, Rice CM.** 1993. Cleavage at a novel site in the NS4A region by the yellow fever virus NS2B-3 proteinase is a prerequisite for processing at the downstream 4A/4B signalase site. J Virol **67:**2327-2335.

236. **Roosendaal J, Westaway EG, Khromykh A, Mackenzie JM.** 2006. Regulated cleavages at the West Nile virus NS4A-2K-NS4B junctions play a major role in rearranging cytoplasmic membranes and Golgi trafficking of the NS4A protein. J Virol **80:**4623-4632.

237. **Speight G, Westaway EG.** 1989. Positive identification of NS4A, the last of the hypothetical nonstructural proteins of flaviviruses. Virology **170:**299-301.

238. **Lin MH, Hsu HJ, Bartenschlager R, Fischer WB.** 2013. Membrane undulation induced by NS4A of Dengue virus: a molecular dynamics simulation study. J Biomol Struct Dyn **32:**1552-1562.

239. **Stern O, Hung YF, Valdau O, Yaffe Y, Harris E, Hoffmann S, Willbold D, Sklan EH.** 2013. An N-terminal amphipathic helix in dengue virus nonstructural protein 4A mediates oligomerization and is essential for replication. J Virol **87:**4080-4085.

240. **Westaway EG, Khromykh AA, Kenney MT, Mackenzie JM, Jones MK.** 1997. Proteins C and NS4B of the flavivirus Kunjin translocate independently into the nucleus. Virology **234:**31-41.

241. **Faggioni G, Ciammaruconi A, De Santis R, Pomponi A, Scicluna MT, Barbaro K, Masuelli L, Autorino G, Bei R, Lista F.** 2009. Evidence of a humoral response to a novel protein WARF4 embedded in the West Nile virus NS4B gene encoded by an alternative open reading frame. Int J Mol Med **23:**509-512.

242. **Faggioni G, Pomponi A, De Santis R, Masuelli L, Ciammaruconi A, Monaco F, Di Gennaro A, Marzocchella L, Sambri V, Lelli R, Rezza G, Bei R, Lista F.** 2012. West Nile alternative open reading frame (N-NS4B/WARF4) is produced in infected West Nile Virus (WNV) cells and induces humoral response in WNV infected individuals. Virol J **9:**283.

243. **Gorbalenya AE, Donchenko AP, Koonin EV, Blinov VM.** 1989. N-terminal domains of putative helicases of flavi- and pestiviruses may be serine proteases. Nucleic Acids Res **17:**3889-3897.

244. **Wengler G.** 1991. The carboxy-terminal part of the NS 3 protein of the West Nile flavivirus can be isolated as a soluble protein after proteolytic cleavage and represents an RNA-stimulated NTPase. Virology **184:**707-715.

245. **Wengler G.** 1993. The NS 3 nonstructural protein of flaviviruses contains an RNA triphosphatase activity. Virology **197:**265-273.

246. **Wang CC, Huang ZS, Chiang PL, Chen CT, Wu HN.** 2009. Analysis of the nucleoside triphosphatase, RNA triphosphatase, and unwinding activities of the helicase domain of dengue virus NS3 protein. FEBS Lett **583:**691-696.

247. **Incicco JJ, Gebhard LG, Gonzalez-Lebrero RM, Gamarnik AV, Kaufman SB.** 2013. Steady-state NTPase activity of Dengue virus NS3: number of catalytic sites, nucleotide specificity and activation by ssRNA. PLoS One **8:**e58508.

248. **Luo D, Xu T, Watson RP, Scherer-Becker D, Sampath A, Jahnke W, Yeong SS, Wang CH, Lim SP, Strongin A, Vasudevan SG, Lescar J.** 2008. Insights into RNA unwinding and ATP hydrolysis by the flavivirus NS3 protein. EMBO J **27:**3209-3219.

249. **Wu J, Bera AK, Kuhn RJ, Smith JL.** 2005. Structure of the Flavivirus helicase: implications for catalytic activity, protein interactions, and proteolytic processing. J Virol **79:**10268-10277.

250. **Xu T, Sampath A, Chao A, Wen D, Nanao M, Chene P, Vasudevan SG, Lescar J.** 2005. Structure of the Dengue virus helicase/nucleoside triphosphatase catalytic domain at a resolution of 2.4 A. J Virol **79:**10278-10288.

251. **Cui T, Sugrue RJ, Xu Q, Lee AK, Chan YC, Fu J.** 1998. Recombinant dengue virus type 1 NS3 protein exhibits specific viral RNA binding and NTPase activity regulated by the NS5 protein. Virology **246:**409-417.

252. **Kapoor M, Zhang L, Ramachandra M, Kusukawa J, Ebner KE, Padmanabhan R.** 1995. Association between NS3 and NS5 proteins of dengue virus type 2 in the putative

RNA replicase is linked to differential phosphorylation of NS5. J Biol Chem **270:**19100-19106.

253. **Yon C, Teramoto T, Mueller N, Phelan J, Ganesh VK, Murthy KH, Padmanabhan R.** 2005. Modulation of the nucleoside triphosphatase/RNA helicase and 5'-RNA triphosphatase activities of Dengue virus type 2 nonstructural protein 3 (NS3) by interaction with NS5, the RNA-dependent RNA polymerase. J Biol Chem **280:**27412-27419.

254. **Umareddy I, Chao A, Sampath A, Gu F, Vasudevan SG.** 2006. Dengue virus NS4B interacts with NS3 and dissociates it from single-stranded RNA. J Gen Virol **87:**2605-2614.

255. **Bazan JF, Fletterick RJ.** 1989. Detection of a trypsin-like serine protease domain in flaviviruses and pestiviruses. Virology **171:**637-639.

256. **Wengler G, Czaya G, Farber PM, Hegemann JH.** 1991. In vitro synthesis of West Nile virus proteins indicates that the amino-terminal segment of the NS3 protein contains the active centre of the protease which cleaves the viral polyprotein after multiple basic amino acids. J Gen Virol **72 (Pt 4):**851-858.

257. **Chambers TJ, Grakoui A, Rice CM.** 1991. Processing of the yellow fever virus nonstructural polyprotein: a catalytically active NS3 proteinase domain and NS2B are required for cleavages at dibasic sites. J Virol **65:**6042-6050.

258. **Aleshin AE, Shiryaev SA, Strongin AY, Liddington RC.** 2007. Structural evidence for regulation and specificity of flaviviral proteases and evolution of the Flaviviridae fold. Protein Sci **16:**795-806.

259. **Kim YM, Gayen S, Kang C, Joy J, Huang Q, Chen AS, Wee JL, Ang MJ, Lim HA, Hung AW, Li R, Noble CG, Lee le T, Yip A, Wang QY, Chia CS, Hill J, Shi PY, Keller TH.** 2013. NMR analysis of a novel enzymatically active unlinked dengue NS2B-NS3 protease complex. J Biol Chem **288:**12891-12900.

260. **Chambers TJ, Hahn CS, Galler R, Rice CM.** 1990. Flavivirus genome organization, expression, and replication. Annu Rev Microbiol **44:**649-688.

261. **Liu WJ, Sedlak PL, Kondratieva N, Khromykh AA.** 2002. Complementation analysis of the flavivirus Kunjin NS3 and NS5 proteins defines the minimal regions essential for formation of a replication complex and shows a requirement of NS3 in cis for virus assembly. J Virol **76:**10766-10775.

262. **Yusof R, Clum S, Wetzel M, Murthy HM, Padmanabhan R.** 2000. Purified NS2B/NS3 serine protease of dengue virus type 2 exhibits cofactor NS2B dependence for cleavage of substrates with dibasic amino acids in vitro. J Biol Chem **275:**9963-9969.

263. **Assenberg R, Mastrangelo E, Walter TS, Verma A, Milani M, Owens RJ, Stuart DI, Grimes JM, Mancini EJ.** 2009. Crystal structure of a novel conformational state of the flavivirus NS3 protein: implications for polyprotein processing and viral replication. J Virol **83:**12895-12906.

264. **Luo D, Wei N, Doan DN, Paradkar PN, Chong Y, Davidson AD, Kotaka M, Lescar J, Vasudevan SG.** 2010. Flexibility between the protease and helicase domains of the dengue virus NS3 protein conferred by the linker region and its functional implications. J Biol Chem **285:**18817-18827.

265. **Patkar CG, Kuhn RJ.** 2008. Yellow Fever virus NS3 plays an essential role in virus assembly independent of its known enzymatic functions. J Virol **82:**3342-3352.

266. **Pijlman GP, Kondratieva N, Khromykh AA.** 2006. Translation of the flavivirus kunjin NS3 gene in cis but not its RNA sequence or secondary structure is essential for efficient RNA packaging. J Virol **80:**11255-11264.

267. **Khromykh AA, Kenney MT, Westaway EG.** 1998. trans-Complementation of flavivirus RNA polymerase gene NS5 by using Kunjin virus replicon-expressing BHK cells. Journal of Virology **72:**7270-7279.

268. **Khromykh AA, Sedlak PL, Guyatt KJ, Hall RA, Westaway EG.** 1999. Efficient trans-Complementation of the Flavivirus Kunjin NS5 Protein but Not of the NS1 Protein Requires Its Coexpression with Other Components of the Viral Replicase. Journal of Virology **73:**10272 – 10280.

269. **Guyatt KJ, Westaway EG, Khromykh AA.** 2001. Expression and purification of enzymatically active recombinant RNA-dependent RNA polymerase (NS5) of the flavivirus Kunjin. Journal of Virological Methods **92:**37-44.

270. **Koonin EV.** 1991. The phylogeny of RNA-dependent RNA polymerases of positive-strand RNA viruses. J Gen Virol **72 (Pt 9):**2197-2206.

271. **Mackenzie JM, Kenney MT, Westaway EG.** 2007. West Nile virus strain Kunjin NS5 polymerase is a phosphoprotein localized at the cytoplasmic site of viral RNA synthesis. J Gen Virol **88:**1163-1168.

272. **Malet H, Egloff MP, Selisko B, Butcher RE, Wright PJ, Roberts M, Gruez A, Sulzenbacher G, Vonrhein C, Bricogne G, Mackenzie JM, Khromykh AA, Davidson AD, Canard B.** 2007. Crystal structure of the RNA polymerase domain of the West Nile virus non-structural protein 5. Journal of Biological Chemistry **282:**10678-10689.

273. **Tan BH, Fu J, Sugrue RJ, Yap EH, Chan YC, Tan YH.** 1996. Recombinant dengue type 1 virus NS5 protein expressed in Escherichia coli exhibits RNA-dependent RNA polymerase activity. Virology **216:**317-325.

274. **Buckley A, Gaidamovich S, Turchinskaya A, Gould EA.** 1992. Monoclonal antibodies identify the NS5 yellow fever virus non-structural protein in the nuclei of infected cells. J Gen Virol **73 (Pt 5):**1125-1130.

275. **Edward Z, Takegami T.** 1993. Localization and functions of Japanese encephalitis virus nonstructural proteins NS3 and NS5 for viral RNA synthesis in the infected cells. Microbiol Immunol **37:**239-243.

276. **Kamer G, Argos P.** 1984. Primary structural comparison of RNA-dependent polymerases from plant, animal and bacterial viruses. Nucleic Acids Res **12:**7269-7282.

277. **Poch O, Sauvaget I, Delarue M, Tordo N.** 1989. Identification of four conserved motifs among the RNA-dependent polymerase encoding elements. EMBO J **8:**3867-3874.

278. **Egloff MP, Benarroch D, Selisko B, Romette JL, Canard B.** 2002. An RNA cap (nucleoside-2'-O-)-methyltransferase in the flavivirus RNA polymerase NS5: crystal structure and functional characterization. EMBO Journal **21:**2757-2768.

279. **Issur M, Geiss BJ, Bougie I, Picard-Jean F, Despins S, Mayette J, Hobdey SE, Bisaillon M.** 2009. The flavivirus NS5 protein is a true RNA guanylyltransferase that catalyzes a two-step reaction to form the RNA cap structure. RNA **15:**2340-2350.

280. **Ray D, Shah A, Tilgner M, Guo Y, Zhao Y, Dong H, Deas TS, Zhou Y, Li H, Shi PY.** 2006. West Nile virus 5'-cap structure is formed by sequential guanine N-7 and ribose 2'-O methylations by nonstructural protein 5. J Virol **80:**8362-8370.

281. **Zhou Y, Ray D, Zhao Y, Dong H, Ren S, Li Z, Guo Y, Bernard KA, Shi PY, Li H.** 2007. Structure and function of flavivirus NS5 methyltransferase. J Virol **81:**3891-3903.

282. **Lu G, Gong P.** 2013. Crystal Structure of the full-length Japanese encephalitis virus NS5 reveals a conserved methyltransferase-polymerase interface. PLoS Pathog **9:**e1003549.

283. **Hannemann H, Sung PY, Chiu HC, Yousuf A, Bird J, Lim SP, Davidson AD.** 2013. Serotype-specific differences in dengue virus non-structural protein 5 nuclear localization. J Biol Chem **288:**22621-22635.

284. **Kumar A, Buhler S, Selisko B, Davidson A, Mulder K, Canard B, Miller S, Bartenschlager R.** 2013. Nuclear localization of dengue virus nonstructural protein 5 does not strictly correlate with efficient viral RNA replication and inhibition of type I interferon signaling. J Virol **87:**4545-4557.

285. **Pierson TC, Kielian M.** 2013. Flaviviruses: braking the entering. Curr Opin Virol **3:**3-12.

286. **Chu JJ, Ng ML.** 2004. Interaction of West Nile virus with alpha v beta 3 integrin mediates virus entry into cells. J Biol Chem **279:**54533-54541.

287. **Chu JJ, Leong PW, Ng ML.** 2006. Analysis of the endocytic pathway mediating the infectious entry of mosquito-borne flavivirus West Nile into Aedes albopictus mosquito (C6/36) cells. Virology **349:**463-475.

288. **Chu JJ, Ng ML.** 2004. Infectious entry of West Nile virus occurs through a clathrin-mediated endocytic pathway. J Virol **78:**10543-10555.

289. **Gollins SW, Porterfield JS.** 1985. Flavivirus infection enhancement in macrophages: an electron microscopic study of viral cellular entry. J Gen Virol **66 (Pt 9):**1969-1982.

290. **Ishak R, Tovey DG, Howard CR.** 1988. Morphogenesis of yellow fever virus 17D in infected cell cultures. J Gen Virol **69 (Pt 2):**325-335.

291. **Nawa M.** 1998. Effects of bafilomycin A1 on Japanese encephalitis virus in C6/36 mosquito cells. Arch Virol **143:**1555-1568.

292. **Ng ML, Lau LC.** 1988. Possible involvement of receptors in the entry of Kunjin virus into Vero cells. Arch Virol **100:**199-211.

293. **van der Schaar HM, Rust MJ, Waarts BL, van der Ende-Metselaar H, Kuhn RJ, Wilschut J, Zhuang X, Smit JM.** 2007. Characterization of the early events in dengue virus cell entry by biochemical assays and single-virus tracking. J Virol **81:**12019-12028.

294. **Hong SS, Ng ML.** 1987. Involvement of microtubules in Kunjin virus replication. Brief report. Arch Virol **97:**115-121.

295. **van der Schaar HM, Rust MJ, Chen C, van der Ende-Metselaar H, Wilschut J, Zhuang X, Smit JM.** 2008. Dissecting the cell entry pathway of dengue virus by single-particle tracking in living cells. PLoS Pathog **4:**e1000244.

296. **Allison SL, Schalich J, Stiasny K, Mandl CW, Kunz C, Heinz FX.** 1995. Oligomeric rearrangement of tick-borne encephalitis virus envelope proteins induced by an acidic pH. Journal of Virology **69:**695-700.

297. **Heinz FX, Allison SL.** 2000. Structures and mechanisms in flavivirus fusion. Adv Virus Res **55:**231-269.

298. **Gollins SW, Porterfield JS.** 1986. The uncoating and infectivity of the flavivirus West Nile on interaction with cells: effects of pH and ammonium chloride. J Gen Virol **67 (Pt 9):**1941-1950.

299. **Blackwell JL, Brinton MA.** 1995. BHK cell proteins that bind to the 3' stem-loop structure of the West Nile virus genome RNA. J Virol **69:**5650-5658.

300. **Shi PY, Li W, Brinton MA.** 1996. Cell proteins bind specifically to West Nile virus minus-strand 3' stem-loop RNA. J Virol **70:**6278-6287.

301. **Riis B, Rattan SI, Clark BF, Merrick WC.** 1990. Eukaryotic protein elongation factors. Trends Biochem Sci **15:**420-424.

302. **Blackwell JL, Brinton MA.** 1997. Translation elongation factor-1 alpha interacts with the 3' stem-loop region of West Nile virus genomic RNA. J Virol **71:**6433-6444.

303. **Davis WG, Basu M, Elrod EJ, Germann MW, Brinton MA.** 2013. Identification of cis-acting nucleotides and a structural feature in West Nile virus 3'-terminus RNA that facilitate viral minus strand RNA synthesis. J Virol **87:**7622-7636.

304. **Davis WG, Blackwell JL, Shi PY, Brinton MA.** 2007. Interaction between the cellular protein eEF1A and the 3'-terminal stem-loop of West Nile virus genomic RNA facilitates viral minus-strand RNA synthesis. J Virol **81:**10172-10187.

305. **Westaway EG, Mackenzie JM, Khromykh AA.** 2003. Kunjin RNA replication and applications of Kunjin replicons. Advances in Virus Research **59:**99-140.

306. **Alvarez DE, De Lella Ezcurra AL, Fucito S, Gamarnik AV.** 2005. Role of RNA structures present at the 3'UTR of dengue virus on translation, RNA synthesis, and viral replication. Virology **339:**200-212.

307. **Corver J, Lenches E, Smith K, Robison RA, Sando T, Strauss EG, Strauss JH.** 2003. Fine mapping of a cis-acting sequence element in yellow fever virus RNA that is required for RNA replication and cyclization. J Virol **77:**2265-2270.

308. **Lo MK, Tilgner M, Bernard KA, Shi PY.** 2003. Functional analysis of mosquito-borne flavivirus conserved sequence elements within 3' untranslated region of West Nile virus by use of a reporting replicon that differentiates between viral translation and RNA replication. J Virol **77:**10004-10014.

309. **Lindenbach BD, Rice CM.** 1997. trans-Complementation of yellow fever virus NS1 reveals a role in early RNA replication. Journal of Virology **71:**9608-9617.

310. **Chu PW, Westaway EG.** 1987. Characterization of Kunjin virus RNA-dependent RNA polymerase: reinitiation of synthesis in vitro. Virology **157:**330-337.

311. **Cleaves GR, Ryan TE, Schlesinger RW.** 1981. Identification and characterization of type 2 dengue virus replicative intermediate and replicative form RNAs. Virology **111:**73-83.

312. **Chua JJ, Ng MM, Chow VT.** 2004. The non-structural 3 (NS3) protein of dengue virus type 2 interacts with human nuclear receptor binding protein and is associated with alterations in membrane structure. Virus Res **102:**151-163.

313. **Leary K, Blair CD.** 1980. Sequential events in the morphogenesis of japanese Encephalitis virus. J Ultrastruct Res **72:**123-129.

314. **Ng ML.** 1987. Ultrastructural studies of Kunjin virus-infected Aedes albopictus cells. J Gen Virol **68 (Pt 2):**577-582.

315. **Ng ML, Hong SS.** 1989. Flavivirus infection: essential ultrastructural changes and association of Kunjin virus NS3 protein with microtubules. Arch Virol **106:**103-120.

316. **Mackenzie JM, Jones MK, Young PR.** 1996. Immunolocalization of the Dengue Virus Nonstructural Glycoprotein NS1 Suggests a Role in Viral RNA Replication. Virology **220:**232 - 240.

317. **Gillespie LK, Hoenen A, Morgan G, Mackenzie JM.** 2010. The endoplasmic reticulum provides the membrane platform for biogenesis of the flavivirus replication complex. Journal of Virology **84:**10438-10447.

318. **Welsch S, Miller S, Romero-Brey I, Merz A, Bleck CK, Walther P, Fuller SD, Antony C, Krijnse-Locker J, Bartenschlager R.** 2009. Composition and three-dimensional architecture of the dengue virus replication and assembly sites. Cell Host Microbe **5:**365-375.

319. **Ma L, Jones CT, Groesch TD, Kuhn RJ, Post CB.** 2004. Solution structure of dengue virus capsid protein reveals another fold. Proc Natl Acad Sci U S A **101:**3414-3419.

320. **Zai J, Mei L, Wang C, Cao S, Fu ZF, Chen H, Song Y.** 2013. N-glycosylation of the premembrane protein of Japanese encephalitis virus is critical for folding of the envelope protein and assembly of virus-like particles. Acta Virol **57:**27-33.

321. **Lorenz IC, Kartenbeck J, Mezzacasa A, Allison SL, Heinz FX, Helenius A.** 2003. Intracellular assembly and secretion of recombinant subviral particles from tick-borne encephalitis virus. J Virol **77:**4370-4382.

322. **Mukhopadhyay S, Kim BS, Chipman PR, Rossmann MG, Kuhn RJ.** 2003. Structure of West Nile virus. Science **302:**248.

323. **Stadler K, Allison SL, Schalich J, Heinz FX.** 1997. Proteolytic activation of tick-borne encephalitis virus by furin. J Virol **71:**8475-8481.

324. **Zhang Y, Kaufmann B, Chipman PR, Kuhn RJ, Rossmann MG.** 2007. Structure of immature West Nile virus. J Virol **81:**6141-6145.

325. **Brandt WE, Cardiff RD, Russell PK.** 1970. Dengue virions and antigens in brain and serum of infected mice. J Virol **6:**500-506.

326. **Smith GW, Wright PJ.** 1985. Synthesis of proteins and glycoproteins in dengue type 2 virus-infected vero and Aedes albopictus cells. J Gen Virol **66 (Pt 3):**559-571.

327. **Deubel V, Kinney RM, Trent DW.** 1988. Nucleotide sequence and deduced amino acid sequence of the nonstructural proteins of dengue type 2 virus, Jamaica genotype: comparative analysis of the full-length genome. Virology **165:**234-244.

328. **Mackow E, Makino Y, Zhao BT, Zhang YM, Markoff L, Buckler-White A, Guiler M, Chanock R, Lai CJ.** 1987. The nucleotide sequence of dengue type 4 virus: analysis of genes coding for nonstructural proteins. Virology **159:**217-228.

329. **Mandl CW, Heinz FX, Stockl E, Kunz C.** 1989. Genome sequence of tick-borne encephalitis virus (Western subtype) and comparative analysis of nonstructural proteins with other flaviviruses. Virology **173:**291-301.

330. **Wright PJ, Cauchi MR, Ng ML.** 1989. Definition of the carboxy termini of the three glycoproteins specified by dengue virus type 2. Virology **171:**61-67.

331. **Crooks AJ, Lee JM, Easterbrook LM, Timofeev AV, Stephenson JR.** 1994. The NS1 protein of tick-borne encephalitis virus forms multimeric species upon secretion from the host cell. Journal of General Virology **75 (Pt 12):**3453-3460.

332. **Mason PW.** 1989. Maturation of Japanese Encephalitis-Virus Glycoproteins Produced by Infected Mammalian and Mosquito Cells. Virology **169:**354-364.

333. **Winkler G, Randolph VB, Cleaves GR, Ryan TE, Stollar V.** 1988. Evidence that the mature form of the flavivirus nonstructural protein NS1 is a dimer. Virology **162:**187-196.

334. **Falgout B, Chanock R, Lai CJ.** 1989. Proper processing of dengue virus nonstructural glycoprotein NS1 requires the N-terminal hydrophobic signal sequence and the downstream nonstructural protein NS2a. Journal of Virology **63:**1852-1860.

335. **Falgout B, Markoff L.** 1995. Evidence that flavivirus NS1-NS2A cleavage is mediated by a membrane-bound host protease in the endoplasmic reticulum. J Virol **69:**7232-7243.

336. **Blitvich BJ, Scanlon D, Shiell BJ, Mackenzie JS, Pham K, Hall RA.** 2001. Determination of the intramolecular disulfide bond arrangement and biochemical

identification of the glycosylation sites of the nonstructural protein NS1 of Murray Valley encephalitis virus. Journal of General Virology **82:**2251-2256.

337. **Wallis TP, Huang CY, Nimkar SB, Young PR, Gorman JJ.** 2004. Determination of the disulfide bond arrangement of dengue virus NS1 protein. Journal of Biological Chemistry **279:**20729-20741.

338. **Pryor MJ, Wright PJ.** 1993. The effects of site-directed mutagenesis on the dimerization and secretion of the NS1 protein specified by dengue virus. Virology **194:**769-780.

339. **Flamand M, Deubel V, Girard M.** 1992. Expression and secretion of Japanese encephalitis virus nonstructural protein NS1 by insect cells using a recombinant baculovirus. Virology **191:**826-836.

340. **Mason PW, McAda PC, Mason TL, Fournier MJ.** 1987. Sequence of the dengue-1 virus genome in the region encoding the three structural proteins and the major nonstructural protein NS1. Virology **161:**262-267.

341. **Pryor MJ, Wright PJ.** 1994. Glycosylation mutants of dengue virus NS1 protein. Journal of General Virology **75 (Pt 5):**1183-1187.

342. **Zhao BT, Prince G, Horswood R, Eckels K, Summers P, Chanock R, Lai CJ.** 1987. Expression of dengue virus structural proteins and nonstructural protein NS1 by a recombinant vaccinia virus. J Virol **61:**4019-4022.

343. **Blitvich BJ, Scanlon D, Shiell BJ, Mackenzie JS, Hall RA.** 1999. Identification and analysis of truncated and elongated species of the flavivirus NS1 protein. Virus Research **60:**67 - 79.

344. **Coia G, Parker MD, Speight G, Byrne ME, Westaway EG.** 1988. Nucleotide and complete amino acid sequences of Kunjin virus: definitive gene order and characteristics of the virus-specified proteins. Journal of General Virology **69 (Pt 1):**1-21.

345. **Dalgarno L, Trent DW, Strauss JH, Rice CM.** 1986. Partial nucleotide sequence of the Murray Valley encephalitis virus genome. Comparison of the encoded polypeptides with yellow fever virus structural and non-structural proteins. J Mol Biol **187:**309-323.

346. **Trent DW, Kinney RM, Johnson BJ, Vorndam AV, Grant JA, Deubel V, Rice CM, Hahn C.** 1987. Partial nucleotide sequence of St. Louis encephalitis virus RNA: structural proteins, NS1, ns2a, and ns2b. Virology **156:**293-304.

347. **Falconar AK, Young PR.** 1990. Immunoaffinity purification of native dimer forms of the flavivirus non-structural glycoprotein, NS1. Journal of Virological Methods **30:**323-332.

348. **Winkler G, Maxwell SE, Ruemmler C, Stollar V.** 1989. Newly synthesized dengue-2 virus nonstructural protein NS1 is a soluble protein but becomes partially hydrophobic and membrane-associated after dimerization. Virology **171:**302-305.

349. **Clark DC, Lobigs M, Lee E, Howard MJ, Clark K, Blitvich BJ, Hall RA.** 2007. In situ reactions of monoclonal antibodies with a viable mutant of Murray Valley encephalitis virus reveal an absence of dimeric NS1 protein. J Gen Virol **88:**1175-1183.

350. **Hall RA, Khromykh AA, Mackenzie JM, Scherret JH, Khromykh TI, Mackenzie JS.** 1999. Loss of dimerisation of the nonstructural protein NS1 of Kunjin virus delays viral replication and reduces virulence in mice, but still allows secretion of NS1. Virology **264:**66-75.

351. **Schlesinger JJ, Brandriss MW, Putnak JR, Walsh EE.** 1990. Cell surface expression of yellow fever virus non-structural glycoprotein NS1: consequences of interaction with antibody. J Gen Virol **71 (Pt 3):**593-599.

352. **Flamand M, Megret F, Mathieu M, Lepault J, Rey FA, Deubel V.** 1999. Dengue virus type 1 nonstructural glycoprotein NS1 is secreted from mammalian cells as a soluble hexamer in a glycosylation-dependent fashion. Journal of Virology **73:**6104-6110.

353. **Lindenbach BD, Rice CM.** 1999. Genetic interaction of flavivirus nonstructural proteins NS1 and NS4A as a determinant of replicase function. Journal of Virology **73:**4611-4621.

354. **Jacobs MG, Robinson PJ, Bletchly C, Mackenzie JM, Young PR.** 2000. Dengue virus nonstructural protein 1 is expressed in a glycosyl-phosphatidylinositol-linked form that is capable of signal transduction. FASEB J **14:**1603-1610.

355. **Noisakran S, Dechtawewat T, Avirutnan P, Kinoshita T, Siripanyaphinyo U, Puttikhunt C, Kasinrerk W, Malasit P, Sittisombut N.** 2008. Association of dengue virus NS1 protein with lipid rafts. J Gen Virol **89:**2492-2500.

356. **Noisakran S, Dechtawewat T, Rinkaewkan P, Puttikhunt C, Kanjanahaluethai A, Kasinrerk W, Sittisombut N, Malasit P.** 2007. Characterization of dengue virus NS1 stably expressed in 293T cell lines. J Virol Methods **142:**67-80.

357. **Crooks AJ, Lee JM, Dowsett AB, Stephenson JR.** 1990. Purification and analysis of infectious virions and native non-structural antigens from cells infected with tick-borne encephalitis virus. J Chromatogr **502:**59-68.

358. **Crabtree MB, Kinney RM, Miller BR.** 2005. Deglycosylation of the NS1 protein of dengue 2 virus, strain 16681: construction and characterization of mutant viruses. Arch Virol **150:**771-786.

359. **Muylaert IR, Chambers TJ, Galler R, Rice CM.** 1996. Mutagenesis of the N-linked glycosylation sites of the yellow fever virus NS1 protein: effects on virus replication and mouse neurovirulence. Virology **222:**159-168.

360. **Somnuke P, Hauhart RE, Atkinson JP, Diamond MS, Avirutnan P.** 2011. N-linked glycosylation of dengue virus NS1 protein modulates secretion, cell-surface expression, hexamer stability, and interactions with human complement. Virology **413:**253-264.

361. **Tajima S, Takasaki T, Kurane I.** 2008. Characterization of Asn130-to-Ala mutant of dengue type 1 virus NS1 protein. Virus Genes **36:**323-329.

362. **Chung KM, Liszewski MK, Nybakken G, Davis AE, Townsend RR, Fremont DH, Atkinson JP, Diamond MS.** 2006. West Nile virus nonstructural protein NS1 inhibits

complement activation by binding the regulatory protein factor H. PNAS **103:**19111 - 19116.

363. **Avirutnan P, Zhang L, Punyadee N, Manuyakorn A, Puttikhunt C, Kasinrerk W, Malasit P, Atkinson JP, Diamond MS.** 2007. Secreted NS1 of dengue virus attaches to the surface of cells via interactions with heparan sulfate and chondroitin sulfate E. PLoS Pathogens **3:**e183.

364. **Alcon-LePoder S, Drouet MT, Roux P, Frenkiel MP, Arborio M, Durand-Schneider AM, Maurice M, Le Blanc I, Gruenberg J, Flamand M.** 2005. The secreted form of dengue virus nonstructural protein NS1 is endocytosed by hepatocytes and accumulates in late endosomes: implications for viral infectivity. J Virol **79:**11403-11411.

365. **Lee CJ, Lin HR, Liao CL, Lin YL.** 2008. Cholesterol effectively blocks entry of flavivirus. J Virol **82:**6470-6480.

366. **Heaton NS, Perera R, Berger KL, Khadka S, Lacount DJ, Kuhn RJ, Randall G.** 2010. Dengue virus nonstructural protein 3 redistributes fatty acid synthase to sites of viral replication and increases cellular fatty acid synthesis. Proc Natl Acad Sci U S A **107:**17345-17350.

367. **Youn S, Cho H, Fremont DH, Diamond MS.** 2010. A short N-terminal peptide motif on flavivirus nonstructural protein NS1 modulates cellular targeting and immune recognition. Journal of Virology **84:**9516-9532.

368. **Gutsche I, Coulibaly F, Voss JE, Salmon J, d'Alayer J, Ermonval M, Larquet E, Charneau P, Krey T, Megret F, Guittet E, Rey FA, Flamand M.** 2011. Secreted dengue virus nonstructural protein NS1 is an atypical barrel-shaped high-density lipoprotein. Proc Natl Acad Sci U S A **108:**8003-8008.

369. **Muller DA, Landsberg MJ, Bletchly C, Rothnagel R, Waddington L, Hankamer B, Young PR.** 2012. Structure of the dengue virus glycoprotein non-structural protein 1 by electron microscopy and single-particle analysis. J Gen Virol **93:**771-779.

370. **Youn S, Li T, McCune BT, Cristea IM, Diamond MS.** 2012. Evidence for a genetic and physical interaction between the NS1 and NS4B that modulates replication of West Nile virus.

371. **Krishna VD, Rangappa M, Satchidanandam V.** 2009. Virus-specific cytolytic antibodies to nonstructural protein 1 of Japanese encephalitis virus effect reduction of virus output from infected cells. Journal of Virology **83:**4766-4777.

372. **Muylaert IR, Galler R, Rice CM.** 1997. Genetic analysis of the yellow fever virus NS1 protein: identification of a temperature-sensitive mutation which blocks RNA accumulation. J Virol **71:**291-298.

373. **Suzuki R, de Borba L, Duarte dos Santos CN, Mason PW.** 2007. Construction of an infectious cDNA clone for a Brazilian prototype strain of dengue virus type 1: characterization of a temperature-sensitive mutation in NS1. Virology **362:**374-383.

374. **Youn S, Ambrose RL, Mackenzie JM, Diamond MS.** 2013. Non-structural protein-1 is required for West Nile virus replication complex formation and viral RNA synthesis. Virol J **10:**339.

375. **Young LB, Melian EB, Khromykh AA.** 2013. NS1' co-localizes with NS1 and can substitute for NS1 in West Nile virus replication. Journal of Virology.

376. **Avirutnan P, Punyadee N, Noisakran S, Komoltri C, Thiemmeca S, Auethavornanan K, Jairungsri A, Kanlaya R, Tangthawornchaikul N, Puttikhunt C, Pattanakitsakul SN, Yenchitsomanus PT, Mongkolsapaya J, Kasinrerk W, Sittisombut N, Husmann M, Blettner M, Vasanawathana S, Bhakdi S, Malasit P.** 2006. Vascular leakage in severe dengue virus infections: a potential role for the nonstructural viral protein NS1 and complement. Journal of Infectious Diseases **193:**1078-1088.

377. **Nascimento EJ, Silva AM, Cordeiro MT, Brito CA, Gil LH, Braga-Neto U, Marques ET.** 2009. Alternative complement pathway deregulation is correlated with dengue severity. PLoS One **4:**e6782.

378. **Kurosu T, Chaichana P, Yamate M, Anantapreecha S, Ikuta K.** 2007. Secreted complement regulatory protein clusterin interacts with dengue virus nonstructural protein 1. Biochemical and Biophysical Research Communications **362:**1051-1056.

379. **Avirutnan P, Fuchs A, Hauhart RE, Somnuke P, Youn S, Diamond MS, Atkinson JP.** 2010. Antagonism of the complement component C4 by flavivirus nonstructural protein NS1. Journal of Experimental Medicine **207:**793-806.

380. **Avirutnan P, Hauhart RE, Somnuke P, Blom AM, Diamond MS, Atkinson JP.** 2011. Binding of flavivirus nonstructural protein NS1 to C4b binding protein modulates complement activation. J Immunol **187:**424-433.

381. **Mason PW, McAda PC, Dalrymple JM, Fournier MJ, Mason TL.** 1987. Expression of Japanese Encephalitis-Virus Antigens in Escherichia-coli. Virology **158:**361-372.

382. **Blitvich BJ, Mackenzie JS, Coelen RJ, Howard MJ, Hall RA.** 1995. A novel complex formed between the flavivirus E and NS1 proteins: analysis of its structure and function. Archives of Virology **140:**145-156.

383. **Hall RA, Kay BH, Burgess GW, Clancy P, Fanning ID.** 1990. Epitope analysis of the envelope and non-structural glycoproteins of Murray Valley encephalitis virus. Journal of General Virology **71 (Pt 12):**2923-2930.

384. **Firth AE, Atkins JF.** 2009. A conserved predicted pseudoknot in the NS2A-encoding sequence of West Nile and Japanese encephalitis flaviviruses suggests NS1' may derive from ribosomal frameshifting. Virology Journal **6:**14 - 19.

385. **Giedroc DP, Cornish PV.** 2009. Frameshifting RNA pseudoknots: Structure and mechanism. Virus Research **139:**193 - 208.

386. **Sun J, Yu Y, Deubel V.** 2012. Japanese encephalitis virus NS1' protein depends on pseudoknot secondary structure and is cleaved by caspase during virus infection and cell apoptosis. Microbes Infect **14:**930-940.

387. **Fan WF, Mason PW.** 1990. Membrane association and secretion of the Japanese encephalitis virus NS1 protein from cells expressing NS1 cDNA. Virology **177:**470-476.

388. **Lin YL, Chen LK, Liao CL, Yeh CT, Ma SH, Chen JL, Huang YL, Chen SS, Chiang HY.** 1998. DNA immunization with Japanese encephalitis virus nonstructural protein NS1 elicits protective immunity in mice. Journal of Virology **72:**191-200.

389. **Melian EB, Hall-Mendelin S, Du F, Owens N, Bosco-Lauth AM, Nagasaki T, Rudd S, Brault AC, Bowen RA, Hall RA, van den Hurk AF, Khromykh AA.** 2014. Programmed Ribosomal Frameshift alters expression of West Nile virus genes and facilitates virus replication in birds and mosquitoes. Submitted to PLoS Pathogens.

390. **Ye Q, Li XF, Zhao H, Li SH, Deng YQ, Cao RY, Song KY, Wang HJ, Hua RH, Yu YX, Zhou X, Qin ED, Qin CF.** 2012. A single nucleotide mutation in NS2A of Japanese encephalitis-live vaccine virus (SA14-14-2) ablates NS1' formation and contributes to attenuation. J Gen Virol **93:**1959-1964.

391. **Winkelmann ER, Widman DG, Suzuki R, Mason PW.** 2011. Analyses of mutations selected by passaging a chimeric flavivirus identify mutations that alter infectivity and reveal an interaction between the structural proteins and the nonstructural glycoprotein NS1. Virology **421:**96-104.

392. **Suzuki R, Winkelmann ER, Mason PW.** 2009. Construction and characterization of a single-cycle chimeric flavivirus vaccine candidate that protects mice against lethal challenge with dengue virus type 2. J Virol **83:**1870-1880.

393. **Kleinschmidt MC, Michaelis M, Ogbomo H, Doerr HW, Cinatl J, Jr.** 2007. Inhibition of apoptosis prevents West Nile virus induced cell death. BMC Microbiol **7:**49.

394. **Samuel MA, Morrey JD, Diamond MS.** 2007. Caspase 3-dependent cell death of neurons contributes to the pathogenesis of West Nile virus encephalitis. J Virol **81:**2614-2623.

395. **Tsao CH, Su HL, Lin YL, Yu HP, Kuo SM, Shen CI, Chen CW, Liao CL.** 2008. Japanese encephalitis virus infection activates caspase-8 and -9 in a FADD-independent and mitochondrion-dependent manner. J Gen Virol **89:**1930-1941.

396. **Takamatsu Y, Okamoto K, Dinh DT, Yu F, Hayasaka D, Uchida L, Nabeshima T, Buerano CC, Morita K.** 2014. NS1' protein expression facilitates production of Japanese encephalitis virus in avian cells and embryonated chicken eggs. J Gen Virol **95:**373-383.

397. **Audsley M, Edmonds J, Liu W, Mokhonov V, Mokhonova E, Melian EB, Prow N, Hall RA, Khromykh AA.** 2011. Virulence determinants between New York 99 and Kunjin strains of West Nile virus. Virology **414:**63-73.

398. **Hanna JN, Ritchie SA, Phillips DA, Shield J, Bailey MC, Mackenzie JS, Poidinger M, McCall BJ, Mills PJ.** 1996. An outbreak of Japanese encephalitis in the Torres Strait, Australia, 1995. Med J Aust **165:**256-260.

399. **French EL.** 1952. Murray Valley encephalitis isolation and characterization of the aetiological agent. Med J Aust **1:**100-103.

400. **Macdonald J, Tonry J, Hall RA, Williams B, Palacios G, Ashok MS, Jabado O, Clark D, Tesh RB, Briese T, Lipkin WI.** 2005. NS1 protein secretion during the acute phase of West Nile virus infection. Journal of Virology **79:**13924-13933.

401. **Schlesinger JJ.** 2006. Flavivirus nonstructural protein NS1: Complementary surprises. Proceedings of the National Academy of Sciences of the United States of America **103:**18879-18880.

402. **Angel TE, Aryal UK, Hengel SM, Baker ES, Kelly RT, Robinson EW, Smith RD.** 2012. Mass spectrometry-based proteomics: existing capabilities and future directions. Chem Soc Rev **41:**3912-3928.

403. **Ishihama Y.** 2005. Proteomic LC-MS systems using nanoscale liquid chromatography with tandem mass spectrometry. J Chromatogr A **1067:**73-83.

404. **Molnar I, Horvath C.** 1976. Reverse-phase chromatography of polar biological substances: separation of catechol compounds by high-performance liquid chromatography. Clin Chem **22:**1497-1502.

405. **Wysocki VH, Resing KA, Zhang Q, Cheng G.** 2005. Mass spectrometry of peptides and proteins. Methods **35:**211-222.

406. **Katoh H, Okamoto T, Fukuhara T, Kambara H, Morita E, Mori Y, Kamitani W, Matsuura Y.** 2013. Japanese encephalitis virus core protein inhibits stress granule formation through an interaction with Caprin-1 and facilitates viral propagation. J Virol **87:**489-502.

407. **Noisakran S, Sengsai S, Thongboonkerd V, Kanlaya R, Sinchaikul S, Chen ST, Puttikhunt C, Kasinrerk W, Limjindaporn T, Wongwiwat W, Malasit P, Yenchitsomanus PT.** 2008. Identification of human hnRNP C1/C2 as a dengue virus NS1-interacting protein. Biochem Biophys Res Commun **372:**67-72.

408. **Ye J, Chen Z, Zhang B, Miao H, Zohaib A, Xu Q, Chen H, Cao S.** 2013. Heat shock protein 70 is associated with replicase complex of Japanese encephalitis virus and positively regulates viral genome replication. PLoS One **8:**e75188.

409. **Gonzalez-Gronow M, Selim MA, Papalas J, Pizzo SV.** 2009. GRP78: a multifunctional receptor on the cell surface. Antioxid Redox Signal **11:**2299-2306.

410. **Hendershot LM.** 2004. The ER function BiP is a master regulator of ER function. Mt Sinai J Med **71:**289-297.

411. **Anderson K, Stott EJ, Wertz GW.** 1992. Intracellular processing of the human respiratory syncytial virus fusion glycoprotein: amino acid substitutions affecting folding, transport and cleavage. J Gen Virol **73 (Pt 5):**1177-1188.

412. **Choukhi A, Ung S, Wychowski C, Dubuisson J.** 1998. Involvement of endoplasmic reticulum chaperones in the folding of hepatitis C virus glycoproteins. J Virol **72:**3851-3858.

413. **Gaudin Y.** 1997. Folding of rabies virus glycoprotein: epitope acquisition and interaction with endoplasmic reticulum chaperones. J Virol **71:**3742-3750.

414. **Hammond C, Helenius A.** 1994. Folding of VSV G protein: sequential interaction with BiP and calnexin. Science **266:**456-458.

415. **Limjindaporn T, Wongwiwat W, Noisakran S, Srisawat C, Netsawang J, Puttikhunt C, Kasinrerk W, Avirutnan P, Thiemmeca S, Sriburi R, Sittisombut N, Malasit P, Yenchitsomanus PT.** 2009. Interaction of dengue virus envelope protein with endoplasmic reticulum-resident chaperones facilitates dengue virus production. Biochem Biophys Res Commun **379:**196-200.

416. **Mulvey M, Brown DT.** 1995. Involvement of the molecular chaperone BiP in maturation of Sindbis virus envelope glycoproteins. J Virol **69:**1621-1627.

417. **Ng DT, Watowich SS, Lamb RA.** 1992. Analysis in vivo of GRP78-BiP/substrate interactions and their role in induction of the GRP78-BiP gene. Mol Biol Cell **3:**143-155.

418. **Segal MS, Bye JM, Sambrook JF, Gething MJ.** 1992. Disulfide bond formation during the folding of influenza virus hemagglutinin. J Cell Biol **118:**227-244.

419. **Wu YP, Chang CM, Hung CY, Tsai MC, Schuyler SC, Wang RY.** 2011. Japanese encephalitis virus co-opts the ER-stress response protein GRP78 for viral infectivity. Virol J **8:**128.

420. **Jindadamrongwech S, Thepparit C, Smith DR.** 2004. Identification of GRP 78 (BiP) as a liver cell expressed receptor element for dengue virus serotype 2. Arch Virol **149:**915-927.

421. **Blazquez AB, Escribano-Romero E, Merino-Ramos T, Saiz JC, Martin-Acebes MA.** 2014. Stress responses in flavivirus-infected cells: activation of unfolded protein response and autophagy. Front Microbiol **5:**266.

422. **Medigeshi GR, Lancaster AM, Hirsch AJ, Briese T, Lipkin WI, Defilippis V, Fruh K, Mason PW, Nikolich-Zugich J, Nelson JA.** 2007. West Nile virus infection activates the

unfolded protein response, leading to CHOP induction and apoptosis. J Virol **81:**10849-10860.

423. **Yang SH, Liu ML, Tien CF, Chou SJ, Chang RY.** 2009. Glyceraldehyde-3-phosphate dehydrogenase (GAPDH) interaction with 3' ends of Japanese encephalitis virus RNA and colocalization with the viral NS5 protein. J Biomed Sci **16:**40.

424. **Mazzola JL, Sirover MA.** 2003. Subcellular localization of human glyceraldehyde-3-phosphate dehydrogenase is independent of its glycolytic function. Biochim Biophys Acta **1622:**50-56.

425. **Robbins AR, Ward RD, Oliver C.** 1995. A mutation in glyceraldehyde 3-phosphate dehydrogenase alters endocytosis in CHO cells. J Cell Biol **130:**1093-1104.

426. **Sirover MA.** 1997. Role of the glycolytic protein, glyceraldehyde-3-phosphate dehydrogenase, in normal cell function and in cell pathology. J Cell Biochem **66:**133-140.

427. **Klingenberg M.** 1989. Molecular aspects of the adenine nucleotide carrier from mitochondria. Arch Biochem Biophys **270:**1-14.

428. **Pebay-Peyroula E, Dahout-Gonzalez C, Kahn R, Trezeguet V, Lauquin GJ, Brandolin G.** 2003. Structure of mitochondrial ADP/ATP carrier in complex with carboxyatractyloside. Nature **426:**39-44.

429. **Pfaff E, Klingenberg M, Heldt HW.** 1965. Unspecific permeation and specific exchange of adenine nucleotides in liver mitochondria. Biochim Biophys Acta **104:**312-315.

430. **Leyva JA, Bianchet MA, Amzel LM.** 2003. Understanding ATP synthesis: structure and mechanism of the F1-ATPase (Review). Mol Membr Biol **20:**27-33.

431. **Yaffe MB, Farr GW, Miklos D, Horwich AL, Sternlicht ML, Sternlicht H.** 1992. TCP1 complex is a molecular chaperone in tubulin biogenesis. Nature **358:**245-248.

432. **Adeva-Andany M, Lopez-Ojen M, Funcasta-Calderon R, Ameneiros-Rodriguez E, Donapetry-Garcia C, Vila-Altesor M, Rodriguez-Seijas J.** 2014. Comprehensive review on lactate metabolism in human health. Mitochondrion **17C:**76-100.

433. **Colombini M.** 1979. A candidate for the permeability pathway of the outer mitochondrial membrane. Nature **279:**643-645.

434. **Lawen A, Ly JD, Lane DJ, Zarschler K, Messina A, De Pinto V.** 2005. Voltage-dependent anion-selective channel 1 (VDAC1)--a mitochondrial protein, rediscovered as a novel enzyme in the plasma membrane. Int J Biochem Cell Biol **37:**277-282.

435. **Merkwirth C, Dargazanli S, Tatsuta T, Geimer S, Lower B, Wunderlich FT, von Kleist-Retzow JC, Waisman A, Westermann B, Langer T.** 2008. Prohibitins control cell proliferation and apoptosis by regulating OPA1-dependent cristae morphogenesis in mitochondria. Genes Dev **22:**476-488.

436. **Wintachai P, Wikan N, Kuadkitkan A, Jaimipuk T, Ubol S, Pulmanausahakul R, Auewarakul P, Kasinrerk W, Weng WY, Panyasrivanit M, Paemanee A, Kittisenachai S, Roytrakul S, Smith DR.** 2012. Identification of prohibitin as a Chikungunya virus receptor protein. J Med Virol **84:**1757-1770.

437. **Kuadkitkan A, Wikan N, Fongsaran C, Smith DR.** 2010. Identification and characterization of prohibitin as a receptor protein mediating DENV-2 entry into insect cells. Virology **406:**149-161.

438. **Kishimoto Y, Hiraiwa M, O'Brien JS.** 1992. Saposins: structure, function, distribution, and molecular genetics. J Lipid Res **33:**1255-1267.

439. **Alcon-LePoder S, Sivard P, Drouet MT, Talarmin A, Rice C, Flamand M.** 2006. Secretion of flaviviral non-structural protein NS1: from diagnosis to pathogenesis. Novartis Foundation Symposium **277:**233-247; discussion 247-253.

440. **Chung KM, Diamond MS.** 2008. Defining the Levels of Secreted Non-Structural Protein NS1 After West Nile Virus Infection in Cell Culture and Mice. Journal of Medical Virology **80:**547 - 556.

441. **Li K, Zhang S, Kronqvist M, Wallin M, Ekstrom M, Derse D, Garoff H.** 2008. Intersubunit disulfide isomerization controls membrane fusion of human T-cell leukemia virus Env. J Virol **82:**7135-7143.

442. **Hussain M, Torres S, Schnettler E, Funk A, Grundhoff A, Pijlman GP, Khromykh AA, Asgari S.** 2012. West Nile virus encodes a microRNA-like small RNA in the 3' untranslated region which up-regulates GATA4 mRNA and facilitates virus replication in mosquito cells. Nucleic Acids Res **40:**2210-2223.

443. **Farabaugh PJ.** 1996. Programmed translational frameshifting. Microbiological Reviews **60:**103-134.

444. **Giedroc DP, Theimer CA, Nixon PL.** 2000. Structure, stability and function of RNA pseudoknots involved in stimulating ribosomal frameshifting. Journal of Molecular Biology **298:**167-185.

445. **Brierley I, Ramos FJD.** 2006. Programmed ribosomal frameshifting in HIV-1 and the SARS–CoV. Virus Research **119:**29 - 42.

446. **Plant EP, Dinman JD.** 2008. The role of programmed-1 ribosomal frameshifting in coronavirus propagation. Frontiers in Bioscience **13:**4873-4881.

447. **Firth AE, Chung BY, Fleeton MN, Atkins JF.** 2008. Discovery of frameshifting in Alphavirus 6K resolves a 20-year enigma. Virol J **5:**108.

448. **Snyder JE, Kulcsar KA, Schultz KL, Riley CP, Neary JT, Marr S, Jose J, Griffin DE, Kuhn RJ.** 2013. Functional characterization of the alphavirus TF protein. J Virol **87:**8511-8523.

449. **Prinzinger R, PreÃŸmar A, Schleucher E.** 1991. Body temperature in birds. Comparative Biochemistry and Physiology Part A: Physiology **99:**499-506.

450. **Fall G, Diallo M, Loucoubar C, Faye O, Sall AA.** 2014. Vector competence of Culex neavei and Culex quinquefasciatus (Diptera: Culicidae) from Senegal for lineages 1, 2, Koutango and a putative new lineage of West Nile virus. Am J Trop Med Hyg **90:**747-754.

451. **de Vries HE, Blom-Roosemalen MC, van Oosten M, de Boer AG, van Berkel TJ, Breimer DD, Kuiper J.** 1996. The influence of cytokines on the integrity of the blood-brain barrier in vitro. J Neuroimmunol **64:**37-43.

452. **Fiala M, Looney DJ, Stins M, Way DD, Zhang L, Gan X, Chiappelli F, Schweitzer ES, Shapshak P, Weinand M, Graves MC, Witte M, Kim KS.** 1997. TNF-alpha opens a paracellular route for HIV-1 invasion across the blood-brain barrier. Mol Med **3:**553-564.

453. **Sultana H, Neelakanta G, Foellmer HG, Montgomery RR, Anderson JF, Koski RA, Medzhitov RM, Fikrig E.** 2012. Semaphorin 7A contributes to West Nile virus pathogenesis through TGF-beta1/Smad6 signaling. J Immunol **189:**3150-3158.

454. **Verma S, Kumar M, Gurjav U, Lum S, Nerurkar VR.** 2010. Reversal of West Nile virus-induced blood-brain barrier disruption and tight junction proteins degradation by matrix metalloproteinases inhibitor. Virology **397:**130-138.

455. **Wang P, Dai J, Bai F, Kong KF, Wong SJ, Montgomery RR, Madri JA, Fikrig E.** 2008. Matrix metalloproteinase 9 facilitates West Nile virus entry into the brain. J Virol **82:**8978-8985.

456. **Verma S, Lo Y, Chapagain M, Lum S, Kumar M, Gurjav U, Luo H, Nakatsuka A, Nerurkar VR.** 2009. West Nile virus infection modulates human brain microvascular endothelial cells tight junction proteins and cell adhesion molecules: Transmigration across the in vitro blood-brain barrier. Virology **385:**425-433.

457. **Bai F, Kong KF, Dai J, Qian F, Zhang L, Brown CR, Fikrig E, Montgomery RR.** 2010. A paradoxical role for neutrophils in the pathogenesis of West Nile virus. J Infect Dis **202:**1804-1812.

458. **Garcia-Tapia D, Loiacono CM, Kleiboeker SB.** 2006. Replication of West Nile virus in equine peripheral blood mononuclear cells. Vet Immunol Immunopathol **110:**229-244.

459. **Wang S, Welte T, McGargill M, Town T, Thompson J, Anderson JF, Flavell RA, Fikrig E, Hedrick SM, Wang T.** 2008. Drak2 contributes to West Nile virus entry into the brain and lethal encephalitis. J Immunol **181:**2084-2091.

460. **Hunsperger EA, Roehrig JT.** 2006. Temporal analyses of the neuropathogenesis of a West Nile virus infection in mice. J Neurovirol**12:**129-139.

461. **Monath TP, Cropp CB, Harrison AK.** 1983. Mode of entry of a neurotropic arbovirus into the central nervous system. Reinvestigation of an old controversy. Lab Invest **48:**399-410.

462. **Samuel MA, Wang H, Siddharthan V, Morrey JD, Diamond MS.** 2007. Axonal transport mediates West Nile virus entry into the central nervous system and induces acute flaccid paralysis. Proc Natl Acad Sci U S A **104:**17140-17145.

463. **Mason PW, Shustov AV, Frolov I.** 2006. Production and characterization of vaccines based on flaviviruses defective in replication. Virology **351:**432-443.

464. **Widman DG, Ishikawa T, Fayzulin R, Bourne N, Mason PW.** 2008. Construction and characterization of a second-generation pseudoinfectious West Nile virus vaccine propagated using a new cultivation system. Vaccine **26:**2762-2771.

465. **Zhang Y, Zhang W, Ogata S, Clements D, Strauss JH, Baker TS, Kuhn RJ, Rossmann MG.** 2004. Conformational changes of the flavivirus E glycoprotein. Structure **12:**1607-1618.

9 Appendices

9.1 Primer sequences for mutagenesis

Table 9.1 Primer sequences for mutagenesis

Primer name	Sequence
NS1' del10 F	GCGCTGCTAGTCCGCGGGAACAAAA
NS1' del10 R	TGTTCCCGCGGACTAGCAGGGCAAT
NS1' del20 F	GGTGGACAGCCAAGATCCGCGGGAACAAAAACTCATCTCAGAAGAGG
NS1' del20 R	GTTTTTGTTCCCGCGGATCTTGGCTGTCCACCTCTTGCGAAGGACC
NS1' Ala F	GTGGACAGCCAAGATGCGGCTGCCGCCGCTGCTGCTGCCGCTGCTAGTTC TAGTGTTTGG
NS1' Ala R	CCAAACACTAGAACTAGCAGCGGCAGCAGCAGCGGCGGCAGCCGCATCT TGGCTGTCCAC
NS1' Cys Mut F	GCATGCCAGCCATACTGATACCCT
NS1' Cys Mut R	CACTAGAACTAGCAGGGGTATCAGT
Stop Mut F	AGCCAAGATTAGCATGCCAGCCATACTGAT
Stop Mut R	GCTGGCATGCTAATCTTGGCTGTCCACCTC
SCMU F	GTGGACAGCCAAGATAAGTATGCCGGCTATCCTTATCGCGCTCCTGGTGC TGGTTTTCGGTGGGATTACGTATACTGATGTGTTACGCTATGTCATTCT
SCMU R	TAGCGTAACACATCAGTATACGTAATCCCACCGAAAACCAGCACCAGGA GCGCGATAAGGATAGCCGGCATACTTATCTTGGCTGTCCACCTCTTGCGA

9.2 Cloning strategies

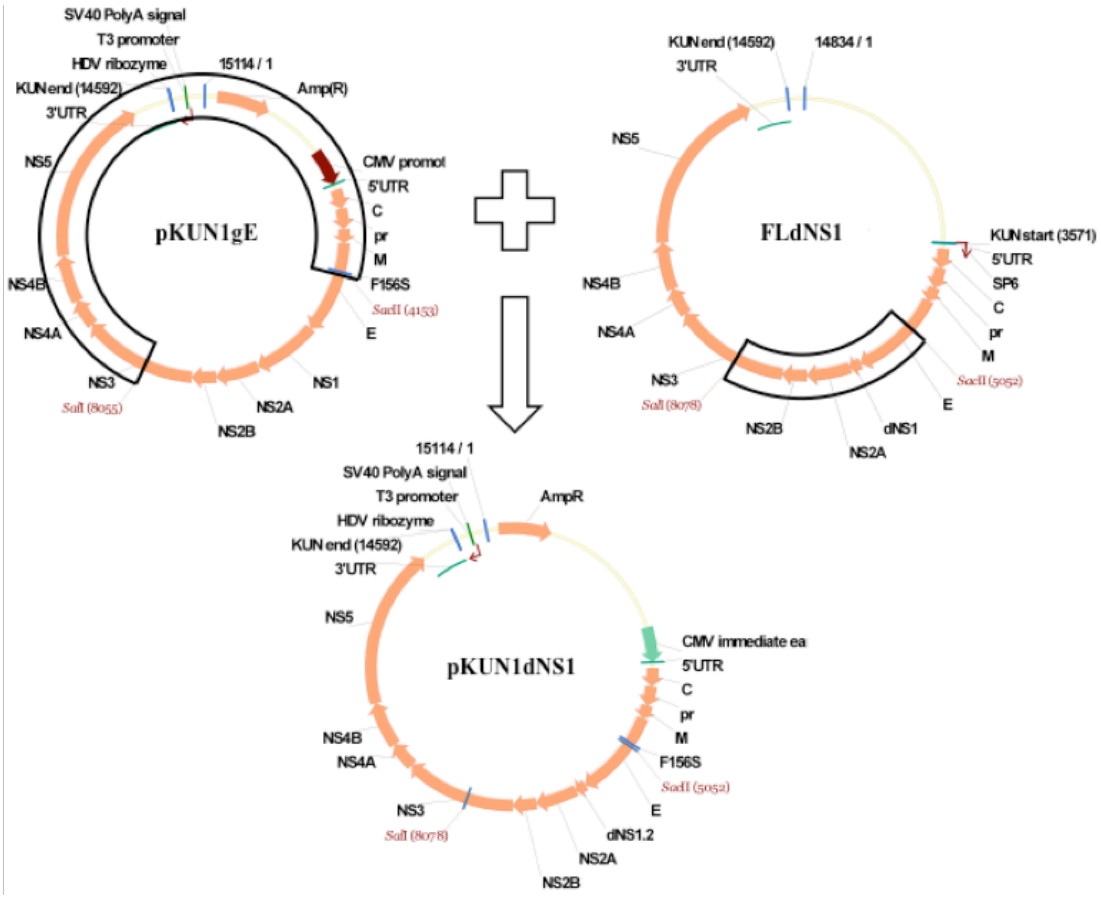

Figure 9.1 Cloning strategy for the generation of pKUNdNS1. pKUN1gE (2) and FLdNS1 (5) were digested with SacII and SalI and indicated fragments were ligated with T4 DNA ligase (New England Biolabs).

9.3 Western on CF from BFA treated cells

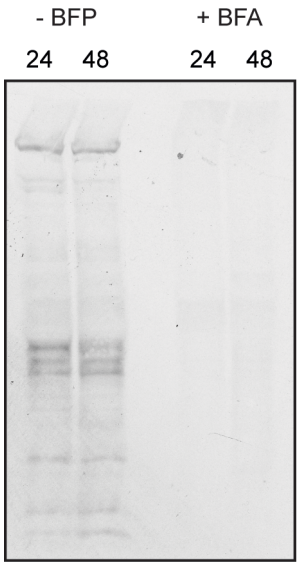

Figure 9.2 Effectiveness of BFA treatment during pulse-chase. Pulse-chase was performed at 24 and 48hpi in the presence or absence of BFA, and culture fluids harvested and clarified by centrifugation. Labelled proteins present in culture medium were subjected to SDS-PAGE, transferred to nitrocellulose membranes and exposed to X-ray film.

9.4 Repeat E and NS5 IP

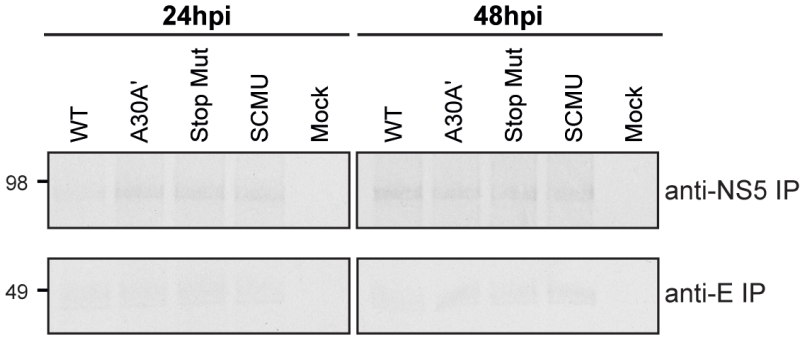

Figure 9.3 Repeat immunoprecipitation of pulse-chase samples to confirm successful first round precipitation. Pulse-chase was performed at 24 and 48hpi and cell monolayers were lysed with RIPA buffer. Protein preparations were immunoprecipitated with anti-NS5 (5H1) or anti-E (3.91D) using Dynabeads® Protein G. Following immunoprecipitation, the unbound fraction was subjected to a repeat of the Protein G Dynabeads® pull-down. Antibody-bound proteins were eluted and samples subjected to electrophoresis. Labelled proteins were transferred to nitrocellulose membranes and exposed to X-ray film.

9.5 Papers published during candidature

Young L, Melian E, Khromykh A. 2013. NS1′ colocalizes with NS1 and can substitute for NS1 in West Nile virus replication. J. Virol. **87**:9384–90.

Young L, Melian E, Setoh YX, Young P, Khromykh A. 2014. Last twenty amino acids of the West Nile Virus NS1' protein are responsible its retention in cells and formation of unique heat stable NS1' homodimers. Submitted to J. Virol.

JVI Journals.ASM.org

NS1′ Colocalizes with NS1 and Can Substitute for NS1 in West Nile Virus Replication

Lucy B. Young, Ezequiel Balmori Melian, Alexander A. Khromykh

Australian Infectious Disease Research Centre, School of Chemistry and Molecular Biosciences, University of Queensland, Brisbane, Australia

NS1′ is a C-terminally extended form of the NS1 protein produced only by encephalitic flaviviruses from the Japanese encephalitis virus serogroup. Here we show that West Nile virus (WNV) NS1′ and NS1 localize to the same cellular compartments when expressed from plasmid DNAs and also colocalize to viral RNA replication sites in infected cells. Using complementation analysis with NS1-deleted WNV cDNA, we demonstrated that NS1′ is able to substitute for the crucial function of NS1 in virus replication.

West Nile virus (WNV) is a mosquito-borne flavivirus within the Japanese encephalitis virus (JEV) serogroup. This serogroup also includes other encephalitic flaviviruses, such as JEV, Murray Valley encephalitis virus, and St. Louis encephalitis virus (1). The natural transmission cycle of WNV is between birds and mosquitoes, primarily the *Culex* species; however, it can cause incidental infections in humans. Since the outbreak of the more pathogenic WNV_{NY99} strain in New York in 1999 (2), WNV has emerged as a major cause of arboviral encephalitis in the United States (3). WNV strains can be divided into two distinct lineages, lineage 1 and lineage 2. Lineage 1 includes both WNV_{NY99} and Kunjin (WNV_{KUN}) (4), the prevalent strain within Australia (5). Despite high sequence similarity to the WNV_{NY99} strain (~98% on the amino acid level) (6), most WNV_{KUN} strains are highly attenuated, with only a small number of human infections and no fatalities reported (5, 7). Since its isolation in early 1960s, WNV_{KUN} has been used extensively as a model for WNV infection (8, 9).

The WNV_{KUN} genome is a single-stranded positive-sense RNA of 11,022 nucleotides (10–12). After translation as a single polyprotein, it is cleaved by host and viral proteases to produce 3 structural (C, prM, and E) and 7 nonstructural (NS1, NS2A, NS2B, NS3, NS4A, NS4B, and NS5) proteins (11, 12). NS1 is a multifunctional glycoprotein that is involved in viral replication (13–16) and modulation of the immune response (17–22). The key role NS1 plays in RNA replication has been shown previously, with mutations or deletions in the NS1 gene resulting in a lack of detectable RNA replication. This function can be complemented in *trans* by the expression of NS1 (14, 15).

An additional nonstructural protein, NS1′, is produced exclusively by the members of the JEV serogroup due to the presence of a −1 programmed ribosomal frameshift at the beginning of the adjacent NS2A gene (23–25). This frameshift, occurring in 30 to 50% of translation events (23, 26), results in the formation of a 52-amino-acid C-terminally extended form of NS1. Although a role in neurovirulence has previously been demonstrated (23), no specific functions for NS1′ in viral replication or virus-host interactions have been identified. In the present study, we show that the NS1′ protein colocalizes with NS1 in viral RNA replication sites in the endoplasmic reticulum (ER) of infected cells and can substitute for the function of NS1 in viral replication.

Plasmid DNA-derived expression of NS1 and NS1′. NS1′ is produced in viral infection due to the presence of a slippery heptanucleotide and 3′ pseudoknot in the viral RNA resulting in a ribosomal shift to the −1 reading frame (23, 25). This results in the addition of 52 amino acids to the C terminus of NS1 protein, including the N-terminal 9 amino acids of NS2A and 43 amino acids after the frameshift, terminating NS1′ synthesis at a stop codon (25). To enable studies on the NS1′ and NS1 proteins, CMV promoter-based plasmids expressing NS1′ or NS1 (pcDNA-NS1′ and pcDNA-NS1, respectively) were designed as shown in Fig. 1A. Both constructs contained the WNV_{KUN} envelope protein (E) signal sequence at the N terminus followed by cDNA for the protein of interest and C-terminal Myc and Flag tags to assist in protein detection. pcDNA-NS1′ was generated by inserting an additional nucleotide (Fig. 1B, boxed nucleotide) at the frameshift site to induce the change in reading frame that leads to NS1′ synthesis. To prevent further frameshifting, we also introduced two single-nucleotide mutations into the slippery heptanucleotide of the frameshift motif, as published previously (23) (Fig. 1B, circled nucleotides). To confirm protein production from the designed plasmids, HEK293T cells transfected with either pcDNA-NS1′ or -NS1 were harvested in radioimmunoprecipitation assay (RIPA) buffer (50 mM Tris HCl, 150 mM NaCl, 1% NP-40, 0.5% sodium deoxycholate, 1% SDS) at 2 days posttransfection. Cell lysates were denatured for 10 min at 70°C, separated by electrophoresis in 10% polyacrylamide gels, transferred to nitrocellulose membranes, and analyzed by Western blotting for the presence of NS1 and NS1′. 4G4, a monoclonal antibody that recognizes both NS1 and NS1′ proteins (27), detected NS1 (monomer) in lysates from pcDNA-NS1-transfected cells and NS1′ proteins (both monomer and dimers) in lysates from pcDNA-NS1′-transfected cells (Fig. 1C). Notably, only NS1′ and not NS1 expression resulted in generation of heat-stable dimers. The results confirmed that pcDNA-NS1 and pcDNA-NS1′ plasmids express NS1 and NS1′, respectively.

The cellular localization of NS1′ is similar to that of NS1 in plasmid DNA-transfected and virus-infected cells. NS1 is

Received 23 April 2013 Accepted 5 June 2013
Published ahead of print 12 June 2013
Address correspondence to Alexander A. Khromykh, a.khromykh@uq.edu.au.

doi:10.1128/JVI.01101-13

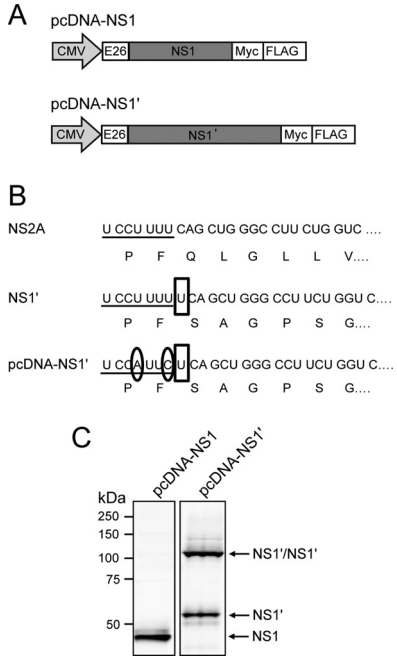

FIG 1 Design and characterization of plasmid DNAs expressing NS1 and NS1′ genes. (A) Plasmid constructs pcDNA-NS1 and pcDNA-NS1′, for expression of NS1 and NS1′, respectively, contain an N-terminal signal sequence consisting of the last 26 codons of the WNV E protein and Myc and Flag tags at the C terminus. (B) Alignment of the nucleic and amino acid sequences of NS2A, NS1′ and pcDNA-NS1′ showing the −1 frameshift occurring at the beginning of the NS2A gene that leads to the generation of NS1′. Underlining shows the slippery heptanucleotide of the frameshift motif, open boxes show inserted nucleotides, and circles show mutated bases. (C) Western blot showing expression of NS1 and NS1′ from pcDNA-NS1 and pcDNA-NS1′, respectively. Lysates were heat denatured and analyzed by Western blotting with anti-NS1 (4G4).

known to localize to the ER of cells during flavivirus infection (16, 28, 29). To examine whether NS1′ also colocalizes to the ER with NS1, we carried out immunofluorescence assays on cells expressing NS1′ or NS1 proteins. HEK293T cells transfected with pcDNA-NS1 or pcDNA-NS1′ plasmids were fixed in 80% acetone–20% phosphate-buffered saline (PBS) at 48 h posttransfection and stained with 4G4, to detect both NS1 and NS1′, and with NS1′-specific antibodies (FS-Ab) (23). As expected, FS-Ab stained only pcDNA-NS1′-transfected cells, while 4G4 stained both pcDNA-NS1- and pcDNA-NS1′-transfected cells (Fig. 2A). Using 4G4 in addition to antibodies recognizing markers for various cellular compartments, we were able to further examine the localization of NS1′ and NS1 in transfected cells. HEK293T cells transfected with pcDNA-NS1 or pcDNA-NS1′ plasmids were fixed at 48 h posttransfection in 4% paraformaldehyde (PFA) with 0.1% Triton X-100 and stained with biotinylated 4G4 and antibodies recognizing markers of the ER (rabbit polyclonal antibody against calnexin [Sigma-Aldrich]), Golgi apparatus (mouse monoclonal antibody against GM130 [Becton, Dickinson]), or endosomes (mouse monoclonal antibody against EEA-1 [BD Transduction Laboratories]). Both NS1 and NS1′ localized predominantly to the ER (Fig. 2B), with a small degree of colocalization with the Golgi apparatus (Fig. 2C) and no distinct localization to the endosomes (Fig. 2D). Moreover, there did not appear to be any differences in the cellular distribution of plasmid-expressed NS1′ compared to NS1, leading us to conclude that NS1′ resides in the same cellular compartments as NS1.

As 4G4 is able to detect both NS1 and NS1′, it is not possible to separate NS1 and NS1′ localization in cells infected with wild-type virus (WNV_{KUN}), as it produces both proteins. FS-Ab, on the other hand, recognizes only NS1′ protein. We previously generated a mutant WNV_{KUN} virus, A30A′, that does not produce NS1′ protein (23). Thus, we used comparative costaining with 4G4 and FS-Ab of cells infected with wild-type or A30A′ mutant WNV_{KUN} viruses in order to assess whether NS1 and NS1′ proteins localize to the same or different cellular compartments. To examine any specific NS1 localization, Vero76 cells infected with either WNV_{KUN} or A30A′ mutant virus at a multiplicity of infection (MOI) of 10 and fixed at 24 h postinfection (hpi) in 80% acetone were costained with 4G4 and FS-Ab. In WNV_{KUN}-infected cells, 4G4-labeled proteins colocalized with FS-Ab-labeled proteins, indicating that NS1 and NS1′ are found in the same cellular compartments (Fig. 3A). To confirm that the cellular distribution of NS1 and NS1′ detected in transfected cells is the same as in infected cells, we carried out immunofluorescence analysis with antibodies detecting marker proteins for ER, Golgi apparatus, and endosomes. Vero76 cells infected at an MOI of 10 with WNV_{KUN} or A30A′ viruses were fixed at 24 hpi (4% PFA in PBS with 0.1% Triton X-100) and stained with biotinylated 4G4 and either anti-calnexin, anti-GM130, or anti-EEA-1 antibodies. As in transfected cells, NS1 and NS1′ localized predominantly to the ER (Fig. 3B), with a small degree of colocalization with the Golgi apparatus (Fig. 3C) and no localization to the endosomes (Fig. 3D). A comparison between WNV_{KUN}- and A30A′-infected cells should also indicate unique NS1′ staining. No differences in anti-NS1 staining between WNV_{KUN}- and A30A′-infected cells indicate that NS1′ and NS1 localize to the same cellular compartments. These results, in combination with the results from plasmid-transfected cells, indicate that NS1′ protein has a cellular distribution similar to that of NS1 during viral infection or when the proteins are expressed as individual proteins.

NS1 has been shown previously to colocalize with double-stranded RNA (dsRNA) at the sites of flavivirus RNA replication in WNV_{KUN}-infected cells (16). To determine whether NS1′ also colocalizes with dsRNA, Vero76 cells infected with WNV_{KUN} or A30A′ (MOI of 10) were fixed at 24 hpi (80% acetone) and costained with anti-dsRNA antibodies and either biotinylated 4G4 or FS-Ab. Proteins stained with both 4G4 and FS-Ab colocalized with dsRNA (Fig. 3E and F, respectively), demonstrating that NS1′ is also associated with dsRNA and therefore with the sites of viral RNA replication.

NS1′ complements replication of NS1-deleted viral RNA. Due to the colocalization of NS1′ with NS1 in the ER and with dsRNA, we hypothesized that NS1′, like NS1, could also play a role in virus replication. To test whether NS1′ can substitute for the function of NS1 in viral replication, we constructed a CMV promoter-driven WNV_{KUN} genomic cDNA with a large (~80%) internal deletion of the NS1 gene (pKUNdNS1) (Fig. 4A). This deletion (dNS1.1) has been used previously by our group in an RNA-based system to demonstrate *trans*-complementation of replication of NS1-deleted viral RNA by the NS1 expressed from WNV_{KUN} replicon RNA (14). We cotransfected HEK293T cells with pKUNdNS1 and either pcDNA-NS1 or pcDNA-NS1′ plasmids to determine whether expression in *trans* of NS1 or NS1′ could rescue replication of replication-deficient

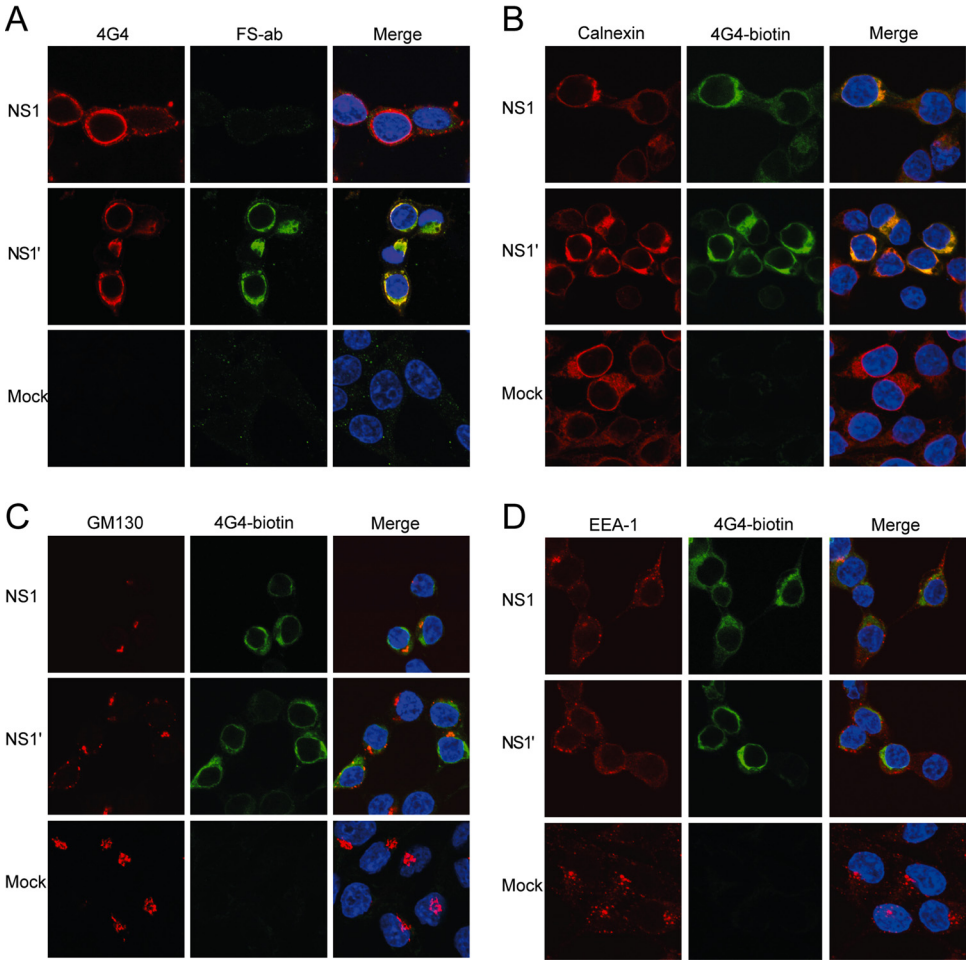

FIG 2 Cellular localization of plasmid-expressed NS1′ and NS1. (A) Immunofluorescence analysis showing production of NS1 and NS1′ using 4G4 (which stains both NS1 and NS1′) and FS-Ab (an NS1′-specific antibody) in transfected HEK293T cells. (B to D) Immunofluorescence analysis showing colocalization of plasmid-expressed NS1 and NS1′ with the ER (B), the Golgi apparatus (C), and endosomes (D). Transfected HEK293T cells were stained with antibodies to appropriate cell markers (calnexin, GM130, and EEA-1, respectively) and biotinylated anti-NS1 (4G4).

pKUNdNS1. Transfection of repBHK cells expressing all of the WNV_{KUN} nonstructural proteins, including NS1 and NS1′, with pKUNdNS1 was also performed as a positive control (14), and cotransfection of pKUNdNS1 with a green fluorescent protein (GFP)-expressing plasmid was included as a negative control. To examine rescue of RNA replication, total RNA was harvested from cotransfected cells at 2 or 4 days posttransfection with TriReagent (Sigma-Aldrich, St. Louis, MO), according to the manufacturer's instructions. Isolated RNA (5 μg) was subjected to denaturing 1.5% agarose gel electrophoresis followed by transfer to Hybond-N membranes (GE Healthcare Limited, Buckinghamshire, United Kingdom). RNA was cross-linked to the membrane by UV irradiation, and Northern hybridization with a ^{32}P-labeled (PerkinElmer, Waltham, MA) WNV_{KUN}-specific 3′ untranslated-region (UTR) probe was carried out to detect accumulation of viral RNA. No viral RNA was detected in mock-transfected cells (Fig. 4B, lanes 9 and 10), and transfection of repBHK cells with pKUNdNS1 resulted in increasing accumulation of viral genomic RNA (Fig. 4B, lanes 11 and 12). A small level of RNA accumulation in the pKUNdNS1-only-transfected cells was detected as expected (Fig. 4B, lanes 1 and 2), due to the transcription of NS1-deficient RNA driven by the CMV promoter. However, the levels of accumulated RNA were notably higher in cells cotransfected with either pcDNA-NS1 (a 5.5-fold increase at day 2 and a 10-fold increase at day 4) (Fig. 4B, lanes 3 and 4) or pcDNA-NS1′ plasmids (a 3-fold increase at day 2 and a 5-fold increase at day 4) (Fig. 4B, lanes 5 and 6) compared to those in pKUNdNS1-only-transfected cells. Notably, some variations in the Northern blot detection of complemented genomic RNA between three different complementation experiments (data not shown) were observed, producing a range of increases for pcDNA-NS1 complementation between 1.5- and 14-fold and for pcDNA-NS1′ complementation between 1- and 5-fold. No distinct band for genomic RNA was detected in cells cotransfected with GFP-expressing plasmid (Fig. 4B, lanes 7 and 8), possibly due to either an inhibitory effect of GFP expression on transcription of KUNdNS1 RNA or enhanced degradation of KUNdNS1 RNA in the presence of GFP expression. *trans*-complementation of viral RNA replication by NS1′ was further supported by immunofluorescence analysis of cotransfected HEK293T cells (fixed in 4% PFA with 0.1% Triton X-100 at 2 days posttransfection) using staining with mouse monoclonal anti-c-Myc antibodies (9E10 hybridoma; ATCC) (NS1 or NS1′ proteins) and rabbit polyclonal anti-NS3 antibodies (16) (pKUNdNS1-expressed NS3 protein). Increased

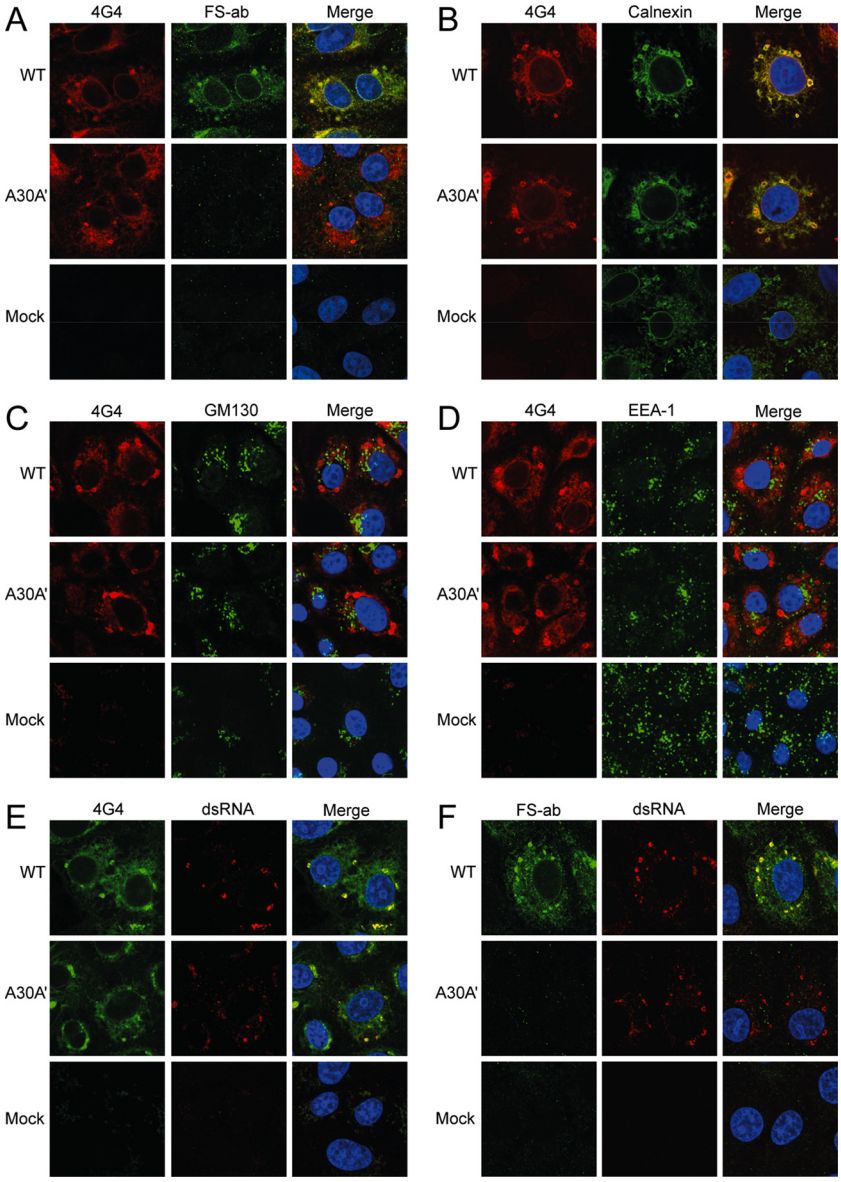

FIG 3 Localization of NS1′, NS1, and dsRNA in WNV_{KUN}-infected cells. (A) Immunofluorescence analysis showing colocalization of NS1 and NS1′ in infected Vero76 cells using 4G4 (which stains both NS1 and NS1′) and FS-Ab (an NS1′-specific antibody). (B to D) Immunofluorescence analysis showing colocalization of virally expressed NS1 and NS1′ with the ER (B), the Golgi apparatus (C), and endosomes (D). Infected cells were stained with antibodies to appropriate cell markers (calnexin, GM130, and EEA-1, respectively) and biotinylated anti-NS1 (4G4). (E and F) Immunofluorescence analysis showing colocalization of NS1 and NS1′ with dsRNA in infected cells stained with anti-dsRNA and either biotinylated 4G4 (E) or FS-Ab (F).

production of NS3 protein in pcDNA-NS1- and pcDNA-NS1′-cotransfected cells, compared to pKUNdNS1-only-transfected cells (Fig. 4C), further demonstrated that *trans*-complementation of replication of the NS1-deleted viral RNA was successful. Therefore, we conclude that NS1′ protein can rescue replication deficiency of NS1-deleted viral RNA.

To detect virus production from cotransfected cells, and thus further confirm successful complementation, culture fluid from transfected HEK293T cells was harvested at 2 days posttransfection and used to infect repBHK cells. If complementation was successful, viral particles containing the NS1-deleted RNA would be able to infect the repBHK cells, replicate, and form viral particles due to the continuing expression of NS1 and NS1′ in the repBHK cells. Prior to infection, the culture fluid was treated with 10 units RQ1 DNase (Promega, Madison, WI) and 10 μg RNase A for 2 h at room temperature to digest any remaining plasmid DNA or uncoated RNA. Two days after infection, cells were fixed (4% PFA with 0.1% Triton X-100) and stained with anti-E antibodies to detect infected cells. Immunofluorescence images of repBHK cells infected with undiluted culture fluids and stained with 3.67G, a monoclonal anti-E antibody (30), showed that only cells that were cotransfected with either pcDNA-NS1 or pcDNA-NS1′ plasmids produced secreted viral particles (Fig. 4D). No secreted viral particles were produced in pKUNdNS1-only-transfected cells or in cells cotransfected with pKUNdNS1 and GFP-expressing plasmid (Fig. 4D). The lack of E-positive repBHK cells infected

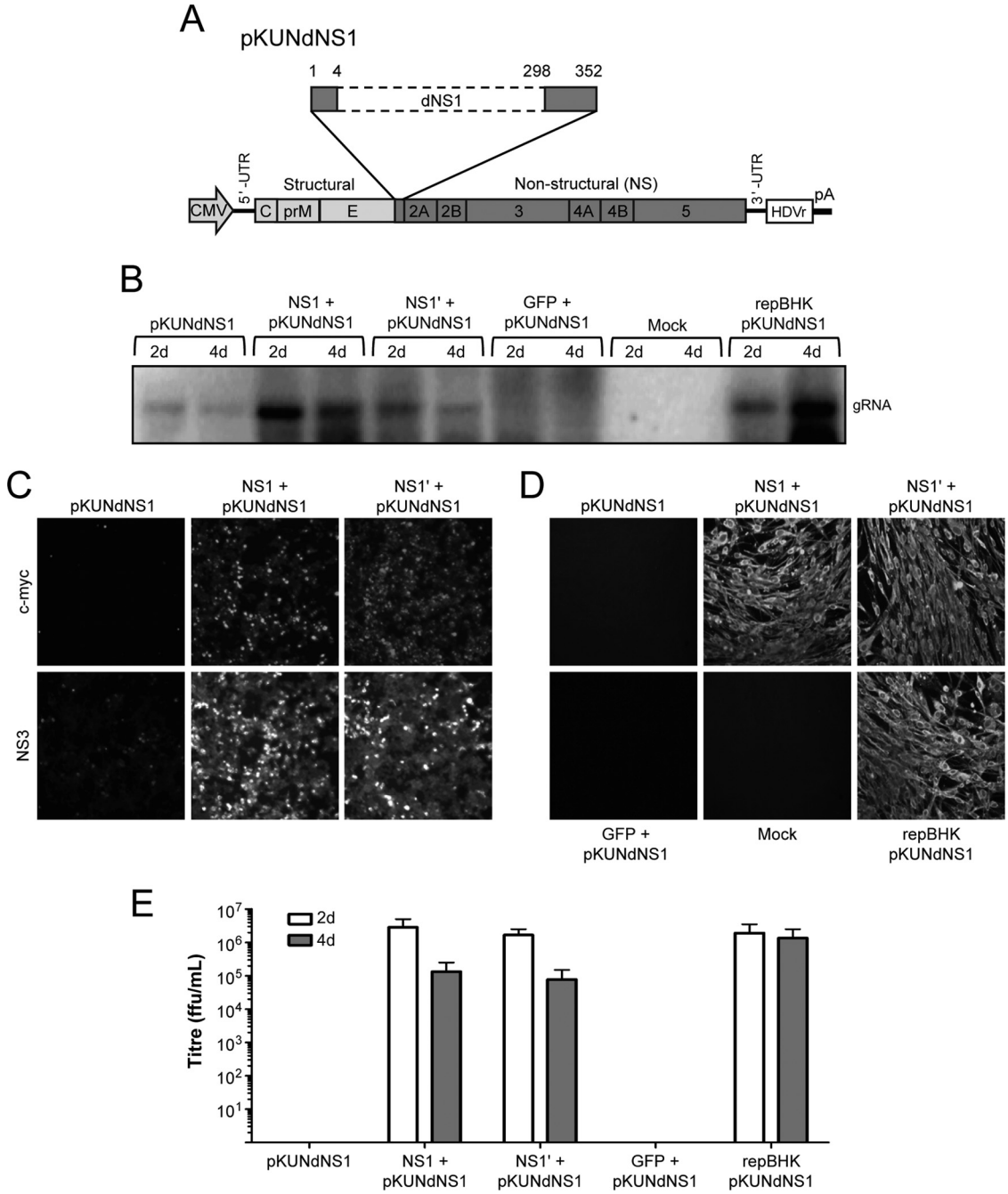

FIG 4 NS1′ complements replication of NS1-deleted viral RNA. (A) Schematic diagram of pKUNdNS1 plasmid DNA containing a large deletion in the NS1 gene (amino acid 4 to amino acid 298) of WNV_{KUN} genomic cDNA. CMV, cytomegalovirus promoter; HDVr, hepatitis delta virus ribozyme; pA, poly(A) signal; UTR, untranslated region. (B) Northern blot with a radiolabeled 3′-UTR probe showing replicating genomic RNA. RNA was harvested from cotransfected cells at 2 or 4 days posttransfection. (C) Immunofluorescence of HEK293T cells cotransfected with pKUNdNS1 and either NS1 or NS1′. Cotransfected cells were stained for c-Myc and NS3. (D) Immunofluorescence analysis showing production of infectious particles from cells cotransfected with pKUNdNS1 and either NS1 or NS1′. Culture fluid (CF) was harvested from cotransfected cells and used to infect repBHK cells. Infected repBHK cells were stained for E. (E) Titers were determined by infection of repBHK cells with serial dilutions of CF from cotransfected cells at day 2 (white bars) or 4 (gray bars) posttransfection and counting E-positive foci at day 2 postinfection. The graph is representative of two independent experiments. The difference between titers of complemented viruses expressing NS1 and NS1′ was not significant ($P > 0.05$), as determined by a standard one-way analysis of variance (ANOVA).

with DNase- and RNase-treated undiluted culture fluids from pKUNdNS1-only-transfected and pKUNdNS1-plus-GFP-expressing-plasmid-cotransfected cells also demonstrates that no transfected DNA or uncoated viral RNA was carried through to infection. To determine the titers of secreted viral particles, repBHK cells infected with serial 10-fold dilutions of collected culture fluids were stained with anti-E antibodies, and foci of E-positive cells were counted. Titration of viral particles was

carried out for two independent complementation experiments, and the average viral titers were determined. The viral titers were similar from NS1- and NS1′-complemented cells, and both were similar to the viral titers obtained in repBHK cells at 2 days after transfection (Fig. 4E). Notably, the accumulation of viral RNA and viral titers in NS1 and NS1′ complementation experiments decreased from day 2 to day 4 after transfections, while transfection of pKUNdNS1 into repBHK cells led to a corresponding increase in RNA level and no decrease in viral titers (Fig. 4B and E). This is likely due to the ability of complemented virus to spread in repBHK cells, where 100% of cells express complementing NS1 and NS1′ proteins, while the spread of complemented virus is not possible in cotransfection experiments, as untransfected cells do not support replication and thus spread of complemented virus. From these results, we concluded that NS1′ could successfully complement deletion of NS1 in virus replication and that there was no significant difference in the efficiency of complementation between NS1 and NS1′.

We have shown in this study that NS1′ has a cellular distribution similar to that of NS1 with respect to the ER, Golgi apparatus, and endosomes, that both NS1 and NS1′ are colocalized in viral RNA replication sites in infected cells, and that NS1′ is able to rescue replication of NS1-deleted viral RNA. From our data it is reasonable to assume that NS1′ may not have a unique function in replication that is different from that of NS1 and thus may simply serve as an additional NS1 protein. Given that NS1′ does contain the entire NS1 protein, it was not entirely unexpected that NS1′ has a similar localization and can perform the same function(s) as NS1 in the virus life cycle. Although here we tested the function of NS1′ only in viral replication, NS1′ may also be involved in other reported functions of NS1, such as interactions with the complement system (17–20, 22) and inhibition of Toll-like receptor 3 (TLR3) signaling (21). Further studies are required to clarify this. However, the presence of the additional C-terminal 52 amino acids in the NS1′ protein compared to NS1 may also result in NS1′ having a unique function(s) in viral infection. Studies focused on identifying potential differences between the NS1 and NS1′ proteins are under way in an effort to explain the *in vivo* differences observed between NS1′-producing and NS1′-lacking WNV_{KUN} viruses (23).

ACKNOWLEDGMENTS

We thank Jennifer Stow for providing antibodies to cellular markers, Roy Hall for providing various monoclonal antibodies, Paul Young for his helpful discussions, and Susann Liebscher for technical assistance with immunofluorescence.

This work was supported by National Health and Medical Research Council of Australia grant APP1009874.

REFERENCES

1. **Lindenbach BD, Rice CM.** 2003. Molecular biology of flaviviruses. Adv. Virus Res. **59:**23–61.
2. **Garmendia AE, Van Kruiningen HJ, French RA.** 2001. The West Nile virus: its recent emergence in North America. Microbes Infect. **3:**223–229.
3. **Rossi SL, Ross TM, Evans JD.** 2010. West Nile virus. Clin. Lab. Med. **30:**47–65.
4. **Lanciotti RS, Ebel GD, Deubel V, Kerst AJ, Murri S, Meyer R, Bowen M, McKinney N, Morrill WE, Crabtree MB, Kramer LD, Roehrig JT.** 2002. Complete genome sequences and phylogenetic analysis of West Nile virus strains isolated from the United States, Europe, and the Middle East. Virology **298:**96–105.
5. **Hall RA, Broom AK, Smith DW, Mackenzie JS.** 2002. The ecology and epidemiology of Kunjin virus. Curr. Top. Microbiol. Immunol. **267:**253–269.
6. **Audsley M, Edmonds J, Liu W, Mokhonov V, Mokhonova E, Melian EB, Prow N, Hall RA, Khromykh AA.** 2011. Virulence determinants between New York 99 and Kunjin strains of West Nile virus. Virology **414:**63–73.
7. **Hall RA, Scherret JH, Mackenzie JS.** 2001. Kunjin virus: an Australian variant of West Nile? Ann. N. Y. Acad. Sci. **951:**153–160.
8. **Westaway EG, Mackenzie JM, Khromykh AA.** 2003. Kunjin RNA replication and applications of Kunjin replicons. Adv. Virus Res. **59:**99–140.
9. **Westaway EG, Mackenzie JM, Khromykh AA.** 2002. Replication and gene function in Kunjin virus. Curr. Top. Microbiol. Immunol. **267:**323–351.
10. **Khromykh AA, Westaway EG.** 1994. Completion of Kunjin virus RNA sequence and recovery of an infectious RNA transcribed from stably cloned full-length cDNA. J. Virol. **68:**4580–4588.
11. **Coia G, Parker MD, Speight G, Byrne ME, Westaway EG.** 1988. Nucleotide and complete amino acid sequences of Kunjin virus: definitive gene order and characteristics of the virus-specified proteins. J. Gen. Virol. **69:**1–21.
12. **Speight G, Coia G, Parker MD, Westaway EG.** 1988. Gene mapping and positive identification of the non-structural proteins NS2A, NS2B, NS3, NS4B and NS5 of the flavivirus Kunjin and their cleavage sites. J. Gen. Virol. **69:**23–34.
13. **Chu PW, Westaway EG.** 1992. Molecular and ultrastructural analysis of heavy membrane fractions associated with the replication of Kunjin virus RNA. Arch. Virol. **125:**177–191.
14. **Khromykh AA, Sedlak PL, Westaway EG.** 2000. *cis-* and *trans*-acting elements in flavivirus RNA replication. J. Virol. **74:**3253–3263.
15. **Lindenbach BD, Rice CM.** 1997. *trans*-Complementation of yellow fever virus NS1 reveals a role in early RNA replication. J. Virol. **71:**9608–9617.
16. **Westaway EG, Mackenzie JM, Kenney MT, Jones MK, Khromykh AA.** 1997. Ultrastructure of Kunjin virus-infected cells: colocalization of NS1 and NS3 with double-stranded RNA, and of NS2B with NS3, in virus-induced membrane structures. J. Virol. **71:**6650–6661.
17. **Avirutnan P, Punyadee N, Noisakran S, Komoltri C, Thiemmeca S, Auethavornanan K, Jairungsri A, Kanlaya R, Tangthawornchaikul N, Puttikhunt C, Pattanakitsakul SN, Yenchitsomanus PT, Mongkolsapaya J, Kasinrerk W, Sittisombut N, Husmann M, Blettner M, Vasanawathana S, Bhakdi S, Malasit P.** 2006. Vascular leakage in severe dengue virus infections: a potential role for the nonstructural viral protein NS1 and complement. J. Infect. Dis. **193:**1078–1088.
18. **Chung KM, Liszewski MK, Nybakken G, Davis AE, Townsend RR, Fremont DH, Atkinson JP, Diamond MS.** 2006. West Nile virus nonstructural protein NS1 inhibits complement activation by binding the regulatory protein factor H. Proc. Natl. Acad. Sci. U. S. A. **103:**19111–19116.
19. **Kurosu T, Chaichana P, Yamate M, Anantapreecha S, Ikuta K.** 2007. Secreted complement regulatory protein clusterin interacts with dengue virus nonstructural protein 1. Biochem. Biophys. Res. Commun. **362:**1051–1056.
20. **Schlesinger JJ.** 2006. Flavivirus nonstructural protein NS1: complementary surprises. Proc. Natl. Acad. Sci. U. S. A. **103:**18879–18880.
21. **Wilson JR, de Sessions PF, Leon MA, Scholle F.** 2008. West Nile Virus nonstructural protein 1 inhibits TLR3 signal transduction. J. Virol. **82:**8262–8271.
22. **Avirutnan P, Fuchs A, Hauhart RE, Somnuke P, Youn S, Diamond MS, Atkinson JP.** 2010. Antagonism of the complement component C4 by flavivirus nonstructural protein NS1. J. Exp. Med. **207:**793–806.
23. **Melian EB, Hinzman E, Nagasaki T, Firth AE, Wills NM, Nouwens AS, Blitvich BJ, Leung J, Funk A, Atkins JF, Hall R, Khromykh AA.** 2010. NS1′ of flaviviruses in the Japanese encephalitis virus serogroup is a product of ribosomal frameshifting and plays a role in viral neuroinvasiveness. J. Virol. **84:**1641–1647.
24. **Mason PW, McAda PC, Dalrymple JM, Fournier MJ, Mason TL.** 1987. Expression of Japanese encephalitis virus antigens in Escherichia coli. Virology **158:**361–372.
25. **Firth AE, Atkins JF.** 2009. A conserved predicted pseudoknot in the NS2A-encoding sequence of West Nile and Japanese encephalitis flaviviruses suggests NS1′ may derive from ribosomal frameshifting. Virol. J. **6:**14–19.

26. **Mason PW.** 1989. Maturation of Japanese encephalitis virus glycoproteins produced by infected mammalian and mosquito cells. Virology **169:** 354–364.
27. **Macdonald J, Tonry J, Hall RA, Williams B, Palacios G, Ashok MS, Jabado O, Clark D, Tesh RB, Briese T, Lipkin WI.** 2005. NS1 protein secretion during the acute phase of West Nile virus infection. J. Virol. **79:**13924–13933.
28. **Mackenzie JM, Jones MK, Young PR.** 1996. Immunolocalization of the dengue virus nonstructural glycoprotein NS1 suggests a role in viral RNA replication. Virology **220:**232–240.
29. **Gillespie LK, Hoenen A, Morgan G, Mackenzie JM.** 2010. The endoplasmic reticulum provides the membrane platform for biogenesis of the flavivirus replication complex. J. Virol. **84:**10438–10447.
30. **Adams SC, Broom AK, Sammels LM, Hartnett AC, Howard MJ, Coelen RJ, Mackenzie JS, Hall RA.** 1995. Glycosylation and antigenic variation among Kunjin virus isolates. Virology **206:**49–56.

Last twenty amino acids of the West Nile Virus NS1' protein are responsible for its retention in cells and formation of unique heat-stable dimers.

Lucy B. Young[1], Ezequiel Balmori Melian[1*], Yin Xiang Setoh[1], Paul R Young[1], and Alexander A. Khromykh[1#]

[1]Australian Infectious Disease Research Centre, School of Chemistry and Molecular Biosciences, University of Queensland, Brisbane, QLD 4072, Australia.

Running title: West Nile virus NS1' protein forms heat-stable dimers

#Address correspondence to Alexander A. Khromykh, a.khromykh@uq.edu.au

*Current affiliation: Queensland Alliance for Agriculture and Food Innovation, University of Queensland.

Summary: 250

Text: 5170

SUMMARY

West Nile Virus (WNV), a mosquito-borne Flavivirus, is the major cause of arboviral encephalitis in the United States. As other members of the Japanese encephalitis virus serogroup, WNV produces an additional nonstructural protein, NS1', a carboxy-terminal extended product of NS1 generated as the result of a -1 programmed ribosomal frameshift (PRF). We have previously shown that mutations abolishing the PRF and consequently NS1', resulted in reduced neuroinvasiveness. However whether this was caused by the PRF event itself or by the lack of a PRF product, NS1', or a combination of both, remains undetermined. Here we show that WNV NS1' forms a unique sub-population of heat- and low pH- stable dimers. C-terminal truncations and mutational analysis employing an NS1'-expressing plasmid showed that stability of NS1' dimers is linked to the penultimate ten amino acids. To examine the role of NS1' heat-stable dimers in virus replication and pathogenicity, a stop codon mutation was introduced into NS1' to create a WNV producing a truncated version of NS1' lacking the last 20 amino acids but not affecting the PRF. NS1' protein produced by this mutant virus was secreted more efficiently than wild type NS1', indicating that the sequence of the last 20 amino acids of NS1' is responsible for its cellular retention. Further analysis of this mutant showed similar to the wild type WNV_{KUN} growth kinetics in cells and virulence in weanling mice after peripheral infection suggesting that full length NS1' is not essential for virus replication *in vitro* and for virulence in mice.

INTRODUCTION

West Nile Virus (WNV) is currently the major cause of arboviral encephalitis in the United States (Petersen, 2009). A member of the Japanese Encephalitis virus (JEV) serogroup, this flavivirus is maintained through a transmission cycle between birds and mosquitoes, primarily the *Culex* species. WNV also causes incidental infections in humans and other mammals, with approximately 5% of symptomatic infections involving neurological symptoms, such as encephalitis and meningitis (Beckham & Tyler, 2009). Kunjin (WNV_{KUN}) is the prevalent strain of WNV within Australia (Hall *et al.*, 2002), and is highly attenuated compared to strains common to the US, such as the strain responsible for the spread of WNV to the US in 1999 (WNV_{NY99}) (Lanciotti *et al.*, 1999). WNV_{KUN} has been used extensively as a model for WNV infection since it was first isolated in 1960 (Doherty *et al.*, 1963; Westaway *et al.*, 2002; 2003).

WNV_{KUN} has an 11kb positive sense single stranded RNA genome encoding for 3 structural (C, prM and E) and 7 non-structural proteins (NS1, NS2A, NS2B, NS3, NS4A, NS4B and NS5). Produced as a single polyprotein, it is cleaved by both host and viral proteases to give rise to the individual proteins (Lindenbach & Rice, 2003). NS1 is a multifunctional glycoprotein involved in the formation of the replication complex (Chu & Westaway, 1992; Khromykh *et al.*, 1999; Khromykh *et al.*, 2000; Lindenbach & Rice, 1997; Westaway *et al.*, 1997; Youn *et al.*, 2012) and the modulation of the host immune response (Avirutnan *et al.*, 2010; Avirutnan *et al.*, 2006; Chung *et al.*, 2006; Crook *et al.*, 2014; Kurosu *et al.*, 2007; Muller & Young, 2013; Schlesinger, 2006; Wilson *et al.*, 2008). After cleavage from the polyprotein (Falgout & Markoff, 1995; Nowak *et al.*, 1989), NS1 is glycosylated and forms a heat-labile dimer in the endoplasmic reticulum (ER) (Pryor & Wright, 1994; Winkler *et al.*, 1989; Winkler *et al.*, 1988). A proportion of

69 the dimerised protein is subsequently trafficked through the Golgi pathway and secreted
70 from cells as a soluble hexamer (Alcon-LePoder *et al.*, 2006; Chung & Diamond, 2008;
71 Flamand *et al.*, 1999; Macdonald *et al.*, 2005).

72 Encephalitic flaviviruses from the JEV serogroup produce an additional non-
73 structural protein, designated NS1', as the result of a -1 programmed ribosomal frameshift
74 (PRF) occurring at the beginning of the adjacent NS2A gene. Produced in 30-50% of
75 translation events, NS1' consists of the entire NS1 protein with a 52 amino acid C-
76 terminal extension encoding the first 9 amino acids of NS2A and 43 additional amino
77 acids (Firth & Atkins, 2009; Mason, 1989; Mason *et al.*, 1987; Melian *et al.*, 2010). We
78 have shown previously that NS1' is localized to the same cellular compartments as NS1
79 and can substitute for the function of NS1 in RNA replication (Youn *et al.*, 2013; Young
80 *et al.*, 2013), indicating that NS1' may function as additional NS1 in viral infection. The
81 PRF event and consequent NS1' production have been shown to be important for the viral
82 pathogenesis of both WNV_{KUN} and JEV as the lack of PRF/NS1' correlated with reduced
83 pathogenicity (Melian *et al.*, 2010; Ye *et al.*, 2012). Recent work has also identified that
84 JEV PRF/NS1' enhanced virus production in avian cells (Takamatsu *et al.*, 2014).
85 However, as mutations used in the above studies abolished both the PRF event and NS1'
86 production (Melian *et al.*, 2010; Takamatsu *et al.*, 2014; Ye *et al.*, 2012; Young *et al.*,
87 2013), the role of these two events independently in virus replication and pathogenesis
88 could not be distinguished and the unique function for NS1' in viral infection has
89 therefore not been identified.

90 In the present study we have focused on characterizing properties of NS1' protein
91 and its putative function in virus replication and pathogenesis. We show that NS1'

produces a unique sub-population of heat-stable homodimers, and that the presence of the frameshifted region results in increased cellular retention of NS1' compared to NS1. By using a mutant virus in which only full-length NS1' production but not the PRF event is affected we show that the last 20 amino acids of NS1' are responsible for the cellular retention of WNV_{KUN} NS1' and that full length NS1' is not essential for neuroinvasiveness in mice.

RESULTS

WNV NS1' is secreted less efficiently than NS1 from both infected and transfected cells. It has been shown previously that JEV NS1', unlike NS1, is not secreted efficiently from infected cells (Fan & Mason, 1990; Mason, 1989). To determine whether this is also the case for WNV_{KUN} NS1', pulse- chase ^{35}S-labelling experiments were carried out. A previously generated NS1'-lacking WNV_{KUN} virus mutant (A30A') was included in pulse-chase labelling experiments to confirm NS1' expression from wild type WNV_{KUN} infected cells. Radiolabelled NS1 and NS1' were detected in both the cell monolayer and culture fluid of WNV_{KUN} infected Vero76 cells at 24 or 72 hpi (Fig. 1a and 1b, respectively). Quantification of individual protein bands and determination of the extracellular/intracellular ratio (E/I) showed that NS1' is consistently secreted to a lower degree compared to NS1 (Fig. 1c). The same could be seen for NS1 and NS1' expressed from pcDNA-NS1 and pcDNA-NS1' transfected 293T cells (both co- and individually-transfected) at 24 and 48 h post transfection (Fig. 2a and 2b, respectively). Again, the E/I ratio showed that NS1' (whether individually- or co-transfected) was secreted to a

114 significantly lower degree than NS1 (Fig. 2c). These results indicate that the frameshifted
115 region of NS1' results in increased cellular retention of NS1' compared to NS1.
116
117 **WNV infection produces unique heat-stable NS1' dimers.** We have shown
118 previously that plasmid-expressed WNV_{KUN} NS1' retains a sub-population of dimers
119 when heated, while heating of plasmid-expressed NS1 disrupted dimers (Young *et al.*,
120 2013). To confirm this stability is not an artifact from plasmid expression, lysate from
121 WNV_{KUN} or A30A' (as a non-NS1' expressing control) infected Vero76 cells was heated
122 or left unheated prior to separation by SDS-PAGE. Proteins were transferred to
123 nitrocellulose membrane and analysed by Western blotting with an anti-NS1 monoclonal
124 antibody (4G4), which detects both NS1 and NS1'. The presence of NS1' dimers is still
125 seen in heated WNV_{KUN} lysate (Fig. 3a, lane 1), confirming that NS1' produced by
126 infected cells also forms a sub-population of heat-stable dimers. Previous studies on JEV
127 NS1' did not show the presence of these heat-stable NS1' dimers (Fan & Mason, 1990).
128 To examine this further, lysates from JEV, Murray Valley encephalitis virus (MVEV),
129 WNV_{NY99} and WNV_{KUN} infected Vero76 cells were subjected to SDS-PAGE and
130 Western blotting with anti-NS1 antibodies to determine the presence or absence of heat-
131 stable NS1' dimers. Heat-stable NS1' dimers were only detected in heated WNV (NY99
132 and KUN) samples (Fig. 3b, lanes 5 and 7), but not JEV or MVEV samples, showing that
133 these dimers are unique to WNV. The intermediate dimer band detected in all unheated
134 samples (lanes 2, 4, 6 and 8) is likely to be an NS1/NS1' heterodimer, which has
135 previously been shown for both JEV and MVEV (Blitvich *et al.*, 1995; Fan & Mason,
136 1990; Lin *et al.*, 1998).

WNV NS1' dimers are resistant to heat and low pH but susceptible to reduction. Previous work by Falconar and Young (Falconar & Young, 1990) has shown that NS1 dimers were stable at low pH (pH 3.5). To assess the pH stability of NS1' dimers, NS1 or NS1' transfected cell lysate (Fig. 4a) and WNV_{KUN} or A30A' infected cell lysate (Fig. 4b) was incubated for 1 h prior to separation by electrophoresis with 1M glycine buffered to the indicated pH. NS1 dimers were indeed stable until the pH was lowered to 3.5, while NS1' dimers were still stable at the lowest pH tested, pH 2.2. A range of temperature treatments was also tested on the same lysates to further examine heat-stability (Fig. 4c and 4d). While NS1 dimers were stable at room temperature, heating to 60°C for 30 min was enough to begin to disrupt this species. NS1' on the other hand, forms a sub-population of dimers that were still stable at the highest temperature tested, 95°C. The sub-population of NS1' that does not have this heat-stable nature has a similar stability to NS1 dimers, with respect to both temperature and pH treatment. However, reduction of lysates with 5% β-mercaptoethanol prior to SDS-PAGE separation resulted in complete disruption of both NS1 and NS1' dimers (Fig. 4e). Therefore, WNV NS1' is able to form a sub-population of heat and low pH stable dimers but these dimers are sensitive to reducing treatment during heating.

NS1' dimer stability resides within the first ten of the last twenty amino acids. As the NS1' heat-stable dimers are distinct from the heat-labile dimers formed by NS1, the stability must be linked to the presence of the frameshifted region of NS1'. To determine the region contributing to this stability, C-terminal 10- and 20-amino acid

truncations of NS1' were generated by PCR mutagenesis of pcDNA-NS1' (Fig. 5a). The presence of heat-stable dimers was determined by SDS-PAGE and Western blot analysis of heated or unheated lysates generated from HEK293T cells transfected with pcDNA-NS1, -NS1', -NS1'del10 or -NS1'del20. NS1' and NS1'del10 both formed a sub-population of heat-stable dimers (Fig. 5b, lanes 3-4 and 5-6 respectively), while NS1'del20 forms only heat-labile dimers (lanes 7-8), similar to those produced by NS1 (lanes 1-2). Interestingly, NS1'del20 also affected the presence of a high molecular weight NS1' multimer that can be observed in both NS1' and NS1'del10 unheated samples (Fig. 5b, lanes 4 and 6 respectively), suggesting that the increased stability of NS1' dimers is associated with the penultimate 10 amino acids.

To determine whether the loss of heat-stable dimers in pcDNA-NS1'del20 transfected cells was due to the specific amino acid sequence, or to a minimum length requirement of the frameshifted region, amino acids 385 to 393 were mutated to alanine (Fig. 5a). SDS-PAGE and Western blot analysis of lysate from pcDNA-NS1'Ala transfected cells showed that NS1'Ala is similar to NS1'del20, as it does not form heat-stable dimers (Fig 5b, lanes 9 and 10). This confirms that the heat-stable dimerisation is linked to the specific sequence of amino acids 385-394, rather than to the length of NS1'.

Due to the presence of a single additional cystiene (Cys) residue within the mutated region of NS1', we reasoned that an inter-chain disulfide bond may be forming between monomeric units, creating the heat-stability seen. This was also supported by the fact that the dimers are sensitive to reducing treatment (Fig. 4e). However, mutagenesis of this Cys residue to Ser (Fig. 5a) failed to affect the formation of the heat-stable NS1' dimers (Fig. 5b, lanes 11 and 12).

Last twenty amino acids of NS1' are important for its cellular retention. To examine the importance of the heat-stable NS1' dimers in the context of viral infection, we designed a mutant virus, Stop Mutant, which should eliminate the formation of stable NS1' dimers. This mutant introduces a premature stop codon 20 amino acids from the end of NS1' (Q385 to Stop), resulting in a truncated version of the protein (Fig. 6a). Notably, the position of the mutation and subsequent truncation of NS1' mimics the pcDNA-NS1'del20 construct, shown previously to not form heat-stable dimers (Fig. 5). This mutation was also introduced in a way so as not to affect the protein coding sequence of NS2A. To confirm the production of a truncated form of NS1' from Stop Mutant infected cells, SDS-PAGE and Western blot analysis of lysate from infected Vero76 cells was carried out. NS1'-specific antibodies detected a protein band corresponding to the predicted size of the truncated NS1' in Stop Mutant samples (Fig. 6b, lanes 3 and 4). This data also confirmed that Stop Mutant NS1', like pcDNA-NS1'del20, does not form heat-stable dimers. Immunofluorescence analysis of WNV_{KUN} and Stop Mutant infected cells stained with anti-NS1 (4G4) and counter-stained with anti-calnexin (ER marker) showed that the truncation of NS1' did not alter cellular localization (Fig. 6c). To determine if the truncation of NS1' in Stop Mutant virus affects NS1' secretion, pulse-chase ^{35}S-labelling experiments were carried out at 24 and 48 hpi as before. Immunoprecipitation of cell lysate or culture fluid, harvested at various chase times following radiolabelling, with anti-NS1 (4G4) showed that Stop Mutant NS1' was secreted during infection (Fig. 6d). Quantification of individual protein bands show that the secretion of Stop Mutant NS1' was in fact increased compared to WNV_{KUN} NS1' (Fig. 6e). The results show that the

206 sequence of the last 20 amino acids of NS1' is responsible for the cellular retention of
207 WNV_{KUN} NS1' protein.
208
209 **Truncation of NS1' does not significantly affect virus replication *in vitro* or**
210 **viral neurovirulence in mice.** To analyse the effect of truncation of NS1' on virus
211 replication *in vitro*, Vero76, C6/36 and mouse embryonic fibroblasts (MEFs) were
212 infected with the wild type WNV_{KUN} and Stop mutant viruses at MOI=1 or 0.1 and virus
213 titres in the culture fluid were determined every 12h (every 24h for C6/36) for up to 120 h
214 after infection. The results showed that truncation of NS1' did not affect virus replication
215 in any of the cell lines (Fig. 7a) demonstrating that full-length NS1' protein is not
216 required for virus replication *in vitro*. The results are similar to our previous *in vitro*
217 findings with A30A' mutant virus in which NS1' production is abolished by mutation of
218 the ribosomal frameshift (Melian *et al.*, 2010). In the same study we also showed that
219 A30A' virus was attenuated in weanling mice compared to WNV_{KUN} (Melian *et al.*, 2010).
220 The attenuation of A30A' may be due to the absence of NS1' itself, the elimination of the
221 frameshift, or a combination of both. In contrast to A30A', Stop Mutant only affects
222 production of full-length NS1', without affecting the ribosomal frameshift. To determine
223 whether NS1' production alone affects virus neurovirulence, 18 day-old mice were
224 infected intraperitoneally with 1000 pfu of either WNV_{KUN} or Stop Mutant and monitored
225 daily for signs of encephalitis. Infection with Stop Mutant resulted in a relatively similar
226 level of mortality compared to the wild type WNV_{KUN} (~40% survival for Stop Mutant
227 compared to ~20% survival for the wild type WNV_{KUN}) (Fig. 7b). This suggests that full-

228 length NS1' protein is unlikely to play a role in viral neurovirulence, indicating that the
229 attenuation seen in PRF/NS1'-lacking mutants is likely due to the loss of the PRF itself.
230
231 **DISCUSSION**
232 We have shown here that NS1' forms a sub-population of heat-stable, secretable
233 homodimers. The stability of these dimers is dependent on amino acids 385-394; though
234 not specifically to the cysteine reside at position 392 (Fig. 5). While NS1' is secreted
235 from both infected and transfected cells, increased cellular retention compared to NS1
236 was noted (Fig. 1 and 2), similar to work published previously for JEV NS1' (Mason,
237 1989). We have also linked this increased cellular retention to the last 20 amino acids of
238 NS1' (Fig. 6). Finally, we have shown that C-terminal truncation of the NS1' protein and
239 loss of heat-stable NS1' dimers in WNV_{KUN} has no effect on viral replication *in vitro* or
240 viral pathogenesis *in vivo* (Fig. 7).
241 The design and use of Stop Mutant was to not only examine heat-stable
242 dimerisation in a viral context, but also to separate the function of full-length NS1' from
243 that of the ribosomal frameshift itself. Due to the intricate relationship between the
244 ribosomal frameshift and the production of NS1', it is difficult to determine whether
245 attenuation of NS1'-lacking viruses is a result of the loss of the NS1' protein, or the
246 frameshift itself (Melian *et al.*, 2010; Ye *et al.*, 2012). It is possible that the frameshift
247 mechanism evolved to primarily control the ratio of structural to non-structural proteins
248 (Melian *et al.*, 2014), and its byproduct NS1' is generated to increase the relative level of
249 functioning NS1. The work presented here showed that truncation of NS1' did not
250 detrimentally affect virus growth in mammalian and insect cell culture, or WNV_{KUN}

pathogenicity in mice after peripheral inoculation (Fig. 7). These results support the hypothesis that full-length NS1' is unlikely to have a unique biological function that contributes to viral pathogenesis in a mammalian system. This suggests that the reduced pathogenicity seen in mice for previously studied WNV_{KUN} viruses lacking both the PRF and NS1' is more likely due to the loss of the PRF.

Work conducted in chicken embryonic fibroblasts and embryonated chicken eggs identified a role for JEV PRF/NS1' in facilitating virus production in avian cells by increasing viral RNA levels (Takamatsu *et al.*, 2014). This is in contrast to virus grown in mammalian or insect culture which has shown that viral replication *in vitro* is not different between viruses lacking PRF/NS1' and those encoding PRF and producing NS1' (Melian *et al.*, 2010; Ye *et al.*, 2012). Our other recent study has also found no difference in replication in avian DF-1 cells between WT and PRF-deficient mutant (A30A') WNV_{KUN} viruses (Melian *et al.*, 2014). Combined together, these results indicate that the role of PRF/NS1' in viral replication may be virus species and perhaps host species specific.

The increased stability observed here for NS1' dimers has given us insight into the cell associated form of NS1', and potentially NS1. Due to the increase in dimer stability, it is possible to observe higher order oligomeric forms in unheated SDS-PAGE analysis of WNV_{KUN} NS1' (see Fig. 3a, 4a-d, 5b, and 6b). Indeed, when this dimer stability was abolished by truncation or mutation, not only were the heat-stable dimers affected, but also the detergent-stable oligomers. Based on the observed size on SDS-PAGE gels, these are likely to be hexamers; however, further confirmation would be required. These higher order oligomers are still observed in SDS-PAGE analysis when cell lysates were treated

with iodoacetamide (to prevent disulfide exchange post-lysis, data not shown), suggesting that the potential hexamer seen is a natural state, not a product of lysis. This data may also shed light on the cell associated form of NS1, which is still unknown (Muller & Young, 2013). The NS1 hexamer is held together by only weak hydrophobic interactions that are disrupted to dimers by detergent treatment (Flamand *et al.*, 1999), such as those required for cell lysis. The observation of higher order oligomers formed by NS1' may indicate that the subtle increase in stability seen for WNV_{KUN} NS1' is enough to allow us to observe the natural state of intra-cellular NS1' without the need for cross-linking.

One key characteristic examined here is the cellular retention of NS1', despite the absence of a distinct hydrophobic region in the frameshifted sequence. This increase in cellular retention compared to NS1 was also linked to the last 20 amino acids of NS1' as shown by more efficient secretion of the Stop Mutant NS1' lacking the last 20 amino acids. It is possible that the increase in secretion of NS1' in cells infected with Stop Mutant may not be due to the loss of a potential cell retention signal in the final 20 amino acids of NS1'. Instead, it is possible that, unlike the heat-stable dimers seen for NS1', this characteristic is dependent on the length of its C-terminal extension. Due to the nature of the ribosomal frameshift, and NS1' being encoded in the -1 open reading frame of NS2A, it is not possible to create an alanine mutant in the viral context similar to the one generated for the plasmid-expressed NS1' alanine mutant, without affecting the coding sequence of the NS2A gene. One way to determine if cellular retention is due to a specific sequence, or a minimum length requirement, would be to examine the secretion of NS1' in other flaviviral species, such as JEV and MVEV, and create similar truncation mutants. Interestingly, the sequence of the frameshifted region is not well conserved

297 between WNV_{KUN}, WNV_{NY99}, JEV and MVEV viruses (Fig. 8) however JEV NS1' has
298 also been shown previously to be inefficiently secreted (Fan & Mason, 1990). If
299 truncation of NS1' in other flaviviral species also results in increased NS1' secretion
300 compared to the wild type NS1', then the cellular retention of NS1' it is more likely to be
301 dependent on its length rather than specific amino acids. Notably, while mutation in the
302 Stop Mutant virus removing the last 20 amino acids increased NS1' secretion, the
303 pathogenesis in mice of this mutant virus was similar to that of the wild type WNV_{KUN}.
304 This suggests that the inefficient secretion, while an intriguing characteristic of NS1' that
305 is distinct from NS1, is unlikely to contribute significantly to virus virulence in the
306 mammalian hosts.

307 The presence of heat-stable, reducing-sensitive NS1' dimers suggested the
308 presence of a disulfide bond; however, mutagenesis of the Cys residue within the
309 frameshifted region indicates that it is not due to a simple interaction between the C-
310 terminal Cys residues of two monomers. It has previously been suggested (M. Lobigs,
311 personal communication) that NS1 may itself catalyse disulfide bond exchange. Viral
312 proteins have been identified previously to contain the disulfide isomerisation motif,
313 CXXC (Li *et al.*, 2008). NS1 contains a CXXC motif that is conserved for DENV, YFV
314 and the JEV serogroup. These Cys residues (C10 and C11) have been shown previously
315 to be important for dimer formation and NS1 secretion (Pryor & Wright, 1993). It is
316 possible that the presence of the frameshifted region in NS1' may in fact impede folding
317 of this C-terminally extended NS1 protein. The heat-stable dimers observed may
318 therefore represent folding intermediates involving intermolecular disulfide bonds
319 between covalently linked NS1' monomers. On the other hand, as these heat-stable

320 dimers appear to be secreted to some degree (Fig. 1 and 2), they are unlikely to represent
321 misfolded protein, as this would be retained in the cell. However, only a small amount of
322 NS1' is secreted from the cell, and it is therefore difficult to conclusively determine the
323 dimer stability. Further work analysing the nature of these heat-stable NS1' dimers and
324 the possibility of the involvement of NS1 part of NS1' in disulfide bond exchange is
325 necessary.

326 While the sequence of frameshifted region is not conserved between different
327 encephalitic flaviviruses, the stop codon and consequently the length of the NS1'
328 extension are (Fig. 8). This suggests that the PRF event leading to production of precisely
329 52 amino acid extension at the C-terminus of NS1 protein may evolve to perhaps ensure
330 that the PRF product, NS1', could function as additional NS1. Given efficient secretion of
331 NS1 from cells, the ability of inefficiently secreted NS1' to function as NS1 in infected
332 cells may provide additional benefit to viral RNA replication. It seems highly unlikely
333 that such a conserved mechanism as -1 PRF producing a stable NS1' protein has evolved
334 in a distinct group of viruses without a significant impact on viral growth/transmission
335 properties in at least one of the vector or host systems. Relatively modest attenuation in
336 mice of PRF- and NS1'-deficient WNV_{KUN} virus (A30A') (49) and our data showing
337 insignificant attenuation of Stop Mutant WNV_{KUN} in mice suggests that mammalian hosts
338 are unlikely to be the primary driver for the evolution of this mechanism. As mammals
339 are only incidental hosts for these viruses, and these viruses predominantly cycle through
340 the *Culex* mosquito vector and avian hosts, it is more likely that this is where the PRF
341 mechanism has initially evolved, and where it is likely to have a significant impact on
342 virus replication and/or transmission. Recent work with WNV_{KUN} and JEV viruses

conducted in the mosquito and avian systems supports this hypothesis, with a difference in pathogenicity in birds, virus growth in avian cell culture, and transmission in *Culex* mosquitoes observed between viruses encoding PRF and expressing NS1' and those lacking PRF and NS1' (Melian *et al.*, 2014; Takamatsu *et al.*, 2014).

In conclusion, we have shown that WNV NS1' forms a sub-population of heat-stable NS1' dimers that are produced and preferentially retained both in the content of virus infection and when the NS1' protein is produced independently from plasmid DNA. We have demonstrated that both the heat-stability and cellular retention can be linked to the last 20 amino acids of NS1', with dimerisation being specifically linked to the penultimate 10 amino acids. We have also shown that viral mutant producing truncated form of NS1' but not deficient in ribosomal frameshift (Stop Mutant) replicates with the same efficiency in cells of different origin and has a relatively similar virulence in mice to the wild type WNV_{KUN}. In combination with previous work (Melian *et al.*, 2014; Melian *et al.*, 2010), this suggests that the PRF itself (and not the NS1' protein) is important for viral pathogenesis in the mammalian system. Further work in the mosquito and avian hosts using Stop Mutant producing truncated NS1' will determine whether full-length NS1' is indeed required for viral replication/transmission in this vector-host system.

MATERIALS AND METHODS

Cell culture. Baby hamster kidney (BHK) and Vero76 (African green monkey) cells were maintained in Dulbecco's modified eagle medium (DMEM) (Gibco, USA) supplemented with 5% heat inactivated Fetal Calf Serum (FCS), 100 U/mL penicillin, 100 µg/mL streptomycin and 2mM glutamax. Mouse embryonic fibroblasts (MEF) and

366 human embryonic kidney (HEK) 293T cells were also grown in DMEM supplemented
367 with glutamax and penicillin/streptomycin as above, with a total of 10% FCS. HEK 293T
368 cells were also grown in 1 mM sodium pyruvate. *Aedes albopictus* cells (C6/36) were
369 grown and maintained in RPMI media (Gibco, USA), containing 10% FCS, glutamax and
370 penicillin/streptomycin as above.

371 **Plasmid construction (i) pcDNA plasmids.** Plasmids for the transient expression
372 of NS1 and NS1' (pcDNA-NS1 and pcDNA-NS1') were described previously (Young *et*
373 *al.*, 2013). Both plasmids contain an N-terminal signal sequence consisting of the last 26
374 codons of the WNV_{KUN} E protein and Myc and Flag tags at the C terminus. Overlapping
375 PCR mutagenesis using *Pfu* DNA Polymerase (Promega) was carried out on pcDNA-
376 NS1' to generate a plasmid containing an amino acid change at residue 392 (NS1' C392S)
377 for cysteine mutagenesis. Overlapping PCR mutagenesis was also used to delete 10 or 20
378 amino acids from the C-terminus of NS1' for truncation analysis, and to introduce several
379 point mutations to change amino acids 385-393 to alanine (NS1'Ala). These reactions
380 were subsequently transformed into *E.coli* DH5α cells and potential clones screened by
381 restriction enzyme digestion prior to sequencing. Positive clones were used to inoculate
382 LB broth and plasmid DNA was purified by NucleoBond®Xtra Midi/Maxi kit as per
383 manufactures instructions. **(ii) FLSDX mutants.** Stop Mutant was generated by
384 overlapping PCR mutagenesis on an intermediate E-NS2A cassette, prior to restriction
385 enzyme digestion and ligation into full-length WNV_{KUN} infectious clone, FLSDX
386 (Khromykh *et al.*, 1998).

387 **Transfection conditions.** 293T cells were seeded at 80-90% confluency in
388 antibiotic free media 24 h prior to experiments. Transfections were carried out using

389 Lipofectamine® 2000 (Invitrogen), according to the manufacturer's instructions. A ratio
390 of 0.8μg DNA to 2μL reagent for a 24-well plate was used as standard, and scaled
391 appropriately for well size.

392 ***In vitro* transcription and electroporation.** Full length cDNA templates
393 (FLSDX and mutants) were linearised with XhoI (New England Biolabs) and purified by
394 phenol-chloroform extraction and ethanol precipitation. *In vitro* transcription and
395 electroporation of BHK cells was carried out as described previously (Leung *et al.*, 2008),
396 virus stocks were harvested at 2 to 4 days post electroporation and titrated on BHK cells.

397 **Virus stocks.** Working virus stocks for WNV_{KUN}, A30A' and Stop Mutant were
398 generated by infection of BHK cells at low multiplicity of infection (MOI=0.1) with
399 WNV_{KUN} or mutant viruses harvested from electroporated BHK cells. Stocks were
400 harvested at day 3 to 5 post infection and titrated as above. WNV_{NY99} stock was
401 generated by infection of Vero76 cells with virus harvested from BHK cells
402 electroporated with RNA transcribed from infectious cDNA clone of NY99 4132 isolate
403 as described previously (Audsley *et al.*, 2011). JEV FU strain, first isolated in 1995
404 (Hanna *et al.*, 1996), and MVEV 1-51, first isolated in 1951 (French, 1952), were kindly
405 donated by Roy Hall.

406 **Virus infection and growth kinetics.** BHK, WT MEF or C6/36 cells were
407 seeded into 6-well plates and infected with WNV_{KUN} or mutant viruses at an MOI of 0.1
408 or 1 for 2 h. Cells were washed 3X and appropriate growth media was added. For growth
409 kinetics, 100 μL per sample was harvested at the indicated times post infection, clarified
410 by centrifugation and stored at -80°C. Virus titres were determined by plaque assay as
411 previously described (Leung *et al.*, 2008).

412 **SDS-PAGE and Western blotting.** Sodium dodecyl sulfate polyacrylamide gel
413 elecrophoresis (SDS-PAGE) was carried out using either a Mini-PROTEAN® Tetra
414 Handcast system (Bio-Rad®) or Bolt® Mini-Gel system (Novex®). Using the Mini-
415 PROTEAN® system, SDS-PAGE gels were prepared with a 10% resolving and 4%
416 stacking gel. Bolt® 4-12% Bis-Tris Plus Gel (Novex®) were used with the Bolt® Mini-
417 gel system. To carry out SDS-PAGE, cell lysate was added to 4X NuPAGE® LDS-
418 PAGE loading buffer (Novex®) and samples were heated (70°C for 10 min) or left
419 untreated as indicated. Protein samples were loaded into an SDS-PAGE gel in Tris-
420 Glycine running buffer and electrophoresed for 1 to 2 h (as required for separation) at
421 130V (Mini-PROTEAN® system) or 200V (Bolt® system). Following SDS-PAGE,
422 samples were transferred from the gel to a nitrocellulose membrane (GE Healthcare
423 Hybond-ECL) using the Mini Trans-Blot System (Bio-Rad®). Membranes to be
424 immunoblotted were removed from the transfer apparatus and washed in 1X PBS Tween-
425 20 (PBST) followed by blocking with 2.5% non-fat milk (Bio-Rad) in PBS overnight at
426 4°C. The blocking solution was removed by 3 x 5 min washes with PBST prior to
427 incubation with the primary antibody at an appropriate dilution in 2.5% non-fat milk for 1
428 h at room temperature. Primary antibody was removed by 3 x 10 min washes in PBST
429 and incubated with the secondary antibody at an appropriate dilution in PBST for 1 h at
430 room temperature protected from light. The secondary antibody was removed by 3 x 10
431 min washes in PBST and signal from membranes was detected using Odyssey machine.
432 **Immunofluorescence.** Vero76 cells were infected with either WNV_{KUN} or Stop
433 Mutant at an MOI of 10 and fixed at 24 h postinfection (hpi) in 80% acetone in PBS.
434 Fixed cells were blocked and subsequently co-stained with 4G4 and an antibody

435 recognizing a marker of the ER (rabbit polyclonal antibody against calnexin [Sigma-
436 Aldrich]). Alexa Fluor 488-conjugated anti-mouse and Alexa Fluor 555-conjugated anti-
437 rabbit antibodies (Invitrogen) were used for secondary labelling. Nuclei were
438 counterstained with DAPI and images captured using an LSM510 META confocal laser-
439 scanning microscope (Carl Zeiss).

440 **Radiolabelling.** Pulse-chase analysis was carried out in 6-well plates of infected
441 Vero cells (infected at MOI=1 with WNV_{KUN} or mutant viruses) or transfected 293T cells
442 (transfected with pcDNA-NS1, pcDNA-NS1' or both plasmids) at 24, 48 or 72 hours. At
443 24 and 72 hpi or 24 and 48 h post-transfection, cells were starved for 30 min in
444 methionine and cysteine free DMEM (Gibco), followed by labelling for 1.5 hours with
445 100μCi 35S-methionine. After labelling, cells were washed once in PBS and twice in
446 DMEM, and chased for 0, 1, 4 or 12 h in DMEM supplemented with 5% heat FCS, 100
447 U/mL penicillin, 100 μg/mL streptomycin and 2mM glutamax. Following radiolabelling,
448 cell monolayers were placed on ice and the culture fluids were removed, clarified by
449 centrifugation at 1500 g for 5 min, and mixed with equal volume of 2X lysis buffer (20
450 mM Tris-HCI, pH 7.5, 150 mM NaCI, 10 mM EDTA, 2% sodium deoxycholate, 2%
451 Triton X-l 00, 0.2% sodium dodecyl sulfate (SDS) containing a 2X concentration of
452 cOmplete protease inhibitor cocktail (Roche)). The cell monolayer was rinsed with ice-
453 cold PBS (pH 7.4), scraped from the plate in 1X lysis buffer (10 mM Tris-HCI, pH 7.5,
454 150 mM NaCI, 5 mM EDTA, 1% sodium deoxycholate, 1% Triton X-l 00, 0.1% SDS)
455 containing protease inhibitors, incubated for 30 min on ice, and clarified by
456 centrifugation for 10 min at 14,000 g. Resulting protein preparations, both from culture
457 fluid and cell monolayer, were immunoprecipitated with 4G4 using 25μL Dynabeads®

458 Protein G per sample according to the manufactures instructions. Briefly, beads were
459 incubated with the described amount of antibody diluted in 200 µL PBST per sample for
460 30 min then washed to remove unbound antibody. The Dynabead®/antibody complex
461 was incubated for 1 h at room temperature with the appropriate protein sample.
462 Subsequent washes were carried out with PBS and proteins were eluted in 30 µL of
463 elution buffer (20 µL 50mM Glycine at pH2.8 plus 10 µL NuPAGE LDS Sample Buffer).
464 Eluted proteins were loaded onto SDS-PAGE gels, electrophoresed and labelled proteins
465 were transferred to nitrocellulose membranes. Membranes were exposed to a phosphor
466 screen and scanned on a Typhoon scanner (GE Healthcare) or exposed to X-ray film in an
467 X-ray cassette at -80°C and developed.

468 **Virulence in mice.** Groups of ten to twenty 18-day-old CD1 mice were infected
469 intraperitoneally with 1000 plaque forming units (pfu) of either WNV_{KUN} or Stop Mutant
470 virus. Mice were monitored daily for signs of illness and euthanized when encephalitic
471 symptoms were evident.

472

473 *Acknowledgements*

474 We would like to thank Roy Hall for providing monoclonal antibodies, JEV FU and
475 MVEV virus stocks; Brian Clark for advice on statistical analysis; Natalie Prow for her
476 assistance with animal work and Mario Lobigs for helpful discussions.

477

478 **REFERENCES**

Alcon-LePoder, S., Sivard, P., Drouet, M. T., Talarmin, A., Rice, C. & Flamand, M. (2006). Secretion of flaviviral non-structural protein NS1: from diagnosis to pathogenesis. *Novartis Foundation Symposium* **277**, 233-247; discussion 247-253.

Audsley, M., Edmonds, J., Liu, W., Mokhonov, V., Mokhonova, E., Melian, E. B., Prow, N., Hall, R. A. & Khromykh, A. A. (2011). Virulence determinants between New York 99 and Kunjin strains of West Nile virus. *Virology* **414**, 63-73.

Avirutnan, P., Fuchs, A., Hauhart, R. E., Somnuke, P., Youn, S., Diamond, M. S. & Atkinson, J. P. (2010). Antagonism of the complement component C4 by flavivirus nonstructural protein NS1. *Journal of Experimental Medicine* **207**, 793-806.

Avirutnan, P., Punyadee, N., Noisakran, S., Komoltri, C., Thiemmeca, S., Auethavornanan, K., Jairungsri, A., Kanlaya, R., Tangthawornchaikul, N., Puttikhunt, C., Pattanakitsakul, S. N., Yenchitsomanus, P. T., Mongkolsapaya, J., Kasinrerk, W., Sittisombut, N., Husmann, M., Blettner, M., Vasanawathana, S., Bhakdi, S. & Malasit, P. (2006). Vascular leakage in severe dengue virus infections: a potential role for the nonstructural viral protein NS1 and complement. *Journal of Infectious Diseases* **193**, 1078-1088.

Beckham, J. D. & Tyler, K. (2009). Clinical Manifestations of Neurological Disease. In *West Nile Encephalitis Virus Infection*, pp. 69-95: Springer New York.

Blitvich, B. J., Mackenzie, J. S., Coelen, R. J., Howard, M. J. & Hall, R. A. (1995). A novel complex formed between the flavivirus E and NS1 proteins: analysis of its structure and function. *Archives of Virology* **140**, 145-156.

Chu, P. W. & Westaway, E. G. (1992). Molecular and ultrastructural analysis of heavy membrane fractions associated with the replication of Kunjin virus RNA. *Archives of Virology* **125**, 177-191.

Chung, K. M. & Diamond, M. S. (2008). Defining the Levels of Secreted Non-Structural Protein NS1 After West Nile Virus Infection in Cell Culture and Mice. *Journal of Medical Virology* **80**, 547 - 556.

Chung, K. M., Liszewski, M. K., Nybakken, G., Davis, A. E., Townsend, R. R., Fremont, D. H., Atkinson, J. P. & Diamond, M. S. (2006). West Nile virus nonstructural protein NS1 inhibits complement activation by binding the regulatory protein factor H. *PNAS* **103**, 19111 - 19116.

Crook, K. R., Miller-Kittrell, M., Morrison, C. R. & Scholle, F. (2014). Modulation of innate immune signaling by the secreted form of the West Nile virus NS1 glycoprotein. *Virology* **458-459**, 172-182.

Doherty, R. L., Carley, J. G., Mackerras, M. J. & Marks, E. N. (1963). Studies of arthropod-borne virus infections in Queensland. III. Isolation and characterization of virus strains from wild-caught mosquitoes in North Queensland. *Aust J Exp Biol Med Sci* **41**, 17-39.

Falconar, A. K. & Young, P. R. (1990). Immunoaffinity purification of native dimer forms of the flavivirus non-structural glycoprotein, NS1. *Journal of Virological Methods* **30**, 323-332.

Falgout, B. & Markoff, L. (1995). Evidence that flavivirus NS1-NS2A cleavage is mediated by a membrane-bound host protease in the endoplasmic reticulum. *J Virol* **69**, 7232-7243.

Fan, W. F. & Mason, P. W. (1990). Membrane association and secretion of the Japanese encephalitis virus NS1 protein from cells expressing NS1 cDNA. *Virology* **177**, 470-476.

Firth, A. E. & Atkins, J. F. (2009). A conserved predicted pseudoknot in the NS2A-encoding sequence of West Nile and Japanese encephalitis flaviviruses suggests NS1' may derive from ribosomal frameshifting. *Virology Journal* **6**, 14 - 19.

Flamand, M., Megret, F., Mathieu, M., Lepault, J., Rey, F. A. & Deubel, V. (1999). Dengue virus type 1 nonstructural glycoprotein NS1 is secreted from mammalian cells as a soluble hexamer in a glycosylation-dependent fashion. *Journal of Virology* **73**, 6104-6110.

French, E. L. (1952). Murray Valley encephalitis isolation and characterization of the aetiological agent. *Med J Aust* **1**, 100-103.

Hall, R. A., Broom, A. K., Smith, D. W. & Mackenzie, J. S. (2002). The ecology and epidemiology of Kunjin virus. *Current Topics in Microbiology and Immunology* **267**, 253-269.

Hanna, J. N., Ritchie, S. A., Phillips, D. A., Shield, J., Bailey, M. C., Mackenzie, J. S., Poidinger, M., McCall, B. J. & Mills, P. J. (1996). An outbreak of Japanese encephalitis in the Torres Strait, Australia, 1995. *Med J Aust* **165**, 256-260.

Khromykh, A. A., Kenney, M. T. & Westaway, E. G. (1998). trans-Complementation of flavivirus RNA polymerase gene NS5 by using Kunjin virus replicon-expressing BHK cells. *Journal of Virology* **72**, 7270-7279.

Khromykh, A. A., Sedlak, P. L., Guyatt, K. J., Hall, R. A. & Westaway, E. G. (1999). Efficient trans-Complementation of the Flavivirus Kunjin NS5 Protein but Not of

the NS1 Protein Requires Its Coexpression with Other Components of the Viral Replicase. *Journal of Virology* **73**, 10272 – 10280.

Khromykh, A. A., Sedlak, P. L. & Westaway, E. G. (2000). cis- and trans-acting elements in flavivirus RNA replication. *Journal of Virology* **74**, 3253-3263.

Kurosu, T., Chaichana, P., Yamate, M., Anantapreecha, S. & Ikuta, K. (2007). Secreted complement regulatory protein clusterin interacts with dengue virus nonstructural protein 1. *Biochemical and Biophysical Research Communications* **362**, 1051-1056.

Lanciotti, R. S., Roehrig, J. T., Deubel, V., Smith, J., Parker, M., Steele, K., Crise, B., Volpe, K. E., Crabtree, M. B., Scherret, J. H., Hall, R. A., MacKenzie, J. S., Cropp, C. B., Panigrahy, B., Ostlund, E., Schmitt, B., Malkinson, M., Banet, C., Weissman, J., Komar, N., Savage, H. M., Stone, W., McNamara, T. & Gubler, D. J. (1999). Origin of the West Nile virus responsible for an outbreak of encephalitis in the northeastern United States. *Science* **286**, 2333-2337.

Leung, J. Y., Pijlman, G. P., Kondratieva, N., Hyde, J., Mackenzie, J. M. & Khromykh, A. A. (2008). Role of Nonstructural Protein NS2A in Flavivirus Assembly. *Journal of Virology* **82**, 4731 – 4741.

Li, K., Zhang, S., Kronqvist, M., Wallin, M., Ekstrom, M., Derse, D. & Garoff, H. (2008). Intersubunit disulfide isomerization controls membrane fusion of human T-cell leukemia virus Env. *J Virol* **82**, 7135-7143.

Lin, Y. L., Chen, L. K., Liao, C. L., Yeh, C. T., Ma, S. H., Chen, J. L., Huang, Y. L., Chen, S. S. & Chiang, H. Y. (1998). DNA immunization with Japanese

encephalitis virus nonstructural protein NS1 elicits protective immunity in mice. *Journal of Virology* **72**, 191-200.

Lindenbach, B. D. & Rice, C. M. (1997). trans-Complementation of yellow fever virus NS1 reveals a role in early RNA replication. *Journal of Virology* **71**, 9608-9617.

Lindenbach, B. D. & Rice, C. M. (2003). Molecular biology of flaviviruses. *Advances in Virus Research* **59**, 23-61.

Macdonald, J., Tonry, J., Hall, R. A., Williams, B., Palacios, G., Ashok, M. S., Jabado, O., Clark, D., Tesh, R. B., Briese, T. & Lipkin, W. I. (2005). NS1 protein secretion during the acute phase of West Nile virus infection. *Journal of Virology* **79**, 13924-13933.

Mason, P. W. (1989). Maturation of Japanese Encephalitis-Virus Glycoproteins Produced by Infected Mammalian and Mosquito Cells. *Virology* **169**, 354-364.

Mason, P. W., McAda, P. C., Dalrymple, J. M., Fournier, M. J. & Mason, T. L. (1987). Expression of Japanese Encephalitis-Virus Antigens in Escherichia-coli. *Virology* **158**, 361-372.

Melian, E. B., Hall-Mendelin, S., Du, F., Owens, N., Bosco-Lauth, A. M., Nagasaki, T., Rudd, S., Brault, A. C., Bowen, R. A., Hall, R. A., van den Hurk, A. F. & Khromykh, A. A. (2014). Programmed Ribosomal Frameshift alters expression of West Nile virus genes and facilitates virus replication in birds and mosquitoes. *Submitted to PLoS Pathogens*.

Melian, E. B., Hinzman, E., Nagasaki, T., Firth, A. E., Wills, N. M., Nouwens, A. S., Blitvich, B. J., Leung, J., Funk, A., Atkins, J. F., Hall, R. & Khromykh, A. A. (2010). NS1' of Flaviviruses in the Japanese Encephalitis Virus Serogroup Is a

592 Product of Ribosomal Frameshifting and Plays a Role in Viral Neuroinvasiveness.
593 *Journal of Virology* **84**, 1641 - 1647.
594 **Muller, D. A. & Young, P. R. (2013).** The flavivirus NS1 protein: molecular and
595 structural biology, immunology, role in pathogenesis and application as a
596 diagnostic biomarker. *Antiviral Res* **98**, 192-208.
597 **Nowak, T., Farber, P. M. & Wengler, G. (1989).** Analyses of the terminal sequences of
598 West Nile virus structural proteins and of the in vitro translation of these proteins
599 allow the proposal of a complete scheme of the proteolytic cleavages involved in
600 their synthesis. *Virology* **169**, 365-376.
601 **Petersen, L. (2009).** Global Epidemiology of West Nile Virus. In *West Nile Encephalitis*
602 *Virus Infection*, pp. 1-23: Springer New York.
603 **Pryor, M. J. & Wright, P. J. (1993).** The effects of site-directed mutagenesis on the
604 dimerization and secretion of the NS1 protein specified by dengue virus. *Virology*
605 **194**, 769-780.
606 **Pryor, M. J. & Wright, P. J. (1994).** Glycosylation mutants of dengue virus NS1 protein.
607 *Journal of General Virology* **75 (Pt 5)**, 1183-1187.
608 **Schlesinger, J. J. (2006).** Flavivirus nonstructural protein NS1: Complementary surprises.
609 *Proceedings of the National Academy of Sciences of the United States of America*
610 **103**, 18879-18880.
611 **Takamatsu, Y., Okamoto, K., Dinh, D. T., Yu, F., Hayasaka, D., Uchida, L.,**
612 **Nabeshima, T., Buerano, C. C. & Morita, K. (2014).** NS1' protein expression
613 facilitates production of Japanese encephalitis virus in avian cells and
614 embryonated chicken eggs. *J Gen Virol* **95**, 373-383.

615 **Westaway, E. G., Mackenzie, J. M., Kenney, M. T., Jones, M. K. & Khromykh, A. A.**
616 **(1997).** Ultrastructure of Kunjin virus-infected cells: colocalization of NS1 and
617 NS3 with double-stranded RNA, and of NS2B with NS3, in virus-induced
618 membrane structures. *Journal of Virology* **71**, 6650-6661.
619 **Westaway, E. G., Mackenzie, J. M. & Khromykh, A. A. (2002).** Replication and gene
620 function in Kunjin virus. *Current Topics in Microbiology and Immunology* **267**,
621 323-351.
622 **Westaway, E. G., Mackenzie, J. M. & Khromykh, A. A. (2003).** Kunjin RNA
623 replication and applications of Kunjin replicons. *Advances in Virus Research* **59**,
624 99-140.
625 **Wilson, J. R., Sessions, P. F. d., Leon, M. A. & Scholle, F. (2008).** West Nile Virus
626 Nonstructural Protein 1 Inhibits TLR3 Signal Transduction. *Journal of Virology*
627 **82**, 8262 - 8271.
628 **Winkler, G., Maxwell, S. E., Ruemmler, C. & Stollar, V. (1989).** Newly synthesized
629 dengue-2 virus nonstructural protein NS1 is a soluble protein but becomes
630 partially hydrophobic and membrane-associated after dimerization. *Virology* **171**,
631 302-305.
632 **Winkler, G., Randolph, V. B., Cleaves, G. R., Ryan, T. E. & Stollar, V. (1988).**
633 Evidence that the mature form of the flavivirus nonstructural protein NS1 is a
634 dimer. *Virology* **162**, 187-196.
635 **Ye, Q., Li, X. F., Zhao, H., Li, S. H., Deng, Y. Q., Cao, R. Y., Song, K. Y., Wang, H.**
636 **J., Hua, R. H., Yu, Y. X., Zhou, X., Qin, E. D. & Qin, C. F. (2012).** A single
637 nucleotide mutation in NS2A of Japanese encephalitis-live vaccine virus (SA14-

14-2) ablates NS1' formation and contributes to attenuation. *J Gen Virol* **93**, 1959-1964.

Youn, S., Ambrose, R. L., Mackenzie, J. M. & Diamond, M. S. (2013). Non-structural protein-1 is required for West Nile virus replication complex formation and viral RNA synthesis. *Virol J* **10**, 339.

Youn, S., Li, T., McCune, B. T., Cristea, I. M. & Diamond, M. S. (2012). Evidence for a genetic and physical interaction between the NS1 and NS4B that modulates replication of West Nile virus.

Young, L. B., Melian, E. B. & Khromykh, A. A. (2013). NS1' co-localizes with NS1 and can substitute for NS1 in West Nile virus replication. *Journal of Virology*.

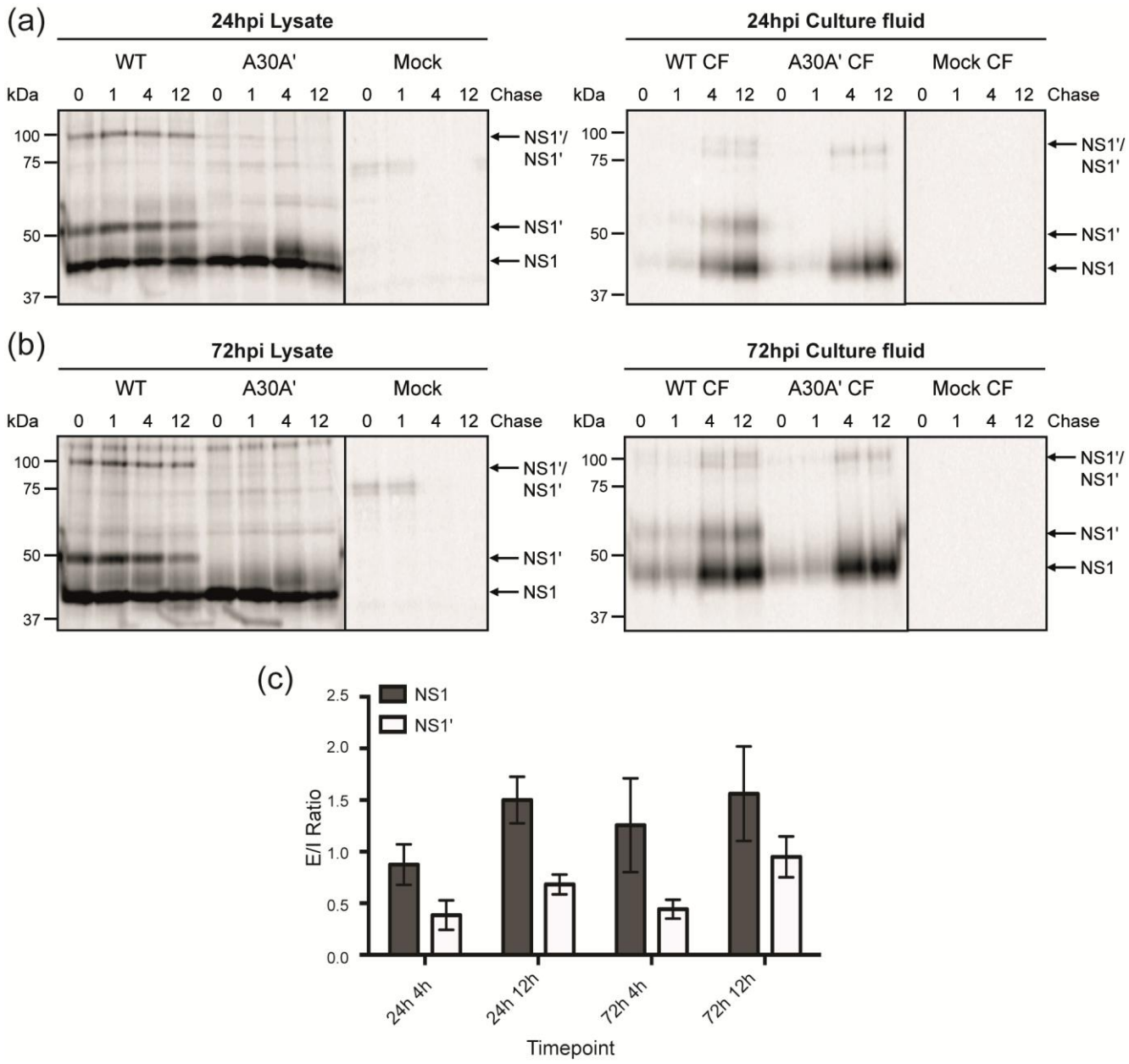

654

655 **FIG 1 NS1' is secreted to a lower degree compared to NS1 from infected cells. (a-b)**
656 Production and secretion of NS1 and NS1' from Vero cells infected with WNV_{KUN} or
657 A30A'. Pulse-chase was performed at (**a)** 24 or **(b)** 72hpi, culture fluids were clarified by
658 centrifugation and cell monolayers were lysed as described. Protein preparations were
659 immunoprecipitated with anti-NS1 (4G4) using Dynabeads® Protein G. Antibody-bound
660 proteins were eluted and samples subjected to electrophoresis. Labeled proteins were

661 transferred to nitrocellulose membranes and exposed to phosphor screen for 1 day. **(c)**
662 Extracellular/intracellular ratio for NS1 (dark bar) and NS1' (white bar) produced by
663 infected cells. Results are expressed as the mean ± SEM of two independent experiments.
664

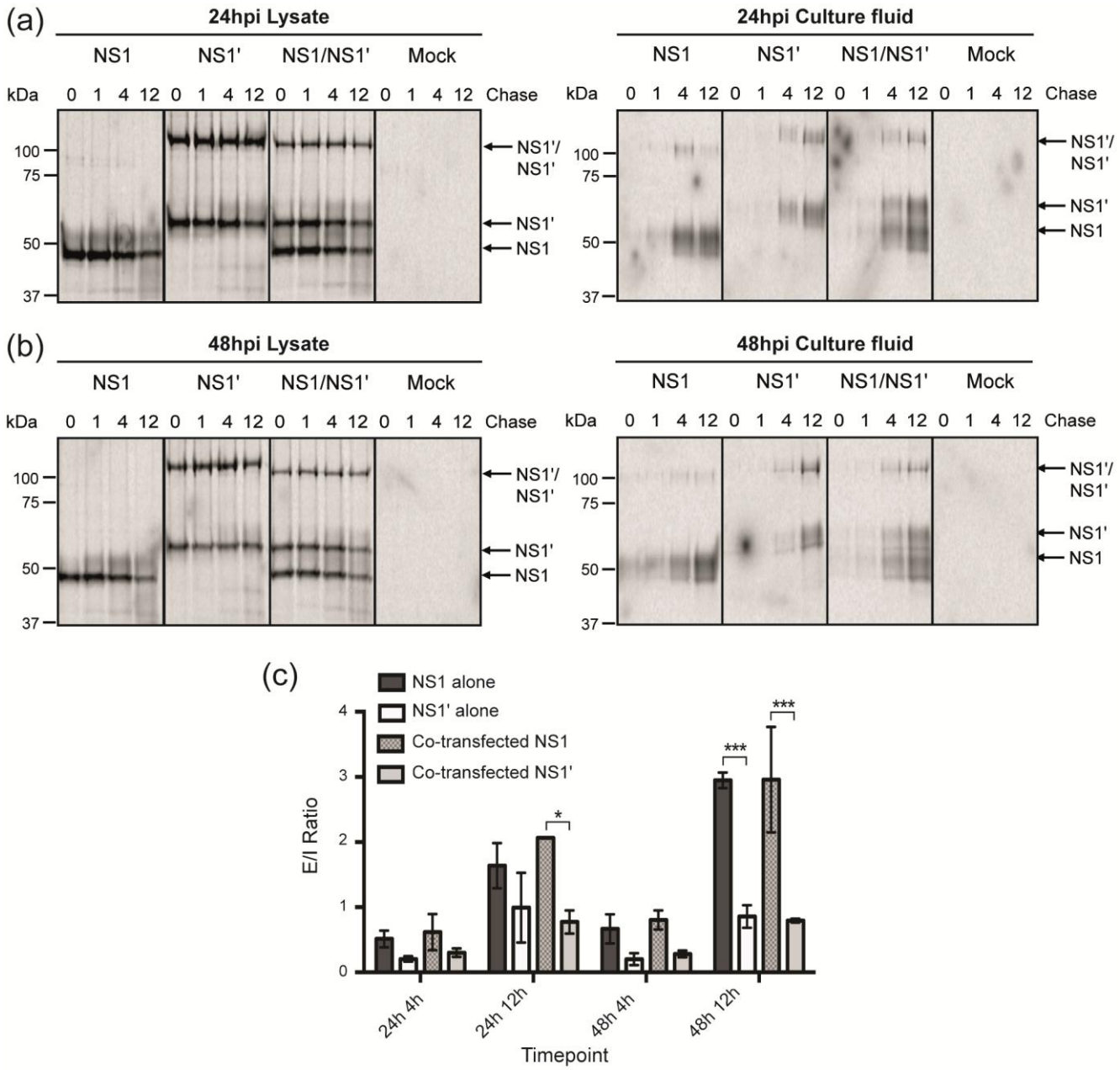

665

666 **FIG 2 NS1' is secreted to a lower degree compared to NS1 from transfected cells. (a-**
667 **b)** Production and secretion of NS1 and NS1' from transfected or co-transfected 293T
668 cells. Pulse-chase was performed at **(a)** 24 or **(b)** 48 hours post transfection and samples
669 processed as outlined in FIG 1. **(c)** Extracellular/intracellular ratio for NS1 and NS1' at 24
670 or 48 h post transfection (with a 4 h or 12 h chase) from singly-transfected (dark or white

671 bar, respectively) or co-transfected cells (medium grey or light grey bar, respectively).
672 Results are expressed as the mean ± SEM of two independent experiments and statistical
673 significance (* [P = 0.01] or *** [P = 0.001]) determined by 2-way ANOVA.
674

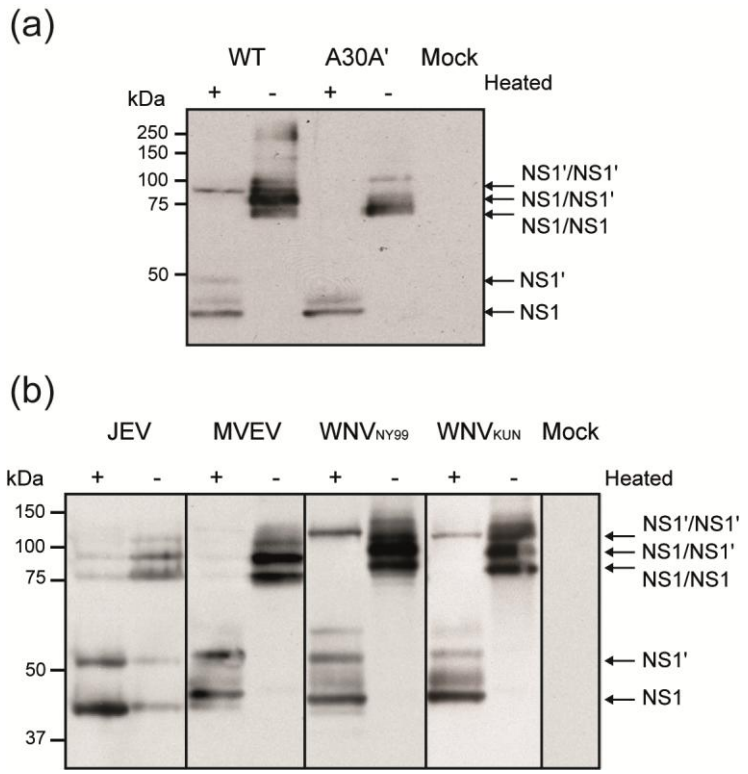

675

676 **FIG 3 Heat-stable NS1' dimers are unique to WNV infected cells. (a)** Western blot
677 showing expression of NS1 and NS1' from WNV_{KUN} and NS1 only from A30A' mutant
678 infected Vero76 cells. Lysates were heat denatured or left untreated and analyzed by
679 Western blotting with anti-NS1 (4G4). **(b)** Lysates harvested from JEV, MVEV,
680 WNV_{NY99} and WNV_{KUN} infected C6/36 cells were heated (70°C for 10 min) or left
681 untreated and proteins were separated by polyacrylamide gel electrophoresis. Proteins
682 were transferred to nitrocellulose membranes and NS1 and NS1' were detected with anti-
683 NS1 (4G4).

684

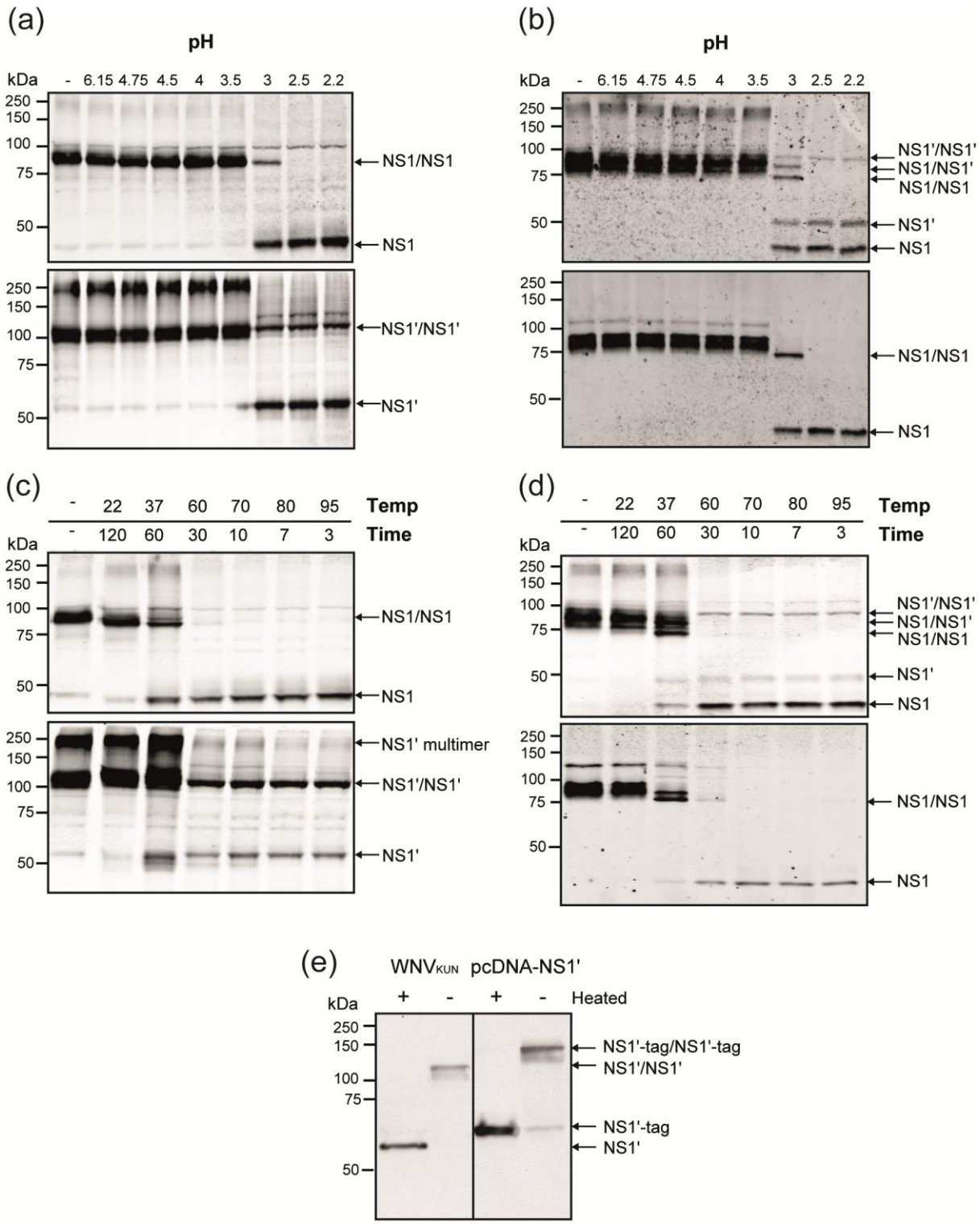

685

686 **FIG 4 Stability of NS1 and NS1' dimers. (a-b)** Lysate from **(a)** transfected or **(b)**

687 infected cells was incubated with 1M glycine at the indicated pH prior to separation by

electrophoresis and western blotting with anti-NS1 (4G4). **(c-d)** Lysate from **(c)** transfected or **(d)** infected cells was incubated at the indicated temperature for the time shown prior to separation by electrophoresis and western blotting anti-NS1 (4G4). Top panel is either pcDNA-NS1 transfected (a and c) or WNV_{KUN} infected (b and d) and bottom panel is either pcDNA-NS1' transfected (a and c) or A30A' infected (b and d). **(e)** Anti-NS1' western blot showing sensitivity of NS1' homodimers to reducing treatment. Lysates from WNV_{KUN} infected Vero76 cells (lanes 1 and 2) or pcDNA-NS1' transfected 293T cells (lanes 3 and 4) were reduced with 5% β-mercaptoethanol and subsequently heat denatured or left untreated prior to Western blotting.

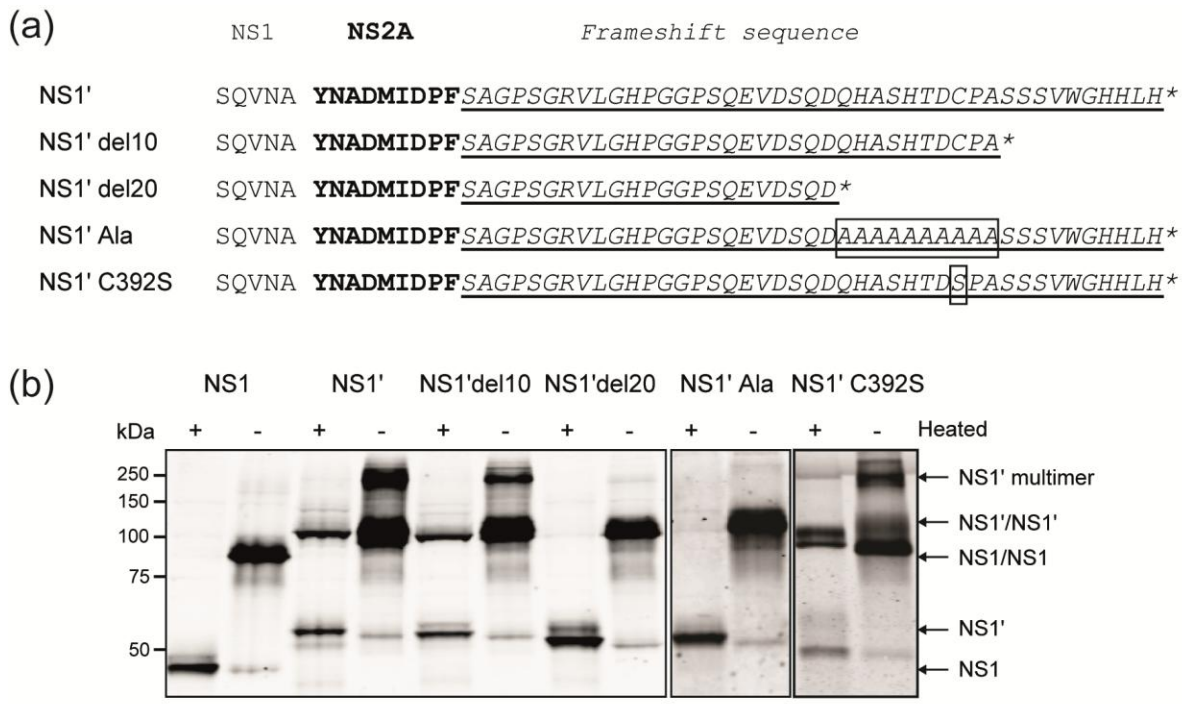

FIG 5 Identification of region in WNV NS1' responsible for formation of heat-stable NS1' dimers. (a) Design of C-terminally truncated (NS1'del10 and NS1'del20) or mutated (NS1'Ala and NS1' C392S) pcDNA-NS1' constructs to assess the region of NS1' contributing to heat-stable dimers. All plasmids retain C-terminal Myc and Flag tags from original pcDNA-NS1' plasmid. Underlining shows the frameshifted region of NS1', boxed nucleotides show mutated bases and asterix (*) shows stop codons. **(b)** Lysates harvested from HEK293T cells transfected with pcDNA-NS1, -NS1', -NS1'del10, -NS1'del20, -NS1'Ala or -NS1' C392S were heated (70°C for 10 min) or left untreated and proteins were separated by polyacrylamide gel electrophoresis. Proteins were transferred to nitrocellulose membranes and detected with anti-NS1 (4G4).

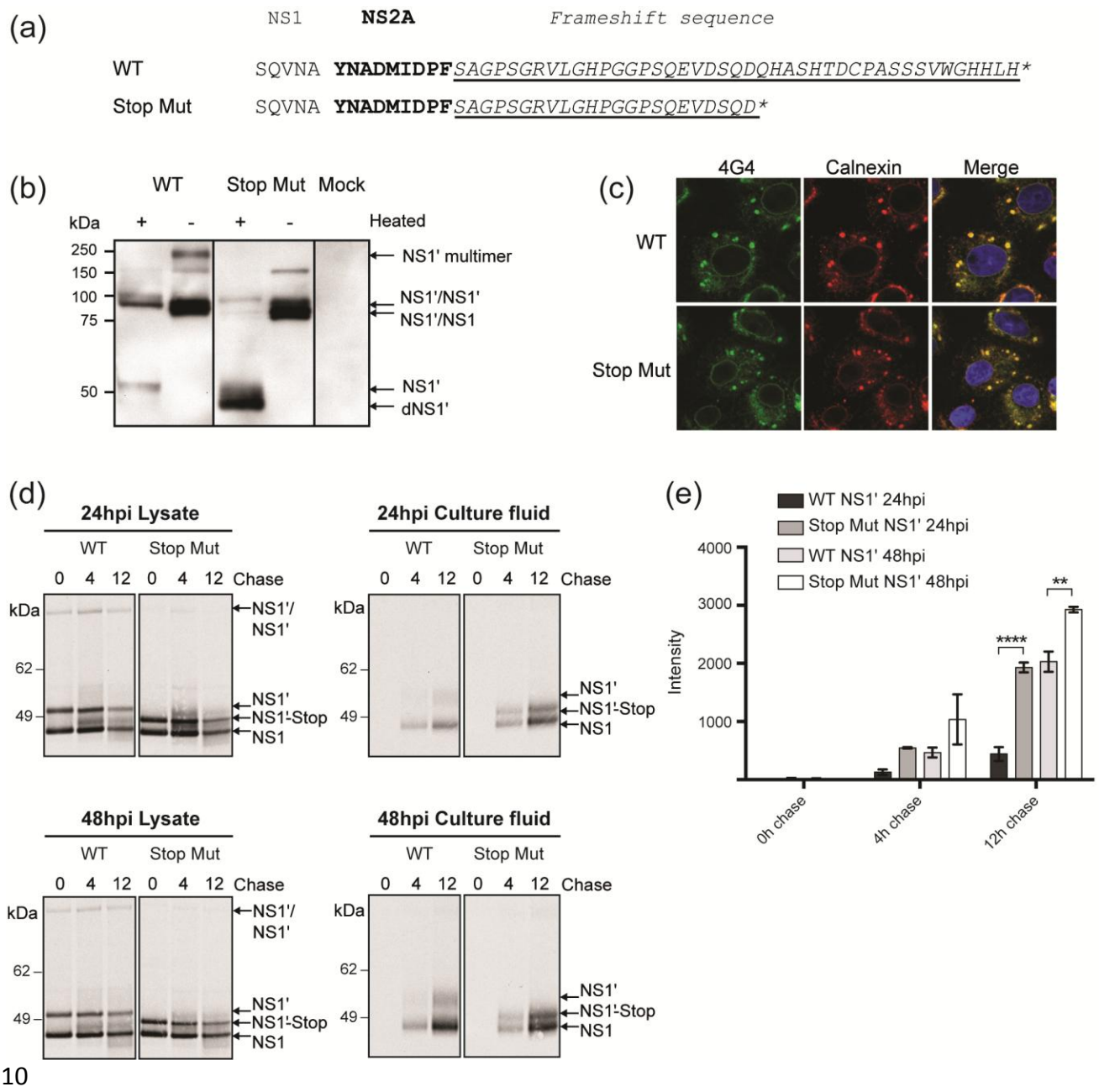

710

711 **FIG 6 Last 20 amino acids of NS1' are important for cellular retention of NS1'. (a)**
712 Design of C-terminally truncated (Stop Mutuant) infectious viral clone. Underlining
713 shows the frameshifted region of NS1' and asterix (*) shows stop codons. **(b)** Lysates
714 harvested from Vero76 cells infected with WNV_{KUN} or Stop Mutant were heated (70°C
715 for 10 min) or left untreated and proteins were separated by polyacrylamide gel

electrophoresis. Proteins were transferred to nitrocellulose membranes and detected with anti-NS1' antibodies. **(c)** Immunofluorescence analysis showing localization of NS1 and NS1' in WNV_{KUN} and Stop Mutant infected cells. Infected cells were fixed and stained with anti-NS1 (4G4; green) and an antibody against calnexin (ER marker; red). **(d)** Production and secretion of NS1 and NS1' from Vero cells infected with WNV_{KUN} or Stop Mutant. Pulse-chase was performed at 24 and 48hpi and samples processed as outlined in FIG 1. **(e)** Quantification of secreted NS1' band intensity from WNV_{KUN} or Stop Mutant infected cells at 24 hpi (dark or medium grey bar, respectively) and 48 hpi (light grey or white bar, respectively). Results are expressed as the mean ± SEM of two independent experiments and significance (**** [$P < 0.0001$] or ** [$P < 0.005$]) determined by 2-way ANOVA.

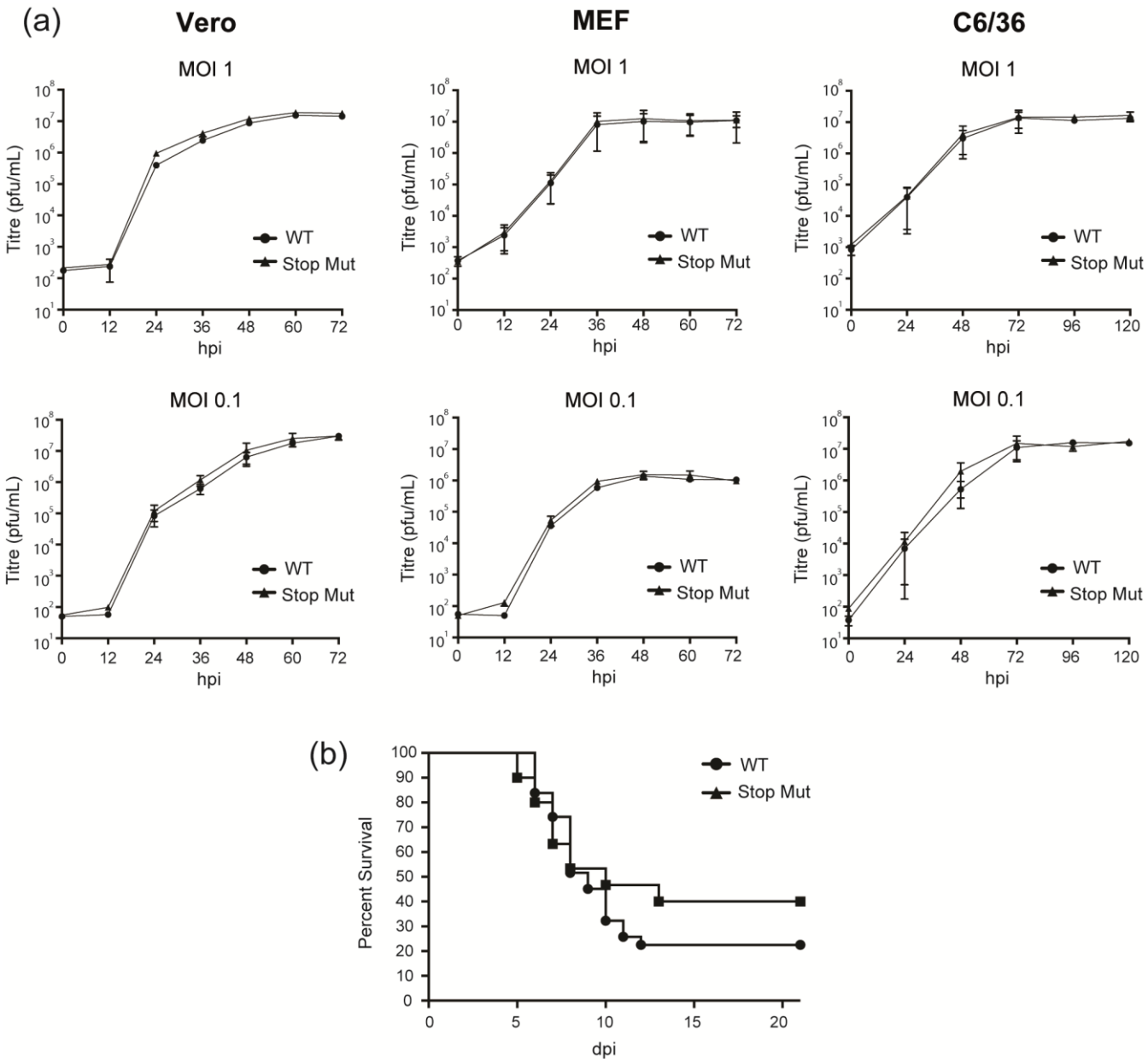

728

729 **FIG 7 Twenty amino acid C-terminal truncation of NS1' does not significantly affect**
730 **viral replication in cells or viral pathogenesis in mice. (a)** Kinetics of viral replication
731 of WNV_{KUN} and Stop Mutant in Vero76, C6/36 or MEF cells. Cells were infected at
732 MOI=1 or 0.1 and viral accumulation was determined up to 120 hpi by plaque assay as
733 described previously (Leung *et al*., 2008). **(b)** Virulence of WNV_{KUN} and Stop Mutant
734 viruses in 18-day old weanling Swiss-outbred CD1 mice. Groups of ten (experiment 1)

735 and twenty (experiment 2) mice were infected intraperitoneally with 1000 pfu of each
736 virus and monitored daily for signs of encephalitis. The graph shows survival rates
737 calculated from the data combined from two experiments.
738

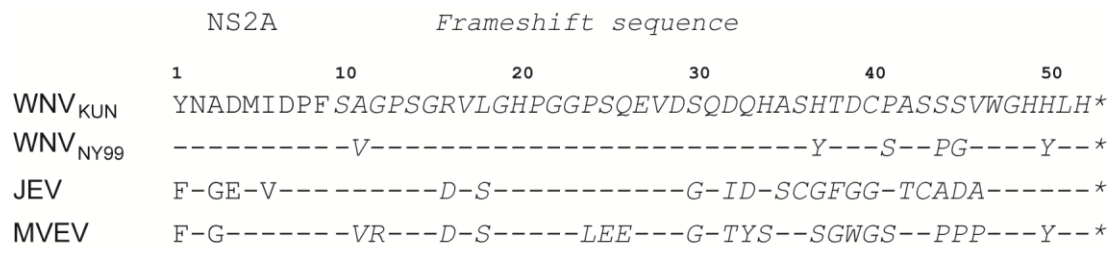

739

740 **FIG 8 Alignment of 52 amino acid C-terminal extension sequences in NS1' of the**
741 **key representative viruses from JEV serogroup.** Dashes (-) indicate amino acids
742 consistent with WNV_{KUN} and asterisk (*) shows stop codons. Virus sequences used:
743 WNV_{KUN} – GenBank:AY274504; WNV_{NY99} – GenBank:NC_009942; JEV –
744 GenBank:NC_001437; MVEV – GenBank:NC_000943.

745